ORGANIC SYNTHESIS ON STRIGOLACTONE CHEMISTRY

A thesis submitted in fulfillment of the requirements for admission to the degree of

Doctor of Philosophy

by

Boheng GUAN

School of Chemistry

the University of Sydney

2025

Statement of Originality & Author Attribution Statement

This thesis is a summary of research work conducted in the School of Chemistry, the University of Sydney, under the supervision of Prof. Christopher S. P. McErlean from October 2021 to February 2025.

All work presented herein is original and performed by myself unless specifically stated. All the figures and schemes were made by myself unless specifically stated. Mass Spectrometry was performed by myself or Ms Chianna Dane, Ms Bernadeth Antonio, Mr. Anthony Ayoub, Mr. Edward Daniel Harvey-Latham and Dr. Nicholas Proschogo (the Mass Spectrometry Facility staff of the University of Sydney). NMR spectra were all obtained and analysed by myself unless specifically stated. All the melting points and IR spectra were obtained and analysed by myself unless specifically stated. The words 'we' and 'our' when used herein refer to myself.

During the preparation of the thesis, the author used ChatGPT for the purpose of text enhancing. Generative AI tool utilization includes checking grammar, correcting typographical errors and fixing sentence structures. The author confirms that where text was modified by generative AI, the content was reviewed for possible errors, inaccuracies and bias. The author takes full responsibility for the submitted thesis and ensures the work is their own and has used generative AI within the parameters of use.

This thesis contained no material published or extracted in whole or in part from a thesis presented by me for any other degree or diploma. No other individuals work has been used without due acknowledgement. Every effort has been made to acknowledge previously published research work. And this thesis contains fewer than 80,000 words.

Boheng Guan

Feb. 2025

Acknowledgements

At the very beginning, I would like to thank my supervisor Prof. Chris McErlean, a knowledgeable organic chemist with inquiring spirit. Like a torch in the endless night, his enthusiasm, persistence and support have encouraged and motivated me to finish my PhD study. I have gained so much from him.

I would like to express my gratitude to China Scholarship Council for providing me with the scholarship and as a Chinese, I will always be proud of my motherland. Also, I would like to thank the University of Syndey for providing me with the chance for my PhD and offering me the PRSS Scholarship to let me survive in Sydney.

Thanks to all the technical staff in the School of Chemistry, particularly Dr. Ian Luck, Dr. Paige Hawkins for training me about the using of NMR, Dr. Nicolas Proschogo for training me about the using of LRMS and all the staff who helped me running my samples in the past three and half years.

Thank you, Dr. Stephen Bulter from the Jolliffe group and Dr. Dennis Cheng, for your help during my early days at the university and the challenging period when COVID was rampant. Without you guys, I can't imagine how long it would have taken me to get familiar with the lab equipment and adapt to working independently and comfortably in the lab.

I would like to thank all the teammates in the CSPM group, Elene, Zhiping (Sam), Fergus, Haochen and Lachlan for the support and friendship as well as the other members of level 5. And I would also like to thank the service room staff Mr. Carlo Piscicelli and Dr. Tahmineh Hashemzadeh for supporting my PhD by providing many research consumable items.

At the same time, I would like to thank the friends I met in the chemistry building, Ivy, Alicia, Chenyou, Haoxiang, Yining, Nian Kee, Jet, Mutian, Zixi, Qinyi, Haobo and Yan

(Huohuo). Our lives intertwined because of this building and I will never forget days after meeting you all. Also, I would like to thank my wonderful and lovely friends outside chemistry: Angel, Bitong, Lora, Xiaosu and Zihan (Lilyellow). I will remember the fantastic life with you guys forever.

Most importantly, I would like to give my biggest thank to my family. Without your supports, I cannot achieve anything. Moreover, I would like to keep the ending part of my acknowledgement to my wife, Jingyao. You are the only one who will walk with me through the whole life, so no words needed here because they exist in every day of the future with you.

Abstract

Strigolactones (SLs) are carotene-derived natural products that play important roles as phytohormones (within plants), as seed germinators of parasitic weeds (between plants), and as chemical communicators between plants and fungi (between kingdoms). A subset of these molecules, called non-canonical SLs, exhibit highly diverse structures that present significant challenges to the synthetic chemist.

The research topic of this thesis is focusing on developing novel synthesis routes from commercially available ionones to two strigolactone molecules: carlactone (CL) and avenaol. Based on the knowledge gained *en route* to CL, further research was conducted towards CL derivatives which shared the same carbon skeleton as CL.

The choice of which non-canonical SLs to target for synthesis was not random. As the biosynthetic precursor of all SLs, and a natural product in its own right, the importance of CL is self-evident. However, total synthesis routes to this molecule remains relatively under-explored. There is still no large-scale preparation that can produce enough CL to enable further biological research. Therefore, inventing a cost-effective and chemoselective synthetic route is necessary.

Avenaol is perhaps the most synthetically challenging non-canonical SL, possessing a unique fused cyclopropane unit that is incredibly sterically congested. We have designed a novel synthetic strategy that intercepts an intermediate in the only reported synthesis of avenaol. We aimed at significantly simplifying the total synthesis of avenaol, thereby facilitating material access for further studies into its potential biological or therapeutic properties.

The first chapter introduces and discusses the discovery, classification and structures of SLs, biosynthesis and biofunctions of SLs, signalling and transporting of SLs as well as current developed total synthetic strategies to species-specific SL molecules.

In Chapter 2, we focus on developing a more effective total synthetic route of the common precursor in SLs biosynthesis, CL. Given the limited understanding of the biosynthesis and biological functions of non-canonical strigolactones, a large-scale supply of CL is crucial for further research. We investigated three totally different synthetic approaches, and although we did not achieve our final aim, this work will inform future research directions and provided valuable knowledge for similar studies.

Chapter 3 describes our effort on modification of Tsukano's total synthesis route towards avenaol. We designed a seven-membered ring intermediate to enable a more efficient synthesis of the key intermediate in the Tsukano route. Additionally, we explored an alternative pathway using free carbene cyclopropanation to construct the main carbon skeleton. We encountered challenging stereochemical issues during the research process. Despite multiple attempts, we were unable to effectively invert the stereochemistry of a key stereocentre in the target structure to give the naturally occurring stereochemistry.

In Chapter 4, we primarily discuss the total synthetic designs on generating CL-type SL derivatives and analogues which become more important in many research fields. Our approach focused on employing olefin metathesis catalyzed by the Grubbs catalyst and Wittig reactions as key transformations, using β-ionone and its hydrogenated derivatives as starting materials. This work aimed to develop a general strategy for synthesizing CL-type SL analogues and derivatives. In this chapter, we detail only preliminary investigations. Due to the unexpected side reactions and byproducts, our initially designed route proved to be unachievable. But based on some promising observations, we still have a clear direction for further investigations.

Moreover, there is a brief conclusion chapter, followed by experimental protocols, related data, and references.

Abbreviations

Å	Ångstrom
ABA	abscisic acid
Ac	acetyl
AIBN	azobisisobutyronitrile
AM	arbuscular mycorrhizae
APCI	atmospheric pressure chemical ionisation
At	*Arabidopsis thaliana*
ATP	Adenosine triphosphate
ATRC	atom-transfer radical cyclization
Bn	benzyl
Boc	*tert*-butyloxycarbonyl
Bu	butyl
Bz	benzoyl
CCD	*Carotenoid Cleavage Dioxygenase*
CCR	Corey-Chaykovsky reaction
CK	cytokinin
CL	carlactone
CLA	carlactonic acid
CLIM	covalently linked intermediate molecule
D	DWARF gene
DABCO	1,4-diazabicyclo[2,2,2]octane
DAD	DECREASED APICAL DOMINANCE gene
dba	dibenzylideneactone
DBU	1,8-diazabicyclo[5,4,0]undec-7-ene
DCC	*N, N'*-dicyclohexylcarbodiimide
DI	deionized
DIBAL	Diisobutylaluminium hydride

DMAP	4-dimethylaminopyridine
DMF	*N, N*-dimethylformamide
DMSO	dimethyl sulfoxide
DNP	dinitrophenylhydrazine
E1cB	unimolecular conjugate base elimination
EDG	electron donating group
eq.	equivalent
ESI	electrospray ionisation
Et	ethyl
EWG	electron withdrawing group
GC-MS	gas chromatography-mass spectrometry
HMPA	hexametylphosphoramide
HPLC	high pressure liquid chromatography
HRMS	high resolution mass spectrometry
HWE	Horner-Wadsworth-Emmons
*i*Pr	isopropyl
IR	infrared
KHMDS	potassium bis(trimethylsilyl)amide
LAK	lipase AK
LBO	*Lateral Branching Oxidoreductase*
LC-MS	liquid chromatography-mass spectrometry
LC-MS/MS	liquid chromatography-tandem mass spectrometry
LCOs	lipochitoolisaccharides
LDA	lithium diisopropylamide
LED	light-emitting diode
LG	leaving group
LiHMDS	lithium bis(trimethylsilyl)amide
LRMS	low resolution mass spectrometry
m.p.	melting point

m.s.	molecular sieve
MAX	MORE AXILLARY GROWTH gene
*m*CPBA	*meta*-Chloroperoxybenzoic acid
MeCLA	methyl carlactonate
MS	mass spectrometry
Ms	methanesulfonyl
NADH	nicotinamide adenine dinucleotide hydride
NBS	*N*-bromosuccinimide
NCAL	Nucleophile-Catalyzed Aldol-Lactonization
NIS	*N*-iodosuccinimide
NMO	*N*-methylmorpholine *N*-oxide
NMP	*N*-metyl-2-pyrrolidone
NMR	nuclear magnetic resonance
nor-AZADO	9-azanoradamantane-N-oxyl
PDC	pyridinium dichromate
PDR1	pleiotropic drug resistance 1
Ph	phenyl
PMB	*p*-methoxybenzyl
PPTS	pyridinium *para*-toluenesulfonate
pyr	pyridine
RSM	RAMOUSUS gene
RT	room temperature
SL	strigolactone
S_N2	bimolecular nucleophilic substitution
TBAF	tetrabutylammonium floride
TBHP	*tert*-butyl hydoperoxide
TBS	*tert*-butyldimethylsilyl
TEA	triethylamine
TEMP	2,2,6,6-tetramethylpiperidine

tert	tertiary
TES	triethylsilane
Tf	triflic
TFDO	methyl(trifluoro methyl)dioxirane
THF	tetrahydrofuran
THP	tetrahydropyran
TIPS	triisopropylsilane
TLC	thin-layer chromatography
TMP	tetramethylpiperidine
TMS	trimethylsilyl
Ts	toluenesulfonic
UV	ultraviolet
μm	micrometer

Table of Content

1 INTRODUCTION

Use of the word 'phytohormone' can be dated back to 1937.[1] Went and Thimann used 'phytohormone' to denote the small molecules existing in plant cells at super low concentrations, which control every aspect of the physiological functions and activities of plants. In subsequent decades, researchers actively isolated and identified phytohormones, which were classified into five groups: abscisic acid (ABA), which is generated by chloroplasts to promote metabolism and production of other phytohormones;[2] auxins, widely known as the initiator of apical dominance;[3] gibberellins, which exhibit multiple different bioactivities across the life cycle;[4] cytokinins (CKs), which affect cell division;[5] and ethylene, which is extremely useful in fruit ripening.[6]

Those five categories were regarded as the only phytohormones for quite a long time.[7] In the more recent past, researchers have delved deeper into plant biochemistry and physiology, and more and more previously undiscovered and unfamiliar hormones have been identified. Strigolactones (SLs) represent one of these new phytohormone classes, which display intriguing chemical structures and unique biological functions.[7,8]

This chapter will provide the reader with an introduction to SLs, including discussions related to their structures, biological functions in plants and fungi, classification, confirmed and proposed biosynthetic routes catalysed by enzymes inside plants, and the current state of total chemical synthesis of a variety of SLs.

1.1 Discovery and Classification of Strigolactones

The first report of a strigolactone appeared in *Science* on 2nd December 1966.[9] Cook and coworkers isolated a molecule from the root exudates of cotton (*Gossypium hirsutum L.*) that did not match any class of known phytohormones. While the structure of the molecule could not be ascertained at that time, it was clear that the molecule contained an alcohol functional group. Those authors named the molecule 'strigol' and described it as a crystalline germination stimulant of the parasitic weeds of the genus *striga*. In the following years, several other related hormones were discovered that contained a lactone unit,[10] so this class of hormones was named 'strigolactones' from their 'mother plant' *Striga asiatica* (*Striga lutea L.*)(Figure 1.1).[11]

Figure 1.1: *Striga asiatica (Striga lutea L.)*. (Image credit RECKON TaiBNET)

1.2 Structures of Strigolactones

1.2.1 General Structure of Strigolactones

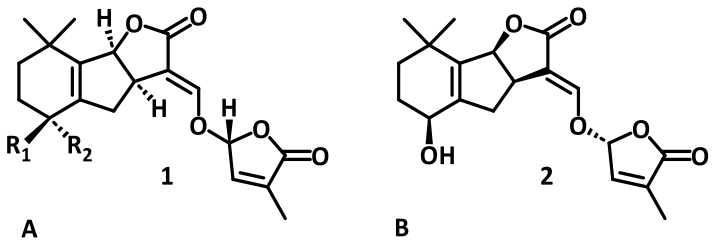

Figure 1.2: (A) Strigol structure (**1**) reported by Cook; (B) Exact structure of (+)-strigol (**2**).

Cook and coworkers proposed the structure of strigol five years after its isolation (Figure 1.2).[12] The structure they reported was confirmed by more sophisticated techniques thirteen years later.[13] Similarly, another molecule was isolated and from the same plant source, whose structure was quite similar to strigol. This molecule was an ester of strigol and was named strigyl acetate.[9,13]

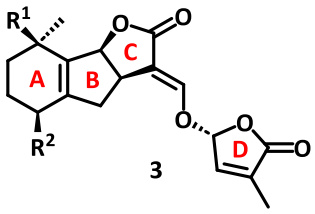

Figure 1.3: General structure of SLs (**3**) in the past.

The generally accepted structure for this 'new' class of strigolactone phytohormones is shown in (Figure 1.3). The four rings were denoted A, B, C and D for convenience. It was proposed that the main ABC ring system was a tricyclic lactone, with individual strigolactones having different substituents appended to this unit. The tricyclic system was linked to a butenolide ring by an enol ether bridge.[8] Indeed, all strigolactones isolated to date possess the same D ring structure,[14] and this feature has become the defining characteristic as to whether new molecules are classified as strigolactones or not.

Strigolactones that conform to the general structure outline in Figure 1.3 are now known as 'canonical strigolactones'.[15]

1.2.2 Canonical Strigolactones: Strigol Type SLs & Orobanchol Type SLs

Strigol (**2**) and strigyl acetate (**4**) were found by Cook and collaborators in 1966.[9] There wasn't any progress in discovering SLs until sorgolactone (**6**) was found in *Sorghum bicolor* by Hauck 26 years later.[16] Sorgolactone (**6**) was found to be even more active than strigol as a germination stimulant for seeds of the parasitic weed genus *striga.*

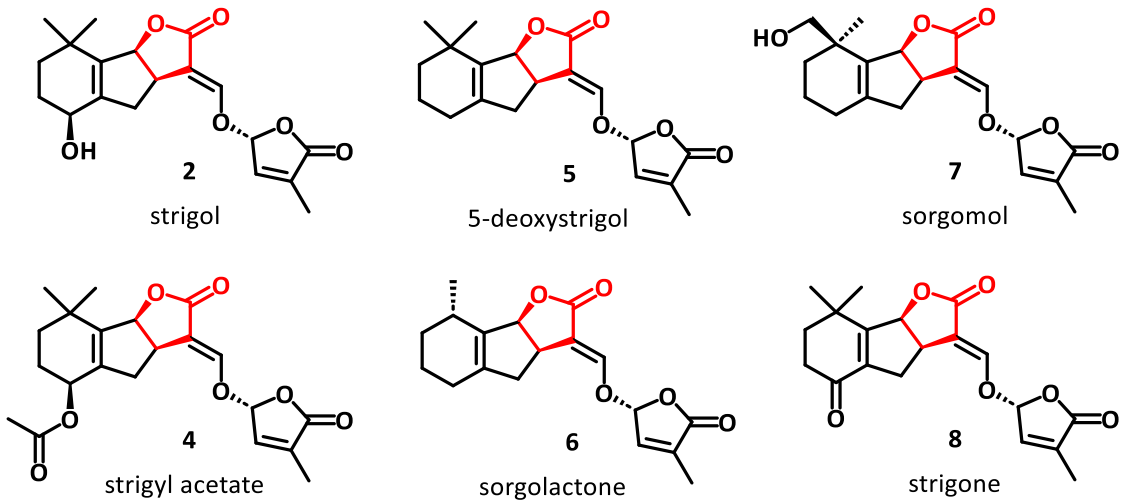

Figure 1.4: Naturally occurring strigol type strigolactones.

In 2005, Akiyama isolated strigol-related molecule 5-deoxystrigol (**5**) from *Lotus japonicus*, and discovered that this phytohormone also acted as a signalling molecule that triggered hyphal branching in arbuscular mycorrhizal fungi.[17]

Xie and Yoneyama discovered another strigol-related molecule from *Sorghum bicolor* that was different from sorgolactone (**6**). This was certified to be a novel strigolactone named sorgomol (**7**), with one more hydroxymethyl group than sorgolactone (**6**).[18]

The most recent discovery of strigol-related SLs was in 2013.[19] Strigone (**8**) was found in *Houttuynia cordata*, famous as a unique herb ingredient in southern west of China.

The strigolactone story took a major turn when the structure of alectrol, that was proposed by Muller in 1992,[20] was disproved. Muller isolated alectrol from *Alectra vogelii Benth.* and proposed a structure (**9**) based on general strigolactone picture displayed in Figure 1.5. However, synthetic efforts by Matsui's group from Japan demonstrated that the proposed structure was incorrect, and that the general structure of SLs mentioned above, might needed to be updated or corrected.[15,21,22]

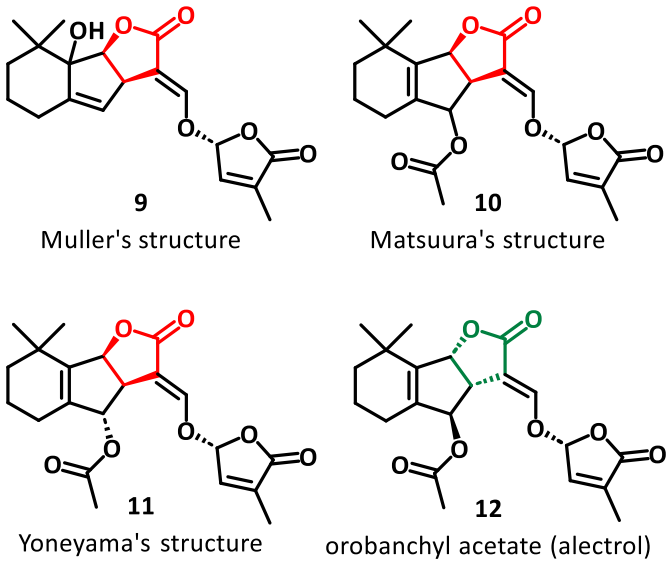

Figure 1.5: Proposed, revised and actual structures of orobanchyl acetate/alectrol (**12**).

Matsuura and Yoneyama gave revised structures of alectrol as molecule (**10**) and (**11**)[23,24] but the issue wasn't resolved until Sugimoto and coworkers elucidated the exact structure of alectrol (**12**), which is now called orobanchyl acetate (**12**) (Figure 1.5).[25] Those researchers were able to confirm that the structures of orobanchol and orobanchyl acetate did possess a tricyclic lactone system, but that it had the opposite stereochemistry to the ABC lactone ring system of strigol. In contrast, the stereochemistry of the butenolide ring remained unchanged.

Subsequent to that work, all canonical SLs, which possess the same atom connectivity on the ABC ring system, have been further classified into Strigol type or Orobanchol type based on the different relative stereochemistry of the ABC ring system.

Despite being discovered much later than the strigol type SLs, the number of orobanchol type strigolactones identified to date, makes this the larger of the two groups.[21] Besides orobanchol (**13**) and orobanchyl acetate (**12**), another two molecules in this category: solanacol (**14**) and solanacyl acetate (**15**) were isolated as germination stimulants for *Orobanche* and *Phelipanche* spp. from tobacco (*Nicotiana tabacum* L.) in 2007.[26] Their structures were initially proposed with the strigol like stereochemistry but were revised two years later.[27]

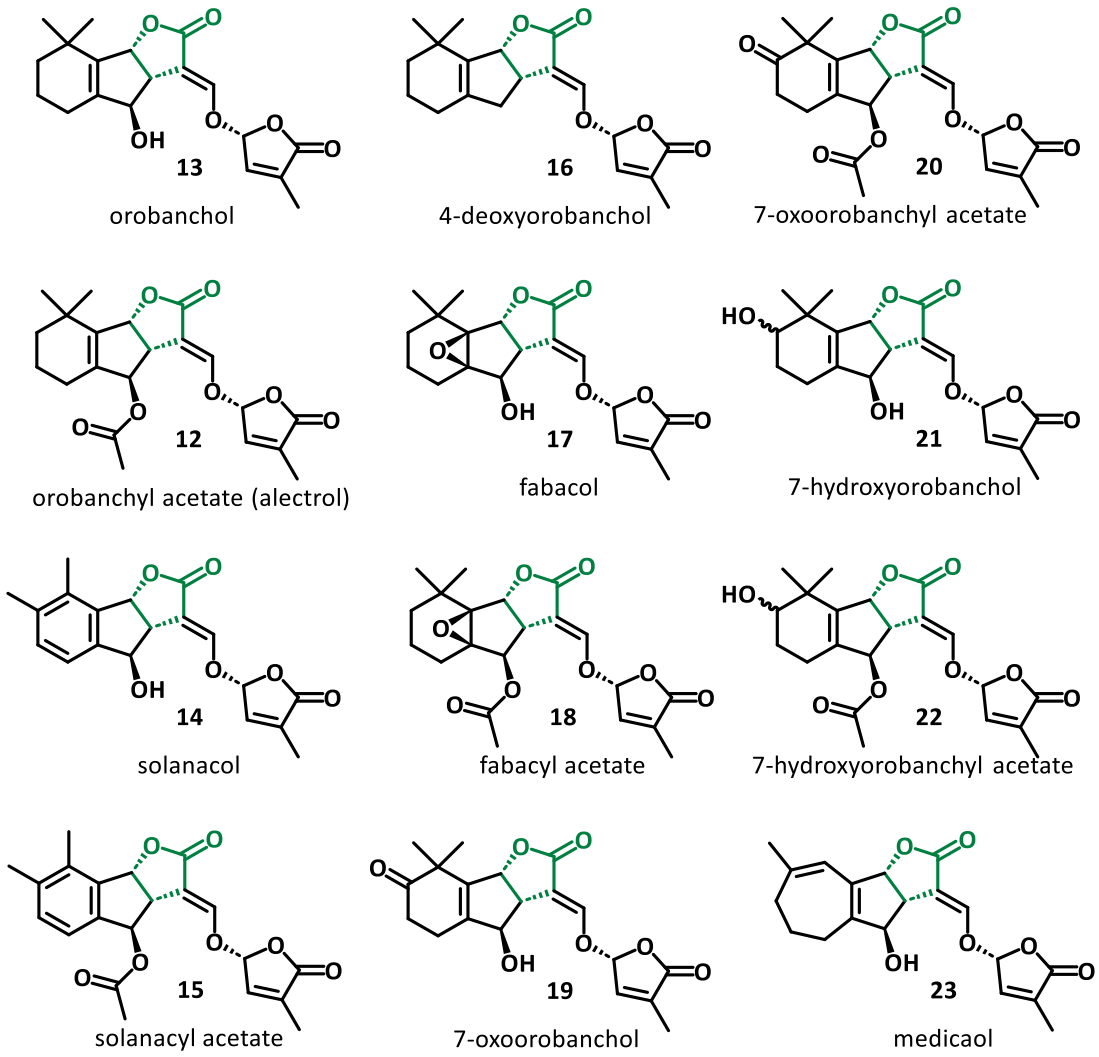

Figure 1.6: Naturally occurring orobanchol type strigolactones.

In analogy to the strigol type phytohormones, the unsubstituted orobanchol type ring system was discovered in 2008, with the isolation of 4-deoxyorobanchol (**16**).[28] Fabacol (**17**) and fabacyl acetate (**18**) were isolated from *Pisum sativum*[29] and at the

same time, four new SLs which contained oxidized and hydroxyl orobanchol (**19**, **20**, **21**, **22**) together with their acetates were also isolated from *Oryza sativa*.[30] The most recently discovered canonical SL, medicaol (**23**), which contains a seven-membered A ring, was classified as an orobanchol type SLs due the stereochemistry of the fused ring system.[31]

1.2.3 Non-Canonical Strigolactones

As mentioned in the previous section, both strigol like and orobanchol like strigolactones possess the same stereochemically defined D ring, connected to a fused ring system via an enol ether bridge.[14] This structural element now defines molecules as strigolactones. Naturally occurring molecules have been isolated from plant hosts, in which the enol ether appended D ring is not attached to a tricyclic fused ring system. These molecules are collectively known as non-canonical SLs.[32]

The earliest reported non-canonical SL was carlactone (**24**), which is now known as the common precursor in the biosynthesis of all SLs in Figure 1.7.[33,34] Alder and coworkers reported carlactone as a molecule with some strigolactone-like bioactivities and discovered a novel biochemical pathway from carotenoids to strigolactones,[34] which will be discussed later in this thesis. An oxidized form of carlactone (**24**), namely carlactonic acid (CLA) (**27**) was reported by Nomura in 2014,[35] and fully characterized four years later.[36]

In 2012, an unidentified strigolactone germination stimulant was observed in the isolation fractions of maize (*Zea mays*), which is the most common host of the parasitic weeds of the genus *Striga*.[37] The mass spectrometric fragmentation pattern confirmed the presence of the strigolactone D ring, but at that time, the structure of the molecule could not be ascertained. Later, researchers isolated two novel non-canonical SLs from the root exudates of black oat (*Avena Strigosa*).[38]

Interestingly, one of these molecules corresponded to the unidentified biological stimulant from maize (*Zea mays*), and was named zealactone (**26**).[39] The structure of the second isolated compound was elucidated as the fused cyclopropane containing molecule, avenaol (**25**).

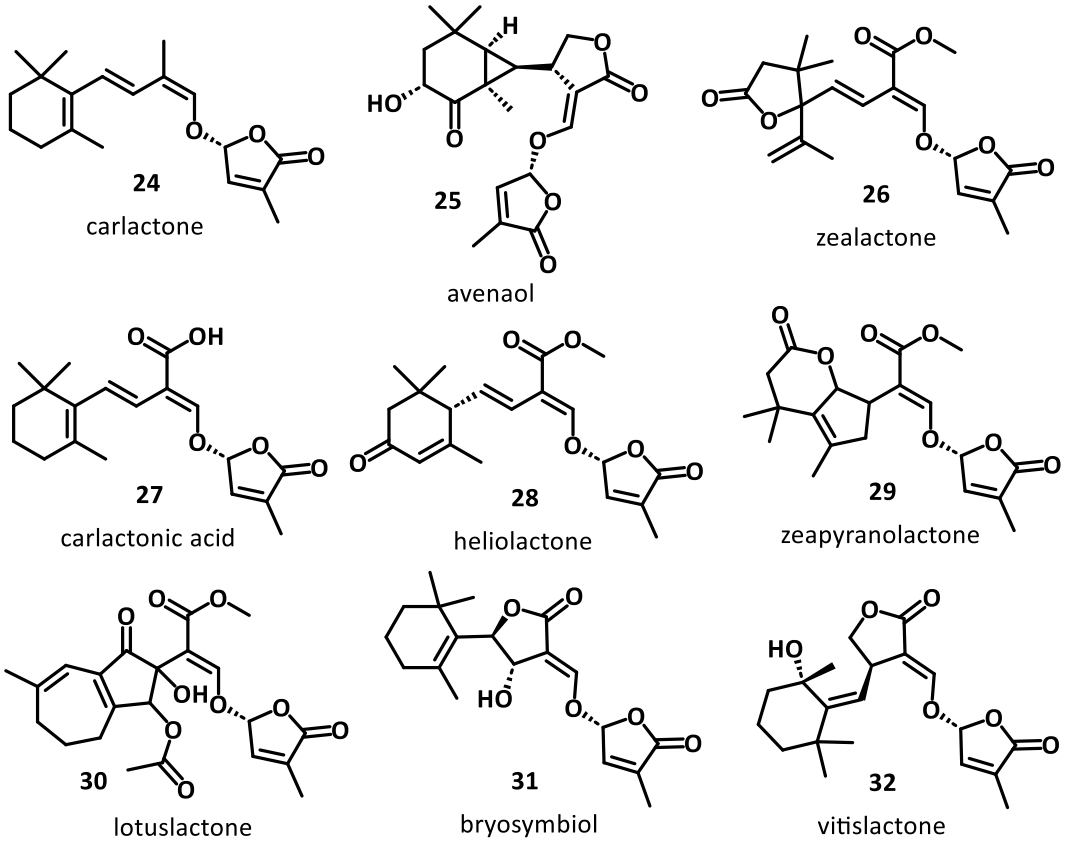

Figure 1.7: Naturally occurring non-canonical strigolactones.

Non-canonical SLs have been isolated in recent years from familiar plants' root exudates. Heliolactone (**28**) was characterized from sunflowers (*Helianthus annuus* L.) as a non-sesquiterpene molecule that has a similar structure to carlactone (**24**).[40] Zeapyranolactone (**29**) and lotuslactone (**30**) were found in *Zea mays*[41] and *Lotus japonicus*[42] respectively, from which zealactone and 5-deoxystrigol had been previously isolated. The most recently isolated non-canonical SL, and coincidentally the most recently isolated strigolactones, are bryosymbiol (**31**) and vitislactone (**32**).[43,44] Bryosymbiol is of note due to the fact that it was isolated from a lower order plant and suggests an ancient evolutionary role for strigolactones. There are also non-

canonical SLs derived from CL (**24**) during biosynthesis processes occurring in plant cells or organs. These will be separately discussed in a later section.

This section of the thesis describes the isolation and classification of a large number of strigolactones from a variety of plant sources. The question of why plants produce such an array of molecules logically follows. Presumably these molecules play some important biological roles that benefit the growing plant. This will be the topic of the following section.

1.3 Biofunctions of Strigolactones in Phytology

1.3.1 Promotion on Parasitic Plant Germination

The first strigolactone, Strigol, and most of the subsequently isolated strigolactones, were found as a result of their ability to act as germination stimulants for the seeds of the parasitic weeds *Striga* and *Orobanche* (parasites lifecycle shown in Figure 1.8). These weeds spend most of their life cycle below ground, where they attach to a host plant and deprive it of nutrients and water. *Striga* and *Orobanche* weeds represent a major risk to global food production, with sustenance crops like maize and sorghum being host plants for *Striga* parasites.[45] Crop losses of up to 90% occur in sub-Saharan Africa due to infestation of crops by these parasitic weeds.

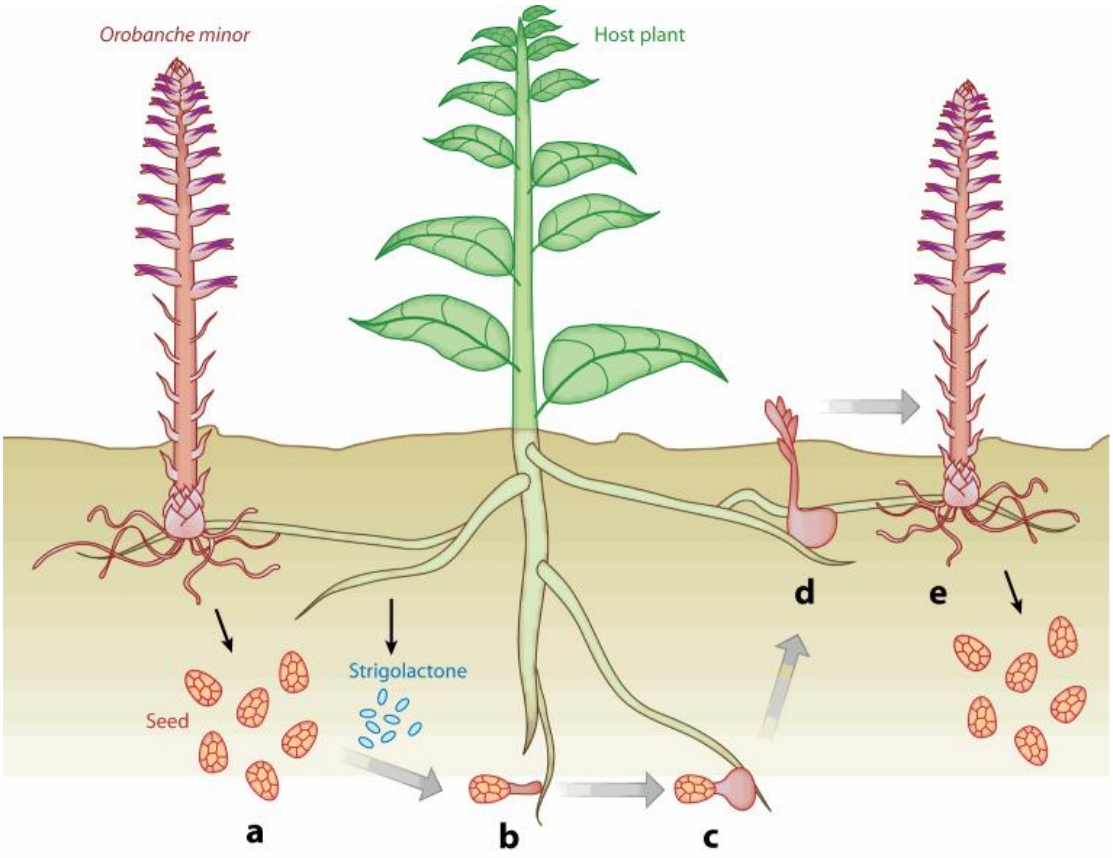

Figure 1.8: Lifecycle of parasites, *Orobanche* as the example. **a.** seed germination induction with the presence of strigolactone; **b.** seedling attaching to the root of the host plant; **c&d.** parasites growth; **e.** cycle closure by releasing more seeds. (Reported by Xie and Yoneyama[10])

Strigolactones that are exuded from the root system of growing plants cause germination of the parasitic weeds at extremely low concentrations.[10,46] So despite the fact that strigolactones are a recognised class of plant hormones, they display activity as an inter-plant signalling agent.

Taking advantage of this aspect of SL activity, suicidal germination was devised as a control strategy for parasitic weeds.[47,48] Soil can be treated with SLs or SL analogues. before planting crops, to germinate the seeds of the parasitic weeds. In the absence of a host to provide nutrients, the parasites perish and farmers can greatly increase harvest yields of subsequently planted crops. Suicidal germination is regarded as the most important application of strigolactones in agriculture.[48]

1.3.2 Coordination on Plant Growth and Architecture

Besides inter-plant activities described above, SLs also play important intra-plant roles. SLs are a class of hormones that affect/coordinate many aspects of plant growth and architecture relative to phosphate availability.[49] Figure 1.9 below summarizes the known biological activities of strigolactones on plant architecture. From this figure it is easily recognized that SLs influence both the upper shoots and the lower roots.

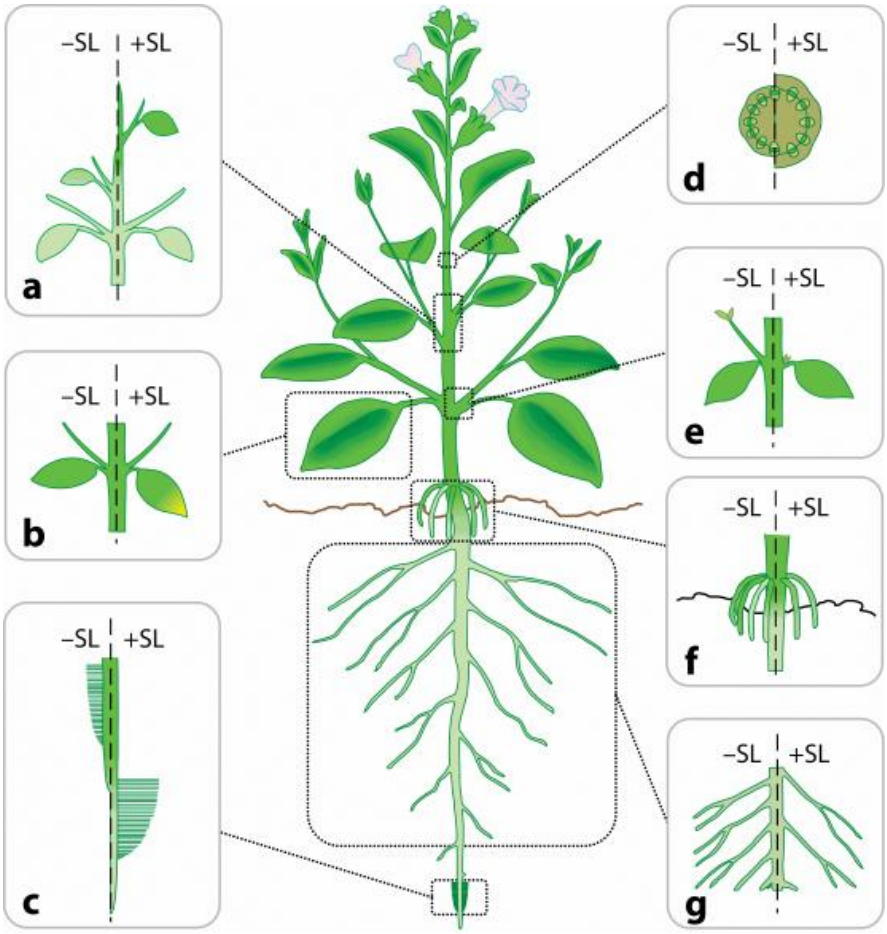

Figure 1.9: SLs coordination on plant growth and architecture. **a.** internode growth stimulation; **b.** leaf ageing promotion; **c.** roof hairs elongation and primary roots growth; **d.** stem thickness increasing and secondary growth induction; **e.** auxiliary bud outgrowth inhibition; **f.** adventitious roots growth inhibition; **g.** lateral roots growth inhibition. (Reported by Al-Babili and Bouwmeester)[49]

Thale cress (*Arabidopsis thaliana*) has become a well-known model plant in agriculture and phytology owing to its easily observed phenotype characteristics. Most strigolactone research uses *Arabidopsis thaliana* as the host plant. Koltai and collaborators observed several main effects of SLs on *Arabidopsis*[50] such as stimulating the growth of primary roots, decreasing the density of lateral roots, and promoting root hair elongation.[51] Surprisingly, SLs also inhibit adventitious root formation in *Arabidopsis* and several other organisms, which was reported by Bouwmeester.[52]

SLs were also found to affect apical dominance,[53] which was defined as an overgrowth inhibition of lateral buds from terminal buds.[54] SLs simultaneously inhibit the outgrowth of auxiliary buds and promote the growth of the internode.[53] In addition to acting as primary phytohormones that directly promote biological processes in plants, SLs are also play a role in influencing phytohormone cross talk. For instance, SLs can regulate the secretion of the phytohormone auxin to control secondary growth in plants as well. Via transport proteins, SLs have been able to initiate or inhibit the production of auxins to regulate further activities[55].

So strigolactones play important inter- and intra-plant roles. But their biological functions do not stop there. SLs also act as inter-kingdom signalling agents.

1.3.3 Essential Molecule in Plant-Fungi Interaction

Research has uncovered that SLs act as signalling molecules in the bidirectional identification between arbuscular mycorrhizae (AM) fungi (Figure 1.10) and their host plants, such as fabaceae, maize, and tomatoes.[24,52] In this symbiotic relationship, hyphal branching is considered to be the key process for establishing the plant-fungi interaction. After extensive observations, it was ascertained that branching activities will only proceed after germinations and hyphal growth which strongly suggested that SLs are the molecules regulating the symbiotic process.[56]

Figure 1.10: Arbuscular mycorrhizae (AM) in the root of *Macrotyloma uniflorum.* (Image credit Rajarshi Rit University of Burdwan)

SLs also play a fundamental role in nutrient transport between the host plant and fungi. Recent investigations show that phosphate deficient plants will generate more SLs to stimulate the branching of AM and cause them to transfer more phosphates to the host.[57] Moreover, SLs are key signalling molecules in both plant-recognizing fungi and in the opposite direction. Acting as promoting molecules, the existence of SLs increases of intracellular calcium and lipochitoolisaccharides (LCOs) concentrations and both of these two species are certified as signals on the recognition of fungi by host plants.[58]

SLs are a privileged family of small molecules that play key biological roles within plants, between plants, and between plants and fungi. Plants are the source of all known strigolactones, and intense research has been conducted to uncover the biological mechanisms by which such a variety of structures are generated.

1.4 Biosynthesis of Strigolactones

1.4.1 Biosynthesis of CL & CLA: Key Precursors in SLs Biosynthesis

The earliest research into the biosynthesis of strigolactones was reported in 2005. Bouwmeester and co-workers hypothesised a possible strigolactone biosynthesis via a carotenoid pathway, in accordance with previous results of carotenoid analysis by using fluoridone, naproxen, tungstate, and ABA treatments.[59] Shortly afterwards, two enzymes from the carotenoid cleavage dioxygenase (CCD) family,[60,61] CCD7 and CCD8, were shown to be critical components of the strigolactone biosynthetic pathway.[28,62] The CYP711As enzyme from the cytochrome P450 family was also implicated in strigolactone biosynthesis.[63] The biosynthetic machinery that produces CL (**24**) and CLA (**27**) is encoded by DWARF 27 (D27), which controls and expresses a carotenoid isomerase and two CCDs (CCD7 and CCD8) which are encoded by MORE AXILLARY GROWTH genes (MAX), RAMOUSUS genes (RSM), DWARF genes (D), or DECREASED APICAL DOMINANCE genes (DAD) in different plant species displayed in Scheme 1.1.[64]

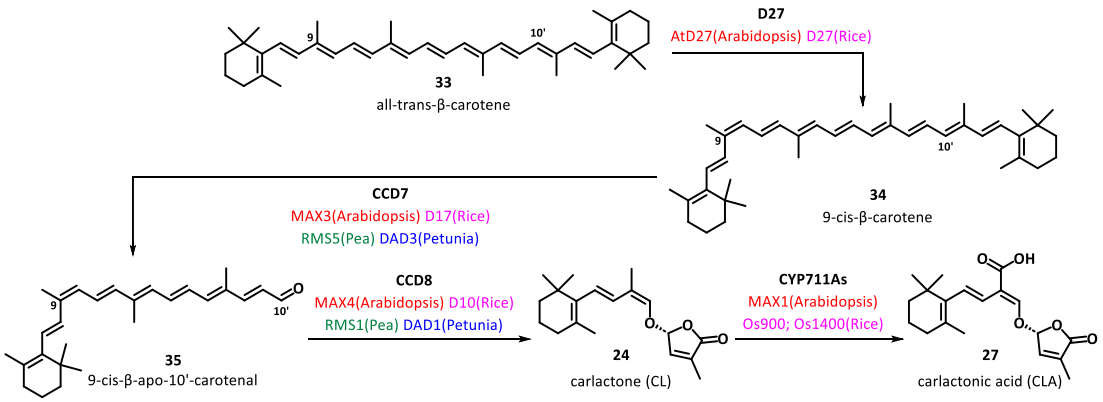

Scheme 1.1: Biosynthesis of CL (**24**) and CLA (**27**).

The first step in the pathway is the isomerization of the double bond between carbon-9 and 10 of all-*trans*-β-carotene (**33**), catalysed by an isomerase This isomerase can also act on other carotenes such as zeaxanthin. CCD7 then cleaves the 9-*cis*-β-carotene (**34**) chain at the double bond between carbon-9' and 10' producing 9-*cis*-β-*apo*-10'-

carotenal (**35**) which installs and locks the *Z*-configuration of the double bond in subsequent biosynthetic pathways. Then, a CCD8-mediated oxidative rearrangement converts compound **35** into CL (**24**). Finally CL (**24**) can be oxidized by CYP711A to give CLA (**27**).[65,66]

A plausible mechanism for the CCD8-mediated oxidative rearrangement has been suggested by Al-Babili and Bouwmeester shown in Scheme 1.2.[49]

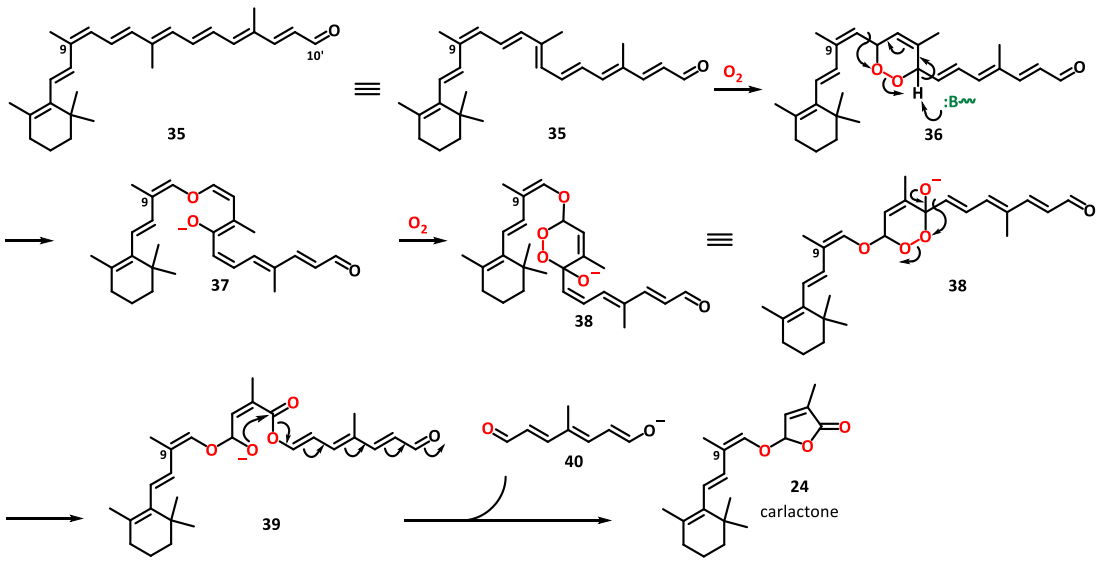

Scheme 1.2: Mechanism of CCD8-mediated oxidative rearrangement.

Firstly, 9-*cis*-β-*apo*-10'-carotenal (**35**) is oxidized by molecular oxygen via [4+2] cycloaddition to generate the oxygenated carotenal **36,** which is deprotonated immediately by bases in plant systems to afford enolate **37**. Another oxygenation follows, giving twice-oxygenated carotenal **38** and ring opened product **39**. Carlactone (**24**) is finally produced by the intramolecular lactonization that releases a symmetric and conjugated enolate anion **40**.

1.4.2 Biosynthesis of Individual SL Molecules from CLA

CLA (**27**) contains the 19-carbon framework that appears in both strigol-like and orobanchol-like canonical strigolactones. It is tempting to speculate that CLA (**27**) could be preferentially cyclized to give deoxy-strigol or deoxy-orobanchol respectively,

and subsequent oxidations produce all of the canonical strigolactones. But the true picture is much more complex and species specific.[64]

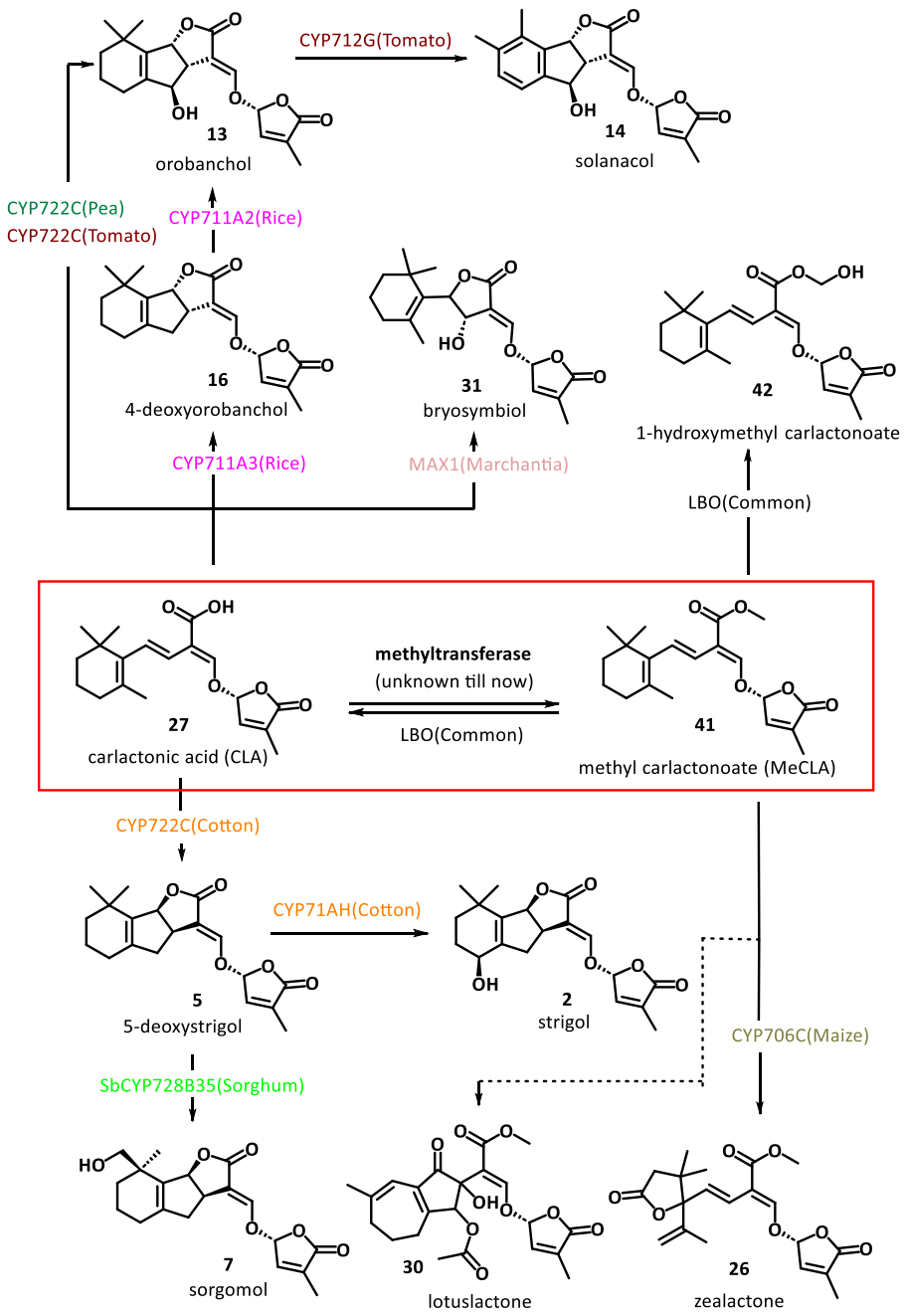

Scheme 1.3: Biosynthesis of specific SLs.

A pertinent example could be found in the biosynthesis of orobanchol. In rice-related species researchers have ascertained that CLA (**27**) is indeed cyclized by CPY711A2 to give deoxy-orobanchol, which is oxidized by CPY711A3 to give orobanchol. However, enzymes in cotton do not convert CLA (**27**) into deoxy-orobanchol. Furthermore, when

deoxy-orobanchol was administered to some other plants, it was discovered that they lacked the ability to convert deoxy-orobanchol into orobanchol. Instead, in cowpeas and tomatoes, the CLA (**27**) was converted directly into orobanchol by the action of CPY722C.[67] But the story becomes more convoluted by the fact that the orobanchol producing enzyme CPY722C was separately isolated from a different species in which it not only cyclizes CLA (**27**) into deoxy- structure, but it does so with the opposite (strigol-like) stereochemistry![68]

Clearly, the biosynthetic picture outlined in Scheme 1.3 is an over-simplification that is lacking some critical (probably oxidation) steps on the path from CL (**24**) or CLA (**27**) to any given canonical strigolactone. In order to cast light on the species-specific biosynthesis of canonical strigolactones, a ready source of radio-labelled and selectively oxygenated CL (**24**) and CLA (**27**) molecules is required.[69,70]

Both CL (**24**) and CLA (**27**) contain the required number of carbons for production of the canonical strigolactones, but the non-canonical strigolactones possess a 20-carbon skeleton. Methyl carlactonate (MeCLA, **41**) was identified in planta in 2014.[36,69] Recently, the methyl transferase necessary to convert CLA (**27**) into MeCLA (**41**) was characterized by Yoneyama and co-workers.[35] Bouwmeester and co-workers have hypothesized that all non-canonical strigolactones are derived from MeCLA with the involvement of lateral branching oxidoreductase (LBO) enzymes,[39,41,42] but the evidence for this is currently lacking. It is known that in maize, CYP706C converts a non-natural isomer of heliolactone (a strigolactone isolated from sunflower species) into zealactone. The parent heliolactone stereoisomer has not been detected in any plant species to date, so the biosynthetic relevance of this transformation remains uncertain. In order to cast light on the species-specific biosynthesis of non-canonical strigolactones, a ready source of radio-labelled and selectively oxygenated MeCLA (**41**) is required.

As depicted in Figure 1.7, there is one recently identified strigolactone that defies categorization as either canonical or non-canonical. In 2022, bryosymbiol (BSB, **31**)

was isolated from the bryophyte *Marchantia paleacea*, which is a (lower order) non-vascular plant.[43]

Bryophytes and vascular plants diverged over 400 million years ago. Bryosymbiol (**31**) was subsequently detected in several vascular plants. The presence of this strigolactone in such an evolutionarily separated genera strongly suggests that their common ancestor produced strigolactones. Amazingly, lower plants lack strigolactone receptors, which suggests that the biological function of the strigolactones in ancestorial plants was not as a phytohormone, but as an inter-plant or inter-kingdom signalling agent. BSB (**31**) contains a 19-carbon skeleton, but it lacks the tricyclic core common to the canonical strigolactones. Nomura and co-workers hypothesize that in bryophytes the same enzyme responsible for conversion of CL (**24**) into CLA (**27**), MpaMAX1, is also capable of epoxidizing the C7–C8 alkene. Subsequent nucleophilic ring opening by the pendant acid would give BSB (**31**).[64] By invoking this unknown epoxidation function of enzyme MpaMAX1, they suggested a possible mechanism for the biosynthesis of BSB (**31**), which is illustrated in Scheme 1.4.

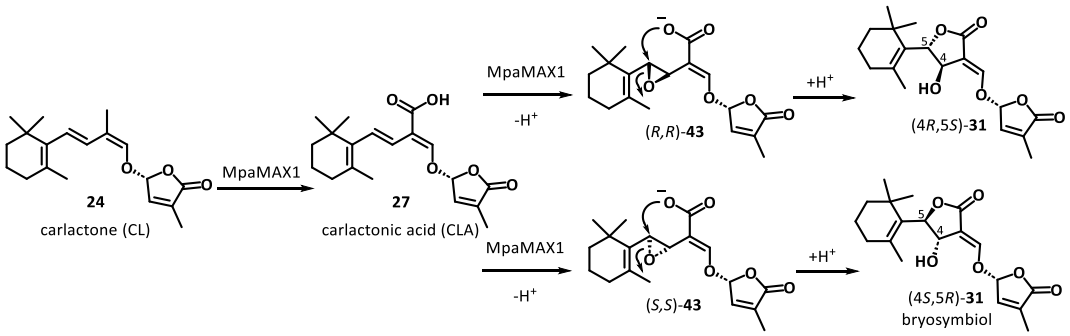

Scheme 1.4: Proposed mechanism of the BSB (**31**) biosynthesis.[64]

However, it cannot yet be determined which step (oxidation to generate the carboxylic acid or epoxidation of the alkene) occurs first yet. Aiming to cast light on the genera- and species-specific biosynthesis of BSB (**31**), a ready source of radio-labelled and selectively epoxidized CL (**24**) and CLA (**27**) molecules is required.

1.4.3 Determination of the absolute stereochemistry of Endogenous CL

Given the previously discussed discussion on the relative stereochemistry of the orobanchol- and strigol-like strigolactones, ascertaining the absolute stereochemistry of the strigolactones was an important goal.

It should be noted that the first stereochemistry inducing step on the pathway to strigolactones is the creation of the stereocentre on the butenolide ring (Scheme 1.2). This absolute stereochemistry is retained in all strigolactones, and as such, the absolute stereochemistry of carlactone sets the relative stereochemistry for the daughter molecules. To determine the absolute structure of CL (**24**), Seto and Yamaguchi first synthesized isotopically labelled, racemic CL (**24**) using 2,6-dimethyl cyclohexanone (**44**) as starting material.[33] The isotopic label was installed by alkylation with methyl iodide containing carbon-13 to generate the trimethyl cyclohexanone (**45**) (Scheme 1.5).

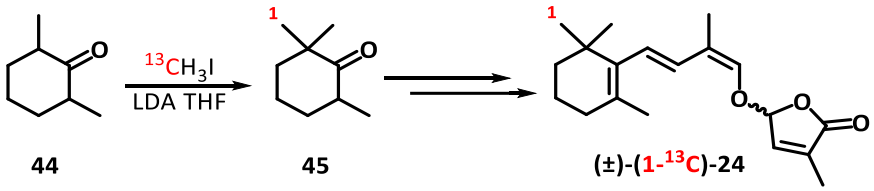

Scheme 1.5: Synthesis of isotope labelled racemic CL (**24**).

Through a lengthy, and very low yielding synthetic sequence, Seto and co-workers successfully produced radio-labelled racemic CL. The individual isomers were carefully separated by semipreparative chiral HPLC to obtain a pair of enantiomers which were used in the feeding experiments of d10-1 mutant rice plants (Scheme 1.6). These experiments unambiguously demonstrated that a single enantiomer of CL (**24**) was transformed into both the orobanchol and strigol-type strigolactones. Furthermore, Seto and co-workers were also able to analyze endogenous CL (**24**) from the root exudates of rice by using LC-MS, and confirmed that naturally occurring CL (**24**) corresponded to a single entiomer.[33,71] But at this stage, they still could not certify the absolute stereochemistry of CL (**24**).

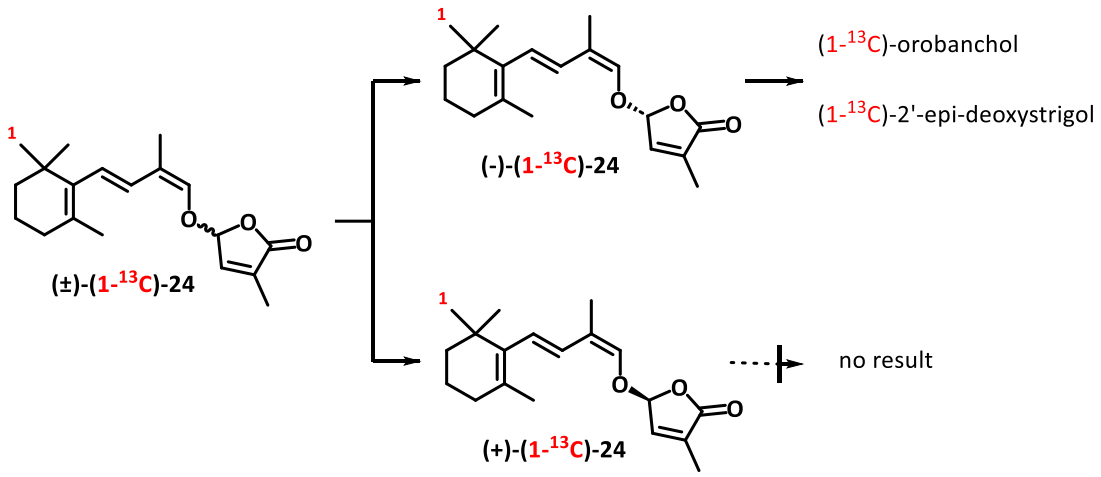

Scheme 1.6: Result of ^{13}C-CL feeding experiments.

The milestone of assigning the absolute stereochemistry of CL (**24**) had to wait until Zwanenburg and co-workers constructed the stereocontrolled D-ring structure by utilizing the homochiral molecule (**49**). As shown in Scheme 1.7, the Diels-Alder adduct of citraconic anhydride (**46**) and cyclopentadiene (**47**), was reduced by kinetic enzymatic resolution with Lipase PS and vinyl acetate, The racemic compound **49** could be selectively converted into butenolide contained compounds (-)-**49** and (+)-**50** with known absolute stereochemistry.[72]

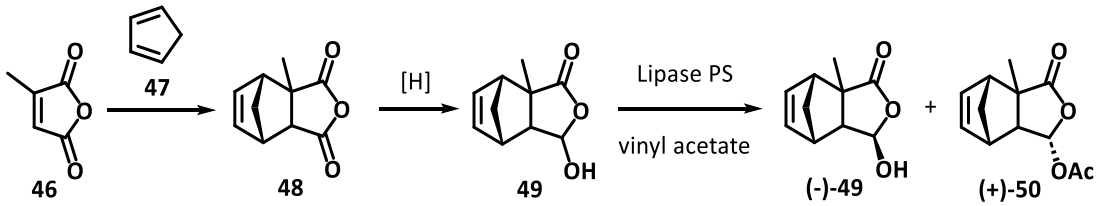

Scheme 1.7: Synthesis of stereo specified compound (-)-**49** and (+)-**50** from synthon **48**.

In this case, the chlorinated molecules (+)-**51** and (-)-**51**, which are produced from compounds (-)-**49** and (+)-**50**, were utilized in the stereoselective synthesis of both enantiomeric CL adducts (+)-**52** and (-)-**52** (Scheme 1.8). Separately, naturally occurring CL was subjected to Diels-Alder reaction with cyclopentadiene (**47**). By comparing the order of elution of the stereochemically defined molecules (+)-**52** and (-)-**52** with the Diels-Alder adducts of naturally occurring CL, Zwanenburg and co-workers were able determine that the absolute stereochemistry of endogenous CL (**24**).

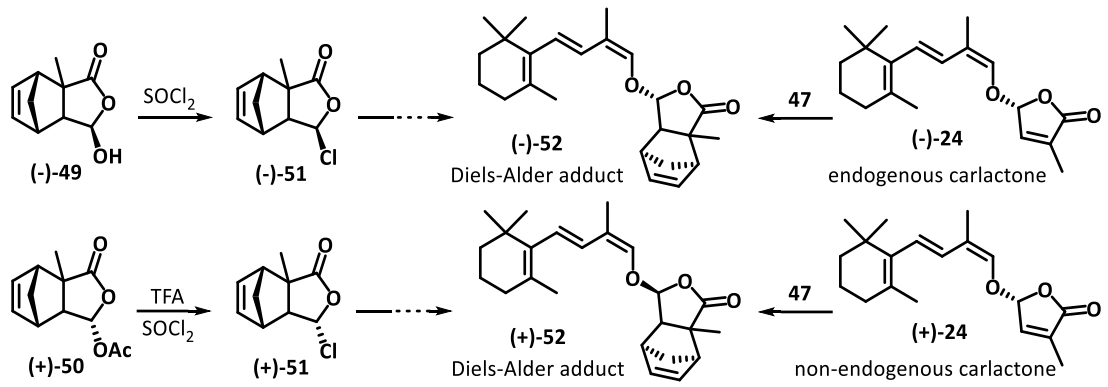

Scheme 1.8: Determination of CL's absolute stereochemistry.

1.4.4 Regulations of SL Biosynthesis

As outlined in the previous sections, the biosyntheses of SLs are elaborate and complex processes that occur in a species-specific manner. It has been observed that strigolactone production is regulated by various endogenous and exogenous factors. This section will discuss several regulation factors that are regarded as having large effects on strigolactone biosyntheses.

Early studies indicated that a deficiency of phosphorus and nitrogen are key regulators of SL biosynthesis. Some plants lacking sufficient phosphorus nutrients were observed to secrete strigolactones in root exudates to promote fungal hyphal elongation and AM's branching. This enhanced the symbiotic relationship by which inorganic phosphorus nutrients could be absorbed by their host plants.[73,74] Similarly, in order to deal with harsh environmental conditions, nitrogen deficiency has also been observed to initiate a strigolactone-regulated system in some other plants.[75] So strigolactone synthesis is regulated by external stimuli. More recently, molecular and gene-level research has provided a beautiful explanation of the nutritional regulation of SL biosynthesis. Nearly all the genes involved in the pathway are expressed under the control and regulation of phosphorus availability and also correlated with some key molecules in host plant roots.[76]

In general, to reach homeostasis of an endogenous level, all phytohormones rely on feedforward regulation and feedback regulation. For the specific case of SLs, biosynthesis pathways are strongly regulated by feedback regulation. Feedback regulation research focuses on CCD7 and CCD8 for their special status in the SL biosynthetic pathway. The two dioxygenases are commonly regarded as targets of feedback regulation.

According to the results of gene expression analysis by several groups, the transcript levels of these two enzymes were obviously increased in the SL-insensitive and SL-deficient mutants of Arabidopsis, cowpea, and rice.[77–79] LC-MS/MS analysis from Seto and Yamaguchi showed that the levels of CL (**24**) and CLA (**27**) sharply increased in those mutants of Arabidopsis and rice, which confirmed the existence of negative feedback regulation in SL biosynthesis pathways.[33,66,71] That is, when SL levels drop, the transcription of CCD7 and CCD8 is increased. So strigolactone biosynthesis is self-regulated by the endogenous level of available strigolactones.

However, the phytohormones profile of plants contain many molecules that are not from the same class, so some influence on each other is expected. Different classes of hormones with different concentration levels promote a variety of biological effects for an individual plant. Aside from SLs, auxins (Figure 1.11) are another kind of important molecule that induce the expressions of CCD7 and CCD8. These interplay of SLs and auxins exerts a delicate balance on transcription regulation.[80]

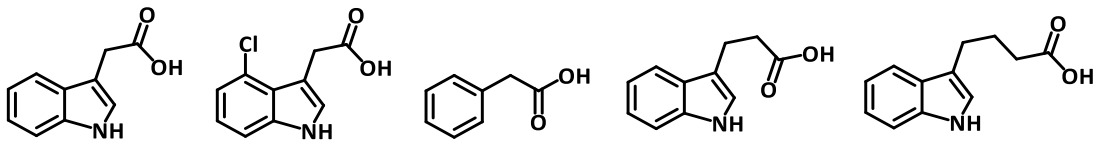

Figure 1.11: Structures of naturally occurring auxins.

In contrast, CK (**58** Figure 1.12) was found to be an antagonist of SL biosynthesis, which inhibited the gene expressions of MAX4 in Arabidopsis thereby impeding the production of SLs.[81]

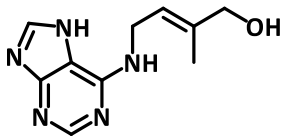

58

Figure 1.12: Structure of cytokinins (CK).

Auxins (**53** to **57**) and CK (**58**) are not the only molecules that can promote or inhibit SL biosynthesis. Besides the three regulations mentioned above, there are still many different kinds of internal and external environmental stimuli that affect the SL biosynthesis regulation.[82,83]

1.5 Signalling and Transport of Strigolactones

1.5.1 DWARF14 (D14)

Since the discoveries of SLs, the debate on possible signalling and perception mechanisms in plants has become a hot topic.[28,84] Aiming at identifying the SLs signalling genes in plants, Arite and co-workers reported a SL-insensitive mutant, d14, from rice whose phenotype showed an accelerated outgrowth on its tillers.

In this mutant, researchers eventually ascertained that the pathogenic genes encoded an α/β-fold hydrolase superfamily protein, DWARF14 (D14).[85] This report overturned many reasonable hypotheses about strigolactone receptors and enabled the identification of D14 as the functional receptor for SL signalling and perception mechanisms.[86,87]

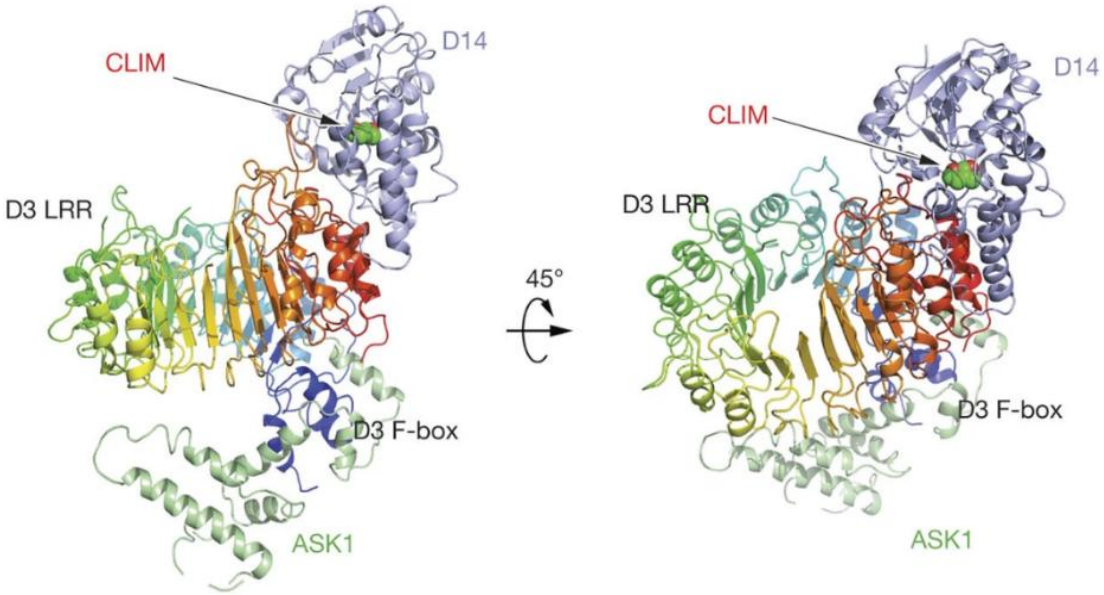

Figure 1.13: 3D structures of the SL-induced complex. (Reported by Rao and Xie[88])

In 2016, Rao and Xie group reported a protein from this superfamily: *Arabidopsis thaliana* D14 (AtD14) which participated in forming a SL-induced complex (Figure 1.13). They firstly reported the 3D x-ray crystallographic structure that showed an open-

to-closed state transition on SL signalling, and demonstrated the hydrolysis of SLs into a covalently linked intermediate molecule (CLIM).[88] At the middle of the CLIM was a cavity that provided enough space and appropriate initiating sites for an enzyme-catalysed reaction (namely, hydrolysis of SLs) by the protein switching between closed and open states.

1.5.2 The Ser-His-Asp Catalytic Triad

The discoveries on D14 gave an explanation of the mechanism of SLs signalling and perception for the first time, and defined the D14 series as non-canonical receptors for SL sensing and signal initiation. This section will introduce a proposed mechanism on the hydrolysis of SLs via the Ser-His-Asp catalytic triad (**62**).

Located in the active site of the protein, a catalytic triad **62** is known as a set of three coordinated amino acids.[89] The Ser-His-Asp catalytic triad combination forms hydrogen bonds among serine (**59**), histidine (**60**) and aspartate (**61**) and plays an extremely important role in SLs hydrolysis (Scheme 1.9).[90]

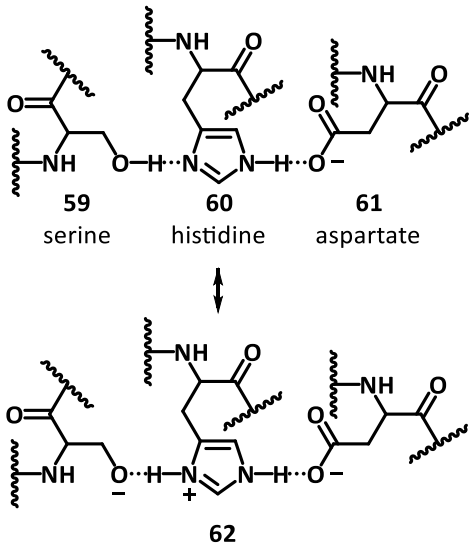

Scheme 1.9: Charge transfer of Ser-His-Asp catalytic triad.

In order to stabilize the negatively charged nucleophilic oxygen on serine (**59**) and maximize its nucleophilicity, the imidazole ring on histidine (**60**) functions as a base to

abstract a proton from serine (**59**). The aspartate (**61**) also stabilizes the positive charge from the other side of histidine (**60**) to aid the charge transfer (Scheme 1.9).[91]

Subsequent to the discovery of SL-induced complex, Zwanenburg and coworkers hypothesized a convincing and logical mechanism of action, using the Ser-His-Asp catalytic triad (**62**) to explain the interactions between SLs and their protein receptors.[92,93] At the same time, they pointed out the short-comings of some less reasonable hypotheses.[94]

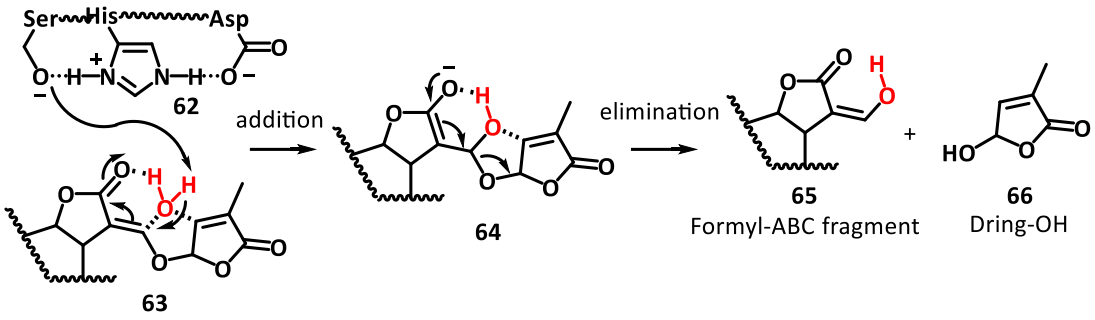

Scheme 1.10: Ser-His-Asp catalytic triad (**62**) inducing SL hydrolysis mechanisms.

The Zwanenburg mechanism in Scheme 1.10 involved a serine-catalyzed addition of a water molecule to the reactive enol ether of the SL molecule, which was hydrogen bonded to the SL substrate. Elimination of the D-ring would result in formal hydrolysis, generating one molecule of formyl-ABC ring fragment (**65**) and one molecule of Dring-OH (**66**), which were known products of SL hydrolysis.

1.5.3 Transport of SLs

To adapt to the environment and promote self-growth, plants have internal transport systems for hormones.[95] Plants have evolved various transport methods for SLs, which play a decisive role in symbiotic perception between host plants and AM fungi as mentioned in regulation section.[73,74] Xie and coworkers discovered SL-related molecules moving via xylem from the root area to the shoots of a growing plant using LC-MS/MS analyses. They ascertained that the intermediates in the SL biosynthetic pathway were mobile signals.[96]

A breakthrough discovery reported by Borghi group upended the assumption SLs were transported by ATP-binding cassette transporters (ABC transporters), which until then were shown to be the major route of phytohormone transport both *in planta* and to external environments. Specifically, Borghi and co-workers found that pleiotropic drug resistance 1 (PDR1) from *Petunia hybrida* transported SLs from the roots to the shoots and also into the rhizosphere.[97] Mashiguchi, Seto and Yamaguchi's review made a comparison among plants (Arabidopsis, rice and *Petunia hybrida*) that highlighted the transport systems in different plants (Figure 1.14).[66] It was ascertained that most of SL biosynthetic intermediates appearing after MAX4/CCD8 step might be mobile signals from the roots to the shoots mutants of Arabidopsis.[98] As for rice, Xie and coworkers confirmed the transport by using stable isotope-labelled orobanchol (**13**) and 4-deoxyorobanchol (**16**).[96]

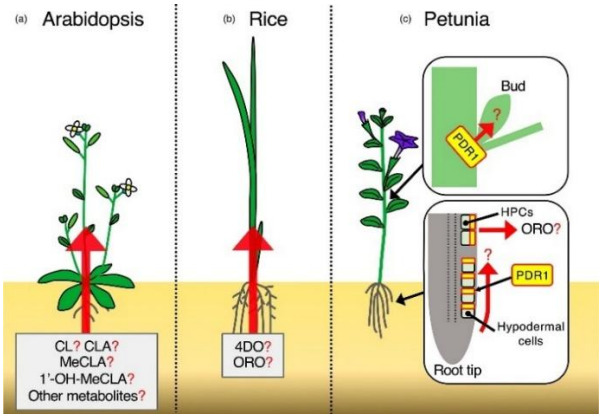

Figure 1.14: Comparison of SLs transport among Arabidopsis, rice and *Petunia hydrida*. (Reported by Mashiguchi, Seto and Yamaguchi).[66]

Given the different mechanisms of strigolactone biosynthesis in different plant species, unravelling this complex system of biosynthetic intermediate transport necessitates a ready supply of radio-labelled and selectively oxygenated CL (**24**) and CLA (**27**) analogues.

1.6 Total Syntheses of Naturally Occurring Canonical Strigolactones

1.6.1 Total Synthesis of Strigols

Strigolactones are produced in minute amounts *in planta* and isolation has proved to be a very challenging task. This lack of material supply provided the impetus for synthetic efforts to produce targeted strigolactones. The first total synthesis route to a SL was published by Sih group in 1974 (Scheme 1.11).[99] They synthesized a pair of strigol **2** racemates with an undefined chiral centre on the butenolide ring (D ring).

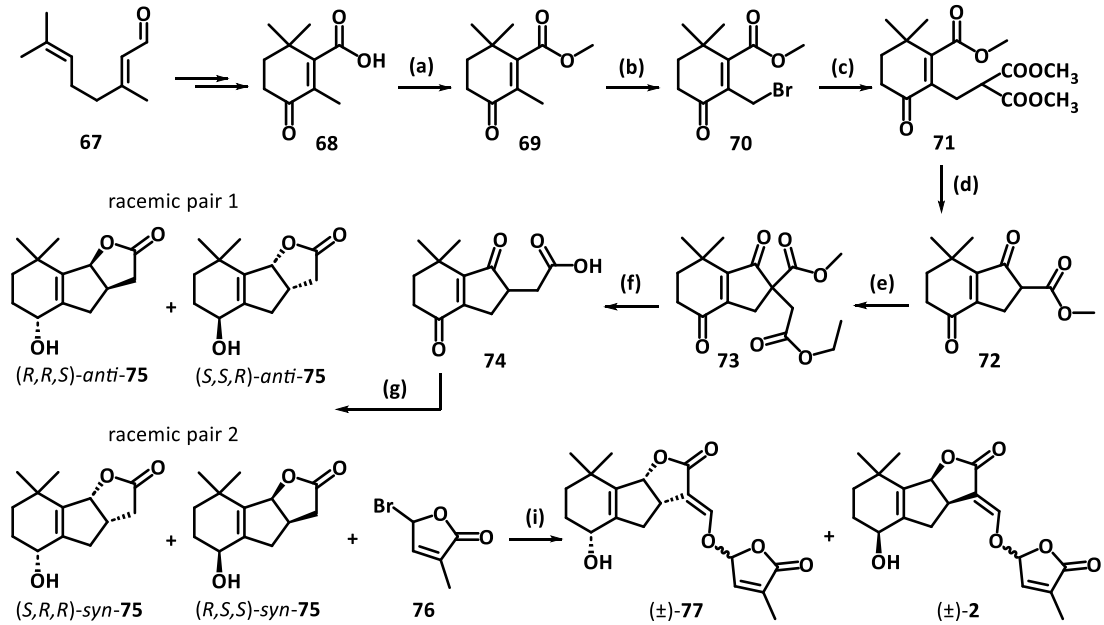

Scheme 1.11: Total Synthesis of strigol racemates by Sih group. Reagent and conditions: (a) MeI, K_2CO_3, acetone, 24h; (b) N-bromosuccinimide, CCl_4, reflux, hν, 1h; (c) $NaCH(COOMe)_2$, MeOH, RT, 24h; (d) reflux, 6h; (e) K_2CO_3, THF, methyl bromoacetate, 72h; (f) AcOH/HCl, reflux, 3h; (g) DIBAL, CH_2Cl_2, -78°C, 2h then H_2SO_4/H_2O; (h) MeOCHO, NaH, Et_2O, 32h then HCl; (i) 60, K_2CO_3, HMPA, 20h.

Sih and coworkers chose citral (**67**) as the starting material and generated carboxylic acid compound **68** as the overall precursor. Then followed esterification to methyl ester **69**, bromination on methyl group to give compound **70**. Alkylation with sodium dimethyl malonate generated the trimethyl ester **71** as the substrate for Dieckman

cyclisation, which built the AB-ring of strigol and generated the β-ketone ester **72**. Another alkylation with methyl bromoacetate followed by decarboxylation via compound **73**, gave the homologate carboxylic acid **74**. DIBAL reduction of compound **74** achieved the construction of C-ring to give a pair of separable diastereomers, *anti*-configured compounds *anti*-**75** and the *syn*-configured compounds *syn*-**75**. The last two steps of the total synthesis were formylation of compounds *syn*-**75** with methyl formate and attachment of the D-ring using bromobutenolide **76**. This two-step sequence gave the final product as a racemic mixture of strigol diastereomers (±)-**2** and (±)-**77**, and has been regarded as the 'standard' endgame for most subsequent SL total syntheses.

In later efforts, access to stereochemically defined ABC-ring system **75** has been regarded as the key synthetic challenge. Raphael,[100] Brooks[101] and Dailey[102] separately reported their own synthetic routes to strigols from various starting materials *via* compounds **75**. And it's obviously that the synthesis of strigyl acetate from strigol was be easily achieved by simple esterification.

However, at this early stage it proved extremely challenging to separate the naturally occurring stereoisomer of strigol from the racemic mixture. After their reported racemic total synthesis, the Sih group made continuous efforts to this end. Their second report on synthesis of strigol brought a chiral auxiliary into their synthetic method. They chose the previously produced lactone isomers *syn*-**75** as the reagent which reacted with (+)-3β-acetoxyandrost-5-ene-17β-carboxylic acid chloride (**78**) to generate isomers of substituted lactones (*S,R,R*)-**79** and (*R,S,S*)-**79** (Scheme 1.12).[99,103] These isomers could be separated by exhaustive chromatography, and diastereomer **62** was carried through to give (+)-strigol. This work realized the first total synthesis of a single isomer strigol.

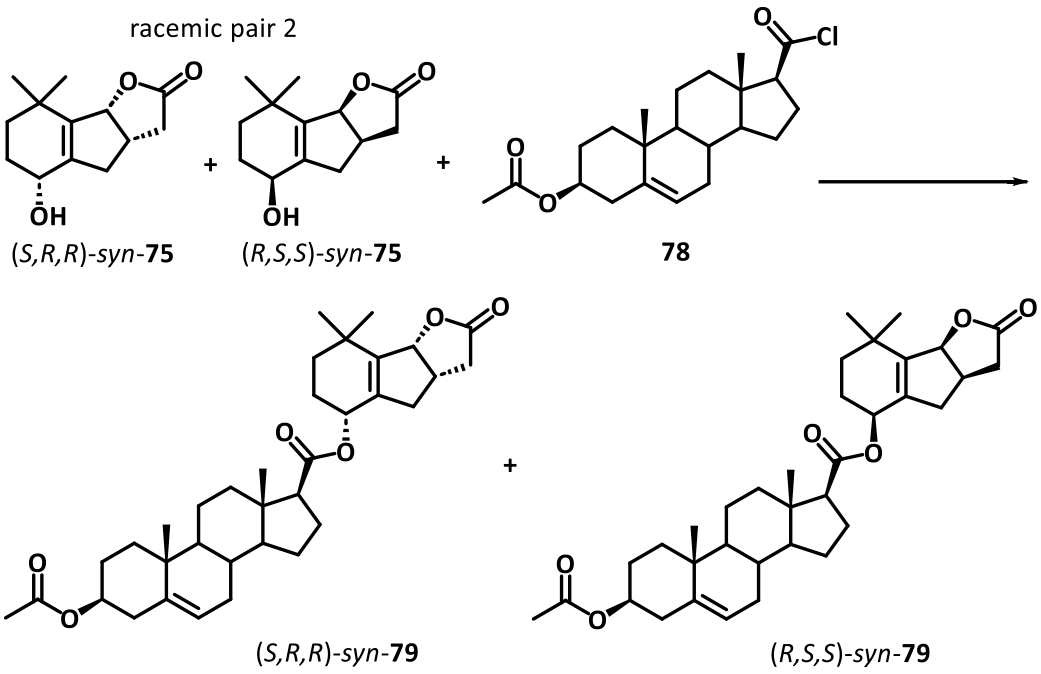

Scheme 1.12: Sih's approach with chiral auxiliary.

Brooks and coworkers made key progress in this area after evaluating several different chiral resolving agents, finding (*R*)-(-)-l-(1-naphthyl)ethyl isocyanate (**80**) as the reagent that reacted with strigols to give easily separable diastereomers **81** and **82**. The use of an auxiliary with known absolute stereochemistry enabled the relative structure of (+)-strigol to be secured by single crystal x-ray diffraction of intermediate **81**.[13]

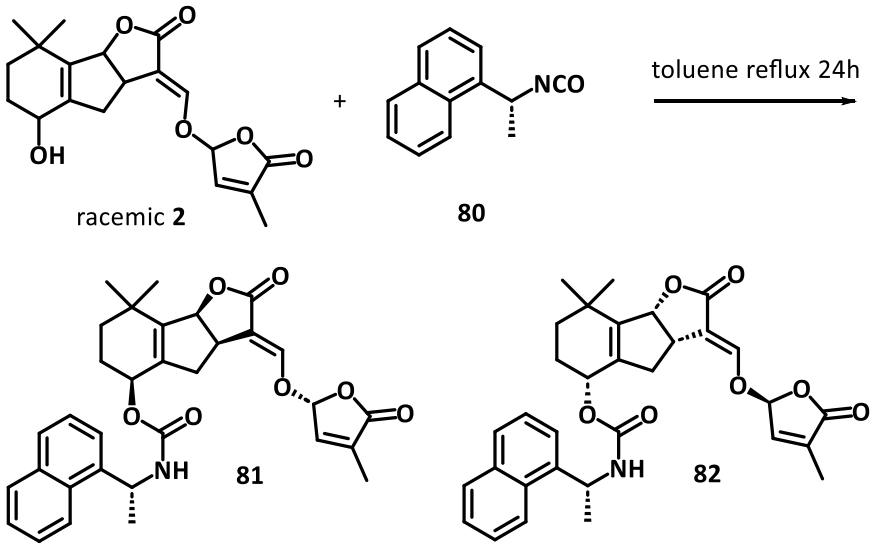

Scheme 1.13: Brooks's synthesis route to absolute strigol.

Since the discovery of lipase AK,[104] researchers have improved several synthetic routes by using this resolving enzyme. Mori and coworkers from Utsunomiya University in Japan, utilized this lipase in their chemoenzymatic approach to strigol (**2**) displayed in Scheme 1.14.[105]

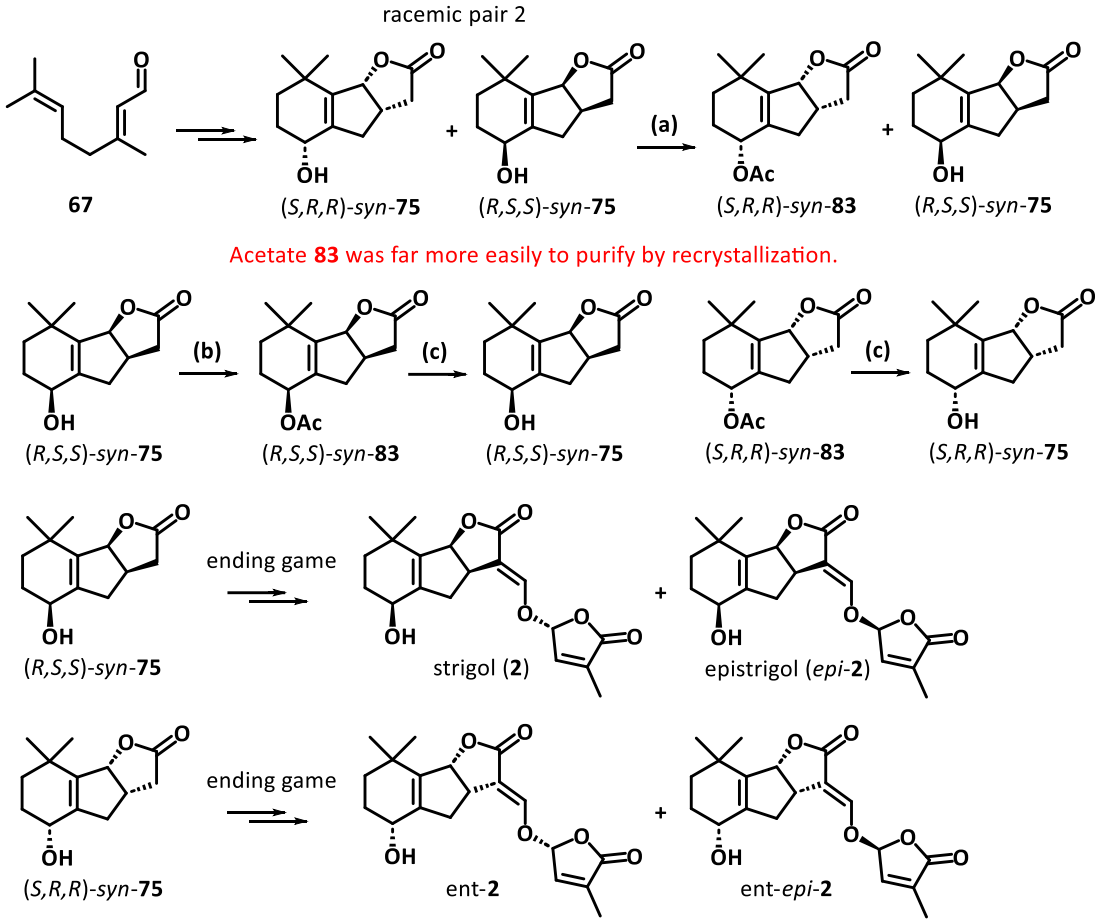

Scheme 1.14: Mori's chemoenzymatic approach with lipase AK. Reagent and conditions: (a) vinyl acetate, lipase AK, THF, RT, 24h; (b) Ac_2O, pyridine; (c)K_2CO_3, methanol (99%).

Finally, the four different isomers of strigol were easy to obtain by employing Sih's 'standard' end game.

1.6.2 Total Synthesis of 5-Deoxystrigol

The traditional racemic tricyclic precursor **84** of 5-deoxystrigol (**5**) had already been synthesized as an intermediate in early total syntheses of strigol (**2**) and orobanchol (**13**).[105,106] It is an obvious synthetic strategy to employ the 'standard' end game to

convert the compound into 5-deoxystrigol (**5**) (Scheme 1.15), but that particular sequence was not reported.[107]

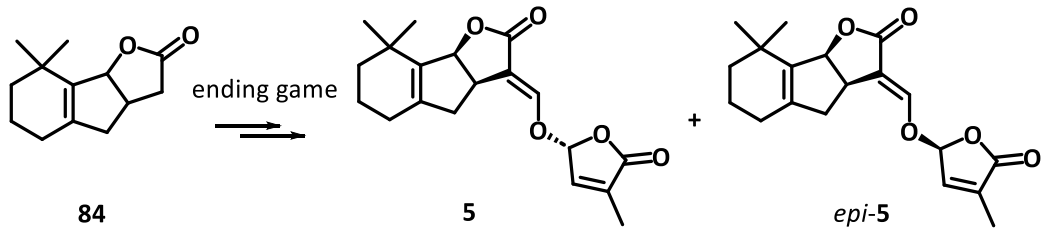

Scheme 1.15: 'Standard' ending steps in synthesizing 5-deoxystrigol (**5**) and isomer *epi*-**5**.

Instead, De Mesmaeker and co-workers at Syngenta Crop Protection, reported the stereoselective total synthesis of 5-deoxystrigol (**5**) in 2014. Up until that work, chiral auxiliaries were employed in strigolactone chemistry as resolving agents. De Mesmaeker's group employed a chiral auxiliary, 2,5-bis(methoxymethyl)-pyrrolidine, as a stereo-controlling unit, which became the highlight of their 5-deoxystrigol (**5**) total synthesis (shown in Scheme 1.16 in different colours). [108]

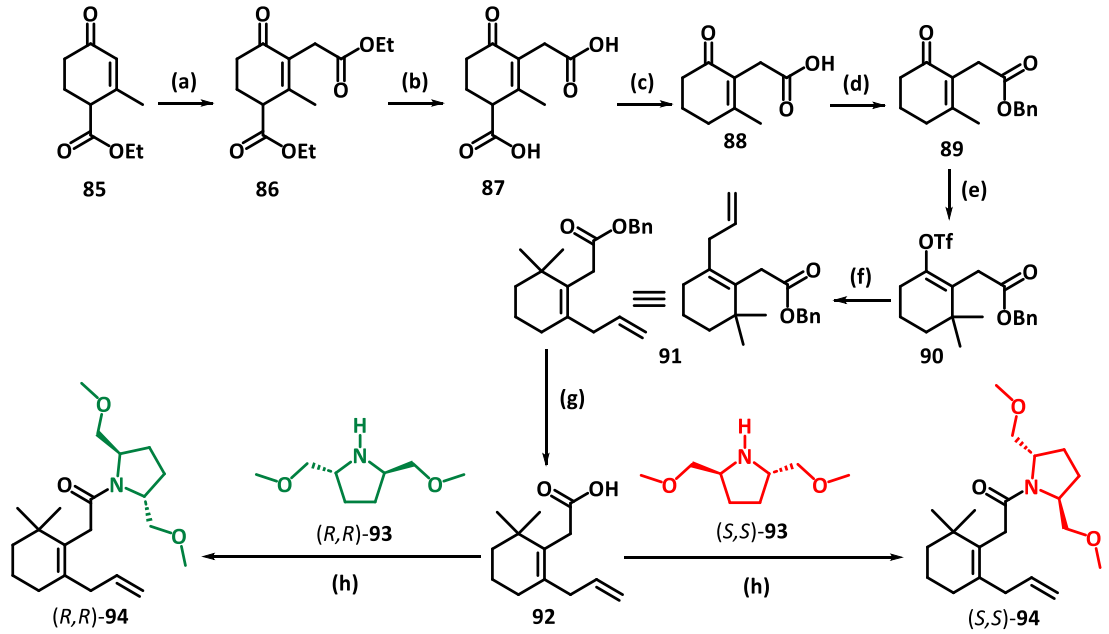

Scheme 1.16: Total synthesis of 5-deoxystrigol isomers Part 1. Reagent and conditions: (a) NaOH, EtOH then $BrCH_2COOEt$; (b) NaOH, $EtOH/H_2O$, then HCl; (c) toluene/DMF, reflux; (d) Cs_2CO_3, BnBr, DMF RT; (e) i: MeLi, CuI, Et_2O, -20°C to 0°C, 15min; ii: then compound **77**, -20°C, 20min; iii: then N-(5-chloro-2-pyridyl)bis(trifluoromethane-sulfonimide), THF, -20°C to 0°C, 15min; (f) allyltributyl stannane, $Pd(PPh_3)_4$, LiCl, dioxane; (g) NaOH, dioxane/H_2O, reflux; (h) 1-hydroxy-7-azabenzotriazole, Et_3N, CH_2Cl_2, RT.

De Mesmaeker and coworkers chose the six-membered ring **85** as the starting material (Hagmann's ester). After reacting with ethyl bromo acetate, the product diester **86** was quenched with sodium hydroxide and neutralized to obtain dicarboxylic acid **87**, followed by heating to achieve decarboxylation to give the single carboxylic acid **88**. Benzyl bromide (BnBr) was used as an esterifying reagent to form ester **77**.

Lithium dimethylcuprate, generated *in situ* from methyllithium and copper iodide, acted as the soft alkylating reagent on **89**, followed by triflation to produce compound **90**. Stille cross-coupling reaction between allyltributyl stannane and compound **90** gave the allyl substituted ester **91**, which was hydrolysed to generate acid **92**. This acid was transformed into the of enantiomeric chiral amides (*S,S*)-**94** and (*R,R*)-**94** by attachment of the chiral auxiliary.

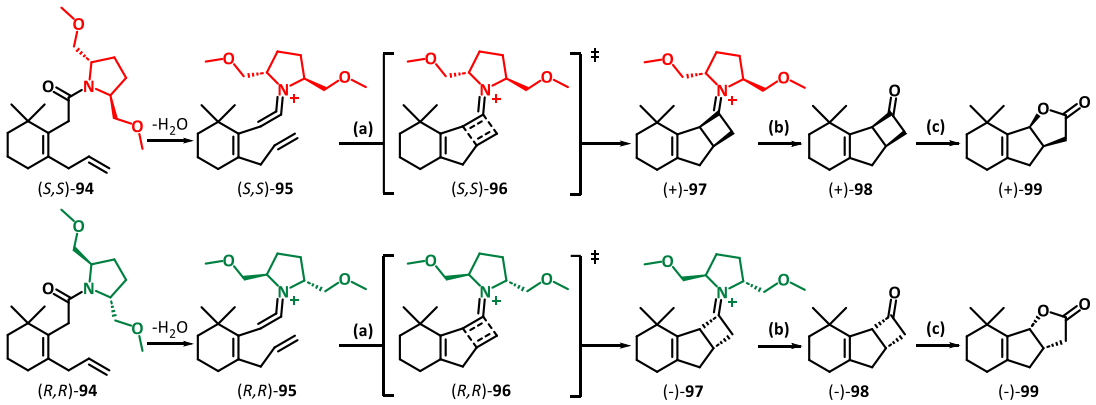

Scheme 1.17: Total synthesis of 5-deoxystrigol isomers Part 2. Reagent and conditions: (a) Tf_2O, 2-fluoropyridine, CH_2Cl_2, RT, 12h; (b) H_2O, CCl_4, reflux; (c) H_2O_2, AcOH, 0°C, 12h.

As depicted in Scheme 1.17, chiral amides (*S,S*)-**94** and (*R,R*)-**94** were individually converted into the corresponding ketene imines, which underwent immediate [2+2] cyclization with the pendent alkenes to produce (after hydrolysis) the highly stereo-enriched cyclobutanones (+)-**98** and (-)-**98**. Bayer-Villager oxidation with hydrogen peroxide in acetic acid, produced precursors (+)-**99** and (-)-**99** respectively**.** Employing the standard end game on (+)-**99** completed their 5-deoxystrigol (**5**) total synthesis.

1.6.3 Total Synthesis of Sorgolactone

Mori and co-workers performed a large amount of work on synthesizing various SLs, including the total synthesis route of sorgolactone.[109] Several steps mentioned above (Scheme 1.11) were utilised during this synthesis, which is shown below in Scheme 1.18.

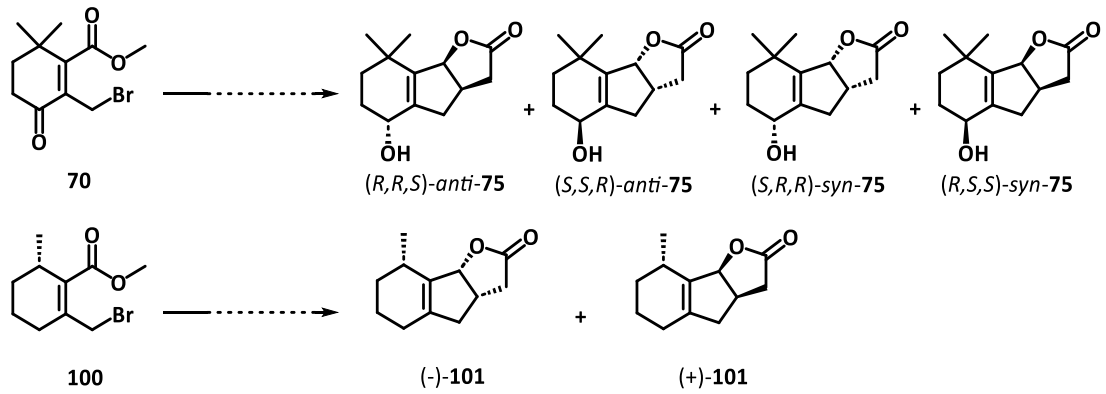

Scheme 1.18: Common steps in Mori's two routes. (Strigol and Sorgolactone)

The synthesis of key intermediate **100** formed the main challenge of Mori's route. In contrast to the strigol synthesis, the stereochemically defined chiral pool material (*S*)-(-)-citronellal **102** was used as the starting material. Making up to eighty percent of the oil from kaffir lime leaves,[110] the (*S*)-(-)-enantiomer of citronellal was easy to purify and greatly simplified the stereochemical challenge associated with the total synthesis of sorgolactone.

The synthesis began with the generation of the methyl ester **103** via oxidation followed by esterification with methyl iodide (Scheme 1.18). Ester **103** was oxidized by mCPBA to form an epoxide **104**, which was cleaved by the action of periodic acid to give aldehyde **105**. After sodium borohydride reduction to give alcohol **106**, the hydroxyl group was substituted by an iodine atom to give compound **107**. Lithium acetylide ethylenediamine complex reacted with **107** to give the terminal alkynyl compound **108** whose α-hydrogen of ester group was substituted by phenylselenyl bromide to afford the α-substituted phenyl selenide **109**. This compound was the precursor material for

formation of the SL A-ring. The cyclization step was initiated by the common radical initiator AIBN and was achieved in the presence of tributyltin hydride. The *in situ* generated secondary radical on the α-carbon of ester cyclized onto the terminal alkyne to afford the cyclohexyl methyl ester **110** after H-atom quenching. Bromination of the double bond by pyridinium tribromide gave compound **111**, which was transformed into the desired intermediate **100** by elimination with sodium hydride (Scheme 1.19). From this point onwards, the synthesis mirrored the previous strigol work using the standard endgame strategy, and provided sorgolactone as a single stereoisomer.

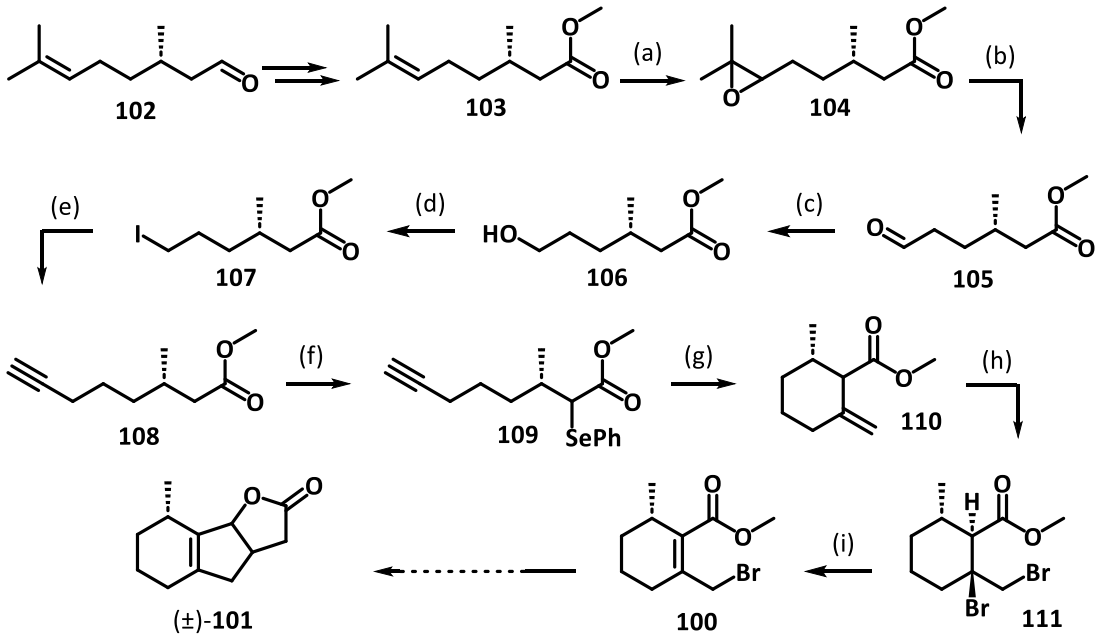

Scheme 1.19: Total synthesis route of sorgolactone. Reagent and conditions: (a) mCPBA, CH_2Cl_2; (b) $HIO_4 \cdot 2H_2O$, THF; (c) $NaBH_4$, methanol; (d) TsCl, pyridine then NaI, acetone; (e) lithium acetylate ethylenediamine; (f) LDA (2 equiv.), THF then phenylselenyl bromide then HCl; (g) $^nBu_3SnH$, AIBN, benzene; (h) pyridinium tribromide, chloroform; (i) NaH, THF.

1.6.4 Total Synthesis of Sorgomol

Takikawa and co-workers reported the first total synthesis of (±)-sorgomol (**7** and *epi*-**7**) in 2011,[111] and subsequently optimized the synthesis. It is that second, optimized route that is discussed here.

Takikawa and co-workers chose the easily accessible compound **112** as the starting material and used a propargylic Grignard reagent to chemoselectively react with the ketone to give alkynyl ether **113** (Scheme 1.20). The three carbon alkyne-containing unit of compound **113** served as a latent α,β-unsaturated ketone, and as the substrate for a Nazarov cyclization. Treatment of compound **113** under acidic reaction conditions effected hydration of the triple bond, hydrolysis of the THP protecting group to get multiple hydroxy-group-containing intermediate **114**, as well as the elimination of primary and tertiary alcohols to give the dienone **115**. Nazarov cyclization of **115** gave the A, B-ring system **116**. After forming B-ring, compound **115** was then alkylated with iodoacetonitrile to give **116**, which was reduced to give lactol **118** (Scheme 1.20). Chemoselective oxidation by silver carbonate on Celite, provided the key precursor **119**. Finally, application of the standard endgame strategy provided sorgomol (**7**).

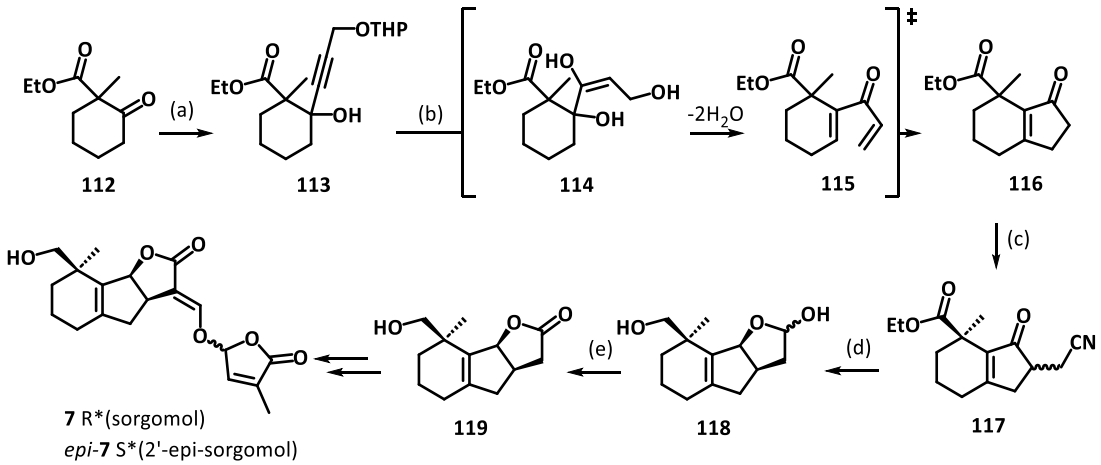

Scheme 1.20: Total synthesis route of sorgomol. Reagent and conditions: (a) Grignard reagent $BrMgCCCH_2OTHP$, THF; (b) H_2SO_4, EtOH; (c) ICH_2CN, LDA, HMPA, THF, -78°C to RT; (d) DIBAL, toluene, -78°C to RT; (e) Ag_2CO_3 on Celite, toluene.

1.6.5 Total Synthesis of Orobanchol

The structure determination of orobanchol was a long story that was finally completed by Sugimoto and co-workers.[25] They synthesized all isomers of orobanchol and used LC-MS/MS, NMR and HPLC comparisons with the plant-derived natural product to determine the exact structure. It transpired that the molecule previously named '*ent*-2'-

epi-orobanchol (**120**) was in fact the correct structure of orobanchol (**13**) (Figure 1.15). This meant that in the years preceding 2011, all synthetic routes towards orobanchol were actually targeting a non-natural isomer.

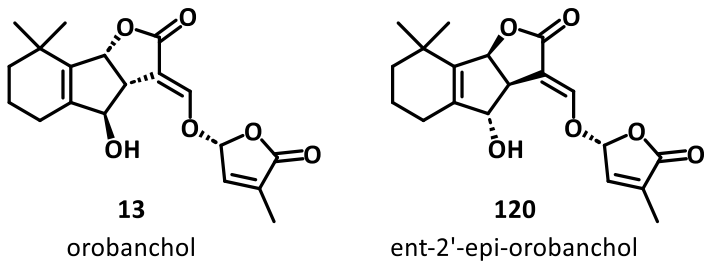

Figure 1.15: Exact structure of orobanchol (**13**) and ent-2'-epi-orobanchol (**120**).

The familiar name of Kenji Mori appears for the third time, because of his research groups efforts on the total synthesis of orobanchol. Mori and coworkers developed and optimized the total synthesis of all isomers of strigol and orobanchol from citral (**67**).[106,107] Their route to orobanchol isomers started from compound (+)-**84**, which was previously reported by Welzel (Scheme 1.21).[112] Compound (+)-**84** was oxidized by chromium trioxide to give a mixture of (+)-**121** and (+)-**122** . After separation and purification, compound (+)-**122** was reduced by sodium borohydride in the presence of cerium chloride to afford two isomers (+)-**123** and (+)-**124**.

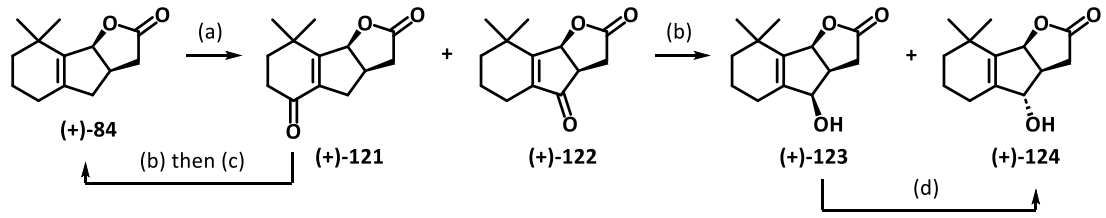

Scheme 1.21: Total synthesis route of key precursors (+)-**123** and (+)-**124**. Reagent and conditions: (a) CrO_3, dimethyl pyrazole, CH_2Cl_2; (b) $NaBH_4$, $CeCl_3 \cdot 7H_2O$, ethanol; (c) PPh_3, CBr_4, dichloromethane then Zn-Cu, THF; (d) EtOOCN=NCOOEt, PPh_3, PhCOOH.

Interestingly, only the anti-configured diastereomer **(+)-124** underwent reaction with ethyl chloroformate and alkylation with the butenolide ring (the standard endgame). Mori and coworkers were able to access the other 'orobanchol' stereoisomers by an

oxidation, reduction sequence. Due to the presence of the highly reactive enol ether appended D-ring, these transformations suffered from low yields.[106,107] Nonetheless, Mori completed the total synthesis of the enantiomer of naturally occurring (-)-orobanchol.

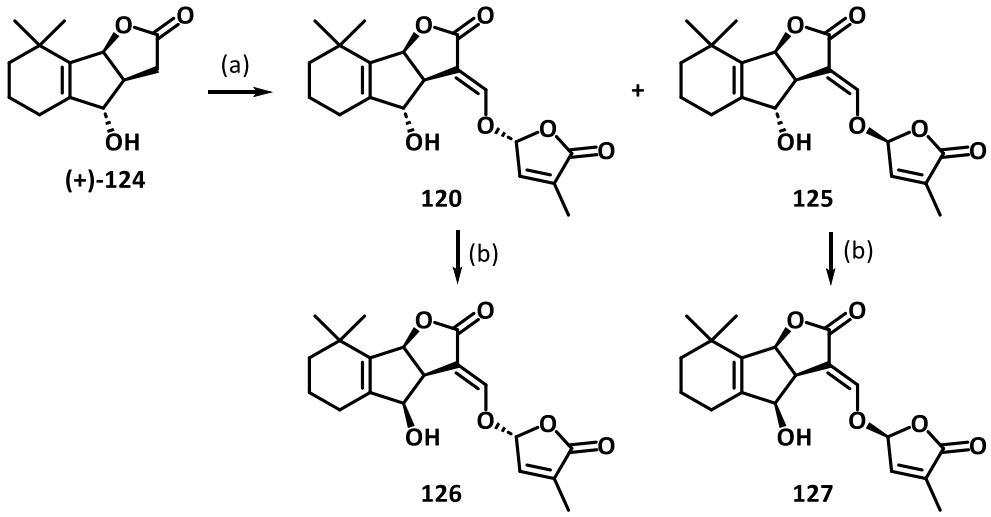

Scheme 1.22: Transformations among isomers. Reagent and conditions: (a) ending steps conditions and reagents; (b) PDC, CH_2Cl_2, RT then $NaBH_4$, $CeCl_3 \cdot 7H_2O$, ethanol.

1.6.6 Total Synthesis of Orobanchyl Acetate (Alectrol)

The exact structure of orobanchyl acetate (alectrol) (**12**) remained a mystery for an extended period after it was isolated. Alectrol (**12**) was isolated by Muller and co-workers, who tentatively proposed the structure **9** as shown in Figure 1.5 mentioned above.[20] Note that this compound had the same relative stereochemistry as strigol, but with the double bond and hydroxyl group in different positions. This structure was disproved by synthesis.[113] In 2008, Matsuura re-analysed isolated alectrol, and proposed a new structure **10**,[23] in which the stereochemistry of the alcohol unit was undefined. Subsequently, Yoneyama and co-workers proposed that alectrol was the acetate of orobanchol (**11**),[24] and suggested the relative stereochemistry was the same as strigol, but the alcohol group was positioned at the 4-position rather than the 5-position of the ring system.

Finally, the matter was settled with Sugimoto's report on the exact structures of orobanchol (**13**) and its acetate (**12**).[25] The synthesis of alectrol (orobanchol acetate) involved esterification of synthesized orobanchol with vinyl acetate and lipase AK**.**

1.6.7 Total Synthesis of Solanacol and Solanacyl Acetate

The first total synthesis of solanacol (**14**) was reported by Boyer and Beau, who ascertained that solanacol was an orobanchol-type strigolactone.[114]

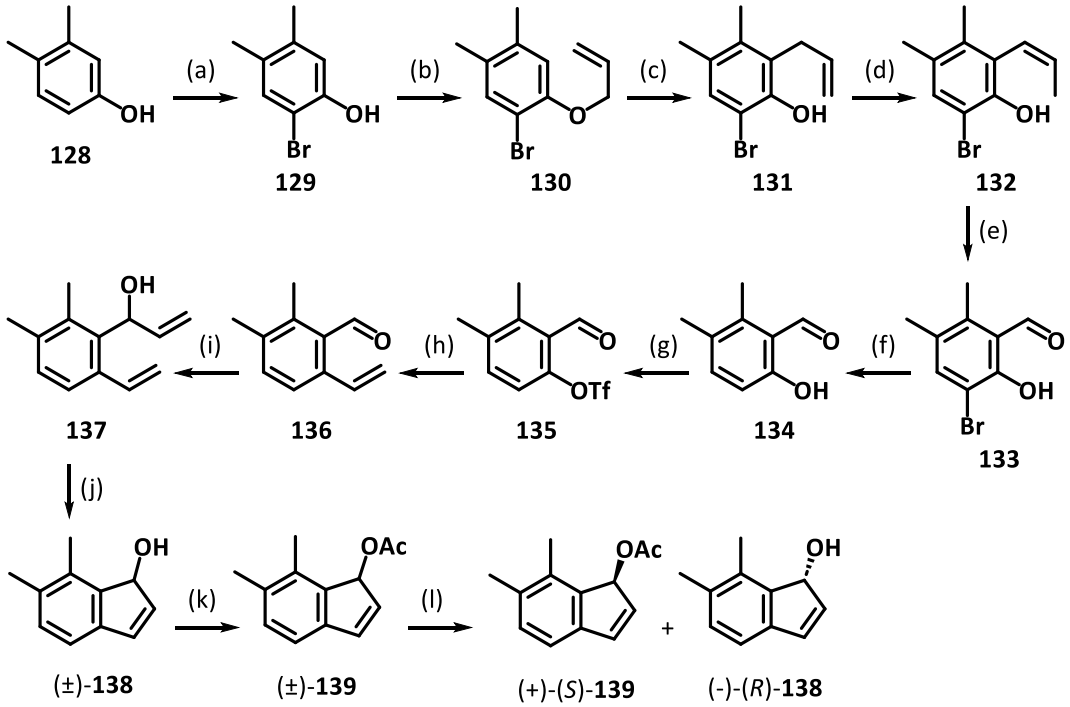

Scheme 1.23: Total synthesis route of designed intermediate (-)-(*R*)-**138**. Reagent and conditions: (a) Br_2, dichloromethane, 0°C, 1h; (b) allylbromide, K_2CO_3, acetone, reflux, 3h; (c) Et_2AlCl, hexane, RT, 6h; (d)tBuOK, THF, RT, 48h; (e) O_3, CH_2Cl_2, -78°C then Me_2S, -78°C to RT, 12h; (f) Pd/C, H_2, NEt_3, MeOH, RT, 2h; (g) pyridine, Tf_2O, CH_2Cl_2, 0°C to RT, 1h; (h) CH_2=$CHBF_3K$, $PdCl_2$, Cs_2CO_3, PPh_3, THF/H_2O, 85°C, 12h; (i) CH_2=CHMgBr, THF, RT, 3h; (j) Grubbs I catalyst, CH_2Cl_2, RT, 12h; (k) Ac_2O, pyridine, THF, 0°C, 15min; (l) immobilized *Candida antarctica* lipase, CH_3CN, H_2O, 24h.

Their synthesis began with a site-selective bromination of dimethyl phenol **128** and subsequent allylation to give allyl phenyl ether **130**. After diethylaluminium chloride catalysed Claisen rearrangement, the double bond was isomerized to give phenol **132**.

Ozonolytic cleavage afforded ortho-hydroxy aldehyde **133**, and the bromine atom was then excised by reduction with hydrogen over Pd/C. The product aldehyde **134** was triflate under standard conditions to give compound **135**. Suzuki cross-coupling with ethylene potassium trifluoroborate gave ortho-vinyl aldehyde **136**, which was reacted with vinyl Grignard to afford alcohol **137**. Ring closing metathesis formed the B-ring and give racemic alcohol (±)**-138**. Esterification with acetic anhydride gave (±)**-139**, which was resolved using immobilized *Candida antarctica* lipase to give ester (+)-(*S*)-**139** and the free alcohol (-)-(*R*)**-138**.

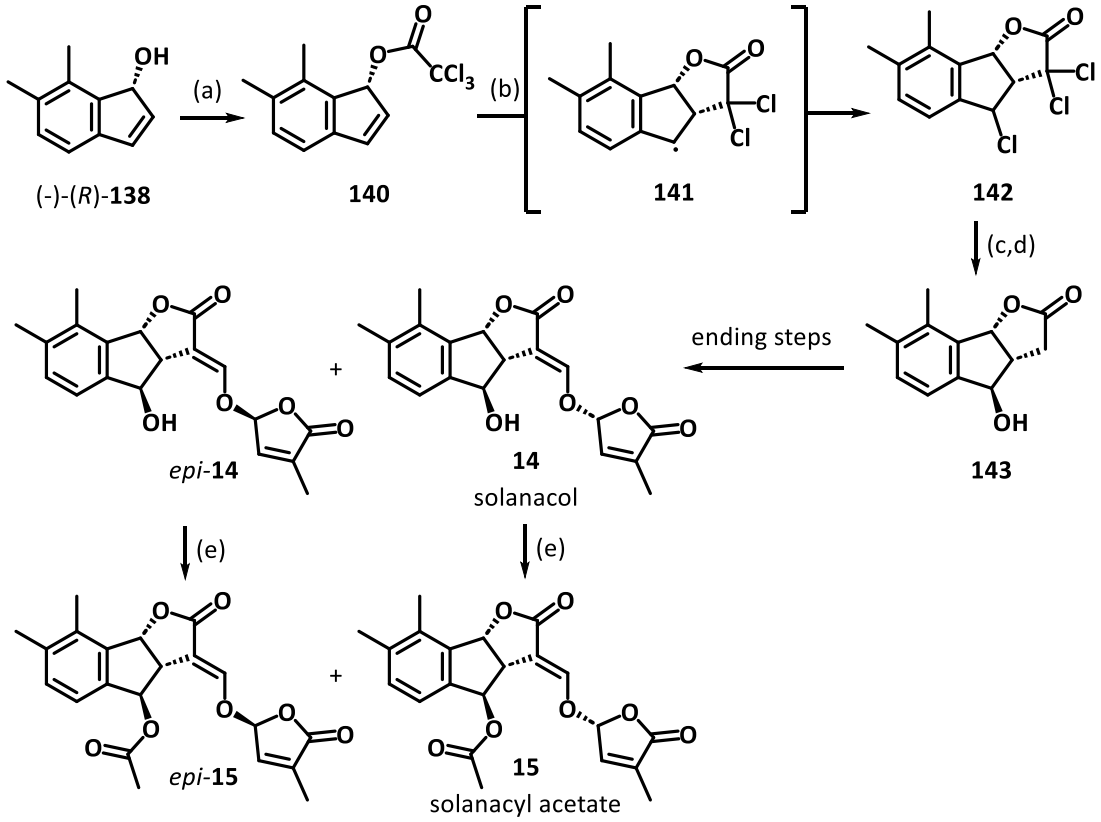

Scheme 1.24: Total synthesis route of solanacol (**14**) and solanacyl acetate (**15**) from (-)-(*R*)-**138**. Reagent and conditions: (a) trichloroacetic anhydride, pyridine, RT, 12h; (b) ATRC, CuCl, dHdipy, $ClCH_2CH_2Cl$, 90°C, 6h; (c) H_2O, hexafluoroisopropanol, 90°C, 30min; (d) zinc dust, NH_4Cl, dry methanol, 0°C to reflux, 2h; (e) Ac_2O, pyridine, RT, 12h.

Stereoselective lactonization was achieved via esterification of (-)-(*R*)**-138** to the corresponding trichloroacetate **140**, and subsequent Copper-catalysed Atom Transfer

Ring Closure (ATRC) to give compound **142**. This sequence installed the C-ring to give the chlorinated tricyclic skeleton of solanacol. Chlorine reduction and substitution, afforded the stereochemically desired tricyclic skeleton **143**. Application of the now familiar endgame strategy furnished solanacol (**14**) and its stereoisomer *epi*-**14**, and solanacyl acetate (**15**) and its isomer *epi*-**15**.

Later, McErlean and co-workers devised an enantioselective total synthesis of solanacol that avoided the use of enzymatic resolution.[115] Instead of enzymes, they chose a single enantiomer ruthenium catalyst to achieve stereo-control.

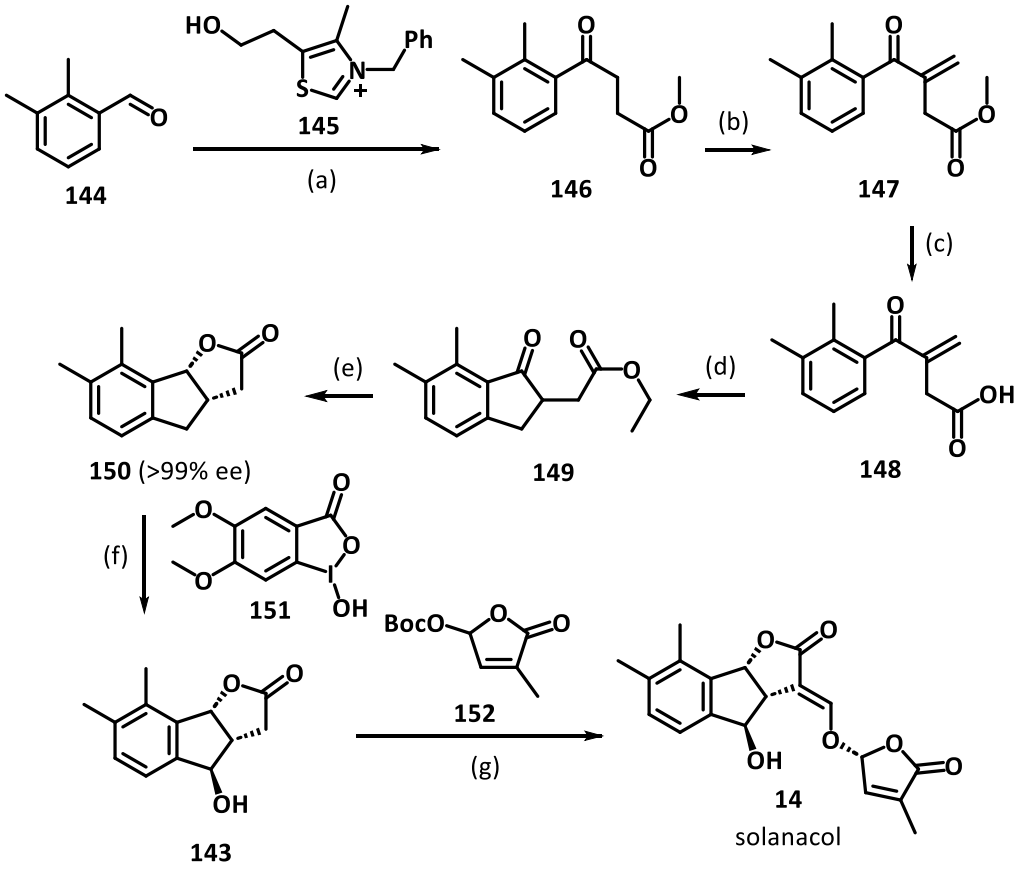

Scheme 1.25: Total synthesis route of solanacol without enzymes. Reagent and conditions: (a) **145** (3×15 mol%), methyl acrylate, caesium carbonate, heat, THF; (b) sodium hydroxide, formalin, H_2O; (c) sodium hydroxide; (d) sulfuric acid, 50°C, then acetyl chloride, ethanol; (e) (R,R)-RuTsDEPN (3 × 4 mol%), formic acid, $NEt(^iPr)_2$, DMF, 40°C then PPTS, toluene; (f) $Ru(bpy)_3Cl_2$, **145**, HFIP/H_2O, blue LED; (g) methyl formate, KO^tBu then $Pd_2(dba)_3$, **152**, (S,S)-DACH-phenyl.

Their synthesis began from dimethyl benzaldehyde (**144**), which underwent *N*-heterocyclic carbene **145** catalyzed addition onto methyl acrylate **146**. Aldol reaction with formalin and elimination gave compound **148**. Simple Nazarov cyclization with sulfuric acid gave bicyclic intermediate **149**. Asymmetric reduction was achieved using transfer hydrogenation in the presence of Noyori's catalyst. Compound **149** was treated with pyridinium *para*-toluenesulfonate (PPTS) to effect lactonization and produce the stereo-defined A,B,C-ring system **150** with high enantio-control. Blue light irradiation of a mixture of **150** and the common ruthenium photoredox catalyst $Ru(bpy)_3Cl_2$, resulted in benzylic oxidation and installed the necessary hydroxyl unit in a stereo-controlled manner. In contrast to most end game strategies, McErlean and co-workers utilized a palladium-catalyzed allylic alkylation to install the butenolide D-ring, giving single isomer solanacol (**14**).

1.6.8 Total Synthesis of Fabacol and Fabacyl Acetate

Because of their obviously related structures, fabacol (**17**) and fabacyl acetate (**18**) appear to be derivatives of orobanchol (**13**). Indeed, Uchida and Takikawa recently developed a strategy for synthesizing fabacol and fabacyl acetate[116]using orobanchol (**9**) as the starting material (Scheme 1.26).

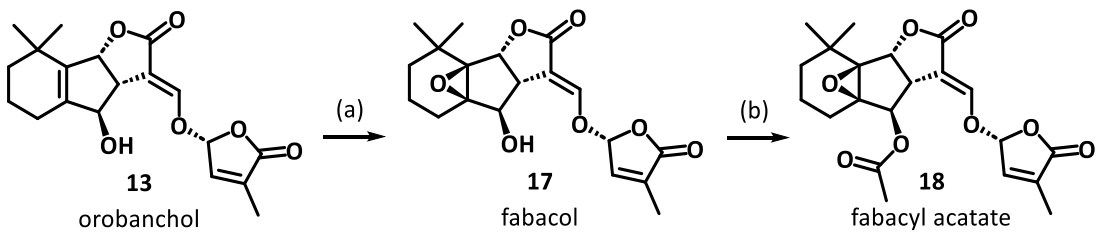

Scheme 1.26: Total synthesis route of fabacol and fabacyl acetate from orobanchol. Reagent and conditions: (a) m-CPBA, sodium bicarbonate, dichloromethane, 0°C to RT; (b) acetic anhydride, DMAP, pyridine, RT.

1.7 Total Syntheses of Naturally Occurring Non-Canonical Strigolactones

1.7.1 Carlactone and Avenaol

As the preceding section illustrates, efforts towards the total synthesis of individual canonical strigolactones have a long history. A wide variety of strategies and methodologies have been applied. In contrast, synthetic efforts towards the non-canonical strigolactones have received much less attention. Because the work described in this thesis relates to novel synthetic approaches to carlactone (**24**) and avenaol (**25**), the details of prior synthetic efforts to those compounds will be described in the following chapters.

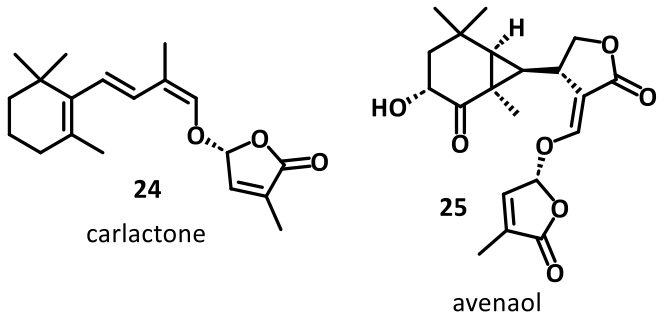

Figure 1.16: Structures of carlactone (CL) (**24**) and avenaol (**25**).

1.7.2 Total Synthesis of CLA and MeCLA

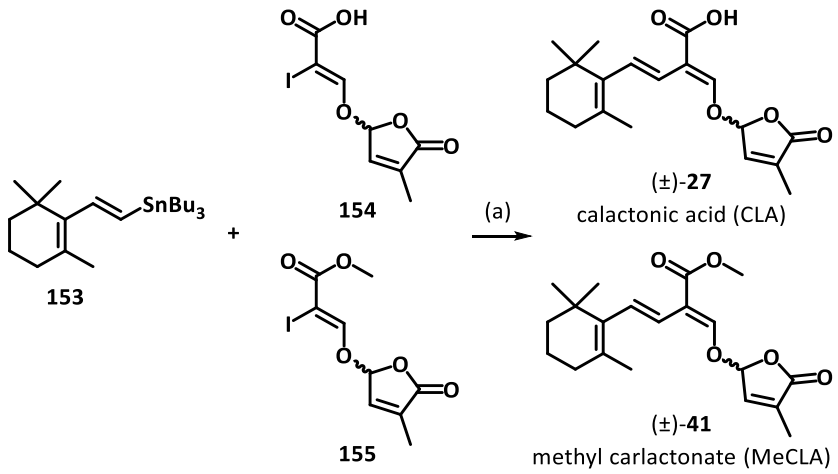

Scheme 1.27: Stille coupling (key step) in the total synthesis of CLA and MeCLA. Reagent and conditions: (a) $Pd_2(dba)_3$, $AsPh_3$, dioxane, 100°C, 45 min.

De Mesmaeker and co-workers made an important strategic contribution towards an efficient route to non-canonical SLs when they reported the total synthesis of carlactonic acid CLA (**27**) and its methyl ester MeCLA (**41**) in 2017.[117] As shown in Scheme 1.27, they chose the Stille cross-coupling reaction as the key bond-forming step to achieve a convergent synthesis of those non-canonical SLs.

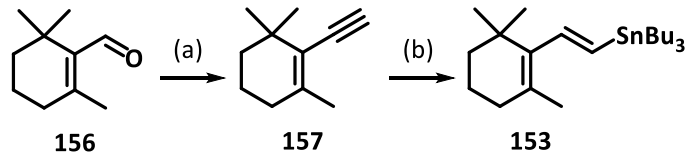

Scheme 1.28: Synthesis of vinyl stannane molecule **147**. Reagent and conditions: (a) $TMSCHN_2$, LDA, THF, -78°C, 6h; (b) $HSnBu_3$, AIBN, 80°C, 24h.

The necessary vinyl stannane compound **153** derived from cyclocitral (**156**) by alkylation using Colvin's procedure,[118] followed by a radical stannylation (Scheme 1.28). Compound **153** represented one half of the target molecules, CLA and MeCLA.

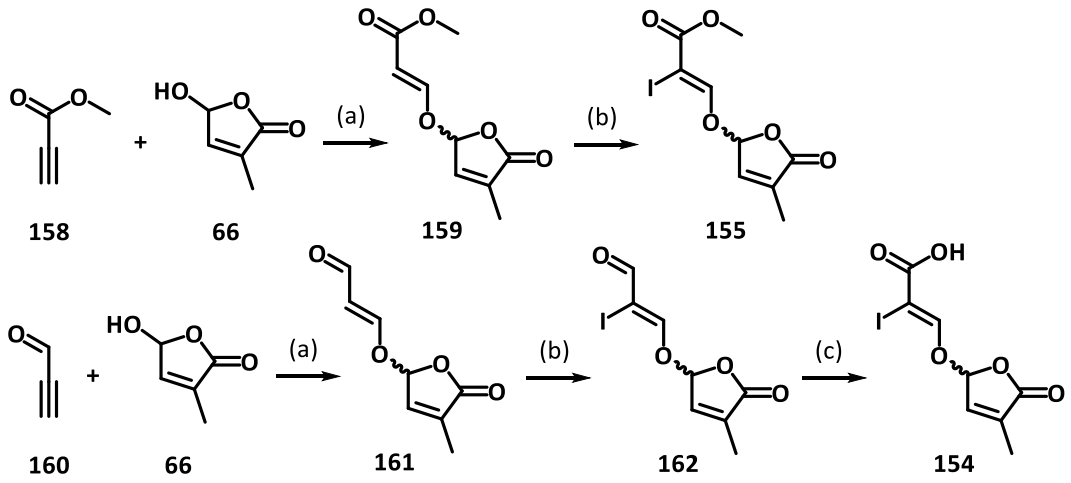

Scheme 1.29: Synthesis of vinyl iodide molecules **148** and **149**. Reagent and conditions: (a) N-methyl morpholine, THF, RT; (b) NIS, AcOH, dichloromethane, RT, 36h then NEt_3, 8h; (c) $CuBr_2$, TBHP, MeCN, RT, 18h.

The second half of the molecules were projected to be the vinyl iodides **154** and **155** (Scheme 1.29). To generate those intermediates, methyl propynoate (**158**) and propyne aldehyde (**160**) respectively, were reacted with the hydroxyl-containing butenolide (**66**).

The *N*-methylmorpholine catalyzed Michael addition exclusively afforded the (*E*)-configured olefins **159** and **161**. Treatment with NIS installed the requisite iodine atoms to give compounds **155** and **162** in excellent yields. Finally, oxidation of compound **162** gave the iodinated carboxylic acid **154**.

With both coupling partners now in hand, De Mesmaeker and co-workers explored many reaction conditions to affect the desired Stille cross-coupling (Table 1.1). The optimized reaction conditions utilized catalytic $Pd_2(dba)_3$ alongside a substantial amount of the highly toxic ligand, $AsPPh_3$ (30 mol%). This combination delivered racemic CLA in 51% yield and racemic MeCLA in 75% yield (entry 4).

Table 1.1: De Mesmaeker's trials on exploring conditions.[117]

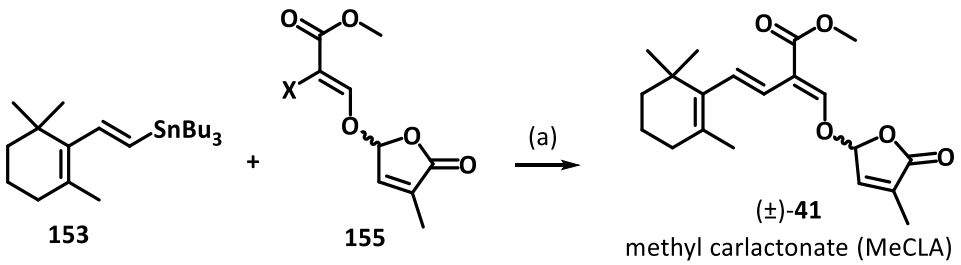

Entry	Reagents & Equiv.	X	Conditions	Conversion/Yield (%)
1	$Pd(PPh_3)_4$ (20 mol%)	I	toluene, 100 °C, 60 min	5/traces
2	$PdCl_2(PPh_3)_2$ (20 mol%)	I	CuI, DMF, 100 °C, 60 min	full conv/10
3	$Pd_2(dba)_3$ (10 mol%); $AsPh_3$ (40 mol%)	I	dioxane, 100 °C, 60 min	full conv/30
4	$Pd_2(dba)_3$ (7.5 mol%); $AsPh_3$ (30 mol%)	I	dioxane, 90 °C, 45 min	full conv/75
5	$Pd_2(dba)_3$ (10 mol%); $AsPh_3$ (40 mol%)	Br	dioxane, 100 °C, 60 min	30/traces

De Mesmaeker and co-workers were also able to complete the first (and to date, the only) stereoselective synthesis of (*R*)-CLA ((*R*)-**27**) and (*S*)-CLA ((*S*)-**27**). To achieve this, the previously synthesized aldehyde intermediate **162** was subjected to

enantioselective HPLC separation (Scheme 1.30). The individual enantiomers (+)**-162** and (**-**)**-162** were then assessed as germination stimulants for seeds of the parasitic weed, *Orobanche Cumana*. Only the (+)**-162** enantiomer was active across a range of concentrations, and since all strigolactones have retained stereochemistry at the butenolide linkage, the (+)**-162** enantiomer was assigned as (*R*)**-155.** This compound was coupled with stannane **153** to give (*R*)-CLA ((*R*)**-27**).

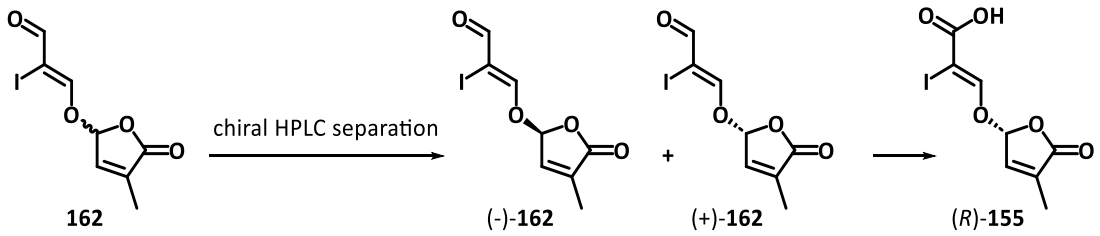

Scheme 1.30: Chiral separation of aldehyde **162** and determination of stereochemistry.

1.7.3 Total Synthesis of Zealactone

De Mesmaeker and co-workers leveraged their new Stille cross-coupling synthetic strategy for the total synthesis of zealactone, making it the most common synthetic strategy to non-canonical SLs.[119]

As depicted in Scheme 1.31, De Mesmaeker and co-workers chose methyl 2-butynoate (**163**) as the material. The triple bond was alkylated by lithium dimethylcuprate and quenched with iodine to afford vinyl iodide **164**. Sonogashira coupling with protected acetylene in the presence of copper(I) gave unsaturated ester **165**, and saponification delivered the carboxylic acid **166**. The acid **166** was converted into the corresponding ketene via the corresponding acid chloride, and the ketene reacted with an extremely large excess of isobutene to produce cyclobutanone **167**. Bayer-Villiger oxidation with *m*CPBA regioselectively inserted an oxygen atom into the allylic position of the cyclobutanone to form the A-ring **168** of zealactone. Following the optimized protocols from the previously discussed CLA synthesis, intermediate **169** was converted into the vinyl stannane **170** in good overall yield. Finally, utilization of the same Stille cross-

coupling methodology united stannane **170** and compound **155** to give the targeted compound, racemic zealactone (**26**).

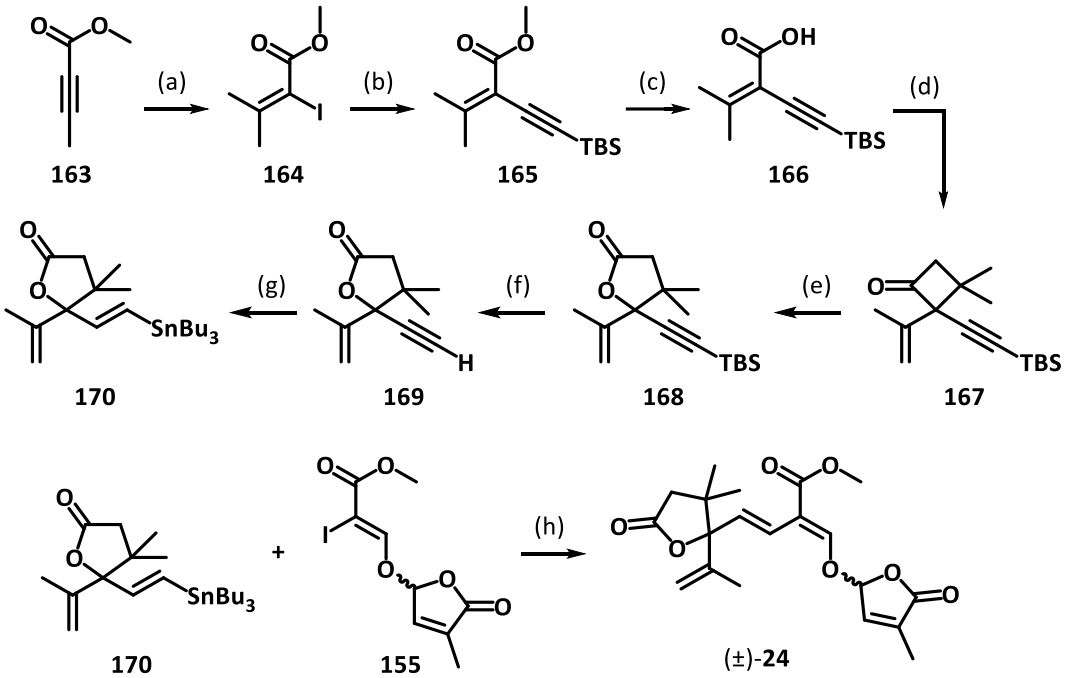

Scheme 1.31: Total synthesis of zealactone **24**. Reagent and conditions: (a) Me_2CuLi, THF, -45°C, 90 min then I_2, -45°C to 0°C, 3h; (b) alkynyl TBS, $Pd(PPh_3)_2Cl_2$, CuI, NEt_3, 1,4-dioxane, 50°C, 90min; (c) LiOH, ^tBuOH, 23°C; (d) oxalyl chloride, DMF, 1,2 dichloroethane, 23°C, 30min then large excess isobutene, TEA, 1,2-dichloroethane, 60°C, 5h; (e) mCPBA, Bu_4NOH, dichloromethane, 23°C, 1h; (f) TBAF, THF, 23°C, 30min; (g) $HSnBu_3$, AIBN, toluene, 80°C, 18h; (h) $Pd_2(dba)_3$, $P(furyl)_3$, dioxane, 120°C, 30 min.

1.7.4 Total Synthesis of Heliolactone

McErlean and Woo reported the racemic and asymmetric total synthesis of heliolactone, and in doing so were able to confirm its proposed stereochemistry.[120] Inspired by the work of De Mesmaeker, they also chose the Stille cross-coupling as the final step in their synthesis. But in contrast to De Mesmaeker's reports, the iodide and stannane units had to be transposed to affect the desired union.

As shown in Scheme 1.32, the synthesis began by conversion of α-cyclocitral (**171**) into dibromo-olefin **172** by the action of tetrabromomethane and triphenylphosphine. A

three-step procedure converted **172** into vinyl iodide **175**. The Corey-Fuchs reaction sequence could not be carried out in the standard manner due to the high volatility of intermediate alkyne **173**, and instability of vinyl stannane **174**. The ketone functionality was introduced onto compound **175** by oxidation with sodium hypochlorite to afford the oxidized vinyl iodide **176**. This molecule represented one of the polarity-reversed partners for the projected Stille cross-coupling reaction. The vinyl stannane coupling partner **177** was generated by radical stannylation of the previously mentioned vinyl iodide **155**. Finally, application of De Mesmaeker's optimized Stille cross-coupling procedure gave racemic heliolactone (**28**).

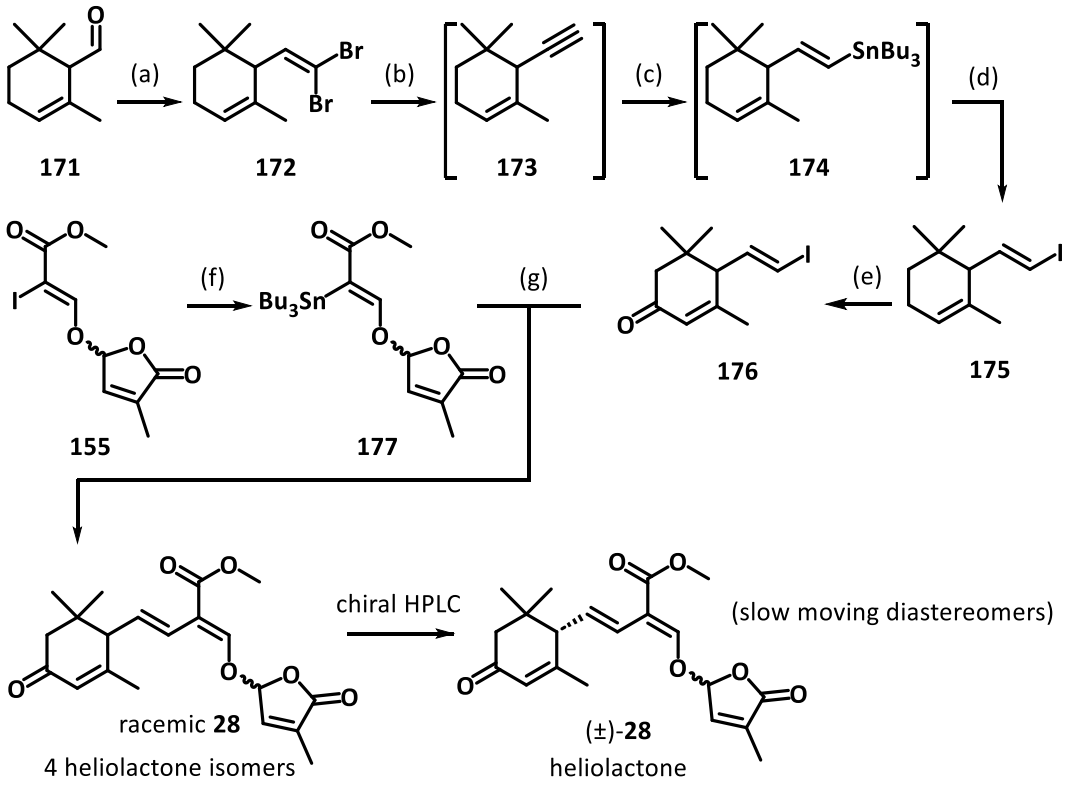

Scheme 1.32: McErlean and Woo's total synthesis of heliolactone. Reagent and conditions: (a) CBr_4, PPh_3, dichloromethane; (b) *n*-BuLi, Et_2O, -78°C; (c) AIBN, Bu_3SnH, PhMe, 90°C; (d) I_2, dichloromethane, 0°C, 5min; (e) NaOCl, TBHP, EtOAc; (f) $(SnBu_3)_2$, Pd_2dba_3, THF; (g) Pd_2dba_3, $AsPh_3$, CuI, NMP.

In order to confirm the stereochemistry of naturally occurring heliolactone, McErlean and Woo revised their strategy to generate single enantiomer coupling partners (**-**)**-176**

and (+)-**177**. As shown in Scheme 1.30, technical grade α-ionone (**178**) was converted into the acid **179** via haloform reaction. Racemic acid **179** was resolved with a chiral amine to give access to (-)-**176**. While direct Hunsdiecker iodination of acid (-)-**176** failed, the sequence of acid activation, decarboxylative borylation, and stereo-retentive iodination successfully delivered the vinyl iodide (-)-**176**. Allylic oxidation provided (-)-**176** as one of the stereochemically defined coupling partners.

The remaining coupling partner was generated from De Mesmaeker's previously described intermediate **155**. Enantioselective HPLC resolution of racemic **155** provided access to (+)-**177**, which contained the naturally occurring (*R*)-stereochemistry. This compound underwent palladium-catalysed stannylation without any impact on the existing stereocentre. Finally, Stille cross-coupling of (+)-**177** and (-)-**176** gave (6S, 11R)-heliolactone **25** and confirmed the stereochemistry of the natural product.

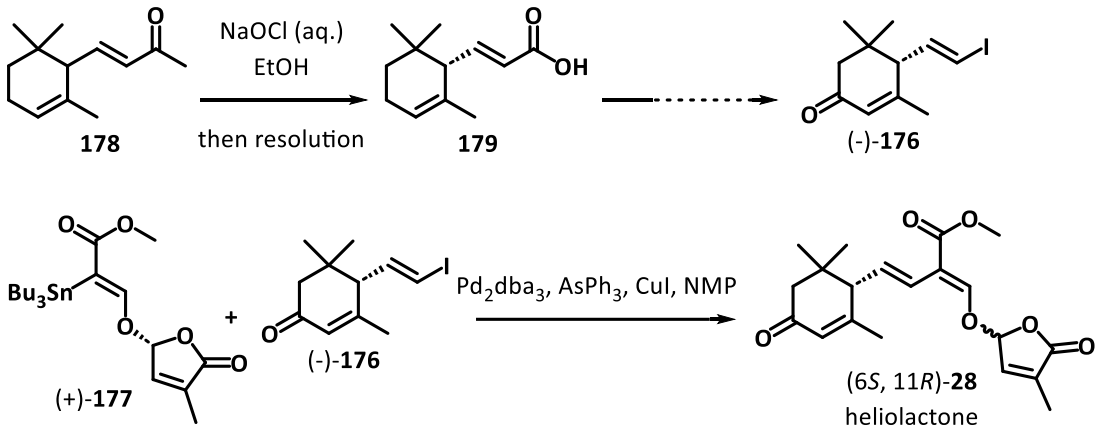

Scheme 1.33: McErlean and Woo's confirmation the stereochemistry of naturally occurring heliolactone (**28**).

1.8 Summary

This chapter aimed to provide the reader with an introduction to the suite of naturally occurring molecules known as strigolactones. The discovery and 'definition' of SLs was described, with an emphasis on the stereochemically defined enol ether appended butenolide ring. A focus on the chemical structure of SLs, enables individual members to be categorized as canonical (possessing a fused tricyclic system) or non-canonical (lacking a fused tricyclic system). The canonical SLs can be further categorized based on the relative stereochemistry of the fused ring system, into either strigol-type or orobanchol-type.

Different strigolactones exhibit different biological functions. Spectacularly, these molecules mediate (or are involved in) in three distinct types of signalling; *intra planta* (i.e. as phytohormones); *inter plantae* (as seed germinators of parasitic weeds); and inter-kingdom (as hyphal branching factors for fungi).

Exploration of the various biosynthetic pathways leading to SLs has demonstrated a species-specific dependency. All SLs are derived from β-carotene, which is transformed (in a conserved manner across species) into the common intermediate, carlactone (CL). A series of enzyme-mediated oxidations and cyclizations converts CL into both canonical and non-canonical SLs. The additional carbon atom that is present in the non-canonical SLs derives from the methyl unit of methyl carlactonate. While some biosynthetic pathways to individual SLs in selected plant species have been elucidated completely, the exact order of many biosynthetic transformations remains unknown. In particular, the biosynthetic hypotheses for the non-canonical SLs remain largely speculative. Unravelling these biosynthetic pathways requires a ready supply of radio-labelled and selectively oxygenated CL and MeCLA analogues.

Our understanding of the molecular basis for SL bioactivities is increasing. Much work has been performed on the signal transduction and transport mechanisms of SLs in

plants. SL signalling is initiated by an α,β-hydrolase enzyme that cleaves the stereochemically defined enol ether appended butenolide ring.

With such potent bioactivities and such low natural abundance, SLs have attracted the attention of synthetic chemists. To date, individual SL molecules have been accessed by unique synthetic routes. No general approach has yet been developed that allows access to all members of this family. However, a common strategy is often employed for the attachment of the butenolide unit. Following Sih's initial work on SLs, most synthesis are completed by Dieckmann reaction of the tricyclic core with ethyl formate, followed by alkylation of the corresponding enol with a halogenated butenolide ring. The few reported syntheses of non-canonical SLs rely upon a Stille cross-coupling reaction for completion of the synthetic route.

Clearly, there is a pressing need for ready supply of radio-labelled and selectively oxygenated CL and MeCLA analogues, as well as a need to provide access to the under-studied non-canonical strigolactones. There is much room to innovate in the area of SL total synthesis.

2 SYNTHETIC WORK TOWARDS CARLACTONE

As mentioned above, carlactone (CL) **24** (Figure 2.1), as the common precursor in every SL biosynthesis, is a pivotal molecule for understanding and developing SL chemistry. Isolation of carlactone from natural sources is not viable due to the fact that the molecule is produced in vanishingly small quantities and undergoes reaction *in planta*. Therefore, CL (**24**) is an important target for total synthesis.

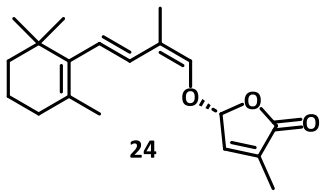

Figure 2.1: Structure of carlactone (**24**).

At a cursory glance, the development of synthetic routes to produce useful quantities carlactone might seem straightforward. However, reality is quite the opposite. Carlactone is light-, acid-, base-, and temperature-sensitive. Since it was first identified (more than twenty years ago), organic chemists have been working tirelessly to develop an efficient and cost-effective total synthesis route. Despite these efforts, existing syntheses are far from satisfactory.

This chapter focuses on the design and investigation of several chemoselective and cost-effective synthetic strategies for the generation of CL (**24**). Three primary approaches are explored: the Darzens reaction (analogous to a previously reported CL route), the Chan-Lam coupling, and a modified Mukaiyama reaction. These methodologies will be discussed in detail in the following sections.

2.1 Previous Total Syntheses of Carlactone

The first total synthesis of CL was reported by Flematti, Smith, and co-workers (Scheme 2.1).[121] Darzens reaction of β-ionone (**180**) and decarboxylative saponification of intermediate **181** gave aldehyde **182**. Enolization of **182** with potassium *tert*-butoxide and *O*-alkylation with the bromobutenolide (**76**) gave racemic CL (**24**) as the minor component in a mixture of (*E*)- and (*Z*)-(±)-CL (**24**). Semi-preparative HPLC was then required to separate these compounds.

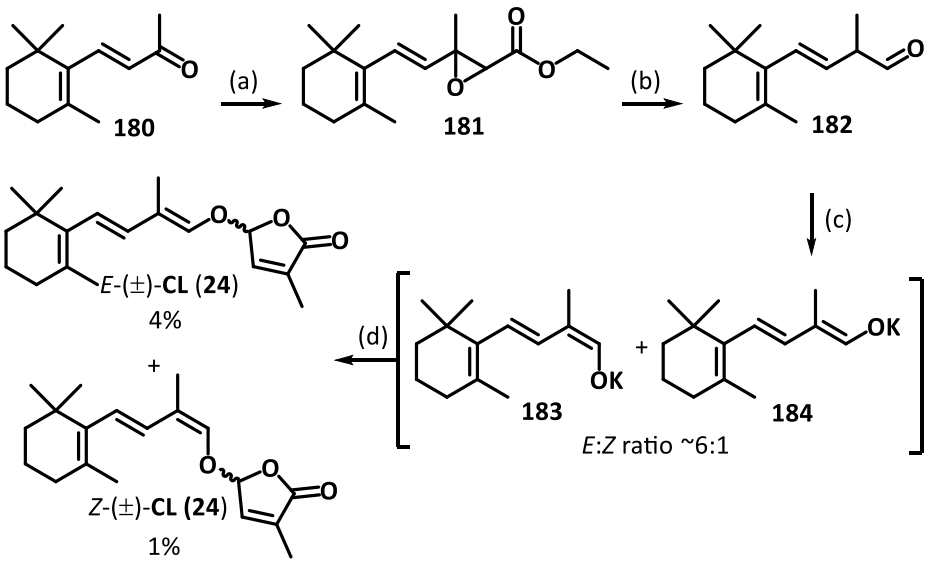

Scheme 2.1: Flematti and Smith's total synthesis route of CL (**24**). Reagent and conditions: (a) ethyl chloroacetate, sodium methylate, phenothiazine, pyridine, 0°C, 2h; (b) sodium hydroxide, methanol then acetic acid; (d) dimsyl potassium, **76**, phenothiazine, DMSO.

Although Flematti and co-workers were able to produce 15 mg of (*Z*)-(±)-CL (**24**), the yield of the final alkylation was a paltry 1%. Despite extensive attempts at optimization, this yield could not be improved upon.

There are two synthetic challenges inherent in Flematti's approach: Firstly, enolization of aldehyde **182** is non-diastereoselective (with the desired (*Z*)-configured enolate being the minor component); and secondly, the sluggish alkylation of the enolate is not

regioselective (i.e. a competition among *C*-alkylation, and *O*-alkylation and no reaction).

In 2014, Seto, Yamaguchi and co-workers reported the a total synthesis of isotopically-labelled CL (Scheme 2.2).[33] In order to insert the ^{13}C atom, they alkylated 2,6-dimethyl cyclohexanone **44** with isotopically-labelled methyl iodide, and carried the material through to give isotopically-labelled β-ionone (**180**). From that point, Seto's approach closely mirrored Flematti's approach.

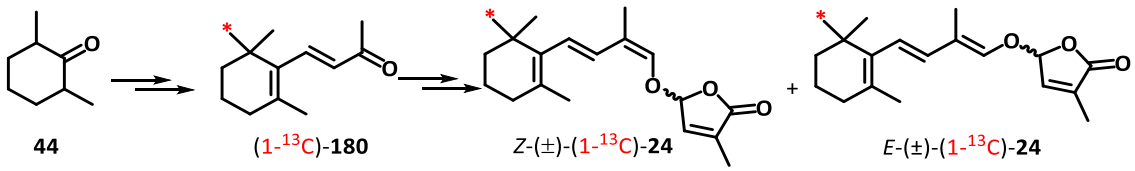

Scheme 2.2: Seto's total synthesis route of isotope-labelled carlactone isomers.

Darzens reaction between ethyl chloroacetate, and the isotope-labelled β-ionone (**180**) gave epoxy ethyl ester, which was deacrboxylatively hydrolysed to afford the aldehyde. Enolization was effected by dimsyl sodium, and reaction of the sodium enolate with brominated D-ring **76** gave a mixture isotopically-labelled carlactone (**24**) and its non-natural isomer. In analogy to Flematti's results, the (*E*)-(±)-CL isomer predominated and was isolated in 4.3% yield. The desired (*Z*)-(±)-CL product (1-^{13}C)-**24** was isolated in a very low yield of just 0.4%.

Clearly, a cost-effective synthetic route that produces carlactone in much higher overall, is a worthy goal.

2.2 Chemoselective Approach via Darzens Reaction

Our synthetic strategy to CL aimed to address the challenges existing in the previous reports, i.e. diastereoselective enolization, and regioselective *O*-alkylation. Key to our approach was the presence of a large, stereo-controlling, and easily removable unit on the enol ether bridge.

2.2.1 Retrosynthetic Analysis

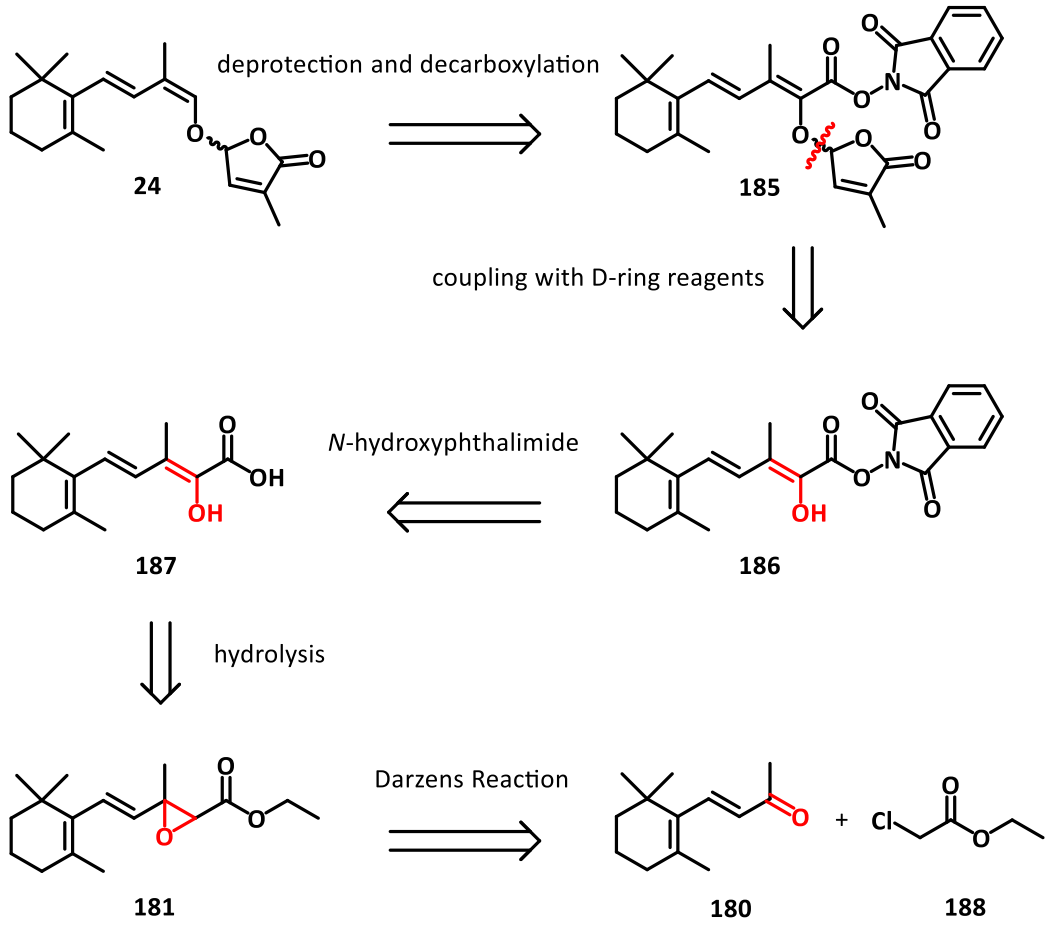

Scheme 2.3: Retrosynthesis of our chemoselective approach.

As shown in Scheme 2.3, our retrosynthetic analysis started not with bond cleavage, but by introduction of an activated ester **185**. We anticipated that the large *N*-hydroxyphthalimido ester **185** unit, which has been widely utilized in radical decarboxylation, would enable diastereoselective generation of the required enol/enolate **186**, and that the group could be easily removed under very mild reaction conditions via metal mediated or photoredox catalyzed pathways. The predicted mechanism has been shown in Scheme 2.4.

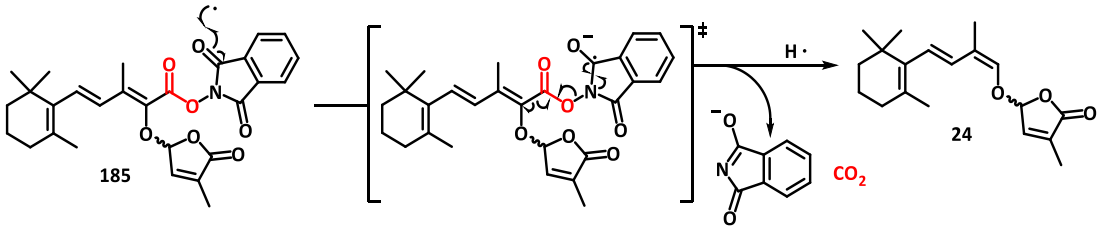

Scheme 2.4: Mechanism of radical decarboxylation.

Following the previously reported synthetic routes, disconnection of the D-ring revealed the bromobutenolide **76** and enol **186**. *N*-hydroxyphthalimido ester **186** was anticipated to come from the corresponding acid **187**, which could be generated by hydrolytic isomerization of epoxy ester **174**. Compound **181** was further disconnected via a retro-Darzens reaction to reveal chloroethyl acetate (**188**) and β-ionone (**180**) as suitable starting materials. Flematti and Seto had previously utilized epoxy ester **181** as an intermediate in their syntheses. In contrast to their work, we anticipated isomerization and ester hydrolysis under milder reaction conditions that prevented decarboxylation.

2.2.2 Synthesis of the D-ring Contained Coupling Reagents

Our synthetic work began with the synthesis of the bromo butenolide **76**. Regardless of the synthetic strategy used, we anticipated that efficient access to an appropriately activated butenolide ring would be an essential for further work. Therefore, we employed the method of Zwanenburg and co-workers.[122]

As shown in Scheme 2.5, acid-catalyzed reaction of methyl malonic acid and glyoxal in refluxing water, delivered the hydroxyl-containing butenolide ring **66** in moderate yield. Appel reaction using tetrabromomethane and triphenylphosphine converted the hydroxyl group into the corresponding bromide, giving the desired brominated compound **76** in good yield. We were keenly aware that optimization of the regioselective *O*-alkylation of enol/enolate **186** may require a metal-catalyzed reaction, and therefore we took the opportunity to convert compound **66** into the corresponding Boc protected compound **190** as well. Such facile formation of the butenolide ring under hot, aqueous conditions deserves further discussion.

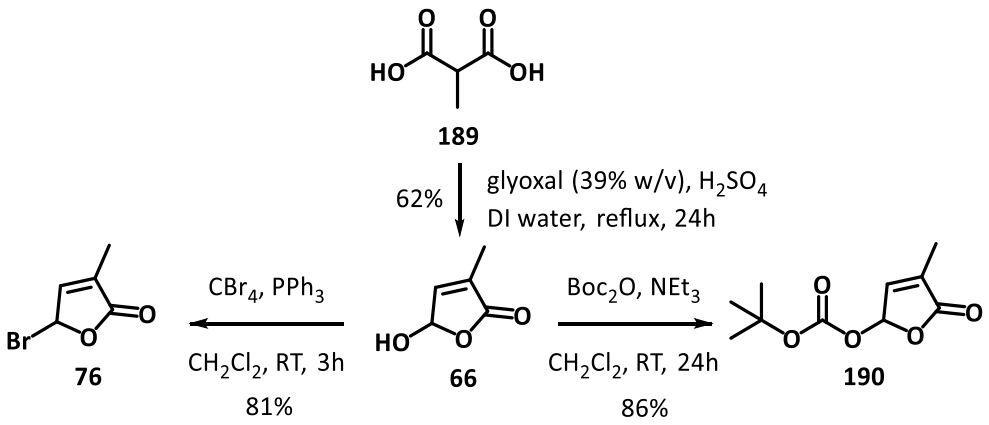

Scheme 2.5: Synthesis of compound **76** and **190** from compound **66**.

Malik, Zwanenburg, and their co-workers were the first to propose a synthetic strategy[122] for the D-ring molecule **66** (D-ring-OH) through a Dobner modification[123] of the Knoevenagel condensation.[124] This approach involved the reaction between methyl malonic acid (**189**) and glyoxal (**192**) in the presence of H_2SO_4 (Scheme 2.6).

Mechanistically, nucleophilic attack by an enolized carboxylic acid on glyoxal (**192**), results in the initial union of the two reactants. Enolization of a carboxylic acid necessitates the use of a strong acid, rationalizing the choice of H_2SO_4. Protonation of the secondary alcohol of **193** initiates a decarboxylative elimination, leading to the formation of an α,β-unsaturated aldehyde **195**. Intramolecular acetalization between the remaining functional groups culminates in formation of the five-membered ring **66**.

Forcefully heating the reaction mixture facilitates elimination of the secondary alcohol, and disfavours unwanted addition of water to the product butenolide **66**.

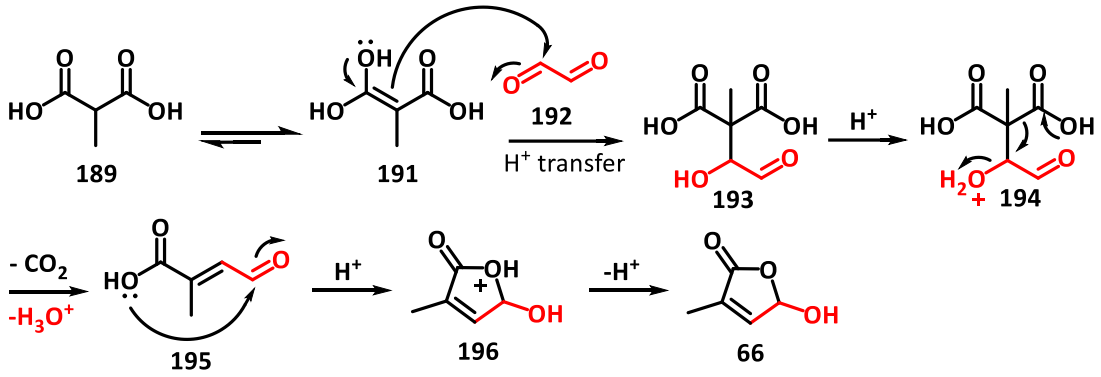

Scheme 2.6: Proposed mechanism of generating D-ringOH.

By employing this methodology, rapid access to the desired bromobutenolide **76** was realized. Attention next turned to generation of the required enol **186**.

2.2.3 Synthesis Efforts and Results of Darzens Approach

Building on the previously reported synthetic strategies to carlactone,[33] this study chose the Darzens reaction as a key step in the pathway to install the required carbon atoms. However, in contrast to those earlier approaches (Scheme 2.1), this method does not involve decarboxylation following hydrolysis of the epoxide ester **181**. Instead, we projected that the epoxide could be rearranged to give the enol ester. Our confidence in this approach was instilled by an historical literature report.

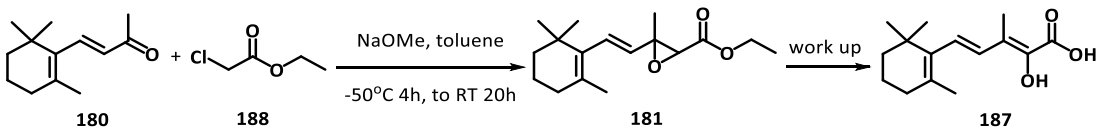

Scheme 2.7: Milas's large-scale Darzens protocol for generating epoxide **181** and acid **187**.

In 1948, Milas and co-workers reported outcomes from the work they performed on vitamin A chemistry during World War II.[125,126] That work reported the large scale

Darzens reaction of β-ionone (**180**) and the regioselective ring opening of the formed epoxide (**181**) displayed in Scheme 2.7.

The Darzens reaction is a condensation reaction that occurs under basic conditions (e.g. sodium ethoxide), in which α-halogenated carboxylic esters react with aldehydes, ketones, or amides to form α,β-epoxy esters.[127] This reaction was first reported in 1904 by the Russian-born French chemist, Auguste Darzens.

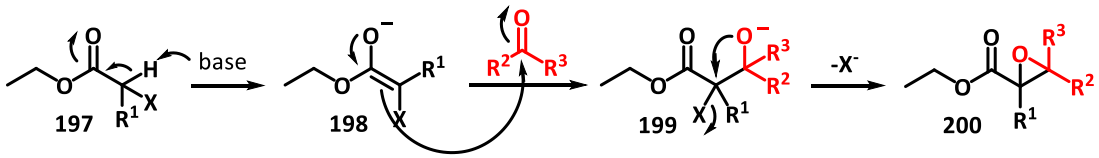

Scheme 2.8: Mechanism of Darzens reaction.

The reaction is initiated under basic conditions, where the halogen substituent aids stabilization of the α-deprotonated carbanion, forming an enolate intermediate **198**. The mechanism is illustrated in Scheme 2.8 with the aldehydes, ketones, or amides were highlighted in red for convenience. The enolate then acts as a nucleophile, attacking the carbonyl compound to form a carbon-carbon bond. This is followed by an intramolecular S_N2 reaction, in which the halogen is displaced, leading to the formation of the epoxy ring at the α,β-position of the ester group **200**.[128]

To find the most suitable conditions for this reaction, we explored different bases and different ratios of reagents and varied the order of reagent addition. As shown in Table 2.1, NaOMe, LDA, and KHMDS were used as bases in this series of reactions, and the ratios of the starting materials were adjusted accordingly.

Among these seven entries from Table 2.1, the third entry achieved the highest yield and was therefore selected as the standard protocol for this Darzens reaction step. It should be noted that the reactant **188** was used as solvent in entries 3 and 4 with the aim of increasing the concentration of reactant to push the reaction forward. This process simplified product purification.

Table 2.1: Various conditions for synthesis of **181**.

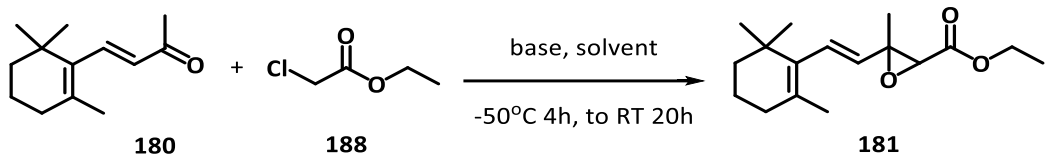

180 **188** **181**

Entry	188 Equiv.	Base	Base Equiv.	Solvent	Order	Yield
1	1.5	NaOMe	1.05	toluene	Protocol A	42%
2	1.5	NaOMe	1.05	toluene	Protocol B	28%
3	2.0	NaOMe	1.05	**188**	Protocol A	46%
4	2.0	NaOMe	1.05	**188**	Protocol B	33%
5	1.5	NaOMe	1.5	toluene	Protocol A	failed
6	1.5	LDA	1.05	toluene	Protocol A	trace
7	1.5	KHMDS	1.05	toluene	Protocol A	< 5%

Protocol A: **180** added in twice (0.5 eq. + 0.5 eq.); base added in twice (0.55 eq. 1h stir then 0.5 eq.).

Protocol B: **180** added in one time; base added in twice (0.55 eq. 1h stir then 0.5 eq.).

After Darzens reaction, we followed the original literature procedures and employed fractional distillation for purification to give the epoxy ester.[125] The distillate was quenched with alcoholic potash and extracted with hexane to remove non-enolized and non-saponifiable by-products. The mixture was then neutralized with dilute HCl solution, followed by repeated enolization with a base and final neutralization with HCl solution. This process yielded the product that had previously been identified as the carboxy-substituted enol structure **187** (Scheme 2.9).

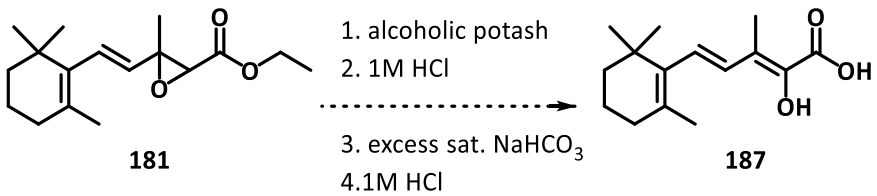

181 **187**

Scheme 2.9: Synthesis of compound **187**.

The esterification of compound **187** with *N*-hydroxyphthalimide to afford the anticipated compound **186** was readily achieved by using DCC (Scheme 2.10) with a yield of 86%. Excess DCC and the resulting urea by-product could be removed through repeated cycles of trituration using minimal solvent rinsing and evaporation, followed by flash column chromatography.

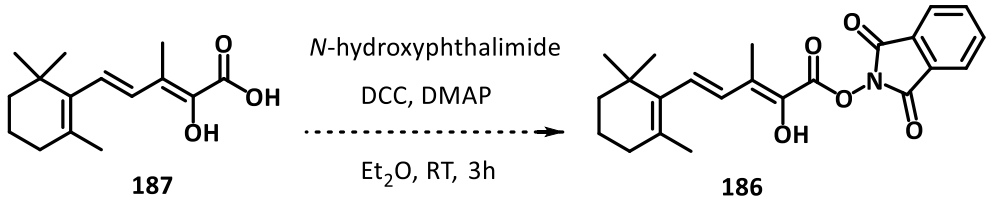

Scheme 2.10: Synthesis of protected compound **186**.

Attachment of the butenolide ring to the geometrically defined enol was then attempted. Despite strictly adhering to Seto's protocol, the coupling step presented unanticipated challenges and complications (Table 2.2). Under a range of reaction conditions, we were unable to append the butenolide ring to the carlactone framework using substitution of the bromo-butenolide. These unexpected outcomes led us to attempt a metal-catalyzed coupling. Following the previous work from McErlean[115,129] and Zwanenburg,[113] a palladium-catalyzed allylic alkylation was attempted with Boc-protected compound **190**. However, these modifications did not lead to any positive outcomes.

Table 2.2: Trials on coupling step of compound **186** & **187**.

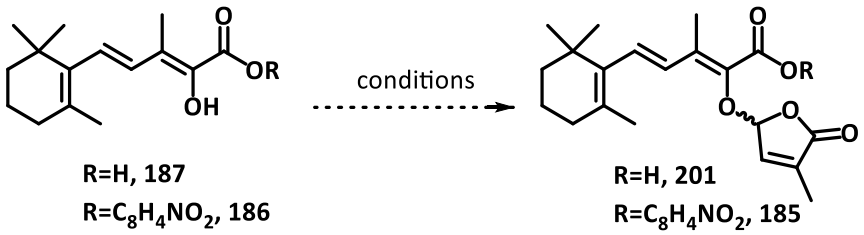

Entry	Reactants & Equiv.	Base	Catalyst	Solvent	Result
1	**186**(1.0 eq.); **76**(1.5 eq.)	Dimsyl sodium	phenothiazine	DMSO	no reaction
2	**187**(1.0 eq.); **76**(1.5 eq.)	Dimsyl sodium	phenothiazine	DMSO	no reaction

3	**186**(1.0 eq.); **76**(1.5 eq.)	K_2CO_3	N/A	DMF	no reaction
4	**187**(1.0 eq.); **76**(1.5 eq.)	K_2CO_3	N/A	DMF	no reaction
5	**186**(1.0 eq.); **190**(1.5 eq.)	Triethylamine	$Pd(dba)_3$	CH_2Cl_2	no reaction
6	**187**(1.0 eq.); **190**(1.5 eq.)	Triethylamine	$Pd(dba)_3$	CH_2Cl_2	no reaction

Considering the failure of these distinct coupling strategies, we hypothesized that the product from the hydrolysis, epoxide rearrangement sequence, might not correspond to the originally determined structure **187**. Likely it was a related compound with similar spectral features.

Mass spectrometric analysis confirmed that the product designated as structure **187** possessed the expected molecular formula. Similarly, the number of chemical environments observed in the NMR spectra matched the anticipated structure. Despite the value of the coupling constants of the olefinic protons being within the anticipated range, careful analysis of the NMR spectra revealed a discrepancy. In molecule **187**, the enolic hydroxyl group, influenced by the pendent alkene and the adjacent carboxyl group, is expected to exhibit a reduced electron cloud density around the hydrogen nucleus. This reduction should result in a downfield shift of the peak. However, this expected shift was not observed in the recorded spectra. Additionally, the hydrogen signal corresponding to the α-H of the hydroxyl group (which was previously assigned as an O-H) was clearly observed in the ^{1}H NMR spectrum (Figure 2.2).

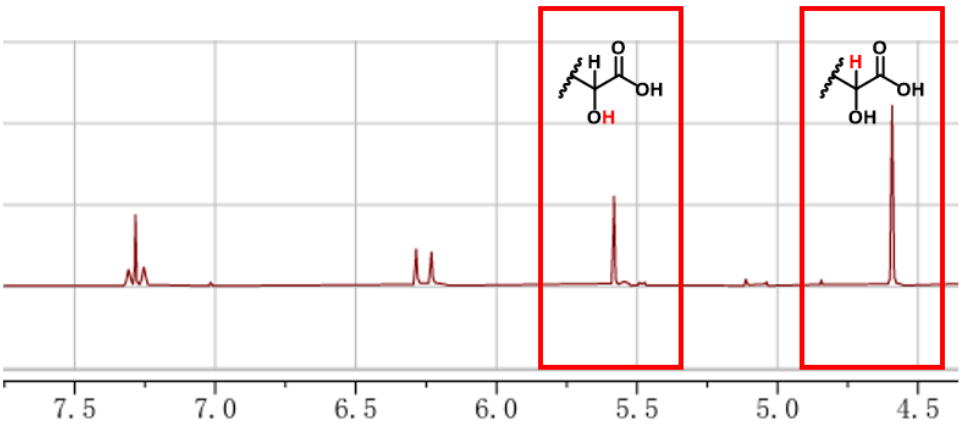

Figure 2.2: Partial ^{1}H NMR spectrum and structural analysis.

Based on the above reasoning, the re-analysis of the characterization data allowed us to assign previously reported hydrolysis, epoxide rearranged as molecule **202** (Scheme 2.11).

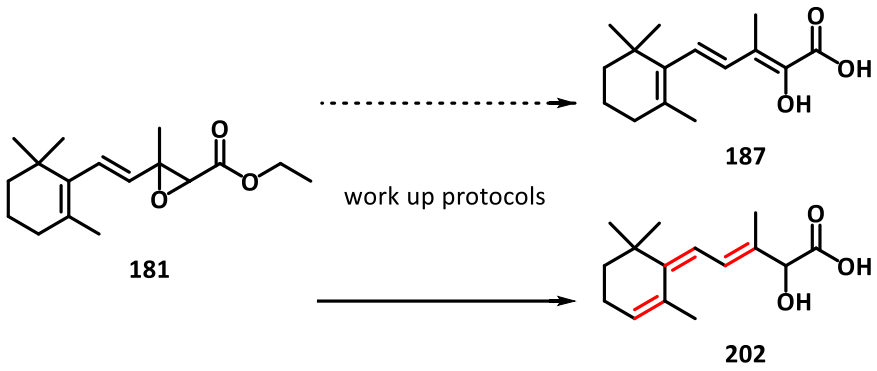

Scheme 2.11: Exact hydrolysis reaction of compound **181**.

In a bid to repeat the literature precedent, the reported procedure was repeated multiple times on α,β-epoxy ester **181**, using modified work-up protocols. In every instance, the product generated was the undesired compound **202**. In contrast to the literature report, protonation of the epoxide oxygen does not result in a [1,2]-hydride shift. Instead, deprotonation of the doubly vinylogous ring proton occurs, giving conjugated triene system of **202**. Considering that NMR spectroscopy had not been developed in the 1940s, the methods available for characterizing compounds at the time were inherently limited. This work corrects that erroneous report.

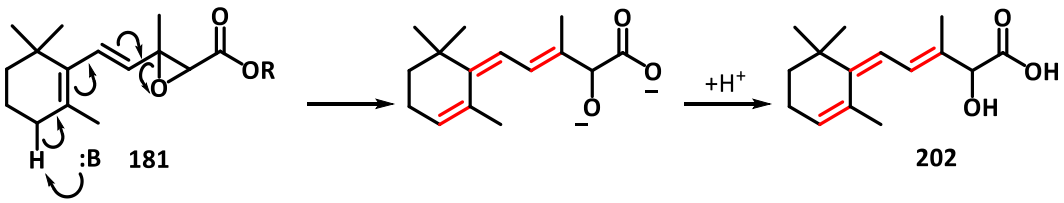

Scheme 2.12: Mechanism of producing non-desired compound **202**.

Consequently, the esterification product with *N*-hydroxyphthalimide is also not the intermediate **185** proposed in the retrosynthetic analysis, but instead the secondary hydroxyl-substituted ester **203** (Scheme 2.13). Since molecule **203** lacks the enolic

structure required for the final coupling step, the failure of the various coupling reactions described in Table **2.2** is therefore explained.

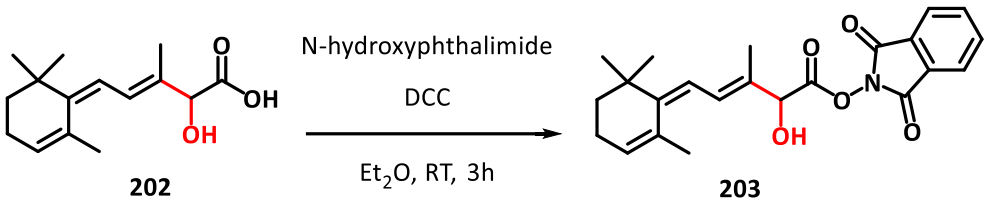

202 **203**

Scheme 2.13: Exact reaction of compound **202**.

Attempts were made to isomerize the triene system of **202** to give the desired enol product **187**. However, treatment of compound **202** with strong acid or base led to compound decomposition. Failure of our efforts to generate intermediate **186** and **187** led us to radically revise our synthetic approach.

2.3 Chemoselective Approach via Cross Coupling

Among the many advancements in synthetic chemistry, cross-coupling reactions have emerged as some of the most famous and widely utilized methods. This section describes the investigation of a cost-effective and chemoselective approach to carlactone, based on a metal-catalyzed cross-coupling reaction.

2.3.1 Retrosynthetic Analysis

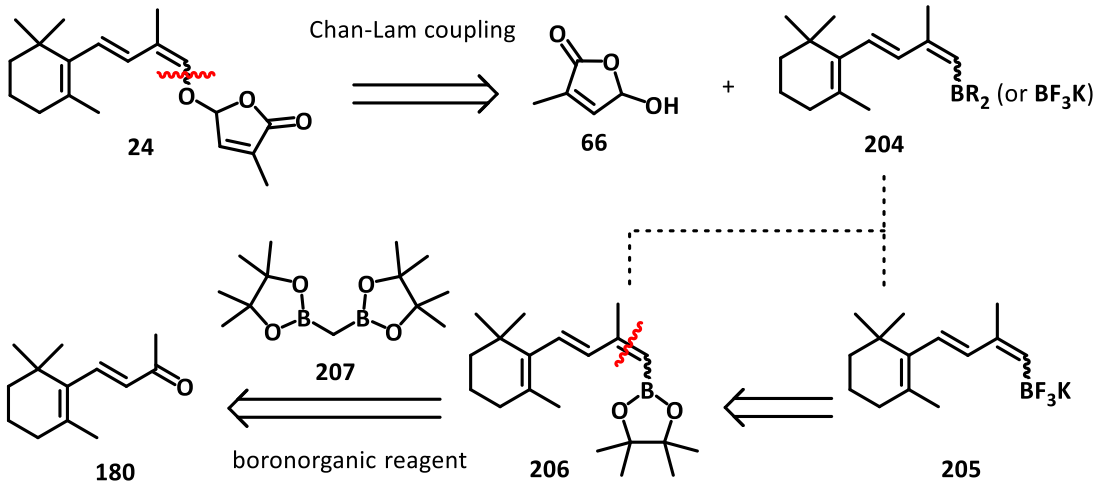

Scheme 2.14: Retrosynthesis of chemoselective approach via cross coupling.

Our revised retrosynthetic analysis is depicted in Scheme 2.14. In contrast to the reported syntheses of CL that rely on enol alkylation, we elected to disconnect the CL structure at the adjacent C-O bond to reveal the known hydroxy butenolide **66** (see Scheme 2.4 for details), and the vinylboron compound **204**. Vinyl boron species **204** was further disconnected via a (retro) boron-Wittig reaction to reveal β-ionone (**180**) as an appropriate starting material.

Key to the success of this strategy, is the metal-catalysed cross-coupling vinyl boron compound **204** with the oxygen atom of compound **66**. Among various cross-coupling reactions, we anticipated the copper-catalyzed Chan-Lam reaction, would be most appropriate.

2.3.2 Cross Coupling Reactions & Chan-Lam Coupling Reaction

Cross-coupling reaction, which have broad substrate scope, unite two molecular fragments to form a new carbon-carbon or carbon-heteroatom (N, O) bond typically with high selectivity (Scheme 2.15).[130] Cross-coupling reactions typically require the use of metal catalysts (palladium,[131,132] copper,[133,134] nickel[135] etc.) to facilitate the bond formation.

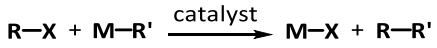

Scheme 2.15: General equation of cross coupling.

The Chan-Lam coupling is a copper-catalysed cross coupling reaction, reported independently by Chan[134] and Lam[133] in simultaneous publications. Both authors reported a novel method for forming C-N and C-O bonds between aromatic boronic acids and alcohols or amines in the presence of copper acetate (Scheme 2.16).

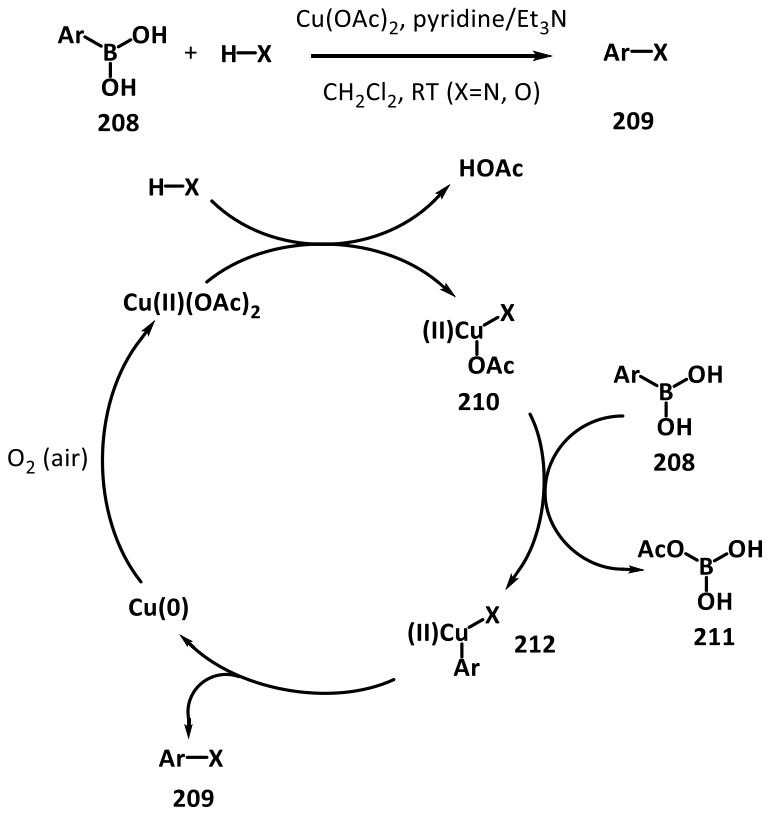

Scheme 2.16: Mechanism of Chan-Lam coupling reaction.

Since that pioneering work, organoboron pinacol esters **213** and organotrifluoroborates **214** have become chief actors in the Chan-Lam chemistry due to their higher reactivity and wider applicability.

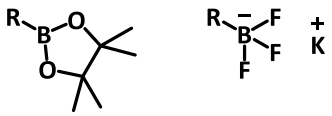

213 **214**

Figure 2.3: General structures of boron pinacol esters **213** and organotrifluoroborates **214**.

In addition to being easily synthesized from bis(pinacolato)diboron, organoboron compounds **213** possess another crucial advantage: their stability in the presence of moisture. Given these advantages, it is unsurprising that such compounds are widely utilized in the field of organoboron coupling reactions.[136,137]

Trifluoroborates **214** have even broader applications,[138] including but not limited to modified Suzuki-Miyaura reactions,[139,140] boron Mannich reactions,[141] organoboron esterification,[142] and rhodium-catalysed coupling reaction.[143] This versatility is attributed to their remarkable stability under various environmental conditions, such as exposure to moisture or oxygen in the air.[144] Additionally, these compounds are typically solid powders or crystals, making them easy to handle and manipulate in the laboratory.

2.3.3 Uncovering Reaction Conditions for the Chan-Lam Coupling

A large number of reaction conditions have been reported for the Chan-Lam coupling. The nature of the incoming nucleophile (an alcohol, an amine, or a carboxylic acid) has a profound impact on the reaction conditions required to effect the cross-coupling. In this work, the projected nucleophile is hydroxy butenolide **66**. The alcohol unit on this molecule is anticipated to have reactivity somewhere on the spectrum between archetypical secondary alcohols (low acidity, competent nucleophilicity) and archetypical carboxylic acids (high acidity, poor nucleophilicity). Additionally, we

anticipated that metal- or base-mediated ring-opening of compound **66** could produce a competitive carboxylate nucleophile. In order to identify appropriate reaction conditions for our projected Chan-Lam coupling, we utilized potassium phenyl trifluoroborate **216** as a model sp^2-boron containing coupling partner.

We began by following the procedure in Quach and Batey's initial report for using trifluoroborate salts in Chan-Lam coupling reactions.[145] We evaluated the differences across multiple aspects including catalyst loading, base loading, reaction duration, solvent identity, and reaction temperature (Table 2.3).

Table 2.3: Trials on Quach and Matey's protocol.[145]

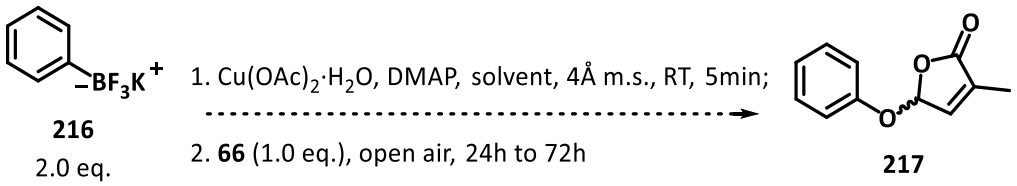

216
2.0 eq.

217

Entry	$Cu(OAc)_2$ Equiv.	DMAP Equiv.	Solv. & Temp.	Time (h)	Result
1	10 mol%	20 mol%	CH_2Cl_2, RT	24h	no reaction
2	20 mol%	20 mol%	CH_2Cl_2, RT	24h	no reaction
3	50 mol%	20 mol%	CH_2Cl_2, RT	24h	no reaction
4	50 mol%	50 mol%	CH_2Cl_2, RT	24h	no reaction
5	50 mol%	100 mol%	CH_2Cl_2, RT	24h	trace
6	10 mol%	20 mol%	CH_2Cl_2, 40°C	24h	no reaction
7	50 mol%	100 mol%	CH_2Cl_2, 40°C	24h	trace
8	10 mol%	20 mol%	CH_3CN, RT	24h	no reaction
9	10 mol%	20 mol%	CH_3CN, 82°C	24h	no reaction
10	50 mol%	100 mol%	CH_2Cl_2, RT	72h	trace

To compare the influence of the catalyst loading, entries 1, 2, and 3 were designed as the catalyst amount increased from 10 mol% to 20 mol% and 50 mol%. Similarly, entries 3, 4, and 5 were used to assess the effect of base loading. Furthermore, entries 5, 7 and 8, 9 investigated the influence of temperature and solvent. Finally, entry 10

was essentially entry 5 with an additional 48 hours of stirring, which helped evaluate the effect of reaction duration. Unfortunately, none of the attempted couplings were successful. However, ^{1}H NMR analysis of the crude reaction mixtures from entries 5, 7, and 10 showed signals that may correspond to the desired product, indicating that the reaction might necessitate a relatively large amount of copper salt and base.

As such the reaction was attempted with increased amounts of copper acetate and DMAP, as shown in Table 2.4.

Table 2.4: Trials focusing on larger amounts of $Cu(OAc)_2 \cdot H_2O$ & DMAP.

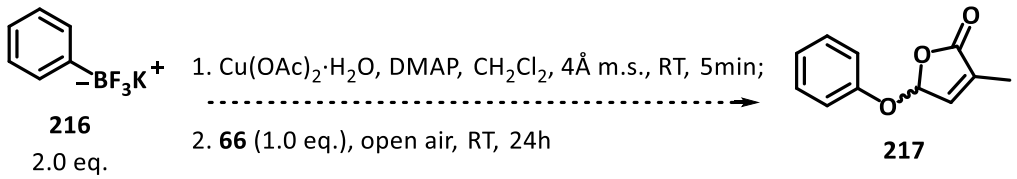

216
2.0 eq.

217

Entry	$Cu(OAc)_2$ Equiv.	DMAP Equiv.	Result
1	100 mol%	100 mol%	trace
2	200 mol%	100 mol%	trace
3	50 mol%	200 mol%	trace
4	50 mol%	300 mol%	trace

Disappointingly, the significantly increased amounts of copper acetate and DMAP had no effort on promoting the reaction cross-coupling.

A recent advance in Chan-Lam coupling reactions reported by Maarseveen and co-workers, attracted our attention. Their work focused on the coupling reaction between the pyridinium complexes of alkenyl boroxines **219** and aromatic carboxylic acids **218**. Maarseveen's optimized conditions used copper triflate as the metal source, triethylamine as the base, and 1,3-diethylurea as a key additives.[146]

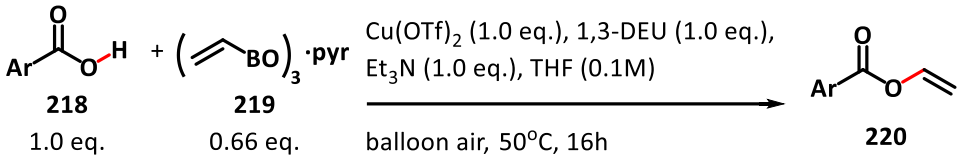

Scheme 2.17: Maarseveen's Chan-Lam coupling method.[146]

As illustrated in Scheme 2.18, we employed identical catalyst loadings and reaction conditions in a bid to affect the cross-coupling of compound **216** and **66**.

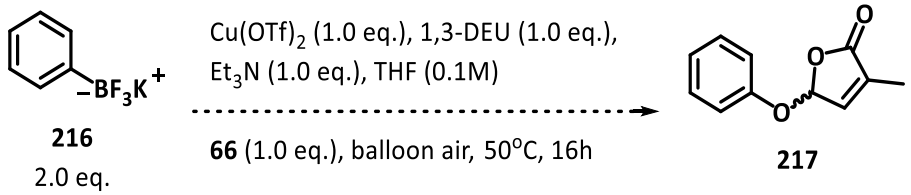

Scheme 2.18: Trials with Maarseveen's condition.

Again, the reaction did not yield any new products, indicating that the optimized reaction conditions were only suitable carboxylic acids and not the less acidic alcohol of compound **66**.

Batey and co-workers have reported Chan-Lan couplings of both alcohols and carboxylic acids. Those researchers found that in addition to commonly employed copper (II) salts (such as copper acetate), copper(I) bromide could also serve as a catalyst for the coupling of alkenyl or aromatic carboxylic acids and trifluoroborates Scheme 2.19.[147]

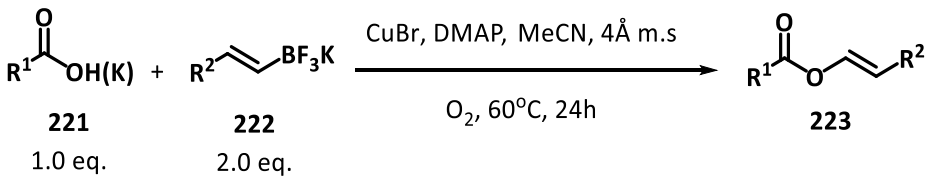

Scheme 2.19: Huang and Batey's Chan-Lam coupling.[147]

Accordingly, we again made modifications to the reaction conditions for the attempted cross-coupling (Table 2.5). Copper acetate monohydrate was replaced with copper(I) bromide, and the solvent was switched from dichloromethane to acetonitrile.

Table 2.5: Trials on Huang and Matey's protocol.[35]

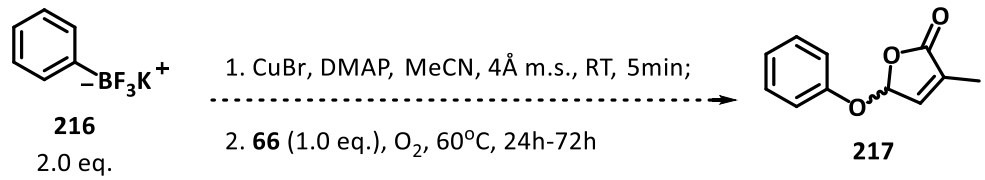

Entry	CuBr Equiv.	DMAP Equiv.	Time (h)	Result
1	10 mol%	20 mol%	24h	no reaction
2	50 mol%	20 mol%	24h	no reaction
3	50 mol%	100 mol%	24h	no reaction
4	50 mol%	100 mol%	72h	no reaction

The outcomes from those efforts were discouraging, with no trace of the desired product being detected even after prolonged reaction times.

Table 2.6: Trials on Sui, Xiong and Ye's protocol.[148]

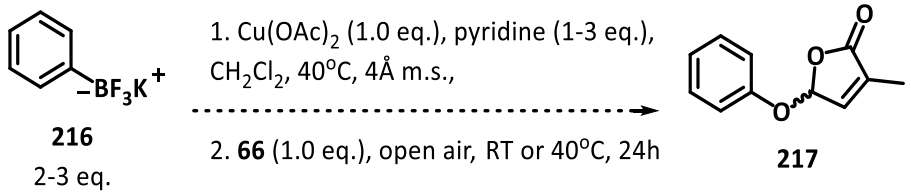

Entry	206 Equiv.	pyridine Equiv.	Temperature	Result
1	2.0 eq.	1.0 eq.	RT	no reaction
2	2.0 eq.	1.0 eq.	40°C	no reaction
3	3.0 eq.	1.0 eq.	40°C	no reaction
4	2.0 eq.	2.0 eq.	RT	trace
5	2.0 eq.	2.0 eq.	40°C	trace
6	3.0 eq.	2.0 eq.	RT	trace
7	3.0 eq.	3.0 eq.	RT	trace

Clearly, Chan-Lam coupling with the hydroxy butenolide compound **66** was far from trivial. We hypothesized that the reactivity of compound **66** may be more similar to a sugar than either an archetypical alcohol or carboxylic acid. As such we followed the work of Sui, Xiong and Ye, who reported the cross-coupling of sugar substrates using pyridine as the base in refluxing dichloromethane, under air. Our efforts to couple compounds under those reaction conditions are shown above in Table 2.6.[148]

Whilst none of the attempted reaction conditions proved to practically useful, it was evident that the base loading had a noticeable influence on the reaction. Entries 4–7 in which super-stoichiometric quantities of pyridine were employed, revealed traces of the desired product by ^{1}H NMR analysis of the crude reaction mixtures.

Up to this point, three different copper salts had been employed as catalysts for the required cross-coupling reaction. However, after testing more than twenty different reaction combinations, we had failed to identify an effective protocol for achieving the Chan-Lam coupling of compound **66**.

2.3.4 Revised Mechanism of Chan-Lam Coupling & Breakthrough Conditions

Most early studies on the Chan-Lam coupling focussed on the identity of the copper salt. In contrast, Merlic and Shade reported a Chan-Lam procedure in which they emphasized the essential role of triethylamine in coupling reactions involving vinyl boronates and alcohols.[149] Jo and co-workers subsequently broadened the scope of potential reaction conditions after an extensive exploration of various bases and solvents.[150] Notably, Vantourout and Watson proposed that the Chan-Lam coupling was more likely to proceed effectively under oxidative conditions, such as in the presence of atmospheric oxygen. These insights opened promising new avenues for reaction optimization.[151]

In 2020, Dong and co-workers provided a detailed study on the mechanism of Chan-Lam coupling reactions catalyzed by copper acetate (Scheme 2.20).[152] Their research

underscored the critical role oxygen played in facilitating the reaction. (For ease of understanding, the starting material and product in the proposed mechanism are represented by the molecules **216** and **217** mentioned earlier). The mechanism proposed by Dong and co-workers was obviously different from traditional copper-catalyzed cross-coupling mechanisms, such as the Ullmann reaction. Instead, Dong proposed that it occurred through a copper (III) intermediate, representing a higher oxidation state of copper. This dual-cycle mechanism highlighted the critical role of the oxidant, offering new ideas for the methodological optimization of the final step in this synthetic route.

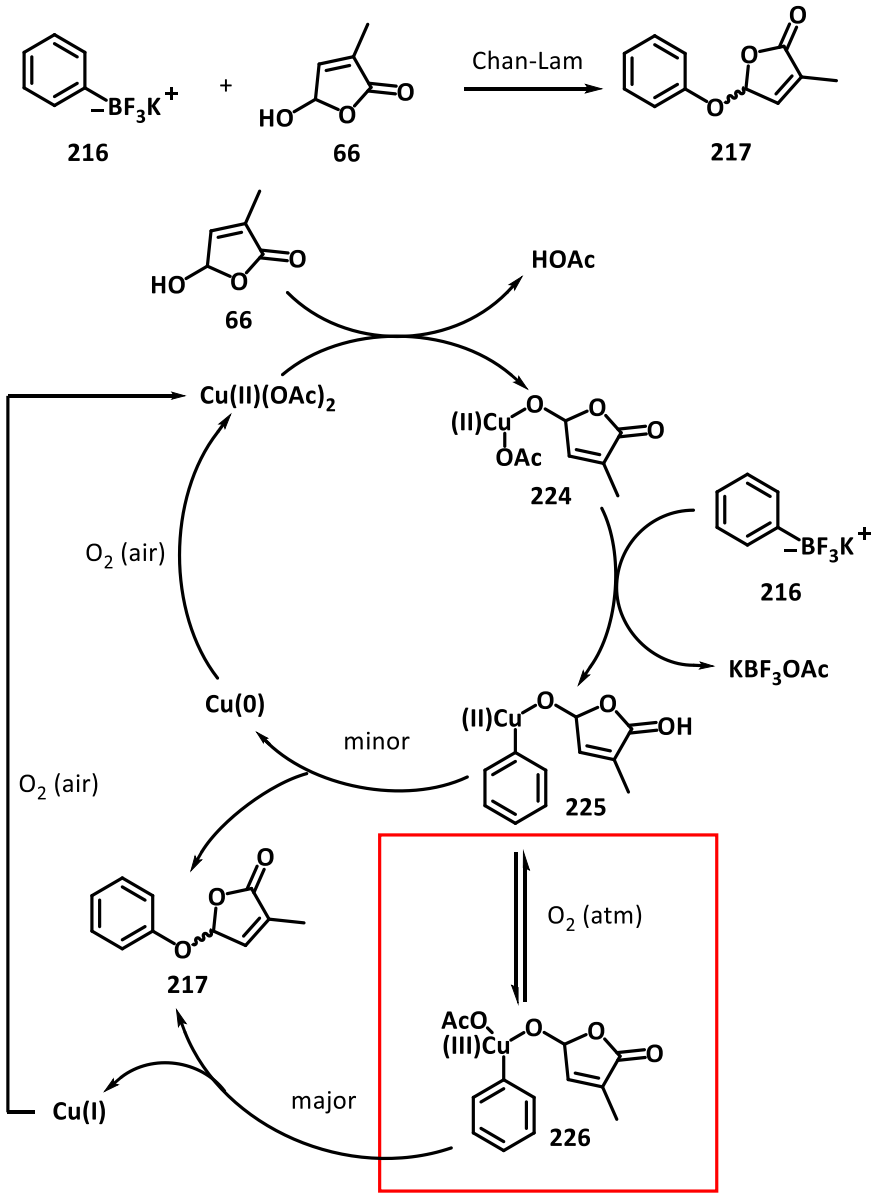

Scheme 2.20: Possible mechanism of Chan-Lam coupling.[149,152]

For the current work, we assessed that the hazards associated with using high purity O_2 under refluxing conditions, and the complexity of the reaction set-up, were sub-optimal. Instead, we examined the use of silver oxide as an alternative oxidant, and compared the outcomes to the O_2 mediated reactions. As a solid powder, silver oxide is not only easier to handle during the addition of reagents but also provides a lower risk profile than gaseous oxygen. The results of our investigation are shown in Table 2.7.

Table 2.7: Trials with O_2 and Ag_2O.

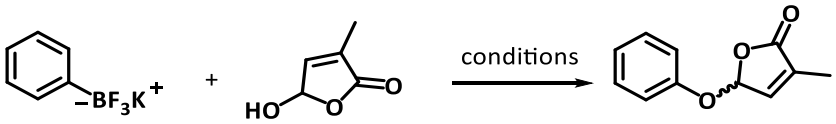

216 **66** (1.0 eq.) **217**

Entry	206 Equiv.	Cu salt & Equiv.	Base & Equiv.	Solv. & Temp.	Oxidants	Result
1	2.0 eq.	$Cu(OAc)_2$; 50mol%	DMAP; 1.0 eq.	CH_2Cl_2; 40°C	O_2 Ag_2O	trace
2	2.0 eq.	$Cu(OTf)_2$; 50mol%	Et_3N; 1.0 eq. 1,3-DEU; 1.0 eq.	THF; 60°C	O_2 Ag_2O	no reaction
3	2.0 eq.	CuBr; 50mol%	DMAP; 1.0 eq.	MeCN; 60°C	O_2 Ag_2O	no reaction
4	2.0 eq.	$Cu(OAc)_2$; 1.0 eq.	pyridine; 3.0 eq.	CH_2Cl_2; 40°C	O_2 Ag_2O	46% 52%
5	3.0 eq.	$Cu(OAc)_2$; 1.0 eq.	pyridine; 3.0 eq.	CH_2Cl_2; 40°C	O_2 Ag_2O	failed 43%

To our delight, reactions conditions that facilitated the desired cross-coupling to produce the product **216** were uncovered. In line with our previous observations, stoichiometric copper (II) acetate proved effective (entries 4 and 5). Similarly, the use of pyridine as the base was successful. And pleasingly, entries 4 and 5 demonstrated that silver oxide was superior to gaseous oxygen as the external oxidant.

After identifying the optimal reaction conditions to effect Chan-Lam cross coupling between the hydroxyl-containing butenolide **66** and an sp^2-trifluoroborate salt, our

attention turned to generation of the remaining coupling partner, compound trifluoroborate salt **205**.

2.3.5 Synthesis of the Organoboron Coupling Reagents

With a view to Chan-Lam coupling with butenolide **66**, two organoboron compounds containing the primary carbon backbone were developed: the potassium trifluoroborate salt **205**, and the corresponding pinacol boronate ester **206**.

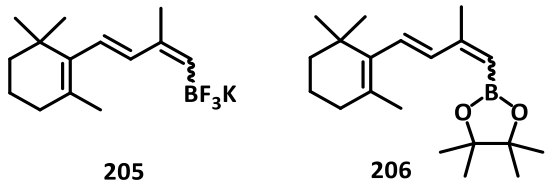

205 206

Figure 2.4: Structures of trifluoroborate **205** and pinacol ester **206**.

In order to employ a boron-Wittig reaction for the one-step synthesis of compound **206** from β-ionone (**180**), bis[(pinacolato)boryl]methane (**207**) was required and the proposed mechanism of its formation is shown in Scheme 2.21.

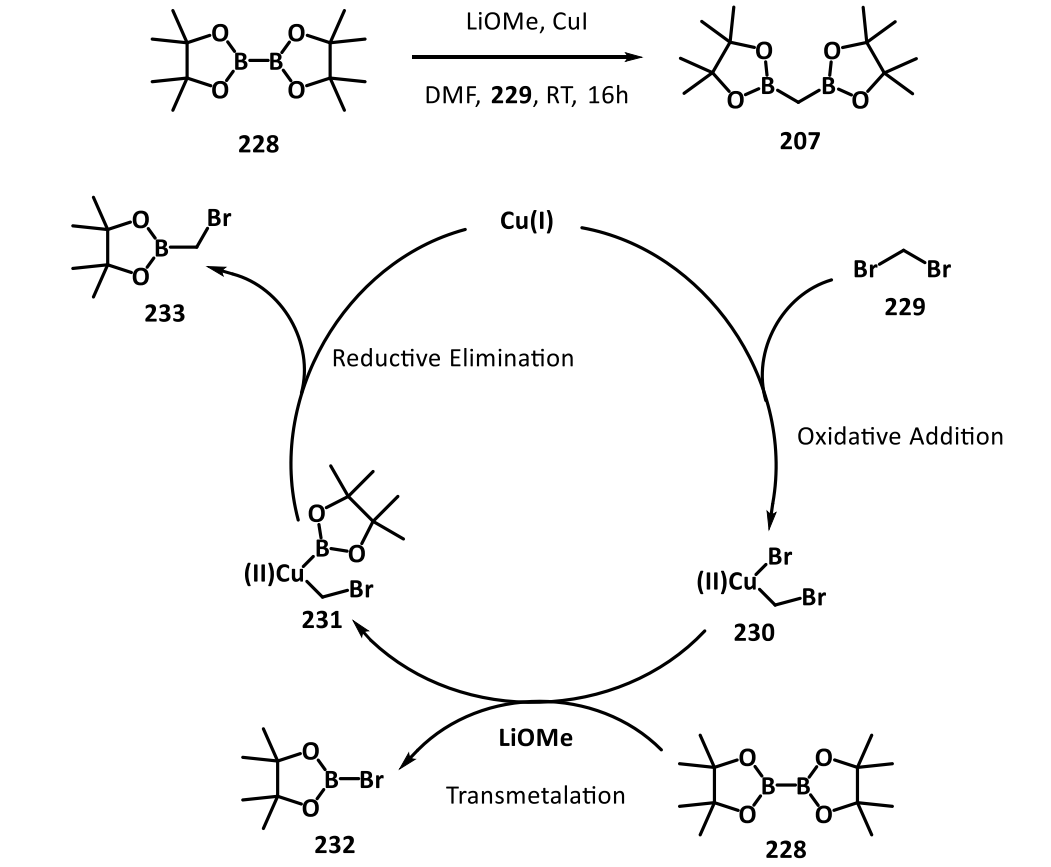

Intermediate **233** via another cycle to reach the product **207**:

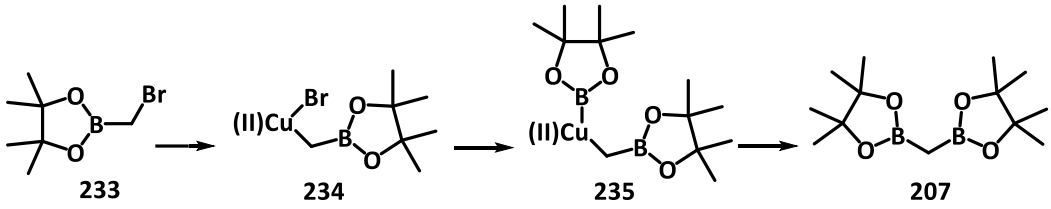

Scheme 2.21: Synthesis and proposed mechanism of methyl diboron **207**.

Reagent **207** was generated by a copper-catalysed double borylation of dibromomethane. Following the protocol for the first copper-catalyzed sp^3-carbon containing Suzuki-Miyaura reaction,[153,154] by a copper(I) iodide catalyzed carbon insertion from dibromomethane (**229**) into the B-B bond of commercial bis(pinacolato)diboron (**228**). This gave the reagent **207** in 63% yield.

Methyl diboronate **207** was then deprotonated with lithium tetramethylpiperidide (LiTMP) (which was generated *in situ* from *n*-BuLi and TMP) and reacted with β-

ionone (**180**) in a boron Wittig reaction. This gave the desired vinylboron ester **206** in 82% yield as a 1.3:1 mixture of geometric isomers (Scheme 2.22). [155,156]

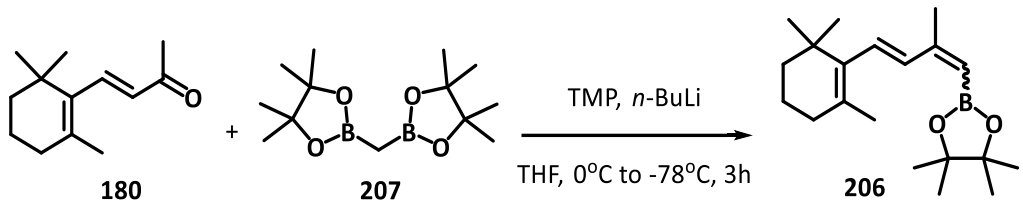

Scheme 2.22: Synthesis of β-ionyl boron ester **206**.

In analogy to the conventional Wittig reaction, the mechanism of this borono-Wittig reaction involved a four-membered ring intermediate (Scheme 2.23).[150] First, the reaction of n-BuLi with TMP generates LiTMP, which deprotonated the methyl group in intermediate **207** to form a carbanion. The use of LiTMP rather than n-BuLi is required to avoid direct addition to the boron atom, as occurs in Matteson-type homologation chemistry. The carbanion intermediate is stabilized by electron donation into the available boron centre. Nucleophilic attack of the carbanion onto the carbonyl unit of β-ionone (**180**), breaks the carbon-oxygen double bond. Formation of the borono-oxetane occurs in an unselective manner between the oxyanion and a pendent boron atom. Finally, the intermediate four-membered ring diastereomers underwent (likely stepwise) ring-opening process to yield the target product **206**.

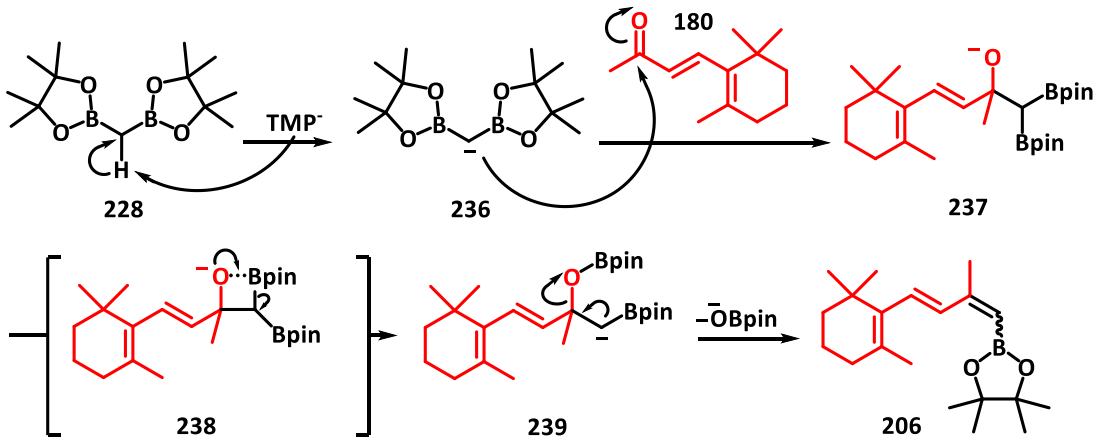

Scheme 2.23: Proposed mechanism of preparation of compound **206**.

At this stage, the 1.3:1 mixture of Z/E isomers of compound **206** (ratio was determined

by ^{1}H NMR analysis of the crude reaction mixture) could not be easily separated *via* flash chromatography. Therefore, the mixture was directly used in the subsequent reactions.

Conversion of the pinacol ester containing **206** into the corresponding trifluoroborate **205** was performed using the protocol of Lennox and Lloyd-Jones.[144] Their approach efficiently converted boronic esters directly into trifluoroborates. The use of tartaric acid as an additive was crucial for removing residual hydroxide to prevent hydrolysis of the tetrafluoroborate.

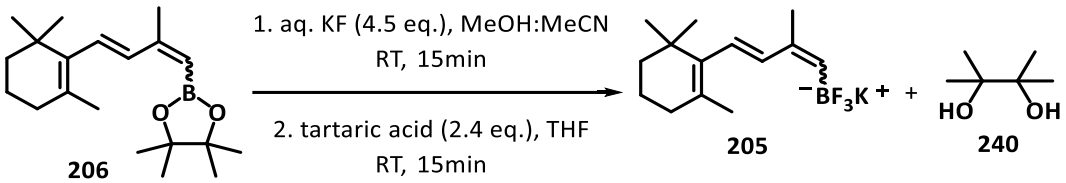

Scheme 2.24: Synthesis of trifluoroborate **205**.

Since the product vinyl boronate **205** was insoluble in dichloromethane, deuterated acetonitrile was chosen as the solvent for measuring the NMR spectra of this compound. These demonstrated that residual pinacol was present. Disappointingly, despite multiple attempts to remove excess pinacol **240** from the crude product through azeotropic evaporation with various alcohols, some pinacol remained. But fortunately, ^{11}B NMR analysis unambiguously revealed two distinct resonances corresponding to the *E*- and *Z*-trifluoroborates. Despite being contaminated with inseparable pinacol, the stage was set for the projected Chan-Lam coupling.

2.3.6 Final Coupling Step

The hydroxy butenolide **66**, the vinyl pinacolatoboronate **206**, and the vinyl trifluoroborate **205** were in hand. Optimized reaction conditions for the sp^{2}-boron alcohol coupling had been identified. Everything was in place for the final Chan-Lam cross-coupling to deliver CL (**24**).

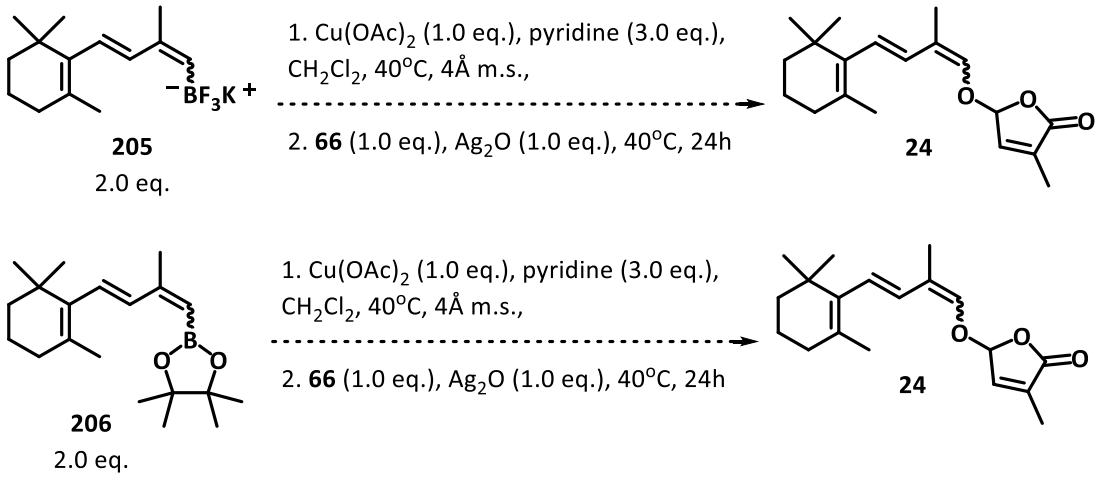

Scheme 2.25: Chan-Lam coupling final step utilizing the optimal conditions.

As depicted in Scheme 2.25, attempted coupling of either the vinyl pinacolatoboronate **206** or the vinyl trifluoroborate **205** with the hydroxy butenolide **66**, under the previously reaction conditions, failed to deliver even traces of CL (**24**).

This disappointing result suggested that the reactivity of the sp^2-C–B bond on both the vinyl boronate **206** and trifluoroborate **205**, were substantially different to the sp^2-C–B bond reactivity on the trifluoroborate salt used to identify the Chan-Lam cross-coupling conditions. Furthermore, ^{1}H NMR analysis of the reaction mixture revealed a highly complex mixture, from which no identifiable by-product could be observed. The organoboron species **206** and **205** did not survive the relatively mild reaction conditions.

Placing this disappointment aside, we attempted to identify Chan-Lam reaction conditions to affect the desired coupling that were compatible with the vinyl boronate reactants.

We began by repeating the original protocols published by Chan, Lam and their co-workers.[133,134] Two equivalents of pinacol boronate **206**, one equivalent of copper acetate, two equivalents of base (triethylamine or pyridine) were employed, with the addition of one equivalent of butenolide **66** (Scheme 2.26) occurring under open air.

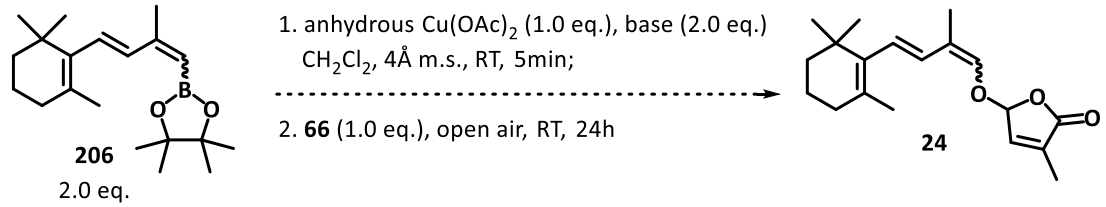

Scheme 2.26: The first trial with Chan and Lam's condition.[133,134]

Even after a reaction time of up to 48 hours, these reaction conditions failed to produce any of the targeted product, CL (**24**). Quach and Batey's report in 2003, which used trifluoroborate salt as starting material, informed our next attempts at the Chan-Lam coupling (Scheme 2.27).[145]

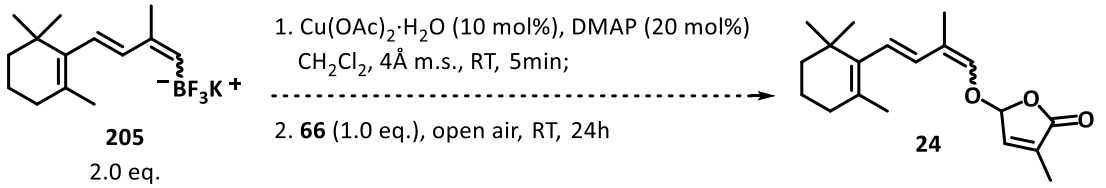

Scheme 2.27: Trial with Quach and Batey's condition.[145]

When catalytic amounts of copper catalyst and base were used, no CL was formed but the two coupling partners were re-isolated from the reaction mixture. This represented the first time that the vinyl boronate survived an attempted Chan-Lam coupling. However, we made some relevant observations: An unexpected colour change was observed after addition of the copper salt to the reaction mixture; and we had already determined that the vinyl boronate sample contained some residual pinacol. After careful consideration, we concluded that the copper was being sequestered by the residual pinacol to form a new complex. Although the identity of this copper complex was not unambiguously determined, it was obviously not catalytically active in the cross-coupling, nor Lewis acidic enough to decompose the vinyl boronate.

To circumvent the issue of residual pinacol in the sample of compound **205**, stoichiometric copper salt was employed to sequester any free pinacol in the reaction system. Increasing the amount of copper acetate monohydrate from 10 mol% to 1.1 equivalents, did not result in CL formation (Scheme 2.28). Further adding to our

frustration, trifluoroborate salt **205** underwent decomposition and could not be recovered

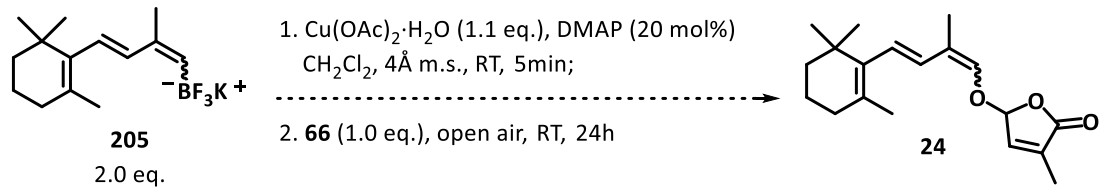

Scheme 2.28: Optimized trial with Quach and Batey's condition.[145]

The projected Chan-Lam coupling would have represented a novel synthetic strategy to CL and analogues. The butenolide and vinyl boronate coupling partners were both synthesized in short order. However, despite optimizing the Chan-Lam reaction conditions on the model substrate, potassium phenyl trifluoroborate (**216**), the desired cross-coupling could not be achieved. It was apparent that the boron compounds mentioned above were not compatible with the copper-catalyzed cross-coupling.

A new strategy for the cost-effective and chemoselective generation of carlactone was required.

2.4 A Nucleophile-Catalyzed Aldol-Lactonization (NCAL) Approach

The projected route to carlactone via the Darzens reaction focused on forming the oxygen-carbon bond between the enol oxygen and the butenolide ring (highlight in red in Figure 2.5). In contrast, the projected Chan-Lam route to carlactone focussed on the generation of the carbon-oxygen bond between the backbone alkene and an oxygen attached to the butenolide ring. This section introduces another approach: formation of the carbon-carbon double bond of the enol.

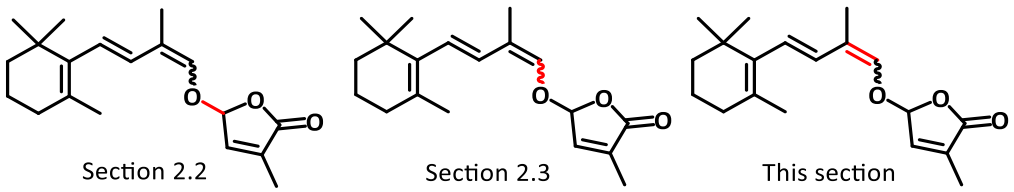

Figure 2.5: Comparison among three strategies mentioned in this chapter.

2.4.1 Retrosynthetic Analysis

Our retrosynthesis is depicted in Scheme 2.29. Many olefination methodologies exist, and our attention was drawn to the decarboxylative olefination of β-lactones. Therefore the initial step in our retrosynthetic analysis was to reconstitute a β-lactone **241** on the enol alkene. Disconnection of the four membered ring revealed β-ionone (**180**) and an hydroxyacetic acid equivalent with the pendent butenolide ring (**242** or **243**). Acid **242** was disconnected to reveal chloroacetic acid (**244**), (obtained from ethyl chloroacetate **188**), and the previously generated hydroxybutenolide **66**. Thiophenyl ester **243** was similarly disconnected to reveal thiophenol (**246**), chloroacetyl chloride (**247**), and hydroxybutenolide **66**.

In the forward sense, reaction between either hydroxyacetic acid equivalent **242** or **243** and β-ionone (**180**) would accomplish a Nucleophile-Catalyzed Aldol-Lactonization (NCAL) sequence to deliver the desired β-lactone. This protocol was first reported by Adam and Fick in 1979, and has been used in several reported syntheses. β-Lactones that contain electron-donating groups are known to undergo facile decarboxylation.[157]

So, we were confident that lactone **241** could be readily decarboxylated to give the target compound CL (**24**). The attraction to this route was the possibility of controlling the geometry of the newly formed alkene, by controlling the relative stereochemistry of the lactone ring.

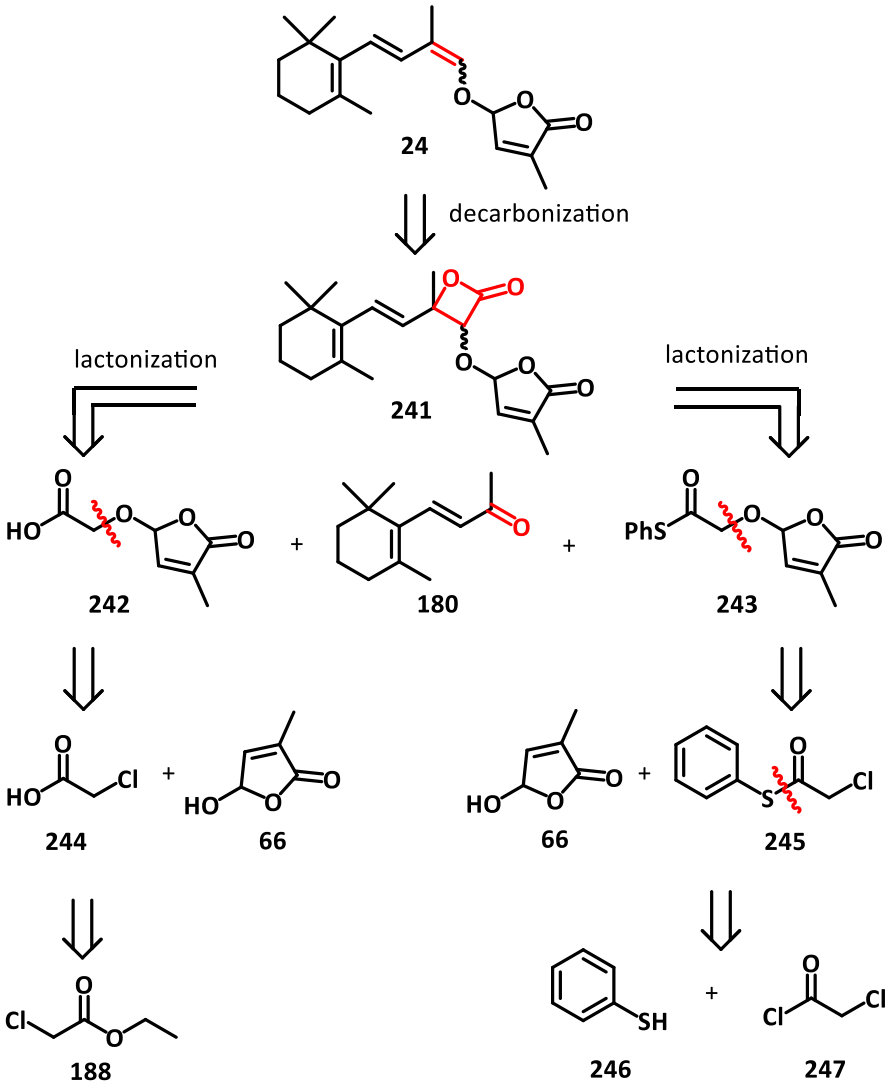

Scheme 2.29: Retrosynthesis of approaches forming the end double bond of conjugated chain.

2.4.2 Mechanism of NCAL and Related Reactions

In Adam and Fick's initial report, the generation of a double bond occurred in an intramolecular fashion from the corresponding hydroxy carboxylic acid **248** (Scheme 2.30).[157] Activation of the alcohol as a phenylsulfonate allowed intramolecular

displacement by the carboxylate to give the β-lactone (**249**). The cheletropic decarboxylation delivered the corresponding alkene (**250**).

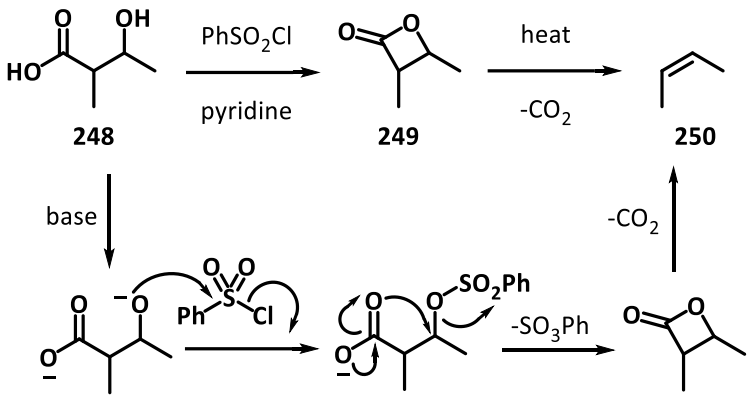

Scheme 2.30: Adam and Fick's strategy.[157]

Basing on that initial report, Romo and co-workers developed an intramolecular, long-chain NCAL using a modified Mukaiyama pyridinium salt (**254**). Achieving the stereoselectivity by utilizing compound **253**, the activation of the acid with salt **254** enabled deprotonation and subsequent NCAL to give lactone **252** (Scheme 2.31).[158,159]

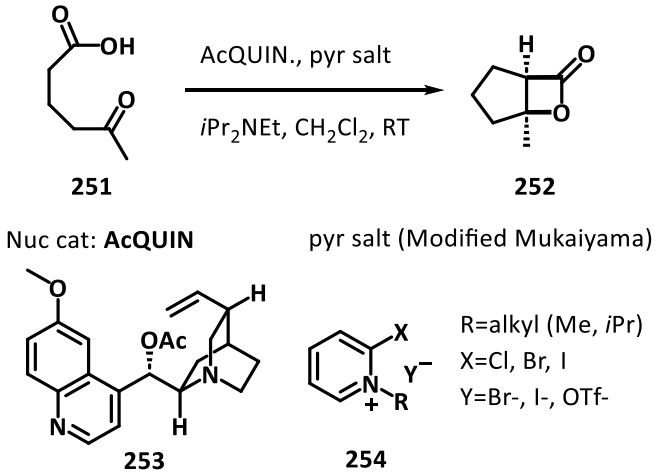

Scheme 2.31: Romo's NCAL strategy.[158,159]

Danheiser and Nowick developed NCAL methodology that was similar to the work of Adam and Fick (Scheme 2.32), but the use of thioesters significantly extended the process to include intermolecular reactions.[160]

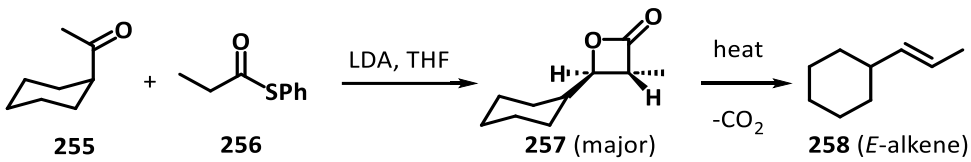

Scheme 2.32: Danheiser and Nowick's strategy.[160]

Furthermore, Danheiser's methodology enabled the stereoselective formation of the lactone through the effect of steric hindrance. Pleasingly, the configuration of the carbon-carbon double bond that results from decarboxylation, correlated to the relative stereochemistry of the lactone. Therefore, this methodology represents a stereoselective olefination.

2.4.3 Synthetic Efforts and Results of NCAL Approach

There are no literature examples in which the NCAL–decarboxylation sequence has been performed on unsaturated, or poly-unsaturated carbonyls. Our work began with a simple question: Were unsaturated carbonyl units competent substrates for the NCAL–decarboxylation process? Our initial work was based on the Romo's pyridinium-mediated NCAL.

The Mukaiyama pyridinium salt **261** was generated by heating a mixture of 2-bromopyridine (**259**) and 1-bromobutane (**260**) overnight, to give the desired compound as a light brown solid after recrystallization (Scheme 2.33).

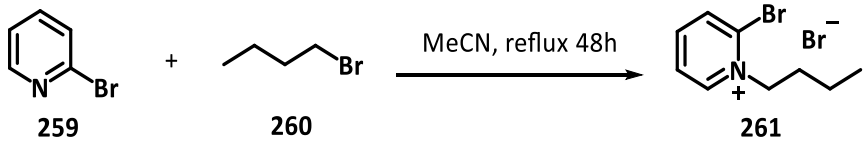

Scheme 2.33: Synthesis of pyridinium salt **261**.

To validate the feasibility of the NCAL–decarboxylation process on unsaturated aldehydes, cinnamaldehyde (**262**) was chosen as the substrate (Scheme 2.34). Heating a mixture of chloromethyl phenoxyacetic acid (**263**), pyridinium salt **261**, and cinnamaldehyde (**262**), in the presence of triethylamine, did indeed affect the desired

NCAL–decarboxylation sequence.

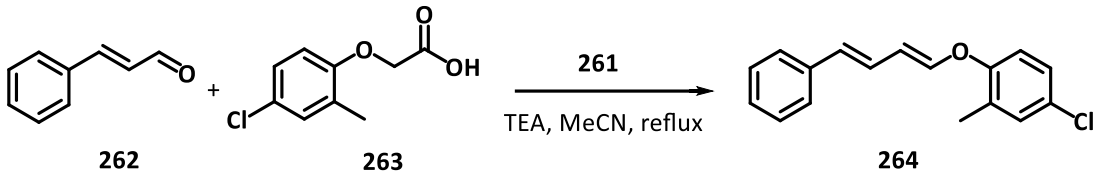

Scheme 2.34: Test reaction with cinnamaldehyde.

Analysis of the reaction mixture by ^{1}H NMR revealed starting material **262** and product **264**, but no intermediate lactone. As shown in Figure 2.6 the diagnostic signals for the dienol ether at 6.20 ppm and 6.64 ppm were easily observed. This ease of lactone decarboxylation augured well for the synthesis of the sensitive enol ether unit of CL.

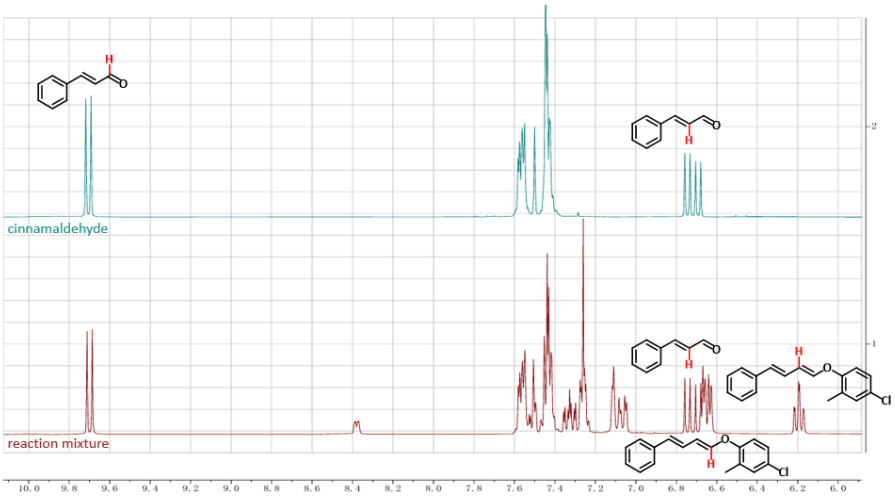

Figure 2.6: Test reaction with cinnamaldehyde **262** and ^{1}H NMR spectra comparison.

After showing that an unsaturated aldehyde underwent the desired reaction sequence, attention shifted to the corresponding unsaturated ketones. This time, 4-methyl pentenone (**265**) was selected as the representative substrate, as shown in Scheme 2.35. However, the reaction yielded a negative result. Heating a mixture of chloromethyl phenoxyacetic acid (**263**), pyridinium salt **261**, and unsaturated ketone **265**, in the presence of triethylamine, did not affect the desired sequence. In fact, those reaction conditions did not result in lactonization.

These outcomes demonstrate that the pyridinium salt method is effective in the NCAL reaction, but its utility does not extend to unsaturated ketones.

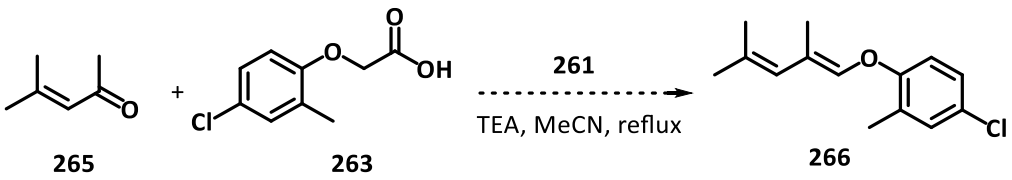

Scheme 2.35: Test reaction with molecule **266**.

We next explored a Danheiser-type procedure, employing thioester **243**. As depicted in Scheme 2.36, chloro-thioester **245** was successfully synthesized from thiophenol (**246**) and chloroethyl acetyl chloride (**247**), using DMAP catalysis. Subsequently, compound **243** was conveniently obtained via esterification with butenolide **66** in the presence of 2 equivalents of potassium carbonate and a catalytic amount of potassium iodide.

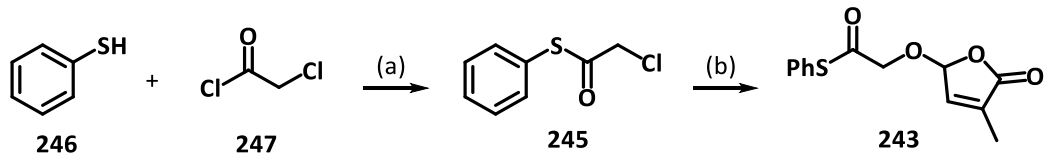

Scheme 2.36: Synthesis of compound **245** and **243**. Reagent and conditions: (a) pyridine, DMAP, CH_2Cl_2, 0℃ 30min then RT, overnight; (b) K_2CO_3 (2.0 eq.), KI (10mol%), acetone, RT, 24h.

The thioester **243** was then put into Danheiser and Nowick's protocol, reacting with LDA in THF to generate our desired *trans*-lactone **241** (Scheme 2.37).

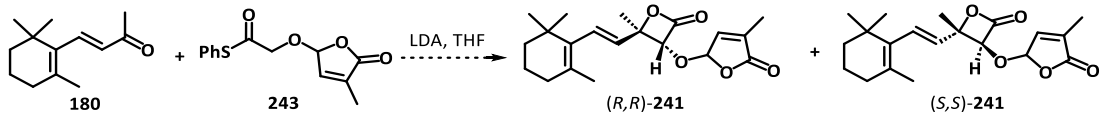

Scheme 2.37: Approach with thioester **243** *via* Danheiser and Nowick's strategy.

Possibly due to the decreased electrophilicity of the poly-unsaturated ketone, or the presence of competing acidic hydrogens on the methyl ketone, we did not detect any lactone products **241**, nor lactone-decarboxylation products in the crude reaction mixture. Frustratingly, neither of the starting materials could be identified or recovered, pointing to unknown reaction pathways. This outcome meant that both attempted NCAL-decarboxylation procedures failed on unsaturated ketones.

2.5 Summary

In this chapter, we explored three novel strategies for the cost-effective and chemoselective generation of carlactone.

The first approach via the Darzens reaction involved introduction of a bulky, leaving groups to lock the configuration of the enol double bond, thereby engendering chemoselectivity into the synthesis. However, this attempt was unsuccessful due to an unexpected double-bond migration during epoxide ring-opening. This outcome is in direct opposition to a literature report, and the actual product **202** could not be isomerized into the desired enol.

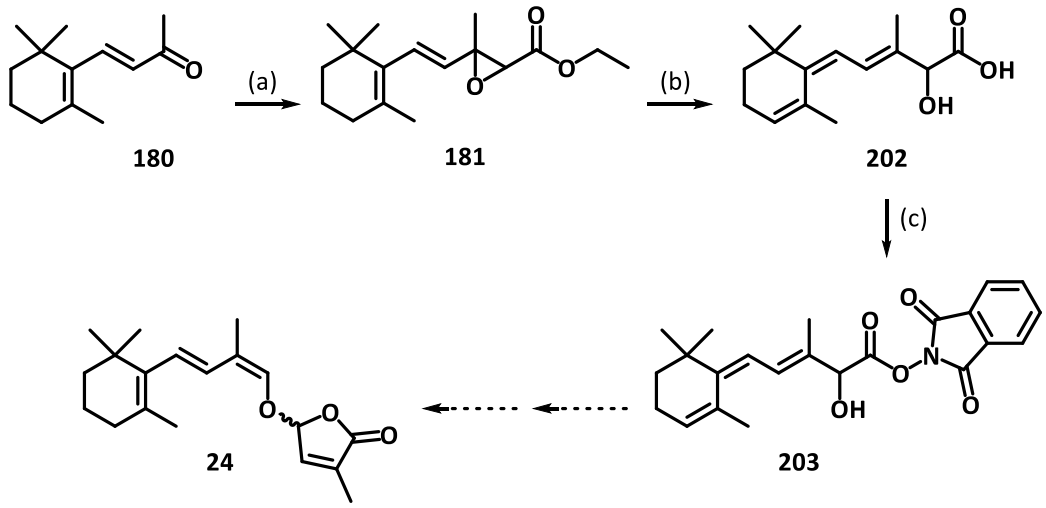

Scheme 2.38: The actual pathway of chemoselective route via Darzens reaction. Reagent and conditions: (a) **188** (2.0 eq.), NaOMe (1.1 eq.), -50°C, 4h then RT, 20h; (b) alcoholic potash then 1M HCl, excess sat. $NaHCO_3$ solution then 1M HCl; (c) N-hydroxyphthalimide, DCC, DMAP, Et_2O, RT, 3h.

The Chan-Lam coupling reaction was investigated as a means to generate the enol ether linkage from the corresponding vinyl boronate, extensively studied with various copper catalysts, bases, solvents, and oxidants such as oxygen and silver oxide by utilizing test molecule potassium phenyl trifluoroborate (**216**). Through this, we confirmed the necessity of oxidants like oxygen or silver oxide for the coupling process. However, as

the reactivity of the sp^2-C–B bond on the organoboron molecules we designed and prepared have been proved to be substantially different to the sp^2-C–B bond reactivity on the molecule used to identify the Chan-Lam cross-coupling conditions. The triene-containing vinyl boronates were incompatible with all attempted Chan-Lam reaction conditions. Based on the above results, we ultimately concluded that this route is not feasible for the chemoselective total synthesis of the carlactone molecule.

In the final part, an intermolecular NCAL–decarboxylation sequence was investigated. Pyridinium and thioester based reagents were employed for the key lactonizations on unsaturated aldehydes and ketones. Based on the current experimental outcomes, unsaturated aldehydes undergo the desired reaction, but unsaturated ketones are incompatible with the required reaction conditions.

There is a pressing need for a short, cost-effective strategy to access quantities of CL (**24**), radio-labelled CL, and selectively oxygenated CL analogues. Three such strategies were investigated in this work, but were ultimately unsuccessful. The quest for rapid access to the light-, acid-, base-, and temperature-sensitive plant-derived natural product, carlactone, remains unresolved.

3 SYNTHETIC WORK TOWARDS AVENAOL

The earliest report on avenaol was published by Yoneyama and co-workers in 2014.[38] They observed a root exudate from black oat during their botanical experiments, which demonstrated greater activity in stimulating the germination of *Orobanche minor* seeds than the corresponding exudates from rye. Moreover, no known SLs were detected in the root exudate using LC-MS/MS analysis. Yoneyama and co-workers isolated the molecule responsible for the bioactivity and named it avenaol (**25**) (Figure 3.1). Structural determination revealed that avenaol contained an immensely sterically congested cyclopropane unit and represented the most structurally complex non-canonical strigolactone isolated to date.

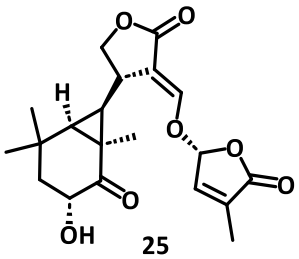

25

Figure 3.1: Actual structure of avenaol (**25**).

This chapter will focus on synthetic studies towards an advanced intermediate *en route* to avenaol. To fully appreciate the magnitude of the synthetic challenge, a discussion on the chemistry of the cyclopropyl structure in avenaol is essential.

3.1 Previous Total Synthesis Route of Avenaol

Due to the unusually sterically congested structure, the total synthesis of avenaol was not reported until 2017. Tsukano and co-workers from Kyoto University completed the synthesis in thirty five steps, achieving an overall yield of 0.14%.[161] Scheme 3.1 shows their successful strategy to the construction of the [4.1.0] ring system of avenaol.

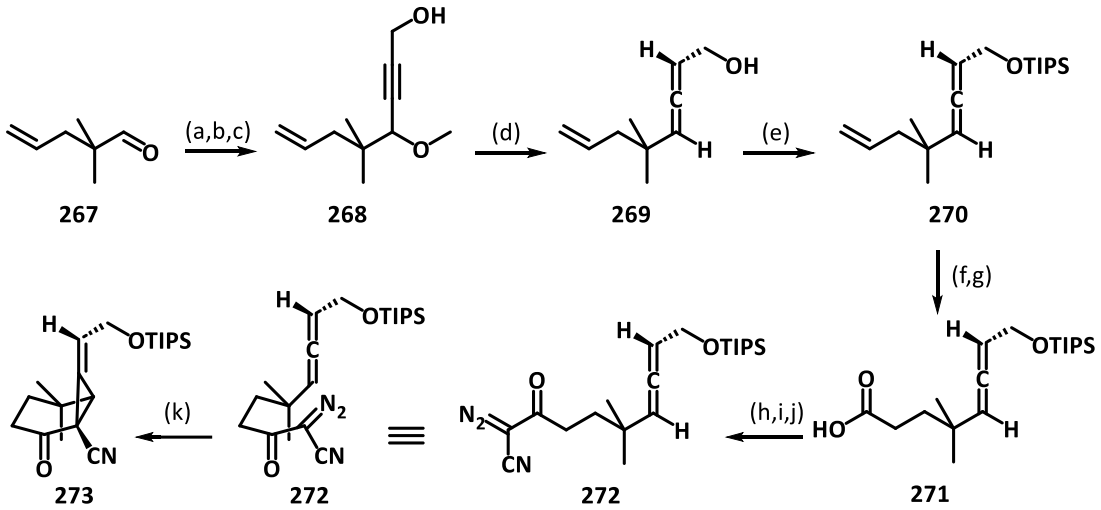

Scheme 3.1: Tsukano's synthesis on building [4.1.0] bridge ring.[161] Reagent and conditions: (a) $CH{\equiv}CCH_2OTHP$, $BnMe_3NOH$; (b) MeI, NaH; (c) *p*-TsOH, methanol; (d) $LiAlH_4$ then I_2, Et_2O; (e) TIPSCl, imid; (f) 9-BBN then NaOH aq., H_2O_2; (g) nor-AZADP, $PhI(OAc)_2$; (h) PivCl then methanol; (i) LiHMDS, MeCN, THF; (j) $imidSO_2N_3$; (k) $Rh(OAc)_4$.

Tsukano's synthetic work started from the commercially available aldehyde **267**, which was reacted with a propargylic acetylide and methylated with methyl iodide to give alcohol **268**. Allene formation was achieved by reaction of the propargyl alcohol with lithium aluminium hydride and subsequent treatment with iodine, to give compound **269**. Protection of the allenoic alcohol as a silyl ether gave compound **270**, which was subjected to a hydroboration, oxidation sequence to give the carboxylic acid **271**. Conversion of **271** into diazocyano compound **272**, the precursor for the key carbenoid cyclization step, was achieved over three steps. Construction of the [4.1.0] fused ring system ring was accomplished by treatment of diazocyano compound **272** with rhodium

tetraacetate, to affect the intramolecular cyclopropanation reaction and give compound **273**.

Compound **273** possessed the atom connectivity corresponding to the fused ring system of naturally occurring avenaol, but introduction of a stereocentre on the fused cyclopropane ring was still required. This proved non-trivial. Tsukano and co-workers achieved an important precursor, compound **276** (Scheme 3.2), through an additional six steps. Compound **276** served as the substrate for their highly innovative stereo-inducing step.

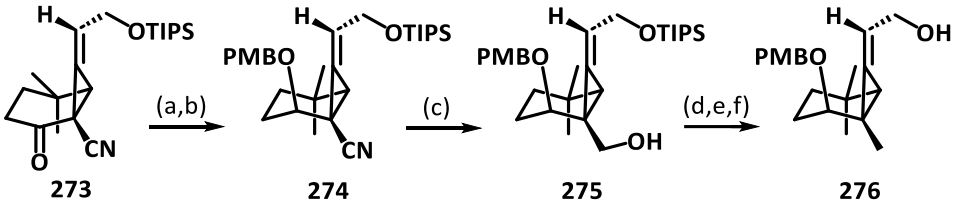

Scheme 3.2: Tsukano's synthesis to precursor **276**.[161] Reagent and conditions: (a) $NaBH_4$, $CeCl_3$, methanol; (b) PMBCl, NaH, NaI; (c) DIBAL-H then $NaBH_4$, methanol; (d) I_2, imid, PPh_3; (e) $NaBH_4$, DMSO; (f) TBAF.

The most remarkable step in Tsukano's total synthesis was the iridium-catalyzed stereoselective isomerization of compound **276**, which utilized steric hindrance as the stereo-selecting factor (Scheme 3.3).

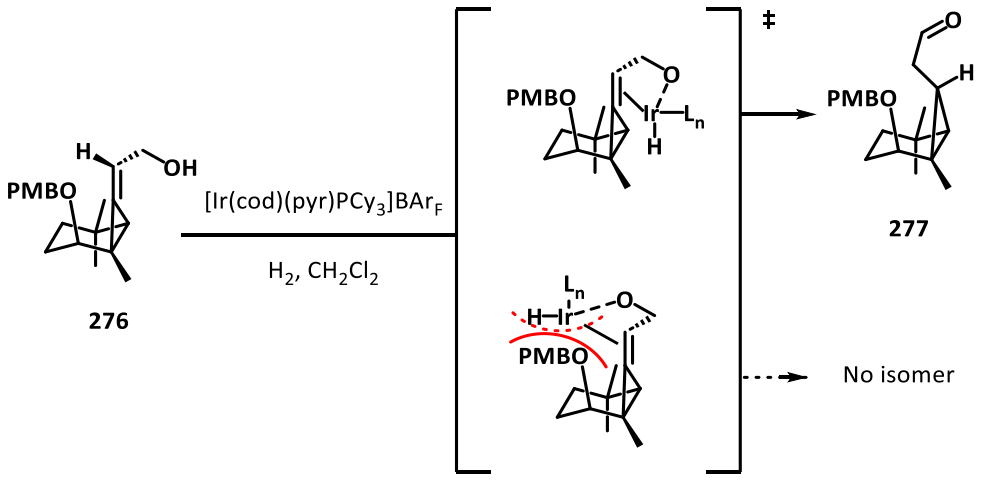

Scheme 3.3: The mechanism of Ir-catalyzed isomerization.

The all-*cis* configuration of avenaol's cyclopropane ring was controlled by the significant steric bulk of the complexed iridium species. As shown in Scheme 3.3 coordination of the tethered metal centre to the alkene was more likely to occur from the less hindered (*exo*) face. Subsequent hydrogen atom transfer to the *exo*-face of the alkene led to the formation of the desired all-*cis* cyclopropyl aldehyde **277**.

It is pertinent to note that construction of the [4.1.0] fused ring system required 18 synthetic operations. This highlights the synthetic challenge associated with the generation of this small, but complex natural product.

Eight further steps were applied to compound **277** to obtain alcohol **281** containing a lactone structure that corresponded to the C-ring in avenaol (Scheme 3.4). Moreover, compound **281** represents not only a significant milestone in Tsukano's synthetic route but also a key intermediate in our design, as will be discussed in the following paragraphs.

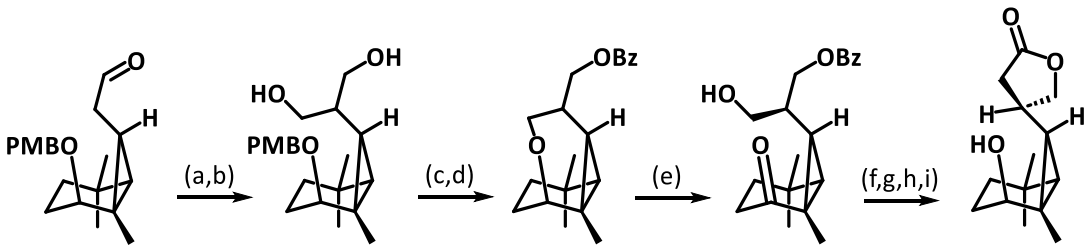

Scheme 3.4: Tsukano's synthesis to key intermediate **281** from compound **277**.[161] Reagent and conditions: (a) CH_2O aq., pyrrolidine, propanoic acid, $NaBH_4$; (b) BH_3·THF, NaOH, H_2O_2; (c) *p*-TsOH, PhSH; (d) BzCl, Et_3N; (e) TFDO; (f) MsCl, Et_3N; (g) NaCN; (h) DIBAL-H; (i) NaOH aq. then HCl aq.

As depicted in Scheme 3.4, non-selective aldol addition of formaldehyde to compound **277** afforded the diol **278**. Fortuitously, intramolecular cyclization of the diol **278** occurred in a stereoselective manner, which differentiated the two alcohol units of **278** and delivered (after protection) compound **279**. Oxidative ring opening with

trifluorodimethyldioxirane (TFDO) gave ketone **280**, which was homologated with cyanide and lactonized to give **281**.

The remaining steps in Tsukano's synthetic route are outlined in Scheme 3.5 and consist of a further seven steps, resulting in the formation of a racemic mixture of avenaol **25** and *epi*-**25**. In short, the alcohol unit of intermediate **281** was converted into an α-hydroxyketone via an elimination–oxidation sequence, and the enol ether appended butenolide (D-ring) was installed using the standard strigolactone end game strategy discussed in the first chapter. These operations delivered racemic avenaol (**25**) and its non-natural isomer *epi*-**25**.

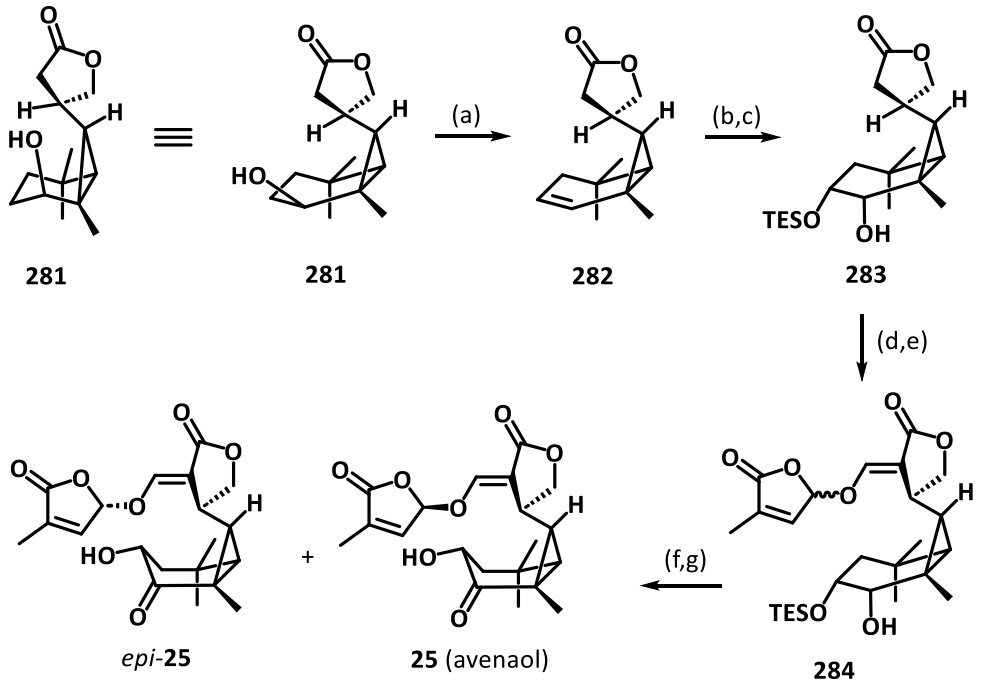

Scheme 3.5: Tsukano's ending strategy to avenaol from intermediate **281**.[161] Reagent and conditions: (a) *p*-TsOH, benzene; (b) OsO_4, NMO; (c) TESCl, imidazole; (d) *t*BuOK, methyl formate; (e) **76**, K_2CO_3, NMP; (f) Dess-Martin periodinane; (g) HF, pyridine.

Tsukano's total synthesis of avenaol is a landmark in strigolactone chemistry. However, with 35 operations required in total, it also highlights the opportunities that exist for innovation and improvement in the total synthesis of non-canonical strigolactones.

3.2 Approach *via* Intramolecular HWE Reaction

In this section, we will discuss a stereoselective synthetic route to avenaol *via* an intramolecular Horner-Wadsworth-Emmons (HWE) reaction to give Tsukano's intermediate **281**.

3.2.1 Retrosynthetic analysis

As depicted in Scheme 3.6, we planned on employing Tsukano's end game strategy, so avenaol was disconnected to reveal compound **281**, which was an intermediate in his reported total synthesis. The 5-membered lactone of **281** was envisaged to arise from a 7-membered lactone **285** via a functional group interconversion. Disconnection of the methoxy unit revealed the unsaturated lactone **286**, which we anticipated to be accessible from intermediate **287** via an intramolecular HWE reaction. Compound **287** contained an epimerizable aldehyde unit attached to the cyclopropane ring, which we planned on utilizing as the stereo-controlling entity. Disconnection of the phosphonate unit revealed a secondary alcohol, and functional group interconversions on the aldehyde, revealed α-hydroxyketone **290** as a likely intermediate. Concomitant disconnection of the secondary alcohol and ring-opening of the cyclopropane unit reveal epoxy ionone **291**, and ultimately α-ionone (**292**) as a suitable starting material.

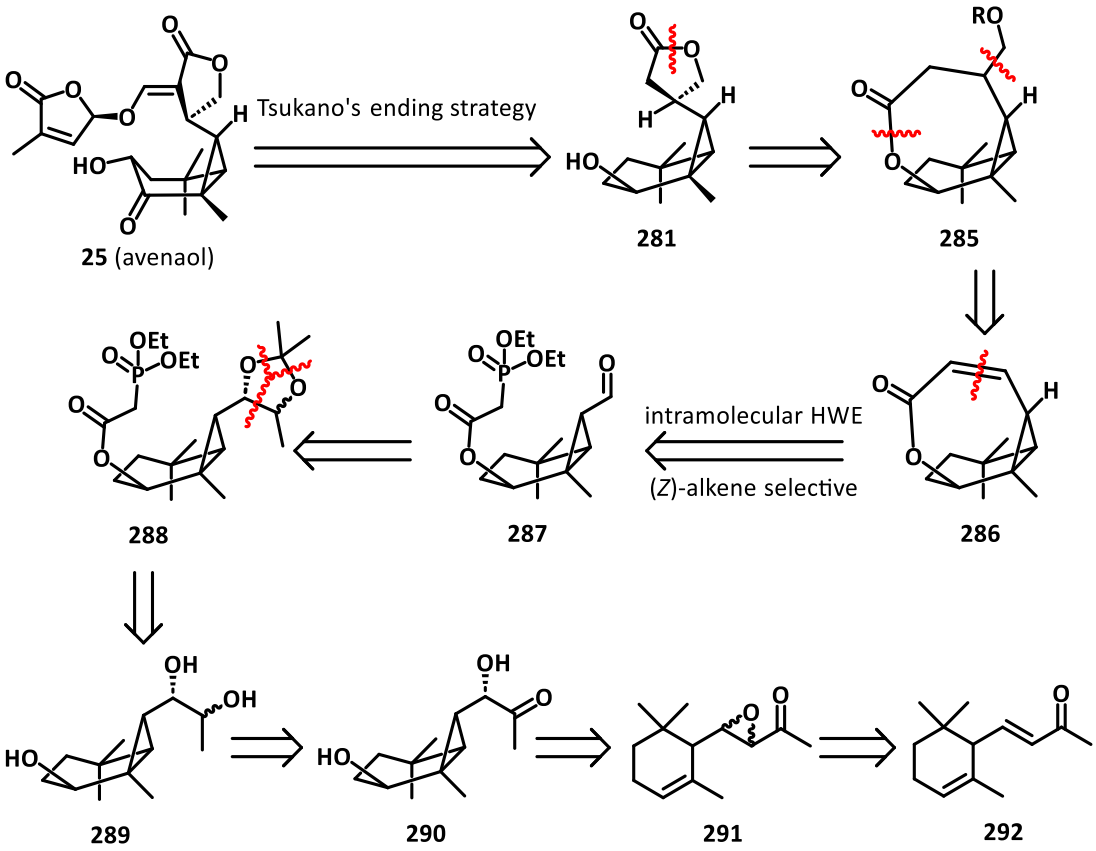

Scheme 3.6: Retrosynthesis to compound **281**.

Key to the success of our strategy was the ability of the *exo*-configured aldehyde in intermediate **287** to undergo epimerization under the HWE reaction conditions. Therefore, a short discussion on the HWE reaction is warranted.

3.2.2 Mechanism of Horner-Wadsworth-Emmons Reaction

The Horner–Wadsworth–Emmons (HWE) reaction is a type of olefination reaction widely used for synthesizing α,β-unsaturated carbonyl molecules by reacting stabilized phosphonate carbanions with the carbonyl units in ketones or aldehydes.[162–164]

The reaction was first published by Horner in 1958 as a modification of traditional Wittig reaction using phosphonium ylides.[165] Horner and co-workers replaced the unstable ylides by more stable phosphonate carbanions, which were more nucleophilic and easier to be alkylated. Moreover, the water-soluble byproducts were easier to remove. Shortly after Horner's report, Wadsworth and Emmons did the further

optimization of the reaction, which is now termed the Horner-Wadsworth-Emmons (HWE) reaction (Scheme 3.7).[166]

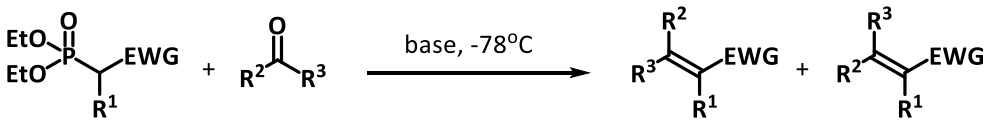

Scheme 3.7: General scheme of HWE reaction (EWG: electron withdrawing group).

2-(Dimethoxyphosphoryl)acetate (**293**) is the archetypically HWE reagent because of its reactivity and commercial availability. Studies of (*E*)-selective HWE reactions of the acetate **293** and aldehydes to give disubstituted alkenes, were reported by Thompson and Heathcock. They found that an increase in steric hindrance around the aldehyde, more forcing reaction conditions, and the use of smaller alkali metal ions, led to an increase in selectivity for the (*E*)-configured product.[167]

The mechanism of the HWE olefination is shown in Scheme 3.8, with the aldehyde component coloured red for ease of comprehension.

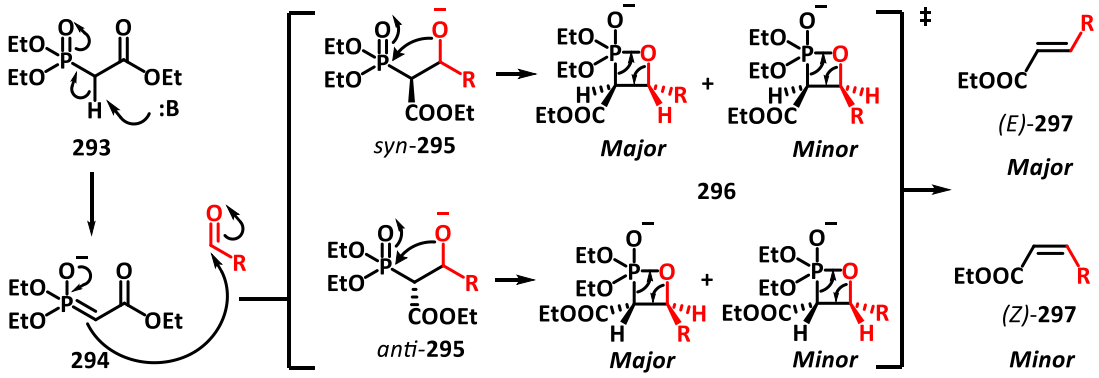

Scheme 3.8: Mechanism of HWE reaction.

Deprotonation of the reagent **293** by base generates the stabilized phosphonate carbanion **294**, which subsequently undergoes a nucleophilic attack on the carbonyl group of the aldehyde, forming the diastereomeric *syn*- and *anti*-hydroxyphosphonates **295**. The negatively charged oxygen in **295** then attacks the pendant phosphorus atom, resulting in the formation of diastereomeric oxaphosphetanes **296**. Steric hinderance

around the 4-membered ring induces diastereoselectivity. These intermediates then undergo cyclo-reversion to yield the major product, (*E*)-alkene **297**, along with the minor product, (*Z*)-alkene **297**.

For the current work towards the total synthesis of avenaol, the projected intramolecular HWE reaction will produce the (Z)-configured enolate, by virtue of the restraints of the 7-membered ring. But critically, the use of basic reaction conditions is anticipated to not only deprotonate the phosphonoacetate but also epimerize the *exo*-cyclopropyl aldehyde to give the necessary *endo*-cyclopropyl aldehyde.

3.2.3 Synthesis on Building Hydroxy [4.1.0] Bridge Ring Carbon Skeleton

In order to put our intramolecular HWE strategy into action, we first had to access the fused cyclopropyl aldehyde **287**. Weyerstahl and co-workers reported a cyclopropane synthesis intramolecular ring opening of a β, γ-unsaturated epoxide under aqueous acid condition. The starting material **298** in that work had an extremely similar structure with α-ionone.[168]

As shown in Scheme 3.9, Weyerstahl reported that the epoxide ring of **298** underwent acid-catalysed intramolecular reaction with the alkene, and subsequent quenching with water to give compound **299**. An intramolecular lactonization then rapidly occurred to form lactone **300**.

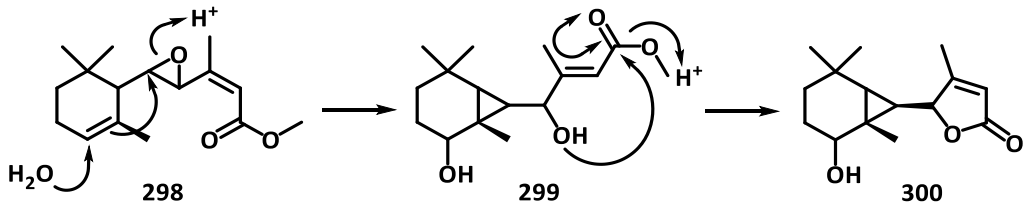

Scheme 3.9: Cyclopropanation by Weyerstahl.[168]

Weyerstahl achieved construction a challenging ring system in a single step which is directly relevant to our devised strategy. We anticipated acid-catalyzed ring-opening of α-ionyl epoxide **291** would form an α-hydroxyketone cyclopropane intermediate.

Or work began with synthesis of epoxide **291** (Scheme 3.10). We utilized hydrogen peroxide under basic conditions to oxidize α-ionone by nucleophilic attack from deprotonated peroxide onto the activated double bond. The steric hinderance provided by the geminal dimethyl unit meant that this reaction was very sluggish. To mitigate against the possible decomposition of the oxidant, additional basic hydrogen peroxide was periodically added to the reaction mixture, which was keep at 0 ºC for an extended period. This protocol provided access to **291** as a racemic mixture of diastereomers.

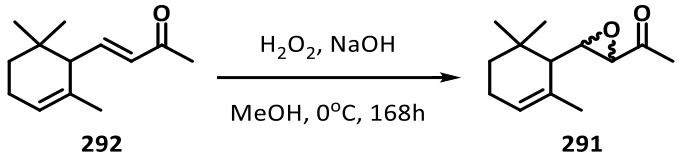

Scheme 3.10: Synthesis of epoxide **291**.

A former Honours student in the McErlean group, Mr. Zhiping Wang, conducted preliminary investigations into the intramolecular cyclopropanation of epoxide **291**. That work formed the basis for our reaction conditions.

Table 3.1: Stereoselective cyclopropanation of compound **291**.

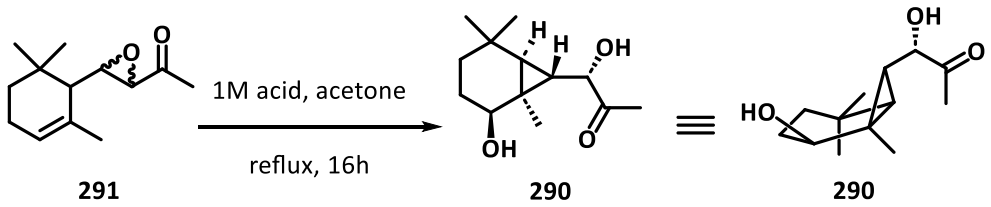

Entry	Acid	Reaction Temperature	Result & Yield
1	1 M H_2SO_4	reflux	stereoselective 25%
2	1 M HCl	reflux	stereoselective 19%
3	*p*-TsOH crystals	reflux	trace

As summarized in Table 3.1, we observed that the reactions catalyzed by sulfuric acid and hydrochloric acid proceeded efficiently, yielding the a single diastereomer of product **290** in moderate yield. However, the reaction catalyzed by *p*-TsOH showed poor performance. Proposed mechanism for the reaction is illustrated in Scheme 3.11.

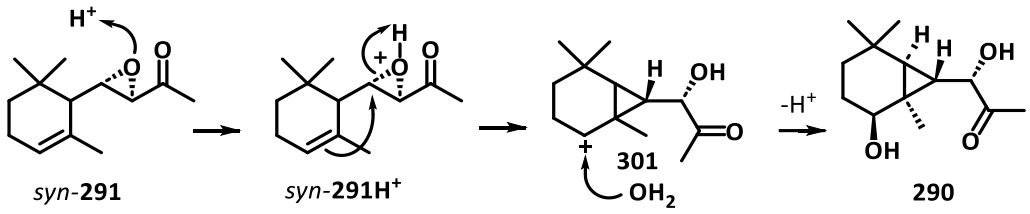

Scheme 3.11: Proposed mechanism of compound **291**'s cyclization.

We could rationalise this high level of diastereoselectivity based on the ground state conformations of the starting *anti*- and *syn*-diastereomers of epoxide **291**. As shown in Figure 3.2, the *anti*-diastereomer showed significant orbital overlap between the antibonding orbital of the breaking epoxide C–O bond of the epoxide and the π-bond of the alkene. Such overlap was absent for the *syn*-diastereomer.

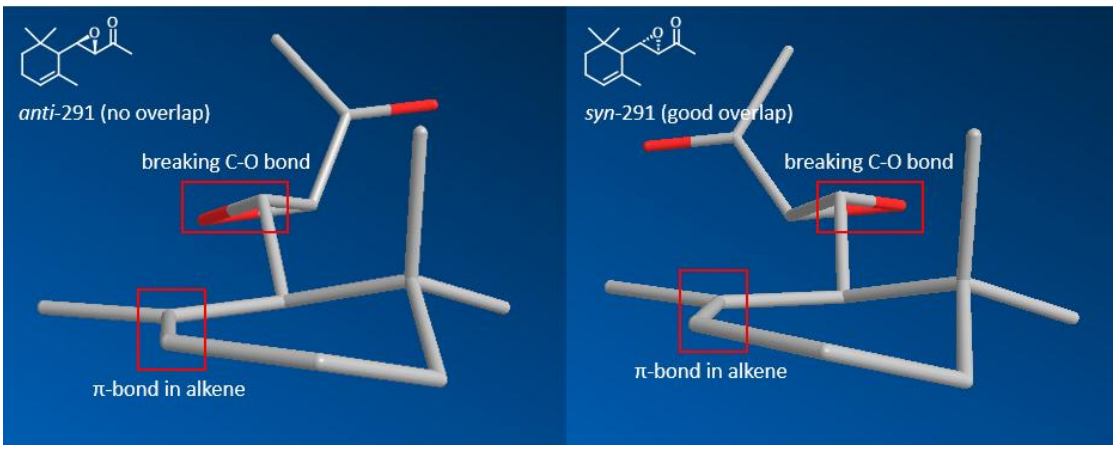

Figure 3.2: Explanation of the overlaps in different isomers *via* Chem3D.

Another noteworthy aspect of this transformation is the final step of the mechanism. According to the conventional reasoning, the hydroxyl group in the product would be stereochemically undefined, as it results from the attack of water onto a planar carbocation. However, in product **290**, the hydroxyl group on the ring is locked into a single relative configuration. Analysis of $^{3}J_{\text{H-H}}$ coupling constants, strongly indicates that the hydroxyl group was equatorially oriented on the ring.

We rationalize this observation by invoking H-bond chelation between the carbonyl group and a water molecule. Such chelation would differentiate the chemical environments of the upper and lower faces of the carbocation intermediate **301**, and

hydrogen bonding would render the chelated water molecule more nucleophilic than bulk water. These two effects account for the stereochemical locking of the hydroxyl group in product **290**. The specific mechanism has been shown in Scheme 3.12.

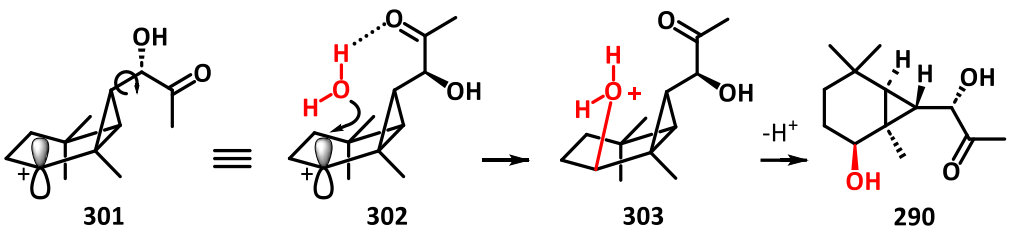

Scheme 3.12: Explanation of configuration-locked hydroxy group in compound **290**.

3.2.4 Construction of Intramolecular HWE Reaction Functional Groups

With hydroxy ketone **290** in hand as a single diastereomer, we proceeded with our planned strategy to incorporate two functional groups into the same compound, as outlined in Scheme 3.13. In this design, the hydroxy group on the A-ring was intended to serve as a handle for the phosphonate (red), while the side chain on the B-ring was to be converted into an aldehyde (green). The order in which to effect these transformations was not clear.

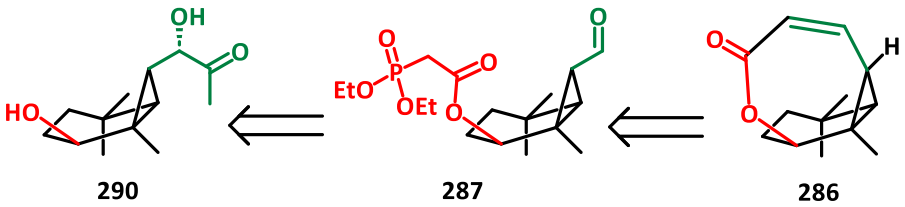

Scheme 3.13: Design idea on molecule **290** to molecule **287** & **286**.

Molecule **290** contains two secondary alcohol groups, and the α-keto alcohol on the side chain proved to be the more reactive. Therefore, attachment of the phosphonate unit to the cyclohexyl alcohol ring required selective protection of side-chain alcohol.

To achieve this, the α-hydroxy ketone was first reduced under Luche conditions, using sodium borohydride and cerium chloride.[169] This yielded diol **289** as an inconsequential mixture of *syn*- and *anti*-diastereomers, which were immediately

protected as the acetonides to afford protected compound **304** (Scheme 3.14).

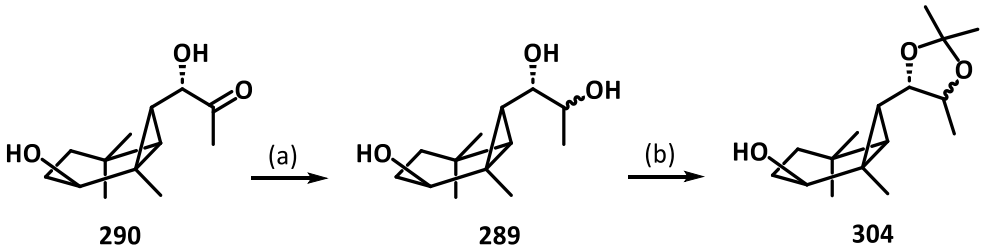

Scheme 3.14: Synthesis route towards acetonide **304**. Reagent and conditions: (a) $CeCl_3 \cdot H_2O$, $NaBH_4$, MeOH, 0°C to RT, 21h; (b) 2,2-DMP, *p*-TsOH, acetone, 0°C to RT, 21h.

As shown in Scheme 3.15, phosphonoacetic acid (**305**) was obtained by hydrolysis of commercially available ethyl phosphonoacetate (**293**). In order to generate the required phosphonoacetyl acetonide intermediate **288**, compound **304** was reacted with phosphonoacetic acid (**305**) under Steglich conditions using DCC and DMAP.[170]

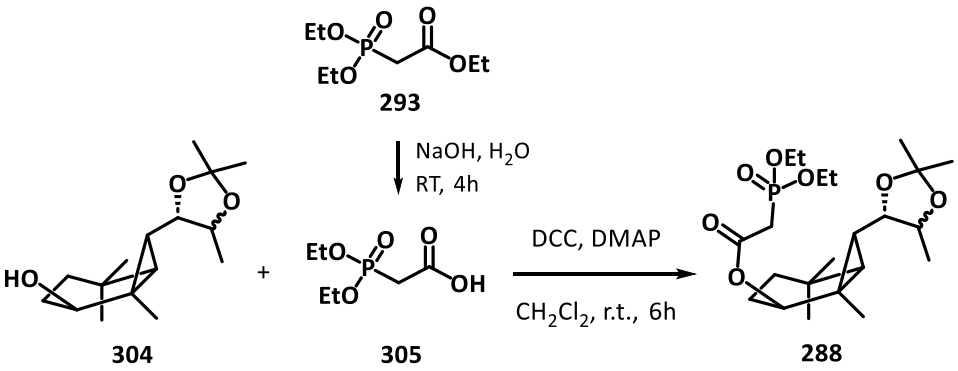

Scheme 3.15: Synthesis of compound **288**.

The accepted mechanism of Steglich esterification is illustrated in Scheme 3.16 and shows that the major by-product to be dicyclohexyl urea. This compound is notoriously difficult to remove from reaction mixtures, and in this instance, several trituration cycles and repeated flash chromatography was required to access uncontaminated phosphonoacetyl acetonide **288**.

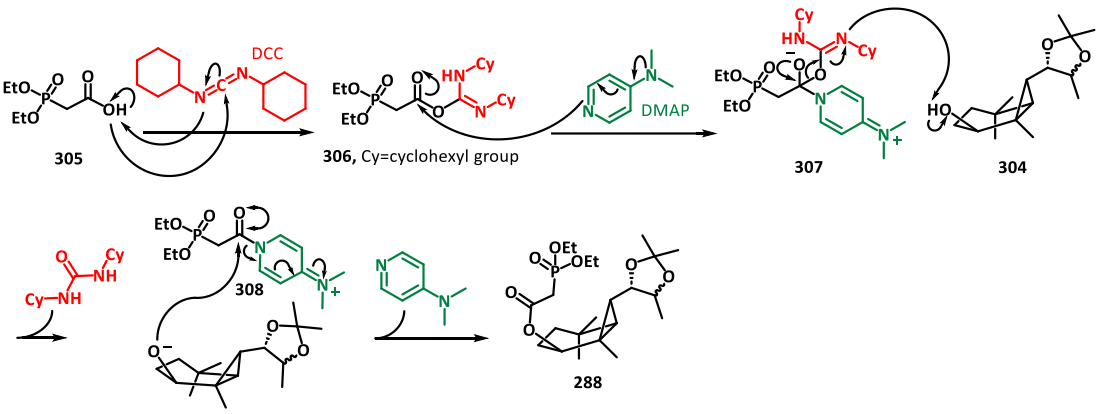

Scheme 3.16: Mechanism of Steglich esterification on synthesizing compound **288**.

Next, the acetonide protecting group of intermediate **288** was removed under acidic conditions, releasing the diastereomeric diols **309** (Scheme 3.17). Oxidative cleavage of the diols with sodium periodate generated the key HWE precursor, molecule **287**.

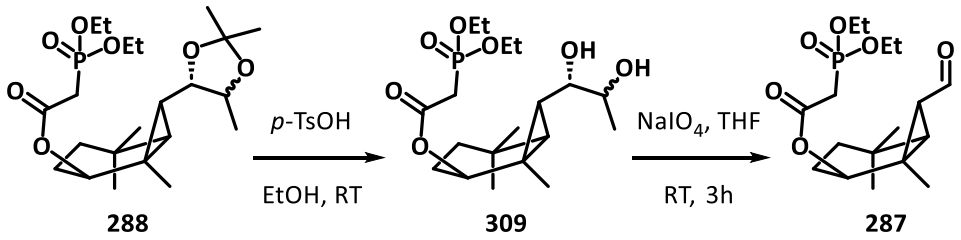

Scheme 3.17: Synthesis of compound **287**.

3.2.5 Intramolecular HWE Reaction

With the successful preparation of the key HWE precursor **287**, the stage was set for the key intramolecular HWE olefination reactions to both epimerize the cyclopropyl aldehyde and construct the seven-membered lactone ring.

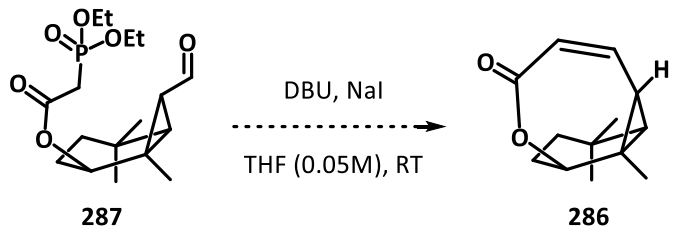

Scheme 3.18: Designed intramolecular HWE olefination step of generating lactone **286**.

To minimize the possibility of undesired intermolecular HWE reactions, the intramolecular HWE reaction of compound **287** was conducted at high dilution at room temperature. Additionally, sodium iodide was used due its high solubility in organic solvents, and its ability on the formation of a complex with the phosphoester that lowers the barrier to deprotonation and facilitates HWE reaction (Scheme 3.18).[171]

As shown in Scheme 3.19, we anticipated the base would deprotonate phosphonate, and perhaps enolize the cyclopropyl aldehyde. Alternatively, the cyclopropyl aldehyde could be enolized in an intramolecular manner. Either way, re-protonation of the cyclopropyl enolate would generate some of the desired *endo*-configured cyclopropyl aldehyde. That the minor *endo*-isomer would undergo intramolecular HWE, and by Le Chatelier's principle, drive production of the desired 7-membered lactone.

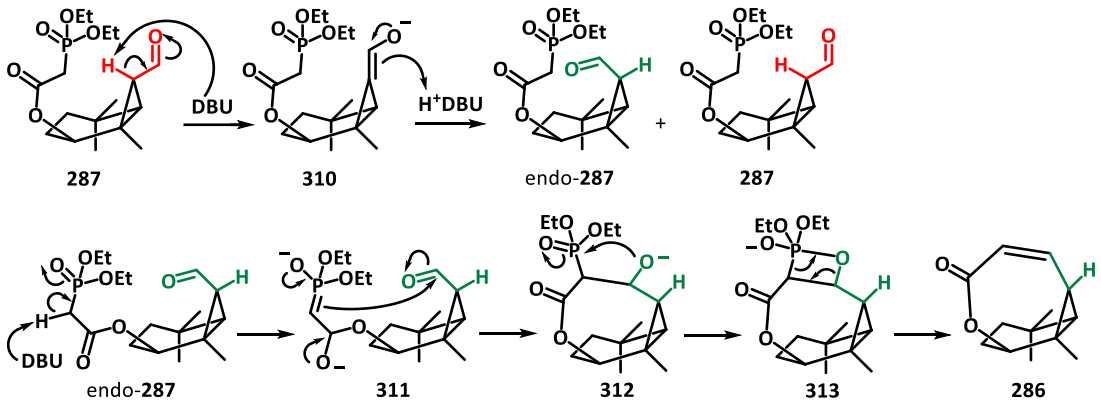

Scheme 3.19: Proposed mechanism of HWE olefination.

As reported in Table 3.2, despite these carefully chosen reaction conditions, the experimental outcomes deviated significantly from our expectations. Analysis of the ^{1}H NMR spectrum of the reaction mixture revealed that molecule **287** remained unreacted even after a substantial reaction time. Heating the reaction mixture led to decomposition, presumably by cyclopropane ring opening, which placed a severe constraint on reaction design. Based on this initial outcome, we reasoned that DBU was not sufficiently basic enough to deprotonate the cyclopropyl aldehyde, and therefore we employed amid bases with a significantly higher pK_a (entries 2–4).

Table 3.2: Results of different bases and temperatures.

Entry	Base	Reaction Temperature	Result
1	DBU, NaI	RT	no reaction
	DBU, NaI	reflux	decomposition
2	LiHMDS	-78°C to 0°C	no reaction
3	LiHMDS	0°C to RT	no reaction
4	LiHMDS	RT to reflux	decomposition

Unfortunately, three different sets of reaction conditions with LiHMDS failed to induce the stereochemical switching of the target carbon, indirectly confirming that the deprotonation step proposed in our mechanism was not occurring.

Based on these experimental results, inverting the stereochemistry of the cyclopropyl aldehyde carbon emerged as the most significant challenge in overcoming this problem. We reasoned that the inability to deprotonated the α-hydrogen atom must be related to the cyclopropane ring system.

3.3 Discussion of Cyclopropane Chemistry

Before further optimizing the mentioned approach *via* HWE reaction, a deeper understanding of cyclopropane structure is necessary, particularly concerning its stereochemistry in avenaol. In small ring contained structures like cyclopropane, the traditional σ-π bonding model fails to account for the unusual bond lengths and bond energies observed (e.g., why the bond angle in cyclopropane is not exactly 60°, why cyclopropane is more stable than cyclobutene, and why cyclopropane has a shorter than expected bond lengths). By virtue of the similarity of the bonding in cyclopropane and the double bond in ethylene,[172] the bent bond theory gives a better explanation for the bond angles and bong lengths observed in cyclopropane (Figure 3.3).[173]

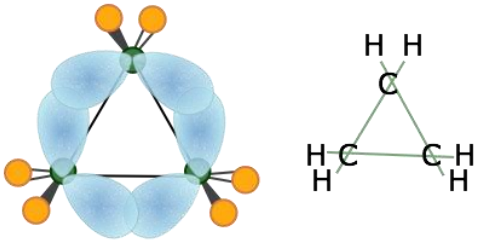

Figure 3.3: Bent bonds in cyclopropane. (Image credit from Coulson-Moffitt Model)

Unlike the traditional bonds, the maximum electron density between carbons in cyclopropane does not lie along the internuclear axis, which leads to the bent bonds. The carbon atoms cannot adopt the standard 109.5° bond angles typical of standard sp^3 hybridization. Instead, increasing *p*-character of the carbon-carbon bonds reduces the bond angles to accommodate the ring strain. Simultaneously, the carbon-hydrogen bonds gain more *s*-character, resulting in shorter bond lengths and stronger bonds.[174] This means that the α-C–H bond on the cyclopropyl aldehyde **287** will be significantly less acidic than the corresponding α-C–H bond on a linear aldehyde. However, the use of the strongly basic LiHMDS reagent was anticipated to be sufficiently powerful to effect the desired deprotonation. Did that mean that the *endo*-isomer was not forming in any meaningful amounts? To answer this question, we needed to slightly change the structure of substrate **287**.

3.4 Strategies for Switching the Stereochemistry of Target Carbon

3.4.1 Direct epimerization strategies

Refocusing on the HWE lactonization strategy, it was clear that epimerization of the cyclopropyl aldehyde was not occurring in the presence of the large phosphonate unit. Therefore, we decided to switch the order of the operations: firstly, epimerize the aldehyde, then install the phosphonate unit for HWE reaction. This slightly revised approach necessitated the installation of a readily removable protecting group on the 6-membered ring alcohol. Molecule **314** was chosen as a suitable substrate (Figure 3.4).

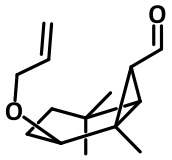

314

Figure 3.4: Structure of molecule **314**.

As shown in Scheme 3.23, intermediate **314** was synthesized through a similar reaction sequence to that previously used. By changing the solvent system from acetone/water to acetone/allyl alcohol, epoxide **281** was smoothly converted into allyl protected ketone **315**. Again, the intramolecular cyclization of the diastereomeric mixture of epoxide **281** produced a single isomer of **315**. Subsequent oxidative cleavage using a periodate salt afforded aldehyde **314** with an overall yield of 60%. It is noteworthy that the desired [4.1.0] fused ring system was synthesised in a total of just 3 steps from commercially available α-ionone (**292**). Compound **314** was now set for aldehyde epimerization.

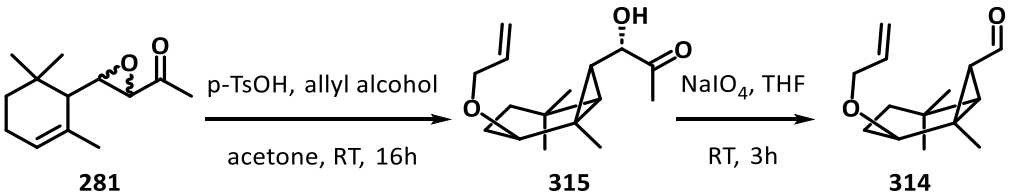

Scheme 3.23: Synthesis of aldehyde **314**.

Our epimerization investigations began by repeating the conditions previously employed on ester **287** (Table 3.3). Epimerization was attempted using DBU and LiHMDS (entries 1 and 2) at several different temperatures, but neither of the bases successfully performed the desired stereochemical inversion. Alkoxide bases have previously been reported for the epimerization of α-carbonyl cyclopropanes, but the use of methoxide (commercial, entry 3, and freshly generated, entry 4) was equally ineffective.

Table 3.3: Stereoswitching trials with different bases.

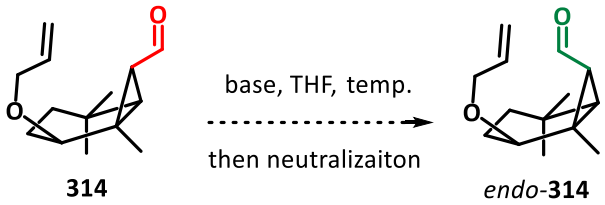

Entry	Base	Reaction Temperature	Result
1	DBU	RT	no reaction
2	LiHMDS	RT to reflux	decomposition
3	NaOMe	-78℃ to RT	no reaction
4	Na in MeOH	-78℃ to RT	no reaction
5	LDA (prepared from *n*BuLi)	-78℃ to RT	unexpected reaction

As shown in entry 5, the use of freshly prepared lithium diisopropylamide (LDA) did result in a deprotonation and isomerization – disappointingly, not the desired one. Instead, the base removed the allylic hydrogen of protecting group, leading to an unexpected formation of the enol ether by-product **316**, as a single geometric isomer. The proposed mechanism for this side reaction is illustrated in Scheme 3.24.

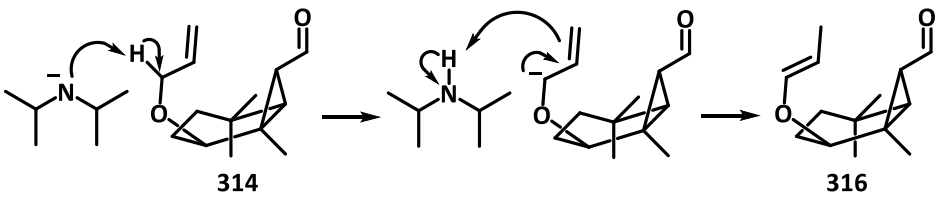

Scheme 3.24: Mechanism of synthesizing byproduct **316**.

Even knowing that the carbon-hydrogen bond strength in the cyclopropane structure is higher than the bonds in common alkanes, the failure of the deprotonation reactions discussed is still perplexing. The deprotonation by LDA suggests that the C-H bond strength at the target carbon in the cyclopropane is substantially stronger than the α-C-H bond in the allyl group. We reasoned that the unique steric environment of the [4.1.0] fused ring system must inhibit the carbonyl adopting a perpendicular arrangement to the α-hydrogen, precluding σ–π* overlap that renders α-hydrogens acidic (Figure 3.5).

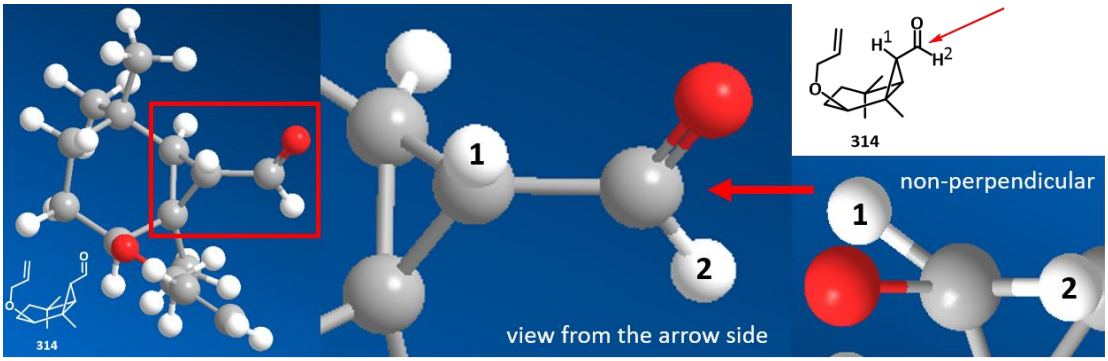

Figure 3.5: General structural explanation for the inhibition of perpendicular arrangement.

To facilitate the deprotonation reaction, we reasoned that the addition of a Lewis acid to the oxygen atom of the aldehyde would alter the steric environment while simultaneously increasing the acidity of the α-hydrogen. The addition of TMSCl was intended to achieve these goals, forming enolate intermediate **317**, thereby driving the reaction forward (Scheme 3.25). Spectacularly, this reaction also failed.

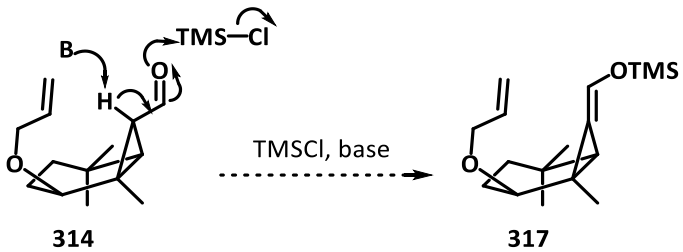

Scheme 3.25: Optimized mechanism on deprotonation.

We had reached a point where a rapid, stereoselective, and cost-effective synthesis of [4.1.0] fused ring system with an aldehyde was achieved, but seemingly trivial

enolization of the aldehyde could not be achieved. We therefore proposed three potential improvements to achieve the desired stereochemical inversion.

The first alteration involved the installation of a bromine atom in place of the α-hydrogen. Under reducing conditions (e.g. in the presence of zinc), the bromine atom could be excised resulting in the formation of an enol structure on the cyclopropane ring. Whilst ambitious given the previous outcomes, we explored installation of the halogen using under basic conditions, and also under radical conditions.

Two brominating reagents were employed: tetrabromomethane (CBr_4) and N-bromosuccinimide (NBS). To achieve the bromination-deprotonation process efficiently, we designed a one-pot reaction protocol, where the brominating reagent was first added at low temperature, followed by the introduction of the base and finally increasing the temperature. This stepwise approach aimed to ensure selective bromination before initiating the unwanted elimination.

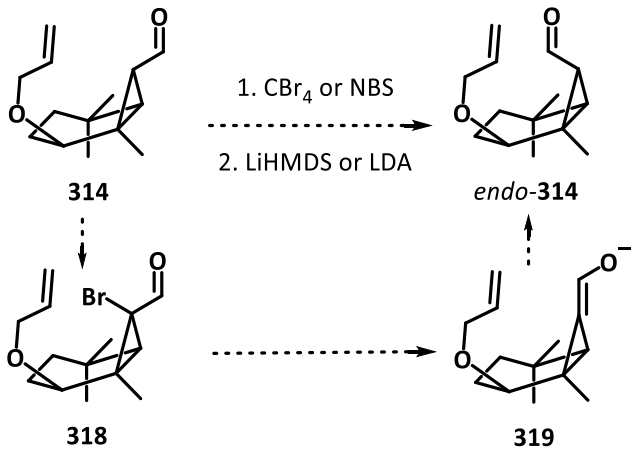

Scheme 3.26: Bromination strategy with CBr_4 and NBS.

Unfortunately, the results of these bromination reactions were even more disappointing than the initial deprotonation attempts. The TLC analysis showed an unclear mixture with indistinguishable spots, and the reaction products proved inseparable. Similar results were obtained by treatment of the aldehyde with NBS and light. Given the complexity of the resulting mixtures, no meaningful conclusions could be drawn as to

what occurred during reaction. However, these observations made it clear that the bromination strategy on the aldehyde had failed.

The second alteration to our strategy was more direct. In consideration of the lack of acidity of the α-hydrogen on the aldehyde, we elected to replace the aldehyde unit with a sterically different electron-withdrawing group. This modification should facilitate deprotonation of the target C–H bond.

Based on the structure of aldehyde **314**, introducing a conjugated system at the aldehyde could alter the local steric environment while still providing a significantly polarized cyclopropyl C–H bond and making it more prone to cleavage. Our first approach involved converting the aldehyde group into an α,β-unsaturated ester *via* a Wittig reaction with triphenylphosphonoethyl acetate **320**.

This modification would install extended conjugation, facilitating the desired stereochemical inversion via extended enolate generation. By applying a recycling deprotonation–reprotonation strategy, the top carbon of the cyclopropane ring could undergo a hybridization shift from sp^3 to sp^2 and back to sp^3, achieving overall epimerization.

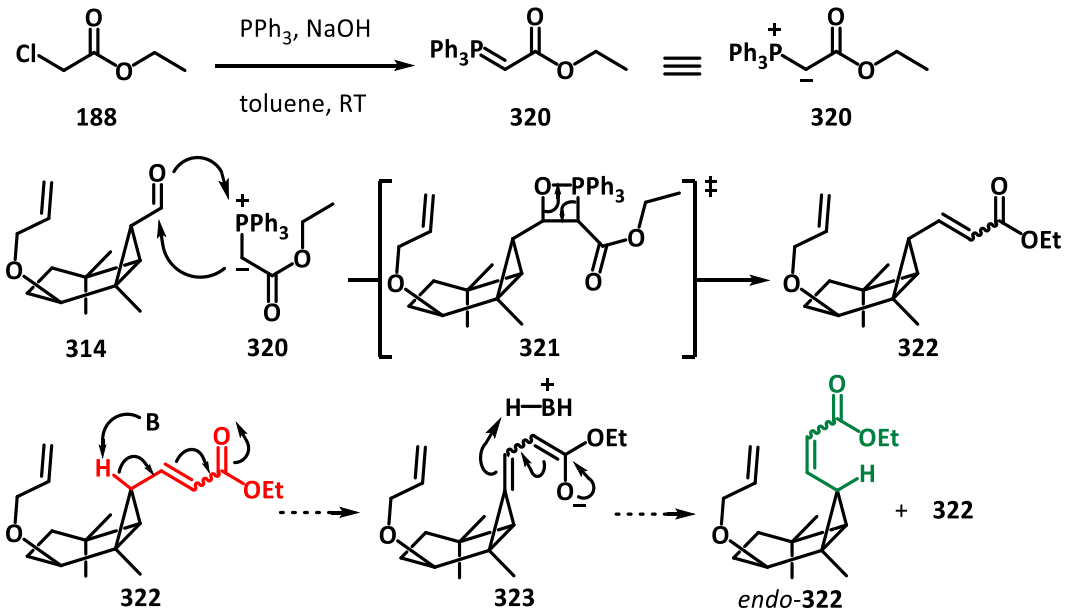

Scheme 3.27: Proposed mechanism of synthesizing *endo*-**322**.

As depicted in Scheme 3.27, the triphenylphosphonoethyl acetate **320** reagent was synthesized from triphenylphosphine and chloroethyl acetate **188**. The Wittig reaction proceeded smoothly upon the addition of base, yielding the desired α,β-unsaturated ester **322**, while retaining the same *exo*-configuration. However, all attempts to induce the stereoswitching through a deprotonation–reprotonation process failed. Each of the reaction conditions reported in Table 3.3 were trialled, but no change in the stereochemistry of the cyclopropane was observed.

The third alteration to our strategy also involved replacing the aldehyde in compound **314** with a different functional group. We drew inspiration by reviewing the successful elements of our synthetic pathway, and our attention was drawn to the α-hydroxy ketone intermediate **315**. Oxidation of the hydroxy group would generate diketone **324**, which appeared to be another enolizable functional group.

As shown in Scheme 3.28, oxidation of compound **315** with Dess-Martin periodinane occurred smoothly. Diketone **324** was reacted with sodium methoxide (both commercial and freshly generated from sodium metal and ultra dry methanol), anticipating sodium ion chelation with the oxyanions would stabilize the enolized structure **325**. However, quenching this reaction returned the starting material **324**. Like its 'predecessors', epimerization of this compound remained a failure.

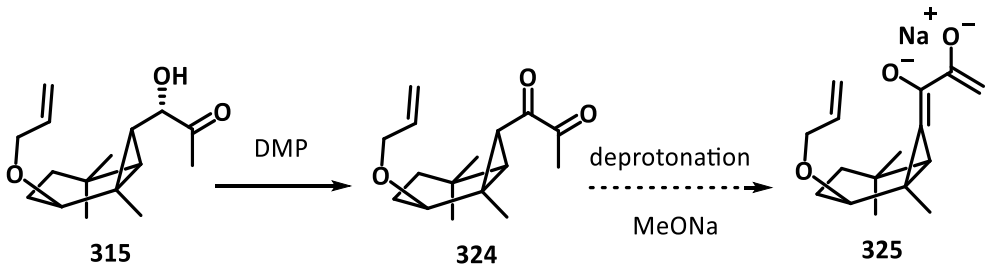

Scheme 3.28: Synthesis of diketone **324** and proposed deprotonated product **325**.

All the above work makes it clear that the direct epimerization of the cyclopropyl aldehyde, or a synthetic equivalent, was not feasible. Therefore, a less direct

epimerization strategy was explored.

3.4.2 Indirect epimerization strategies

We anticipated that an *endo*-configured unit could be installed on the cyclopropane unit by reduction or conjugate addition to the enone **327** (Scheme 3.29). The α,β-unsaturated system could be generated by elimination of a suitable leaving group, which could be derived from the known intermediate **315**. We settled upon a bromide as the leaving group of choice.

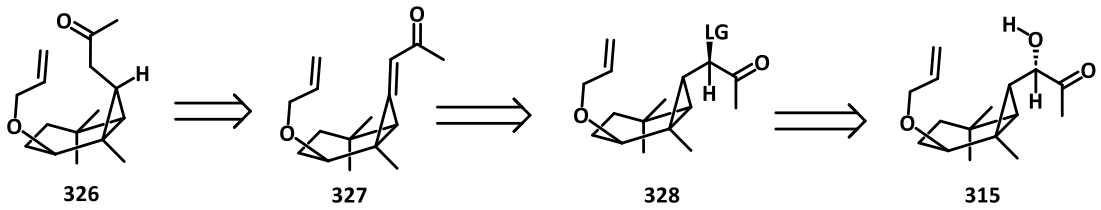

Scheme 3.29: Retrosynthetic analysis of the indirect epimerization strategy.

Bromination of compound **315** with tetrabromomethane smoothly gave two new and easily separable products, **329** and **331**. However, neither of them was the desired enone **327** as there were no NMR signals corresponding to the allyl group. Careful structure elucidation, based on NMR and MS data, demonstrated that the reaction had produced the ring-opened diketone **329** and bromoketone **331**. Our proposed mechanisms for the formation of these unwanted products are illustrated in Scheme 3.30.

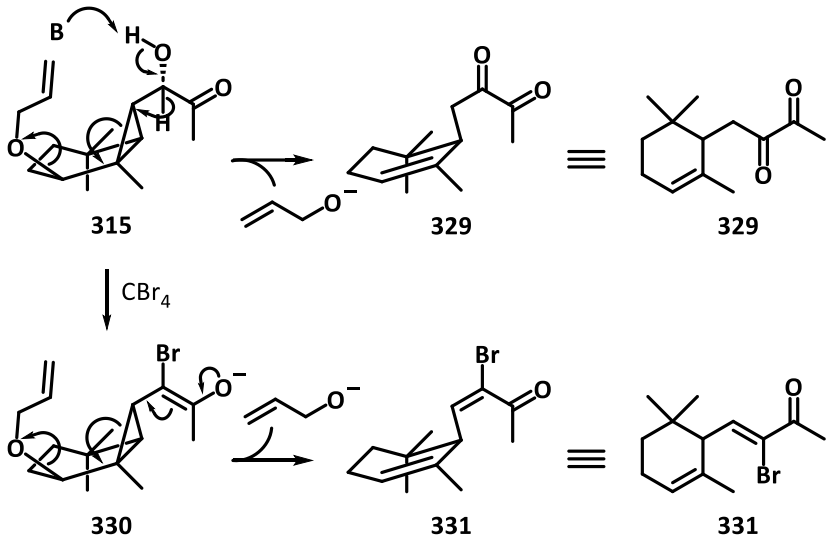

Scheme 3.30: Proposed mechanisms of generating byproduct **329** & **331**.

Formation of diketone **329** is likely the result of the α-hydroxyketone **315** undergoing deprotonation, with subsequent ring-opening of the strained cyclopropane and elimination of the allyl unit as its alkoxide. This reaction is competitive with the bromination of the α-hydroxyketone **315**. When bromination of α-hydroxyketone **315** is successful, rather than elimination of the halogen, $E1_{CB}$ reaction from enolate **330** occurs with analogous ring-opening and elimination of the allyl unit as its alkoxide of the to generate **331**.

3.4.3 Summary of epimerization strategies

Up until this point, our achievement had been the rapid, 2-step construction of a [4.1.0] fused ring system that mapped well onto the structure of our target molecule, avenaol. The oxygen atom on the 6-membered ring (either an alcohol or an ether) provided a synthetic handle to install the α-hydroxy ketone seen in avenaol. But the cyclopropane unit required epimerization to match the stereochemistry seen in the natural product. We assessed various methods to achieve stereo-inversion of the target cyclopropyl carbon, but none of them succeeded.

The direct epimerization of aldehydes **287** and **314** were explored under a variety of reaction conditions (Figure 3.6). Failure to accomplish the epimerization led us to

attempt the direct epimerization of molecules containing related functional groups, **322** and **324**. Again, our attempts failed to invert the cyclopropane stereochemistry. We reasoned that these negative outcomes stemmed from the inherently strong C–H bonds in the cyclopropane structure. Reaction conditions forcing enough to effect the deprotonation, led to competitive cyclopropane ring-opening. Therefore, an indirect epimerization was explored. Unfortunately, although partial bromination of molecule **315** was achieved, the relatively mild basic reaction conditions led exclusively to cyclopropane ring-opening.

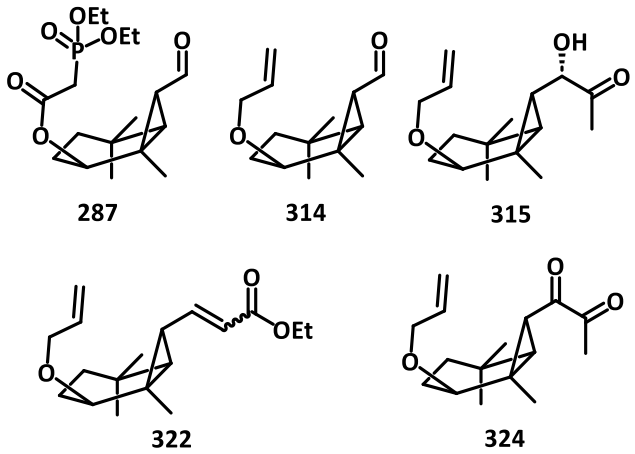

Figure 3.6: Molecules in stronger EWG strategy attempts.

As a result, we decided to radically rethink our approach and shifted our focus to exploring alternative synthetic pathways for the total synthesis.

3.4.4 Other Stereoselective Synthesis to Cyclopropyl Structures

Installation of the sterically congested cyclopropane ring of avenaol is challenging because each of the large substituents are appended to the same face of the small ring. Methods for the direct construction of such all-*cis* cyclopropanes are lacking. The most commonly employed cyclopropane synthesis is the Simmons-Smith reaction (Scheme 3.31), which utilizes a Cu-Zn couple and a dihalogenated methane to effect an [2+1] cycloaddition.[175] For disubstituted alkenes, the stereochemistry of the alkene is retained in the product.

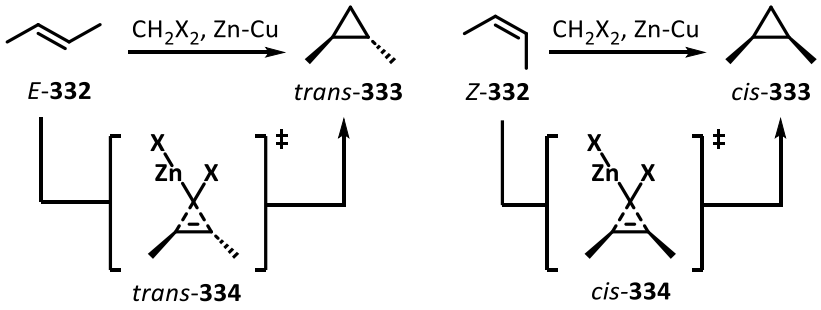

Scheme 3.31: Stereochemistry and general mechanism of Simmons-Smith reaction.[175]

Another famous cyclopropanation is the Corey-Chaykovsky reaction (CCR) which has been widely utilized to synthesize epoxides **337**, aziridines **339** and cyclopropanes **341** from sulfur ylides (Scheme 3.32).

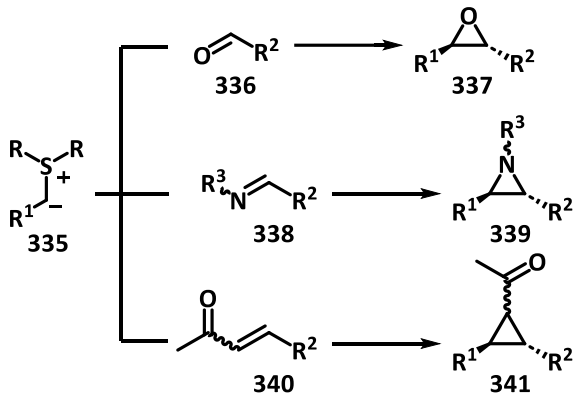

Scheme 3.32: Corey-Chaykovsky reaction (CCR).

It is noteworthy that regardless of the configuration of the double bond in the starting material, CCR consistently proceed the formation of a *trans*-configured cyclopropane product (Scheme 3.33).

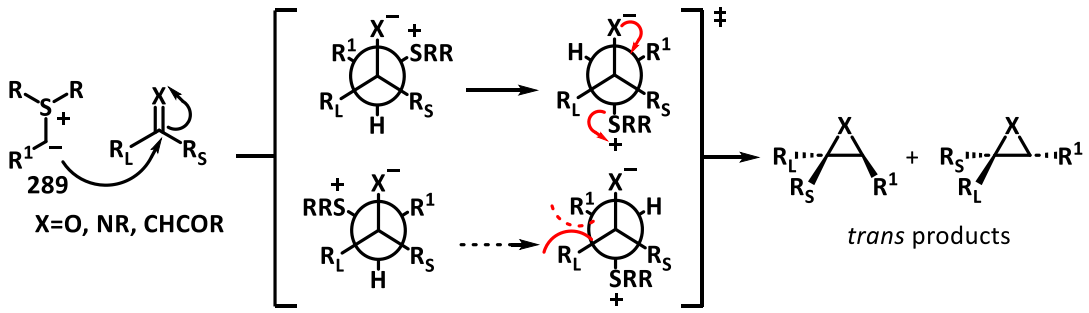

Scheme 3.33: Mechanism of generating *trans* rings.

The key step of this reaction involves addition of a nucleophilic sulfur ylide to an electrophilic substrate is followed by displacement of the sulfur unit and ring-closure. The ability of the intermediate to undergo bond rotation means that the CCR strongly favours the thermodynamically more stable, least sterically congested product.[176,177]

Besides these frequently employed methods, there are also several reactions to stereochemically synthesize the cyclopropanes *via* diazole species[178] or carbenes.[179]

However, none of these methods are capable of directly generating the all-*cis* cyclopropane found in avenaol. Therefore, a suitable method for inverting the stereochemistry of the cyclopropyl ring remains essential for achieving our desired total synthesis of avenaol.

3.5 Approach *via* Radical Reactions and Free Carbene Cycloaddition

Considering the special challenging stereochemistry of the cyclopropane ring of avenaol, we devised another strategy based on the selective reaction of a di-functionalized cyclopropane ring. This new strategy was based on previous work by Kikuchi and McErlean.[180]

3.5.1 Retrosynthetic Analysis

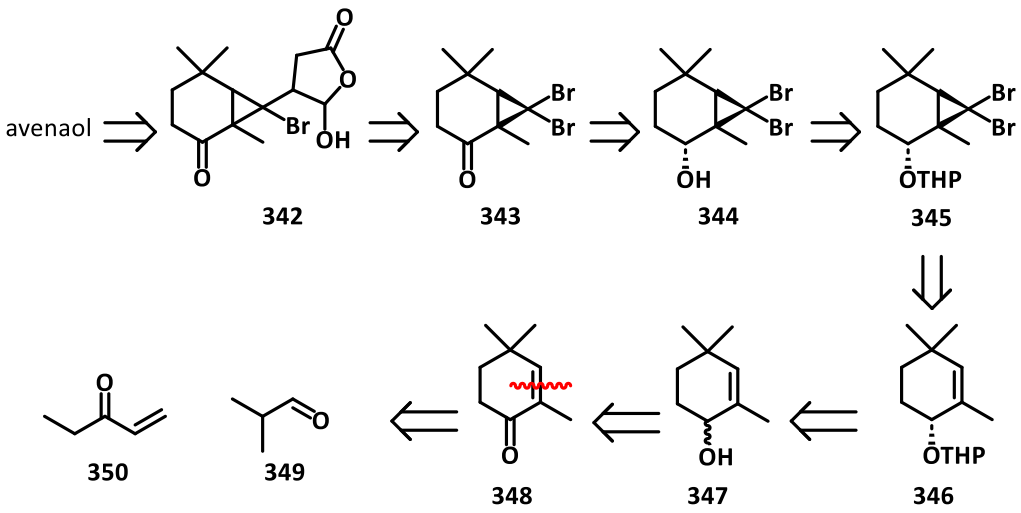

Scheme 3.34: Retrosynthesis of approach *via* radical reactions.

Our retrosynthetic analysis is depicted in Scheme 3.34. Standard manipulations of avenaol revealed the bromocyclopropyl containing compound **342** as key intermediate. Disconnection of the activated lactone ring revealed dibromocyclopropane **343**. The generation of molecule **343** eliminated the issue of stereochemical control during the cyclopropanation reaction. We envisaged that the *exo*-configured bromine atom would be more available for reaction, providing the necessary stereocontrol. The ketone unit of **343** derived from an alcohol **344**, which enabled the introduction of a large protecting group **345**. Disconnection of the cyclopropane ring revealed the alkene **346**. We anticipated that the large protecting group on the alcohol of **346** would enable stereochemical control of a cyclopropanation of the alkene with dibromocarbene. The protected alcohol **346** could be easily accessed from the ketone **348**, which was the

Robinson annulation product of reaction between isobutyraldehyde (**349**) and ethyl vinyl ketone (**350**).

3.5.2 Mechanism of Free Carbene Cyclopropanation

The cycloaddition between a free carbene and an alkene is a popular method for the construction of complex structures in natural products.

Free carbenes are mostly derived from the corresponding diazo-compounds or by elimination of halogenated molecules. Containing two unshared valence electrons, carbenes can be classified into singlet species and triplet species by their electron configuration (Figure 3.7).[181,182]

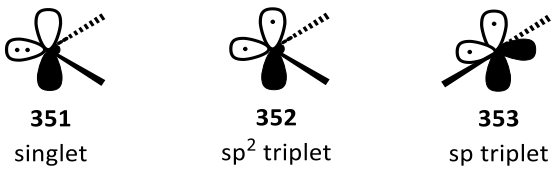

Figure 3.7: Structures of singlet and triplet carbenes.

Von E. Doering and Hoffmann reported that chloroform (**354**) could generate the singlet free carbene *via* α-elimination under ultra basic condition,[179] which is exactly the method we planned utilize in this work (Scheme 3.35). Those authors were the first to propose a spirocyclic transition state **357** for the cycloaddition mechanism between dichlorocarbene (**355**) and cyclohexene (**356**), which explained formation of cyclopropane **358**. In this work, such a spirocyclic transition state would minimize steric interactions with the geminal diethyl group of substrate **345**.

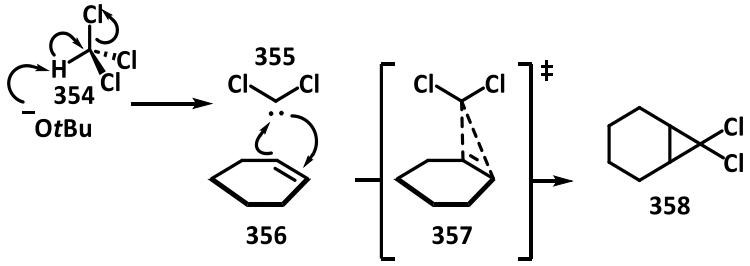

Scheme 3.35: Mechanism of dichloro carbene cyclopropanation.[179]

3.5.3 Synthesis of the [4.1.0] Carbon Skeleton

In contrast to the previous approaches starting from α or β-ionone, the first step of the new strategy started with the construction of cyclohexyl ring (the A-ring of avenaol). Robinson annulation,[183] a reaction combining Michael addition and aldol condensation, seemed the logical choice for construction of this ring. As depicted in Scheme 3.36, large-scale Robinson annulation between ethyl vinyl ketone (**350**) and isobutyraldehyde (**349**) was efficiently performed using a Dean-Stark apparatus, yielding the A-ring-containing ketone **348** in a good yield. The mechanism of the Robinson annulation is depicted below.

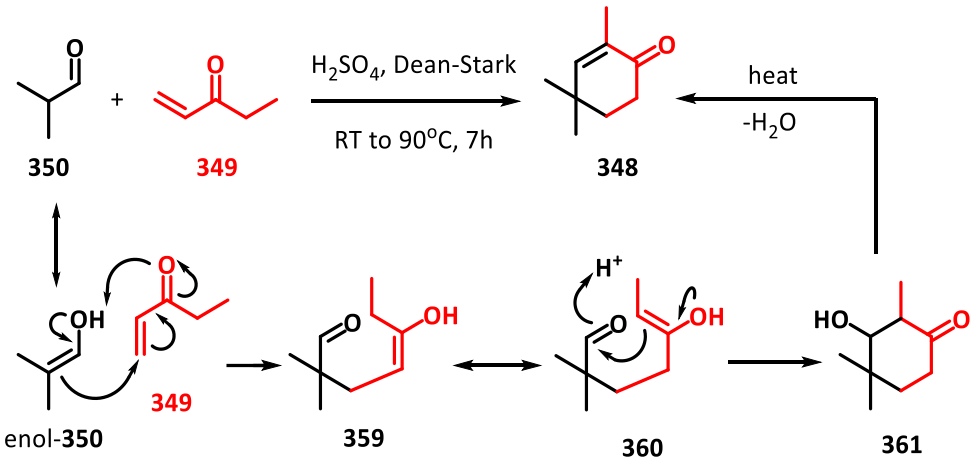

Scheme 3.36: Scheme and Mechanism of Robinson annulation on preparing ketone **348**.

Fractional distillation was employed to purify the desired product **348**, with the fraction boiling at 55°C yielding the desired product **348** with a 47% yield. With compound **348** in hand, the next step was converting it to alcohol **347** *via* Luche reduction using sodium borohydride and cerium chloride.[169] The resulting alcohol was then reacted with dihydropyran in the presence of aluminium chloride, leading to the formation of the THP-protected product **346** (Scheme 3.37).

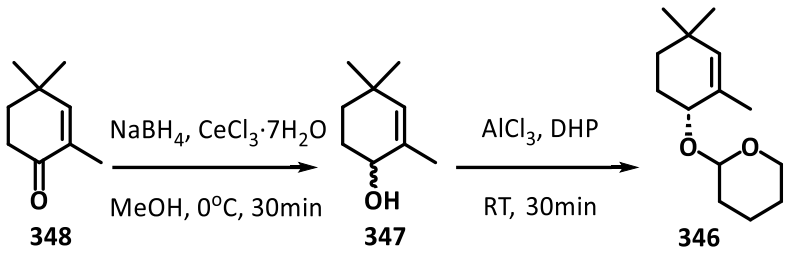

Scheme 3.37: Synthesis of THP-protected alcohol **346**.

According to previous research by Kikuchi and McErlean,[180] the steric hindrance created by the THP protecting group forced carbene addition to occur on the opposite face of the alkene, which led to a high level of diastereo-control. As shown in Scheme 3.38 carbene addition onto compound **346** was very sluggish, but provided the desired dibromocyclopropane **345**. The THP group could be efficiently deprotected using *p*-TsOH in methanol, resulting in a near quantitative yield of alcohol **344**.

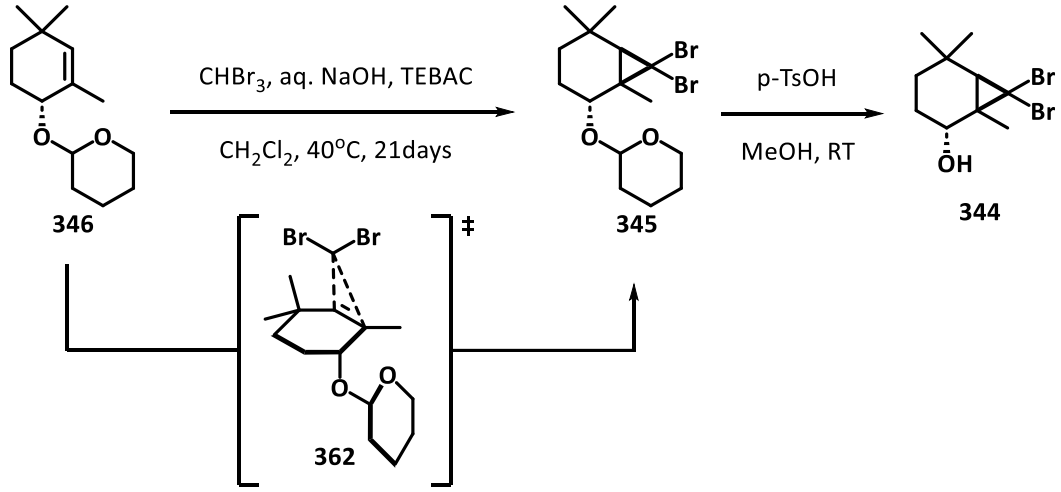

Scheme 3.38: Stereo controlled cycloaddition mechanism and preparation of alcohol **344**.

The subsequent oxidation step was efficiently carried out by Dess-Martin periodinane to give ketone **343** (Scheme 3.39).

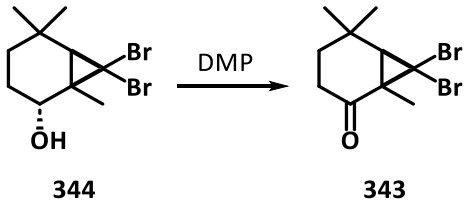

Scheme 3.39: Synthesis of ketone **343**.

3.5.4 Coupling Approaches

The [4.1.0] fused ring system of compound **343** corresponded the A, B-ring ring system of avenaol. The next step was the projected radical coupling of the cyclopropane ring and a suitably activated butenolide (C-ring). In the previously reported work, Kikuchi and McErlean attempted the Giese-type radical addition of a bromocyclopropyl radical onto the parent butenolide (Scheme 3.40).[180] Unfortunately, in that instance, the initially formed bromocyclopropyl radical preferentially abstracted a H-atom, with the subsequent cyclopropyl radical adding slowly onto the butenolide. This resulted in the non-natural *exo*-stereochemistry on the cyclopropane. In order to install the correct stereochemistry, butenolide addition must occur first. Therefore a more reactive butenolide ring was required.

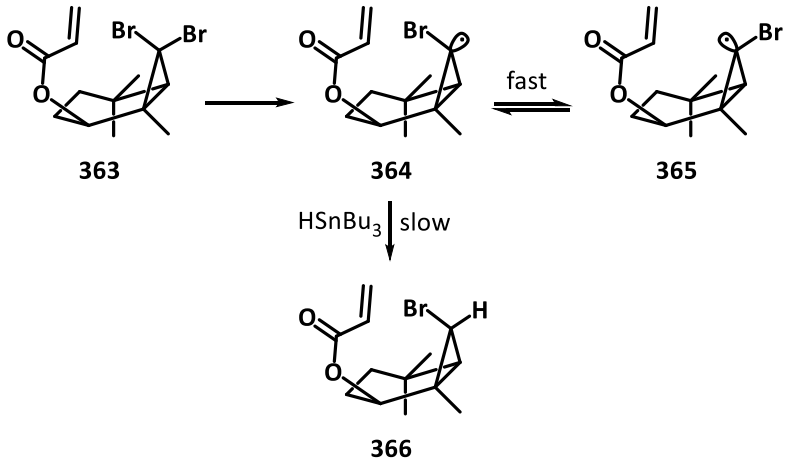

Scheme 3.40: Kikuchi and McErlean's Giese-type radical trial.

A recent publication by Feringa and co-workers, highlighted the increased reactivity of hydroxybutenolide **368** relative to the parent butenolide.[184] Moreover, according to that report, molecule **368** had no activity in homo-polymerization, which decreased the possibility of side reactions. Considering our plan to directly introduce a butenolide unit, hydroxyfuranone **368** emerged as a suitable candidate.

The preparation of furanone **368** was relatively straightforward (Scheme 3.40). By slowly adding Oxone to a vigorously stirred mixture of furan (**367**) and water, molecule **364** could be obtained on a gram-scale in 67% yield, without need for further purification.[185]

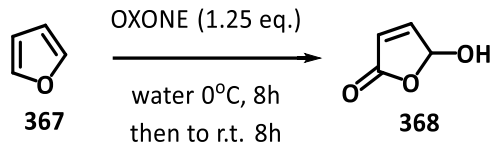

Scheme 3.41: Synthesis of coupling reagent furanone **368**.

With both the dibromocyclopropane **343** and the activated butenolide **368** coupling partners in hand, we turned our attention to the radical-based coupling. We explored two potential approaches for the coupling step: a photoredox reaction and an AIBN-initiated radical reaction.[180]

As illustrated in Scheme 3.42, the photocatalytic method employed the organic photocatalyst **369** and triisopropylsilane (TIPS) as the H-atom source and source of silyl radicals. The reaction involved mixing ketone **343** and furanone **368** in a small amount of acetonitrile with DABCO as a base. The mixture was then subjected to ~450 nm light in a photoreactor for 48 hours.

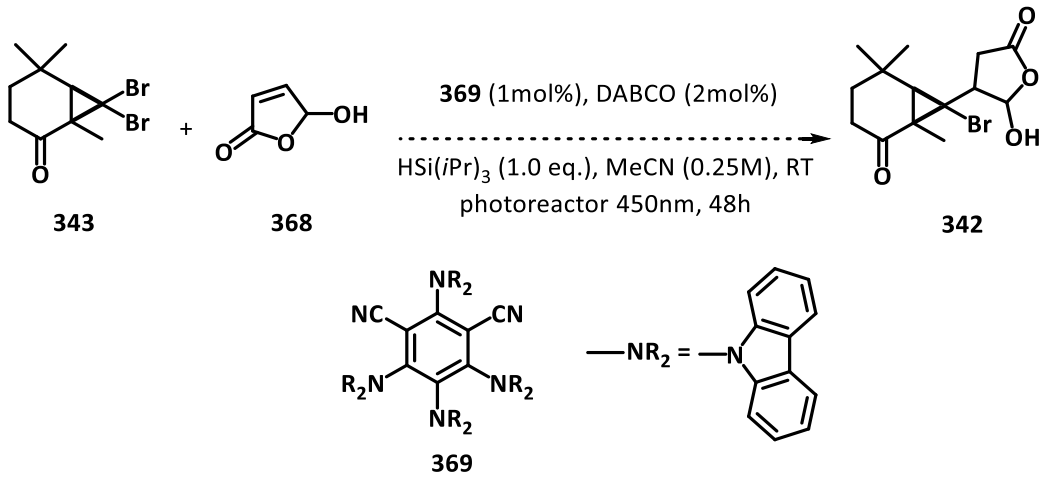

Scheme 3.42: Photocatalytic coupling attempt.

Unexpectedly, the reaction did not proceed. After 48 hours of stirring, the starting materials remained unreacted, indicating that the photocatalytic method was ineffective in this case.

After the photocatalytic method, we also explored the AIBN-initiated radical reaction on dibromoketone **343** and the furanone partner **368** as displayed in Scheme 3.43. TIPS was utilized as the H-atom source as well as the source of silyl radicals. Ultra dry acetonitrile (with additional drying over molecular sieves) was employed and the mixture was then reacted at room temperature for 48 hours.

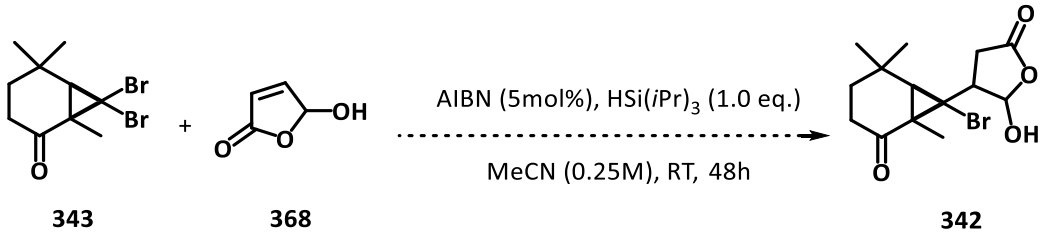

Scheme 3.43: AIBN-initiated radical attempt.

Similarly, the resulting crude of the AIBN radical attempt was proved to be mostly starting material. At this point, a modification on the scale of TIPS was developed onto the reaction above. We slightly increased the equivalents of TIPS and increased the concentration of the reaction mixture (Scheme 3.44).

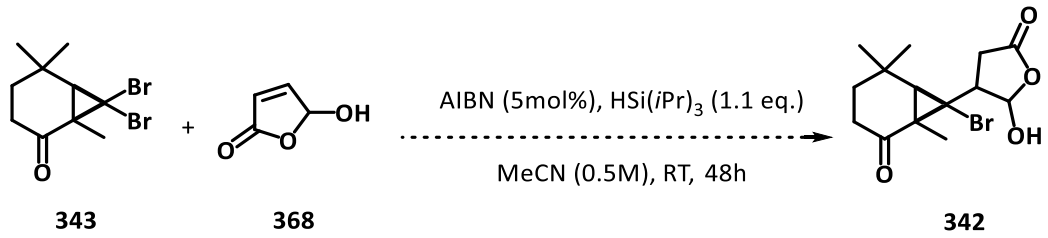

Scheme 3.44: Modified AIBN-initiated radical attempt.

However, no obvious difference was observed between the original attempt and the modified one. As the two reactions were both failed, we rationalized that the hydroxybutenolide **368** was not a suitable reaction partner.

Initially, we thought that hydroxybutenolide **368** would prefer to undergo the ring-opening via radical catalysis, thereby preventing the formation of our expected coupling molecule. However, NMR analysis of the reaction mixture showed that there still remained a large amount of starting material, indicating that there were not any structural changes on the hydroxybutenolide **368**.

Therefore, the only remaining explanation is that our starting materials were lacking enough reactivity for a Giese-type radical coupling. Compared to commonly used Giese reactants, molecule **368** had a similar unsaturated carbonyl structure, but the electron-withdrawing effect provided by the carbonyl in the lactone unit was likely attenuated. In addition, the hydroxyl group on the opposite side could also provide unpredictable effects on the reaction. This electronic ambiguity may have led to the unexpected result.

It was also possible that the reaction did not proceed due to the mismatched orbitals between the substrate's LUMO and the SOMO of the radical intermediate. But this remains speculative at this stage.

3.6 Summary

In this chapter, we explored various synthetic approaches toward the total synthesis of avenaol **25**, with a particular focus on the construction of the key intermediate **281**. Our initial strategy involved a strategy featuring a seven-membered lactone **286,** formed via intramolecular HWE reaction. Despite the elegance of this pathway, an unexpected challenge arose concerning the stereochemistry of the cyclopropane ring, which proved difficult to control.

In response, we delved into stereoswitching strategies aimed at altering the configuration of this critical carbon center. Despite considerable efforts and experimental trials, no viable solution emerged. Consequently, we shifted our focus to the construction of a non-stereospecific cyclopropane ring through free carbene addition, successfully synthesizing dibromo cyclopropyl ketone **343**, followed by a series of downstream reactions.

As with the previous chapter, the coupling step remained a significant challenge in the total synthesis process. We explored both photoredox catalysis and AIBN-initiated radical reactions for coupling **343** with a C-ring-containing fragment. Unexpectedly, neither method yielded the desired outcome, with starting materials largely unreacted under various conditions.

Although the previously mentioned approaches were unsuccessful, the seven-membered ring intermediate we designed remains a key target that would significantly simplify Tsukano's total synthesis to avenaol. Future work will shift away from the current design strategies and explore alternative approaches to construct the core unit of this intermediate.

Similarly, research on the photoredox and other catalyst-mediated radical reactions is still far from complete. Further work will focus on identifying molecules that are more suitable than hydroxybutenolide **368**. By observing the results or outcomes of radical

coupling reactions using optimized substrates, it should be possible to discover the most appropriate reactants. Once this key challenge is overcome, the following steps on the modification of Tsukano's route are expected to proceed smoothly.

Despite these setbacks, investigations of innovative strategies for the total synthesis of avenaol remains ongoing. Drawing from Tsukano's route, future efforts will build on the insights gained from these experiments. While the challenges faced thus far highlight the complexity of avenaol's unique structure, they also pave the way for further approaches.

4 SYNTHETIC WORK ON CL-TYPE ANALOGUES

Since the first total synthesis of strigol (**2**), the original strigolactone (SL) phytohormone, reported in 1974, research into the chemistry, biology, and agricultural applications of SLs have spanned nearly half a century. During this time, numerous researchers have focused on applying synthetic SLs to plants to further investigate the underlying mechanisms of plant biology and uncover valuable agricultural applications. However, achieving these goals poses significant challenges due to the complex synthetic routes required to obtain natural SLs and the difficulty of long-term preservation of these compounds.

To address these challenges, research into SL analogues has emerged as a critical area of study. Among these analogues, the most notable is GR24 **370** (Figure 4.1), a synthetic strigolactone analogue that is structurally similar to strigol, first reported by Besserer and co-workers in 2008. Analogue GR24 holds substantial biological significance, as it has been shown to rapidly increase intracellular NADH levels, enhance NADH dehydrogenase activity, and boost ATP production without requiring new gene expression.[186]

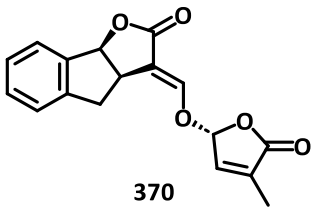

370

Figure 4.1: Structure of GR24 **370**.

Even in recent years, GR24 continues to drive new biological discoveries unstoppably. In 2021, Samaj and co-workers explored a novel mechanism connecting cytoskeletal behaviour to light-regulated SL perception, further expanding the understanding of SL-related cellular processes through light-responsive GR24 analogues.[187]

Surprisingly, no non-canonical strigolactone analogues have displayed the same utility as GR-24.

4.1 Designed CL-type Analogues

Interestingly, Akiyama and co-workers synthesized several CL-type SL analogues to investigate the structural influence on hyphal branching in arbuscular mycorrhizal fungi.[188] Their study demonstrated that the bioactivity of these analogues is strongly correlated with the oxidation state of the methyl group on the conjugated double bond chain, rather than the presence or formation of the B- and C-rings in SLs or their analogues. Figure 4.2 illustrates the CL-type analogues synthesized by Akiyama and co-workers.

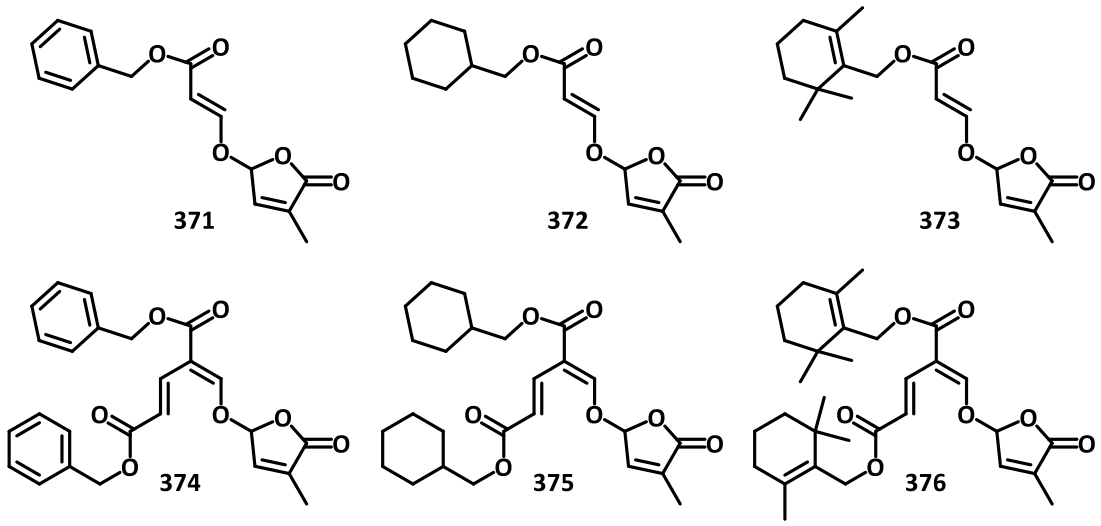

Figure 4.2: CL-type SL analogue structures synthesized by Akiyama and co-workers.

Based on the above research findings, we proposed the synthesis of several synthetic analogues that are structurally similar analogues to CL (**24**), CLA (**27**), and MeCLA (**41**), aiming to develop more stable and easily storable compounds under conventional conditions. The availability of such analogues would significantly facilitate biological and agricultural studies on CL-type strigolactones, making experimental processes more efficient and controllable.

To develop a novel SL biosynthesis inhibitor, Ito and co-workers synthesized a series of carlactone derivatives and analogues.[189] They evaluated these compounds through in vitro enzymatic assays, measuring the content of target substances in root exudates

to assess the inhibitory effect on SL biosynthesis. Among the various derivatives synthesized by Ito and co-workers, one specific molecule **377** caught our particular interest (Figure 4.3).

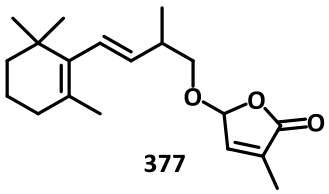

Figure 4.3: Derivative **377** of carlactone reported by Ito and co-workers.

Inspired by Ito's work, and in line with the principle of maintaining the core structures of CL and MeCLA, we have designed several structurally modified analogues with enhanced stability**,** aiming to serve as practical substitutes for the original plant hormones. These analogues retain the essential functional groups responsible for biological activity while optimizing the chemical stability to withstand storage and handling under standard laboratory and agricultural conditions.

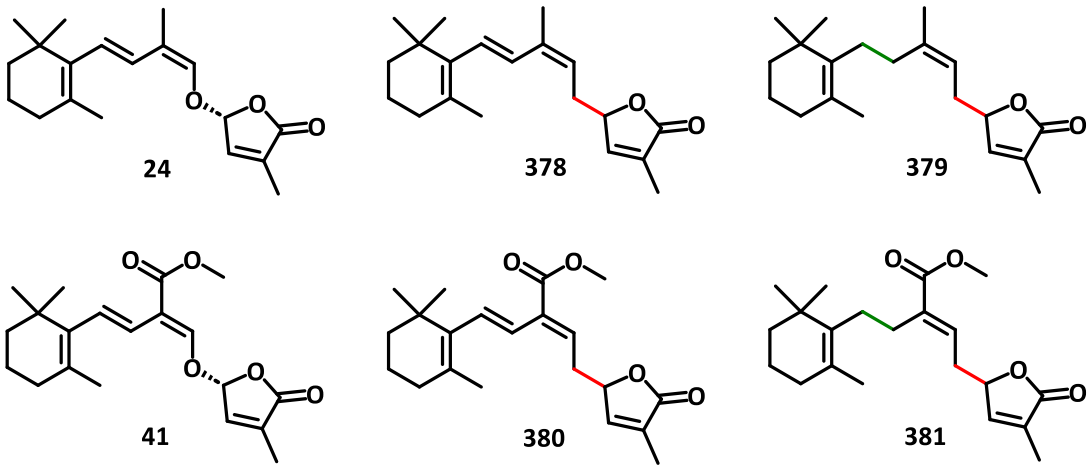

Figure 4.4: Designed CL-type analogues.

By replacing the oxygen atom attached to the butenolide D-ring in CL (**24**) and MeCLA (**41**), we designed two new derivatives, **378** and **380**, aimed at improving the stability of these compounds while preserving their biological activity. Furthermore, by removing the conjugated double bond in the middle of the chain structure, two additional analogues, **379** and **381**, were proposed (Figure 4.4).

4.2 CL-Type Derivatives Synthesis Approach *via* Grubbs Catalyst

4.2.1 Retrosynthetic Analysis

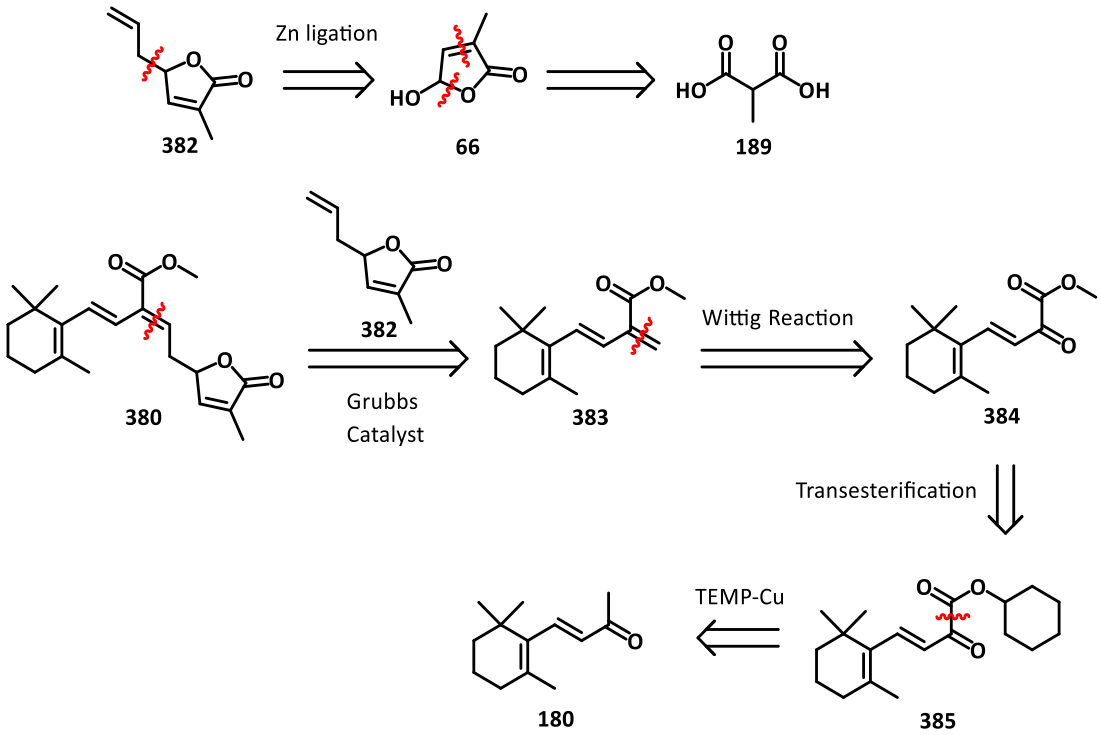

Scheme 4.1: Retrosynthesis of derivative **380** *via* Grubbs olefination.

In this chapter, we made efforts to synthesize derivative **380** and the retrosynthetic analysis of the proposed analogue **380** is shown in Scheme 4.1. A common disconnection of the highlighted olefin reveals disubstituted alkene **383**, along with the allylated butenolide **382**. In the forward direction, we projected that the partners could be united using a cross-metathesis reaction. The A-ring containing intermediate **383,** underwent functional group interconversion to reveal the corresponding carbonyl compound **384**. We projected that Wittig reactions on ketones **384** would install the required olefins. Further functional group interconversions revealed that the ketone intermediate could be derived from β-ionone **180**. For instance, oxidation of the methyl ketone in β-ionone **180** would deliver the α-ketoester **385**.

The allylated butenolide **382** could be easily prepared from zinc catalyzed allylation of D-ring-OH **66**. The synthesis of D-ring-OH **66** was shown in Chapter 2.

4.2.2 Mechanism of TEMP-Cu(I) Co-Catalyzed Oxidation

In 2015, Jiao and co-workers reported a new method for the conversion of methyl ketones into a-ketoesters *via* a co-catalyzed oxidative pathway by 2,2,6,6-tetramethylpiperidine and copper(I).[190] In their protocol, more than 2 equivalents of cyclohexanol **382** was employed as the alcoholic reagent to form the α-ketoesters in high yields (Scheme 4.2).

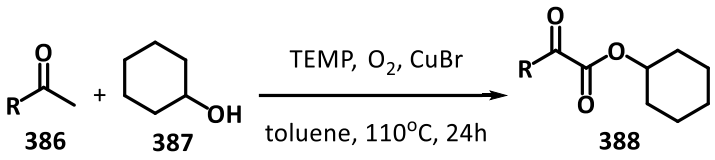

Scheme 4.2: Jiao's method on generating α-ketoesters **388**.

By varying reactions conditions, monitoring the reaction by electron paramagnetic resonance spectroscopy, and conducting radical scavenger reactions, Jiao and co-workers identified the glyoxal monohydrate **390** as a key intermediate in the mechanistic pathway (Scheme 4.3).

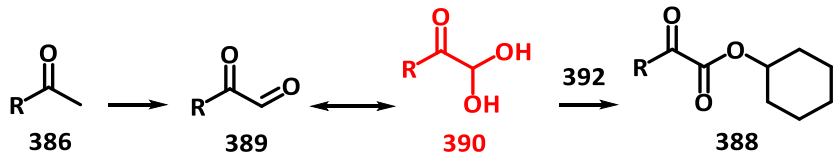

Scheme 4.3: Proposed intermediate **390** in Jiao's report.

Jiao and co-workers proposed a potential mechanism, which is shown in Scheme 4.4.

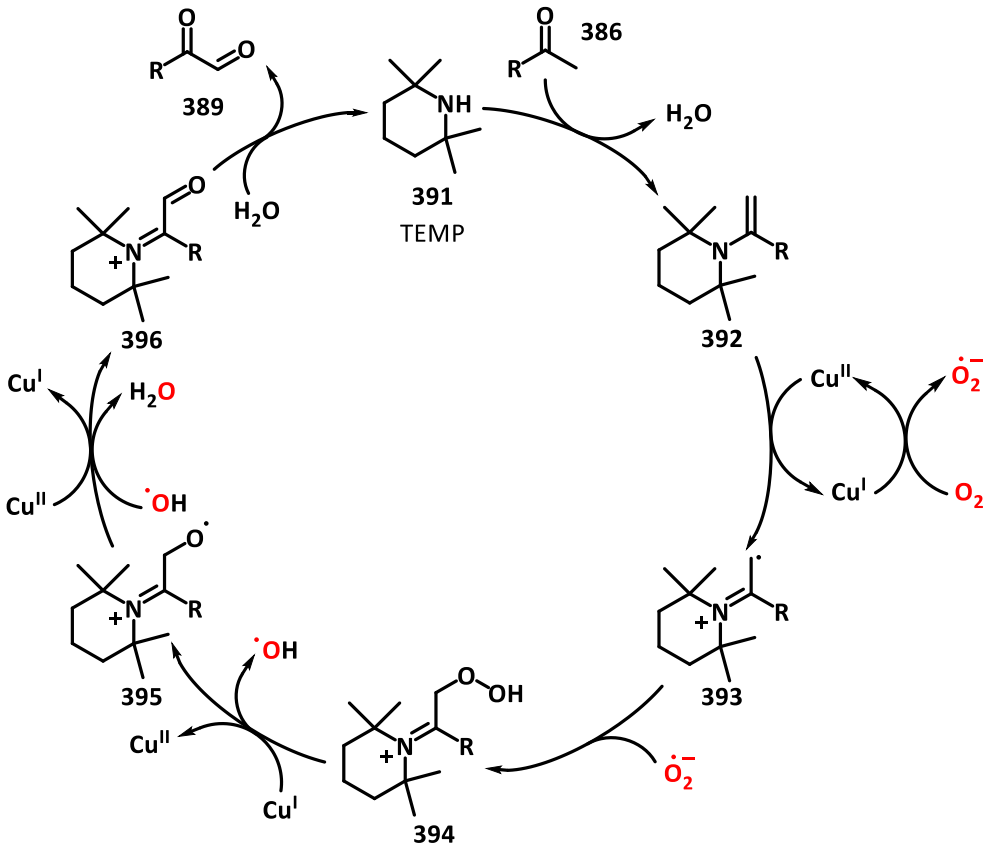

Scheme 4.4: Proposed mechanism to intermediate **389**.

In their proposed mechanism, reaction of ketone **386** with TEMP, accompanied by the release of one molecule of water, provided adduct **392**. The interaction between molecular oxygen and copper(I) leads to the formation of copper (II) and a superoxide radical ($O_2^{-}\cdot$). The resulting copper (II) species rapidly oxidizes the enamine adduct **392**, generating a radical cation **393**, which subsequently reacts with the superoxide radical to form the peroxide intermediate **394**. Following this step, additional redox steps between copper (I) and copper (II) promotes the generation of further oxygen-centered radicals which cleave the peroxyl group in compound **394** into an aldehyde and water, to yield aldehyde **396**. The final hydrolysis of aldehyde **396** affords the diketone intermediate **389**, the core structure of glyoxal monohydrate **390**. Oxidation of **390** in the presence of cyclohexanol provides the α-keto ester **388**.

4.2.3 Grubbs Catalysts

Grubbs' ruthenium-based catalysts were first reported by Grubbs in 1992 (Figure 4.5). In the first iteration, the ruthenium centre was decorated with a alkylidene, and the catalyst proved active in olefin metathesis reactions.[191] Grubbs was awarded a Nobel Prize for this contribution, and Grubbs' catalyst has been widely utilized in organic synthesis for the generation double bonds due to its air-stability and good solubility in most organic solvents. Till now, at least three generations of these catalysts have been developed and used by organic chemists.[192,193] Hoveyda and co-workers investigated the effect of the ligands on catalyst activity, and developed the Hoveyda-Grubbs catalyst, which contained a carbene ligand in addition to a chelating alkylidene.[194] The Hoveyda-Grubbs catalyst is frequently used for cross-metathesis reactions.

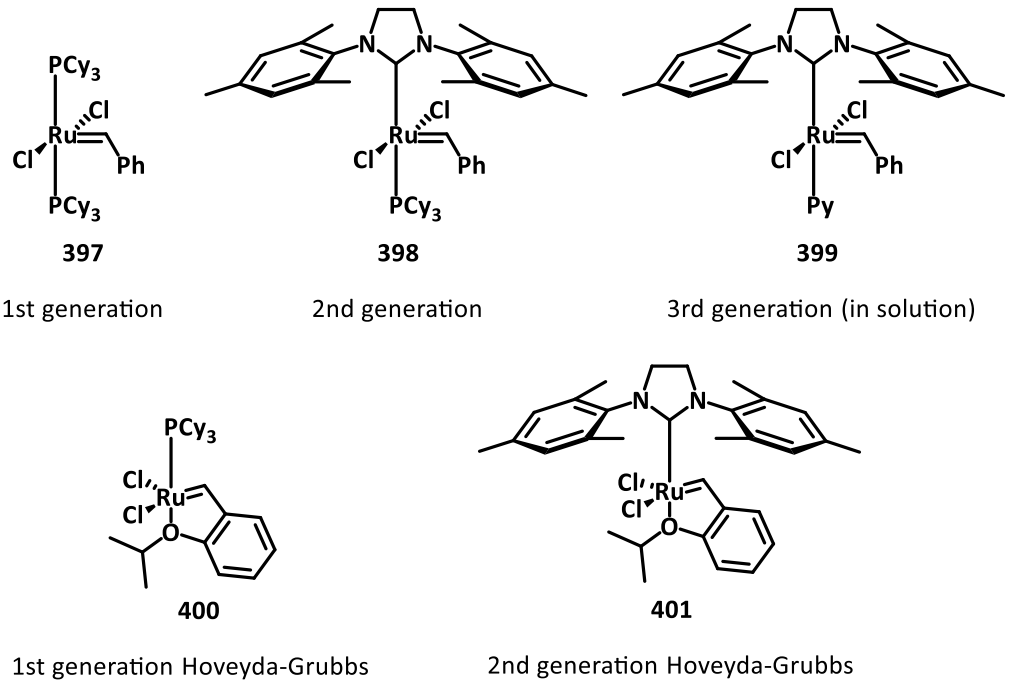

Figure 4.5: Structures of each generation Grubbs and Hoveyda-Grubbs catalysts.

Due to commercial availability, in this work the second generation Grubbs catalyst was selected as the catalyst of choice to generate CL-type derivatives.

4.2.4 Results, Challenge on Synthesizing MeCLA Analogue 380

Our first target was MeCLA derivative **380** (Scheme 4.5) and we selected Jiao's TEMP–Cu(I) co-mediated oxygenation to convert the starting material β-ionone **180** into cyclohexyl ester **385**.[190] As such, β-ionone **180**, cyclohexanol, TEMP, and copper(I) bromide were dissolved in toluene and purged with oxygen before heating under reflux for 20 hours. This delivered cyclohexyl ester **385** in good yield.

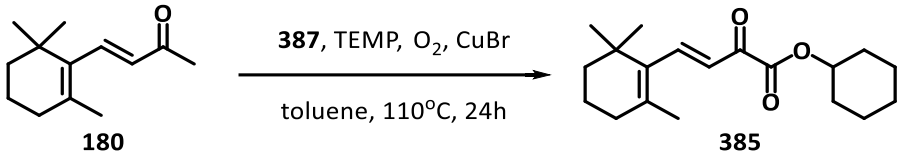

Scheme 4.5: TEMP-Cu(I) oxidation to synthesize cyclohexyl ester **385**.

Transesterification using a methanol solution of sodium methoxide at room temperature, converted the cyclohexyl ester **385** into the methyl ester **384** (Scheme 4.6). Methyl ester **384** was subsequently subjected to a Wittig reaction with triphenylphosphonomethyl bromide under basic conditions, to efficiently convert the α-carbonyl group into a carbon-carbon double bond **383**. Compound **383** was the desired intermediate for the projected cross-metathesis reaction.

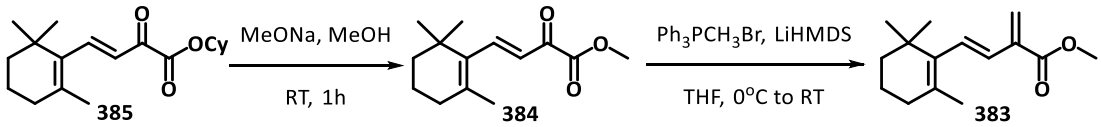

Scheme 4.6: Synthesis of compound **384** and **383**.

The other olefinic partner for the cross-metathesis reaction, compound **382**, was prepared as shown in Scheme 4.7. The previously generated hydroxy butenolide **66** was dissolved in THF containing allyl bromide at 0°C, followed by the addition of a large excess of zinc powder. The zinc was activated by the slow addition of saturated ammonium chloride solution at 0°C. After stirring the reaction mixture overnight, the desired allylated butenolide **382** was obtained in good yield.

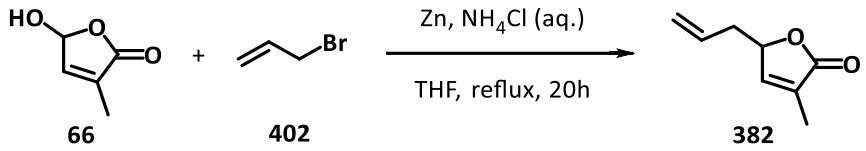

Scheme 4.6: Synthesis of allyl Dring **382**.

With both alkene coupling partners **382** and **383** in hand, the stage was set for the cross-metathesis.

Unexpectedly, subjecting a mixture of **382** and **383** to the action of Grubbs 2nd generation catalyst provided the two products **403** and **404** (Scheme 4.7). These undoubtedly arise via intermolecular Diels-Alder reaction of the starting ester **383**. To provide a clear visualization of how this side reaction occurred, products **403** and **404** are colour coded with red and green in Scheme 4.7.

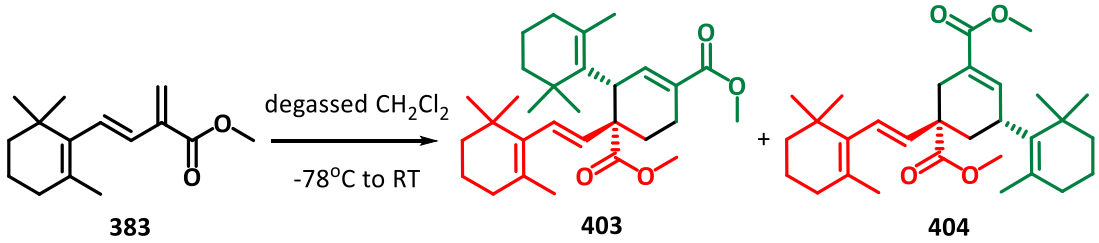

Scheme 4.7: Unexpected Diels-Alder reaction of final step.

Based on this experimental result, we made modifications to the olefin metathesis protocol. In a nitrogen-protected reaction vessel, we first dissolved alkene **382** in degassed dichloromethane and added the Grubbs catalyst next. Subsequently, a diluted dichloromethane solution of molecule **383** was added dropwise to the reaction mixture at -78°C to minimize the occurrence of the Diels-Alder reaction**.** However, these changes showed no significant improvement, as the only reaction products remained the adducts **403** and **404**.

4.3 Summary

This chapter focused on the synthesis of a MeCLA-type strigolactone analogue, for potential applications in chemistry, biology, agriculture, and even therapeutic research. A short sequence of TEMP-Cu(I)-mediated oxygenation, transesterification, and Wittig methylenation provided one substrate for a planned cross-metathesis reaction. The second partner, an allylated butenolide, was also generated in short order (2 total steps). However, an unexpected Diels-Alder reaction occurred in the presence of the Grubbs ruthenium-based catalyst, and precluded the desired cross-metathesis reaction.

Nonetheless, we have at least confirmed that the Wittig reaction could proceed effectively with current structures. In further studies, the synthetic route towards derivative **380** may be restructured to position the Wittig reaction as the key step. Specifically, the step originally intended for the Wittig reaction could be moved to the final stage of the synthesis, allowing the target molecule to be constructed. The updated retrosynthesis has been illustrated in Scheme 4.8.

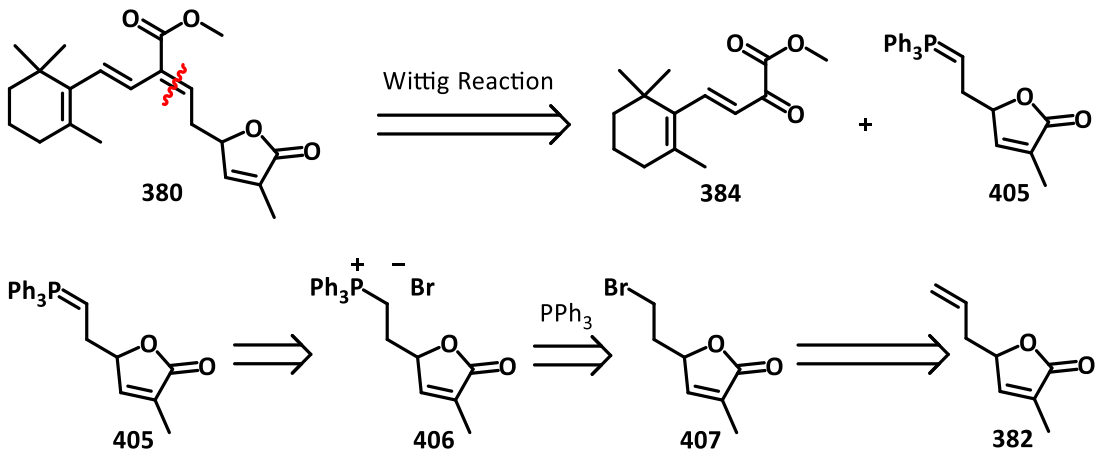

Scheme 4.8: Retrosynthetic analysis for further work.

Taking the Wittig reaction in Scheme 4.1 as a reference, derivative **380** can also be obtained via the Wittig reaction between carbonyl methyl ester **384** and Wittig reagent **405**. So, future work could focus on the synthesis of an alternative substrate, Wittig reagent **405**. Molecule **405** can be easily obtained by elimination of one molecule of

HBr from the phosphonium salt **406**, which are produced by the addition between brominated butenolide **407** and triphenylphosphine. The previously mentioned molecule **382** can be readily converted into molecule **407** through a series of common reactions.

5 THESIS CONCLUSIONS

To understand the biosynthesis and biological mechanisms of action of the class of phytohormones known as strigolactones, synthetic access to these molecules is required.

This thesis discussed the investigation of a number of strategies to address the shortcomings of current strigolactone chemistry. The central tenet of this work was to uncover scalable and cost-effective strategies to generate CL (**24**) and CLA (**27**), and their radio-labelled and selectively oxygenated analogues. Strategies for the synthesis of the highly sterically congested non-canonical strigolactone, avenaol, were also investigated.

The magnitude of the challenge associated with synthesis of these targets cannot be understated. The linear triene system of CL (**24**) and CLA (**27**), and the presence of an enol ether linked butenolide, render these molecules labile to acid, base, and light. Similarly, the non-canonical strigolactone, avenaol, possesses a highly strained, all-*cis* cyclopropane unit that is labile to ring-opening when heated.

Nonetheless, detailed investigations into the applicability of a Darzens reaction–epoxide rearrangement strategy, a Chan-Lam coupling strategy, a nucleophile-catalyzed aldol lactonization (NCAL)–decarboxylation strategy, and a cross-metathesis strategy were undertaken for the synthesis of CL (**24**), CLA (**27**), and analogues. These were all demonstrated to be unsuitable for the generation of the target molecules.

As all three of the previously proposed synthesis routes have been proven to be unfeasible at this stage, future research will primarily proceed by two directions. The first is the development of an entirely new synthetic route that is significantly different from the three existing approaches. The second is the optimization of the most challenging steps within the current three strategies.

For example, in the Chan-Lam coupling approach, we could explore a broader range of coupling substrates containing the D-ring unit in combination with mentioned organoboron reactants. Additionally, efforts could be made to eliminate the potential effect of pinacol by replacing the pinacol ester with other boron esters.

Similarly, in the NCAL strategy, a small-scale methodological study could be conducted to further optimize the reaction conditions, which may include the synthesis and evaluation of a series of structurally diverse substrates to identify the molecules resembling carlactone in both structure and reactivity, thereby enabling more representative studies.

In Chapter 3, the rapid generation of the single diastereomer [4.1.0] ring system corresponding to the A, B-ring system of avenaol, was reported. In order to invoke an intramolecular Horner-Wadsworth-Emmons (HWE) reaction, epimerization of a key cyclopropyl aldehyde intermediate was studied. Despite much effort, conditions to effect this epimerization were not uncovered. Therefore, modification of a previously unsuccessful radical-based approach to avenaol was investigated. Again, rapid access to a single diastereomer [4.1.0] ring system was achieved. However, attempted radical-mediated coupling of this intermediate to an activated butenolide fragment proved elusive.

While the outcomes until now have not meet our expectations, there has still been some positive results. As previously mentioned, the novel seven-membered ring intermediate we designed continues to be a key component in the optimization of Tsukano's route. Future research may focus on the stereoselective synthesis of this intermediate.

And finally in Chapter 4, we aimed at synthesizing derivatives of carlactone to replace the naturally occurring molecule, which is unstable under many conditions, for utilizing in subsequent experiments. By replacing the oxygen atom that serves as the bridge between the carbon framework and the D-ring with a carbon atom, and by optimizing

the double bond system, we designed several structural derivatives. In this chapter, we described a series of synthetic efforts on the preparation of molecule **380**.

Although the initial attempts resulted in unanticipated side reactions leading to Diels-Alder products, they also inspired us to develop a new synthetic route basing on the Wittig reaction.

The work in this thesis will inform the next iteration of researchers who undertake the challenge of simplifying the synthesis of strigolactones. I firmly believe that optimized total synthesis pathways to natural SL molecules and analogues, will be realized in the near future.

6 EXPERIMENTAL

6.1 General Experimental

All non-aqueous reactions were performed under an inert argon or nitrogen atmosphere in oven-dried glassware unless otherwise stated. Methanol (MeOH), (*N*, *N*)-dimethylformamide (DMF), tetrahydrofuran (THF), dichloromethane (CH_2Cl_2), diethyl ether (Et_2O), acetonitrile (MeCN or CH_3CN) and toluene (PhMe) were purified and dried by passage through 3 Å molecular sieves and alumina column with an Innovative Technology Puresolv System. Some solvents including dichloromethane (CH_2Cl_2), methanol (MeOH) and acetonitrile (MeCN or CH_3CN) were ultra-dried over 4 Å molecular sieves under particular circumstances. Deuterated solvents chloroform-d ($CDCl_3$), methanol-d_4 (CD_3OD), acetonitrile-d_3 (CD_3CN), water-d_2 (D_2O) and dichloromethane-d_2 (CD_2Cl_2) were kept and stored in 3 Å molecular sieves and all other solvents were used without further purification unless otherwise stated.

Flash column chromatography was performed using Merck Kieselgel 40-63 μm (230-400 mesh) silica gel. Analytical thin-layer chromatography (TLC) was performed on Merck Kieselgel 60 F_{254} precoated aluminium sheets, visualized using UV light (at 365 nm and 254 nm), and developed using acidic ethanolic anisaldehyde stain with heat, basic aqueous potassium permanganate stain with heat and acidic butanoic dinitrophenylhydrazine (DNP) stain with heat.

α-ionone and β-ionone were purified through column chromatography on silica gel via 5% ethyl acetate (EtOAc) in hexane (small scale) and distillation (large scale). Triethylamine (TEA or Et_3N) was freshly distilled from potassium hydroxide. Dicyclohexylcarbodiimide (DCC) was purified by recrystallisation from a mixture of ethyl acetate (EtOAc) and water. *N*-bromosuccinimide (NBS) was purified by recrystallisation from water. Other commercially available chemicals were used neat from their reagent containers as received, or purified by using commonly known

standard protocols.

Nuclear magnetic resonance (NMR) spectroscopy was conducted at 300K on Bruker AVANCE DPX300 (^{1}H at 300Hz) or 500(^{1}H at 500Hz) spectrometers with samples dissolved in deuterated solvents mentioned above. Chemical shifts are reported as parts per million (ppm) and all coupling constants are reported in hertz (Hz) unless otherwise stated. ^{1}HNMR residual solvent peaks: $CDCl_3$ (δ = 7.26), CD_3OD (δ = 3.31), CD_3CN (δ = 1.94), D_2O (δ = 4.79), CD_2Cl_2 (δ = 5.32). ^{13}CNMR residual solvent peaks: $CDCl_3$ (δ = 77.16), CD_3OD (δ = 49.00), CD_3CN (δ = 1.32 & 118.26), D_2O (δ = N/A), CD_2Cl_2 (δ = 53.84). Multiplicity is reported as these following abbreviations: s = singlet, d = doublet, t = triplet, q = quartet, m = multiplet, br = broad, dd = doublet of doublets and dt = doublet of triplets.

Gas chromatography-mass spectrometry (GC-MS), low resolution electrospray ionisation (ESI) and atmospheric pressure chemical ionisation (APCI) mass spectra were obtained using a Bruker Amazon SL spectrometer with a nebulizer spray source. And high resolution mass spectra were obtained using a Bruker Apex II FTICR 7 T mass spectrometer equipped with an off-axis Analytical ESI and APCI source.

Melting points were uncorrected and determined using a Stanford Research Systems Optimelt automated melting point system in open capillaries.

Infrared (IR) spectra were acquired on a Bruker Alpha FT-IR spectrometer with a diamond ATR or zinc-selenium accessory and processed using OPUS software.

6.2 Synthesis of Reagents

2-methylmalonic acid

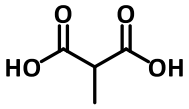

189

To a cooled solution of aqueous KOH (100 mL, 0.5 mol, 5 M, 8.9 eq.) was added diethyl methylmalonate (9.75 g, 9.6 mL, 0.056 mmol, 1.0 eq.) at 0°C, and stirred for 5 minutes. The reaction was then allowed to warm to room temperature and stirred for 48 hours. The reaction mixture was washed with diethyl ether (2 × 40 mL) and the aqueous layer was acidified with aqueous HCl (100 mL, 4 M). The aqueous layer was extracted and washed with EtOAc (5 × 50 mL) and the combined organic layers were dried over Na_2SO_4, filtered, and concentrated *in vacuo*, to give the product **189** as a white solid (6.24 g, 94.4%). **m.p.**: 134.4 °C~136.0 °C; **^{1}H NMR** (300 MHz, DMSO) δ 12.63 (s, 2H), 3.35 (q, *J* = 7.2 Hz, 1H), 1.26 (d, *J* = 7.2 Hz, 3H); **^{13}C NMR** (75 MHz, DMSO): δ 172.1, 46.1, 13.9; **LRMS** (ESI, *m/z*) calculated for $C_4H_5O_3$ $[M-H]^-$ 117.02, found 117.07; **IR** (neat/cm^{-1}): 3008, 2883, 2714, 2612, 2543, 1686, 1468, 1410, 1289, 1209, 1092, 896, 770, 669, 568, 508, 440. Data is in agreement with literature.[122]

5-hydroxy-3-methylfuran-2(5H)-one

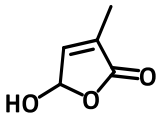

66

To a stirring solution of glyoxal (3.6 mL, 39% w/v in H_2O, 1.8 eq.) in deionised water (30 mL) was added methyl malonic acid (2.73 g, 23 mmol, 1.0 eq.) at room temperature, followed by dropwise addition of H_2SO_4 (6 drops, 98%). The reaction mixture was then heated at reflux for 27 hours, before being cooled and solid NaCl was added. The aqueous layer was extracted with EtOAc (4 × 20 mL) and the combined organics were dried with Na_2SO_4, filtered and concentrated *in vacuo*. The residual crude was purified using flash chromatography, eluting with 40% EtOAc in hexanes, to give the furanone product **66** as a light yellow solid (1.62 g, 62% product not super pure). **m.p.** 53.9 °C~56.3 °C; **^{1}H NMR** (300 MHz, $CDCl_3$) δ 6.88 (dd, *J* = 1.6 Hz, 1H), 6.08 (d, *J* = 7.2 Hz, 1H), 3.92 (s, 1H), 1.95 (s, 3H); **^{13}C NMR** (75 MHz, $CDCl_3$) δ 172.1, 144.1, 134.0, 96.6, 10.5; **LRMS** (ESI, *m/z*) calculated for $C_5H_7O_4$ $[M+OH]^+$ 131.04, found 131.46; **IR** (neat/cm^{-1}) 3355, 3094, 2949, 1726, 1411, 1348, 1202, 1006, 914, 792, 647, 560. Data is in agreement with literature.[122]

5-bromo-3-methylfuran-2(5H)-one

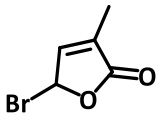

76

DringOH **48** (4.39 g, 39.0 mmol, 1.0 eq.) and tetrabromomethane (16.00 g, 48.0 mmol, 1.2 eq.) were dissolved in dichloromethane (50 mL). Followed by adding triphenylphosphine (12.70 g, 48.5 mmol, 1.2 eq.) in dichloromethane (25 mL) at 0°C. The reaction mixture was stirred for 3 h. The solvent was then removed in vacuo. The concentrated crude was purified by column chromatography, eluting by 10% EtOAc in hexanes, to give the compound **76** (5.78 g, 81%) as a yellow oil. **^{1}H NMR** (300 MHz, $CDCl_3$) δ 7.20 (dq, *J* = 1.6 Hz, 1H), 6.83 (dq, *J* = 1.4 Hz, 1H), 2.00 (t, *J* = 1.6 Hz, 3H). **^{13}C NMR** (75 MHz, $CDCl_3$) δ 170.3, 146.2, 130.8, 74.85, 53.48, 10.50; Mass spectrum cannot be found. Data is in agreement with literature.[103]

tert-butyl (4-methyl-5-oxo-2,5-dihydrofuran-2-yl) carbonate

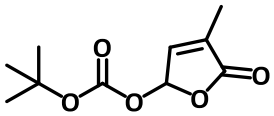

190

To a solution of methyl butenolide 48 (1.14 g, 10 mmol, 1.0 eq.) in dichloromethane (30 mL) was added di-*tert*-butyl decarbonate (3.29 g, 15 mmol, 1.5 eq.) followed by triethylamine (1.4 mL, 10 mmol, 1.0 eq.) and the reaction was stirred to react at room temperature for 16 hours. The solvent was removed in vacuo and the crude mixture was purified by flash column chromatography with 5% to 10% EtOAc in hexanes to obtain the title compound (1.83 g, 86%) as a colourless oil. **m.p.**: 42.1°C~44.4°C; **^{1}H NMR** (300 MHz, $CDCl_3$) δ 6.85 (s, 1H), 6.64 (s, 1H), 1.88 (s, 3H), 1.43 (s, 9H); **^{13}C NMR** (75 MHz, $CDCl_3$) δ 170.6, 151.0, 141.3, 134.4, 94.1, 84.1, 27.2, 10.0; **LRMS** (ESI, *m/z*) calculated for $C_{10}H_{14}O_5Na$ $[M+Na]^+$ 237.07, found 237.31; **IR** (neat/cm^{-1}) 3088, 2989, 2928, 1752, 1453, 1367, 1255, 1161, 1094, 1026, 957, 877, 852. Data is in agreement with literature.[103]

Straight forward synthesis of Darzens acid 202:

ethyl (*E*)-3-methyl-3-(2-(2,6,6-trimethylcyclohex-1-en-1-yl)vinyl)oxirane-2-carboxylate

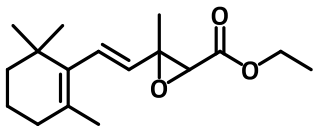

181

A mixture of 3.4 mL (30 mmol, 1.5 eq.) of ethyl bromoacetate, [**Method A:** 1.9 mL (1.0 mmol, 0.5 eq.); **Method B:** 3.8 mL (20 mmol, 1.0 eq.) of β-ionone] and 10mL of dry thiophene-free toluene was cooled to -78°C in a flask supplied with a stirrer, a nitrogen inlet and a dropping funnel attached to a flask containing 1.13 g (21 mmol, 1.05 eq.) of alcohol-free sodium methoxide in 5mL toluene. A little over one-half of the sodium methoxide was slowly added with vigorous stirring in the course of one-half hour, [**Method A:** then an additional 1.9 mL of β-ionone was added dropwise with rest sodium methoxide in the course of one-half hour alternately; **Method B:** the rest sodium methoxide was added in half an hour.] The mixture was then packed at -78°C and allowed to stir gently overnight, warming up slowly to room temperature. The mixture was then heated in nitrogen on the water-bath for four hours, then cooled quickly to -5°C and maintained at this temperature while the aqueous solution of tartaric acid was added to it. The toluene layer was separated, washed with water, dried, and the toluene and excess ethyl bromoacetate removed on the water-bath under reduced pressure. The crude mixture was then purified by fractional distillation and the fraction with boiling point around 156°C was collected to obtain the title compound **181** (3.41 g, yield 61.2%) as an orange oil (Method A & B were mentioned in **Chapter 2**, ***section 2.3.3***). **m.p.**: 36.4 °C~37.9 °C; **^{1}H NMR** (500 MHz, $CDCl_3$) δ 7.27 (dd, *J* = 16.4, 1.1 Hz, 1H), 6.11 (dd, *J* = 16.4, 1.1 Hz, 1H), 3.88 (s, 1H), 2.29 (s, 3H), 2.07 (t, *J* = 6.4 Hz, 3H), 1.76 (d, *J* = 0.9 Hz, 3H), 1.69 – 1.54 (m, 2H), 1.57 – 1.43 (m, 3H), 1.37 – 1.20 (m, 2H), 1.07 (s, 6H).

The failed method of entries **6** and **7**: Cool a solution of lithium bis(trimethylsilyl)amide (LiHMDS 1.05 eq.) or lithium diisopropyl amine (LDA 1.05 eq.) in THF to -78°C under

a positive pressure of argon followed by adding the solution of ethyl chloroacetate (1.0 eq.) dropwise to the reaction. After stirring for 15 minutes, β-ionone (1.0 eq.) was added dropwise over 5 minutes. Allow the reaction to warm to 25°C and stir for 2 hours. Quench the reaction by adding 10%HCl and dilute the reaction with diethyl ether. Wash the organic phase with 10%HCl, deionized water and brine. Dry the organic phase with sodium sulphate and remove the solvent.

(3*E*,5*Z*)-2-hydroxy-3-methyl-5-(2,6,6-trimethylcyclohex-2-en-1-ylidene)pent-3-enoic acid

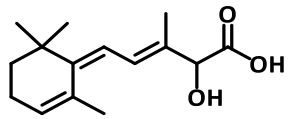

202

The hydroxy ester **174** (3.41 g, 12.4 mmol, 1.0 eq.) was hydrolyzed by potassium hydroxide in the 1:1 mixture of water and methanol, then diluted with one volume of water and extracted several times with hexane to remove the non-saponifiable materials. The water layer was then neutralized with diluted hydrochloric acid and extracted with ether several times. Then the solution was extracted with excess sodium bicarbonate solution to form the strongly enolic structure. And then the title product **186** was covered by acidification with diluted hydrochloric acid. The crude acid thus obtained was dissolved in the least volume of ether to the solution was added enough hexane until a cloudiness resulted. The mixture was allowed to stand in fridge for several days to obtain the orange acid **202** with both solid and liquid formations (2.28 g, yield 73.5%). **m.p.**: around room temperature (both liquid and solid formations under common circumstance). **^{1}H NMR** (500 MHz, $CDCl_3$) δ 6.88 (d, *J* = 11.6 Hz, 1H), 6.20 (dd, *J* = 11.7, 2.7 Hz, 1H), 5.85 – 5.76 (m, 1H), 4.70 (d, *J* = 13.4 Hz, 1H), 2.20 (s, 1H), 2.18 – 2.00 (m, 2H), 1.90 (q, *J* = 1.6 Hz, 3H), 1.82 (d, *J* = 1.4 Hz, 3H), 1.51 (q, *J* = 6.1 Hz, 2H), 1.33 – 1.18 (m, 6H); **^{13}C NMR** (126 MHz, $CDCl_3$) δ 145.8, 144.5, 134.03, 65.87, 34.85, 33.89, 31.59, 29.00, 28.79, 25.75, 21.69, 19.21, 15.25, 14.12, 11.75; Mass spectrum cannot be found.

1,3-dioxoisoindolin-2-yl (3*E*,5*Z*)-2-hydroxy-3-methyl-5-(2,6,6-trimethylcyclohex-2-en-1-ylidene)pent-3-enoate

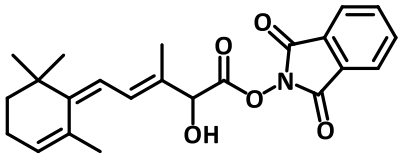

203

To a solution of acid **186** (500 mg, 2.0 mmol, 1.0 eq.) in diethyl ether (20 mL) was added N-hydroxyphthalimide (340 mg, 2.1 mmol, 1.05 eq.), DCC (412 mg, 2.0 mmol, 1.0 eq.) and DMAP (12 mg, 0.1 mmol, 5mol%). The reaction was stirred at room temperature for 3 hours. After finishing, the reaction mixture was filtered and the filter cake was washed with a minimum volume of diethyl ether and repeated the protocol above several times to remove the DCC urea. The residue was concentrated *in vacuo* and purified by flash column chromatography eluting by 15% to 25% EtOAc in hexanes, to give the compound **203** as a light orange solid (709 mg, yield 89.7%). **m.p.**: 31.6 ℃~33.0 ℃; **^{1}H NMR** (500 MHz, $CDCl_3$) δ 7.92 (dd, *J* = 5.5, 3.1 Hz, 2H), 7.87 – 7.75 (m, 2H), 6.99 (d, *J* = 11.4 Hz, 1H), 6.25 (dd, *J* = 11.5, 2.1 Hz, 1H), 5.82 (t, *J* = 4.6 Hz, 1H), 5.22 – 5.02 (m, 1H), 1.97 (d, *J* = 1.4 Hz, 3H), 1.95 – 1.89 (m, 2H), 1.72 (s, 3H), 1.61 – 1.41 (m, 2H), 1.40 – 1.25 (m, 6H); **^{13}C NMR** (126 MHz, $CDCl_3$) δ 174.6, 170.9, 156.6, 140.3, 134.0, 133.5, 130.0, 129.3, 129.3, 128.8, 127.9, 90.89, 57.48, 35.13, 28.53, 23.72, 21.21, 18.71; **LRMS** (ESI, *m/z*) calculated for $C_{23}H_{24}NO_5$ $[M-H]^-$ 394.16, found 393.96.

bis(4,4,5,5-tetramethyl-1,3,2-dioxaborolan-2-yl)methane

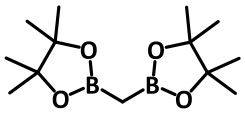

207

To a flask with dry methanol (20 mL) at 0°C ice bath was added small pieces of Li metal (0.695 g, 100 mmol). As soon as Li metal coated with LiOMe on the surface of small lithium pieces, a glass shield was used and dry MeOH was added incredibly slowly dropwise until the reaction resumed. Once all the Li metal had dissolved, the solvent was concentrated in vacuo to give LiOMe (3.47 g, yield 91%) as a white solid. To the newly prepared LiOMe (3.47 g, 91.3 mmol, 1.5 eq.) was added CuI (0.579 g, 3.04 mmol, 5 mol%) and bis(pinacolato)diboron (15.4 g, 60.8 mmol, 1.0 eq.). The flask was purged with argon and DMF (60 mL) was added slowly. The reaction mixture was sonicated for 15 minutes and then cooled to 0°C using an ice bath. Dibromomethane (4.2 mL, 10.6 g, 60.9 mmol, 1.0 eq.) was then added dropwise with vigorous stirring. Following completion of the addition, the cooling bath was removed and the reaction mixture was stirred at room temperature overnight. After monitoring the reaction with TLC, diethyl ether (200 mL) was added to the reaction mixture and then filtered through a short plug silica, rinsed with diethyl ether (50 mL) and the filtrate was then concentrated in vacuo. To the crude residue was then added hexanes (100 mL), washed with water (100 mL) ten times (as many as possible) to remove most of DMF, dried over Na_2SO_4, filtered and concentrated *in vacuo*. Followed by further drying under highvac afforded the compound as a white solid (10.3 g, yield 63.2%). **m.p.** 52.9 °C~55.5 °C; **^{1}H NMR** (300 MHz, $CDCl_3$): δ 1.23 (s, 24H), 0.35 (s, 2H); **^{13}C NMR** (75 MHz, $CDCl_3$) δ 24.78, 83.06; **^{11}B NMR** (128 MHz, $CDCl_3$) δ 33.83; **LRMS** (ESI, *m/z*) calculated for $C_{13}H_{26}B_2O_4Na$ $[M+Na]^+$ 291.19, found 291.22; **IR** (neat/cm^{-1}) 2977, 2932, 1354, 1307, 1267, 1138, 966, 896, 844, 674, 578. Data in agreement with literature.[196]

4,4,5,5-tetramethyl-2-((3*E*)-2-methyl-4-(2,6,6-trimethylcyclohex-1-en-1-yl)buta-1,3-dien-1-yl)-1,3,2-dioxaborolane

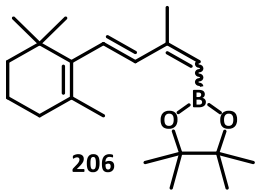

206

To a cooled solution of tetramethylpiperidine (1.71 mL, 10.0 mmol, 1.0 eq.) in dry THF (20 mL) at 0°C under argon was added dropwise 2.5M (2.14 M by titration) n-butyllithium (4.7 mL, 10.0 mmol, 1.0 eq.) and stirred for a further 15 minutes. To the reaction mixture was then added a solution of $CH_2(Bpin)_2$ (2.72 g, 10.1 mmol, 1.01 eq.) in THF (5 mL) at 0°C and stirred for another 15 minutes. The reaction mixture was then cooled to -78°C and a solution of β-ionone (1.8 mL, 9.1 mmol, 0.91 eq.) in THF (5 mL) was added dropwise. The reaction mixture was stirred at -78°C for 1 hour, then warmed to 0°C and stirred for another 2 hours. Water (100 mL) was added and the aqueous layer was extracted with diethyl ether (3 × 50 mL). The combined organics were dried over Na_2SO_4, filtered and concentrated *in vacuo*, to give a cis-trans isomeric mixture of dioxaborolane as a yellow oil (2.37 g, yield 82.4%). **^{1}H NMR** (500 MHz, $CDCl_3$) (*Z* : *E* ≈ 1 : 1.2) δ 7.23 (s, 1H), 6.36 (d, 1H), 6.08 (d, 1H), 5.26 (s, 1H), 2.03 (d, 3H), 1.77 (d, 3H), 1.49 – 1.43 (m, 5H), 1.26 (s, 12H), 1.09 (s, 6H); δ 7.17 (s, 1H), 6.27 (d, 1H), 6.13 (d, 1H), 5.28 (s, 1H), 2.15 (d, 3H), 1.67 (d, 3H), 1.64 – 1.56 (m, 5H), 1.28 (s, 12H), 1.00 (s, 6H); **^{13}C NMR** (125 MHz, $CDCl_3$) δ 156.07, 139.26, 137.48, 133.30, 129.91, 129.61, 82.79, 82.74, 40.32, 39.49, 34.19, 34.15, 33.63, 32.93, 28.95, 28.88, 24.86, 24.59, 21.69, 21.61, 19.24, 16.48; **HRMS** (ESI, *m/z*) calculated for $C_{20}H_{34}BO_2$ $[M+H]^+$ 317.2752, found 317.2756; **IR** (neat/cm^{-1}) 2976, 2927, 2864, 1598, 1446, 1362, 1265, 1141, 968, 852.

potassium trifluoro((3*E*)-2-methyl-4-(2,6,6-trimethylcyclohex-1-en-1-yl)buta-1,3-dien-1-yl)borate

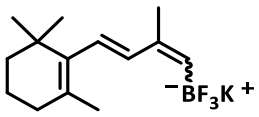

205

To a suspension of alkenylboronic isomers (235 mg, 0.75 mmol, 1.0 eq.) in MeOH and CH_3CN was added a solution of potassium fluoride (193 mg, 3.38 mmol, 4.5 eq,) in water at room temperature. After stirring for 15 minutes, a solution of L-(+)-tartaric acid (280 mg, 1.82 mmol, 2.45 eq.) in THF (2 mL) was added dropwise to the rapidly stirring biphasic reaction mixture, causing the instant formation of a white precipitate, which flocculated for a further 5 minutes. The reaction mixture was then diluted with CH_3CN and filtered. Following further washes of the flask and filter cake with CH_3CN, the filtrate was concentrated *in vacuo*. The residual was then dissolved in 50:50 aqueous methanol and concentrated *in vacuo*. The residual was then dried under reduced pressure for 5 hours, and then freeze-dried over 24h, to give the titled compound as a mixture of *E* and *Z* isomers, as an impure solid (299 mg cannot calculate yield because of the pinacol impurities). Clean **^{1}H NMR & ^{13}C NMR** spectra cannot be obtained. **^{11}B NMR** (96 MHz, CD_3CN) δ 29.7, 5.19.

potassium trifluoro(phenyl)borate

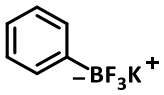

216

To a stirring solution of phenyl boronic acid (250 mg, 2.1 mmol, 1.0 eq.) in a minimum amount of MeOH was added aqueous KHF_2 (750 mg, 7.2 mmol, 3.5 eq.). A white precipitate was formed and the reaction mixture was stirred for a further 15 min before filtered using vacuum filtration. The crude residual was then recrystallised from hot CH_3CN, filtered and evaporated in vacuo to give the product as a white crystalline solid (197mg, yield: 52 %). **m.p.**: ~ 286 °C; **^{1}H NMR** (300 MHz, MeOD): δ 8.12 (d, J = 6.8 Hz, 2H), 7.88 (t, J = 7.1 Hz, 2H), 7.81 (d, J = 7.1 Hz, 1H); **^{13}C NMR** (75 MHz, MeOD): δ 141.1, 136.0, 127.1, 126.3; **LRMS** (ESI, *m/z*) calculated for $C_6H_5BF_3$ $[M]^-$ 145.04, found 144.89; **IR** (neat/cm^{-1}) 3051, 3012, 1434, 1216, 934, 903, 750, 710, 603. Data in agreement with literature.[197]

General protocol of Chan-Lam Coupling Final Step:

To a suspension of **coupling reagent** (potassium trifluoroborate salt or ionyl bis(pinacolato)diboron); **copper catalyst** (several different copper salts); **base** (DMAP, pyridine or TEA) in **solvent** (dichloromethane or acetonitrile) added powdered 4Å molecular sieves and was stirred for 5 minutes at room temperature. To this stirring suspension was added the **D-ring-OH**. The stirring reaction mixture was then sealed with a rubber septum and stirred under **oxidant** (an atmosphere of oxygen or adding silver oxide powder) at **temperature** (room temperature or was heated to reflux). Following a **period** (24 hours to 72 hours), the crude mixture was filtered through a plug of celite to remove the molecular sieves and any insoluble by-products and then concentrated in vacuo.

3-methyl-5-phenoxyfuran-2(5H)-one

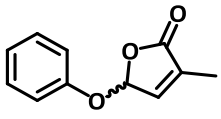

217

Reagents: Potassium phenyl trifluoroborate (1.84 g, 10 mmol, 2.0 eq.); DringOH (570 mg, 5 mmol, 1.0 eq.); pyridine (1.43 g, 15 mmol, 3.0 eq.); silver oxide (3.47 g, 15 mmol, 3.0 eq.) or oxygen atmosphere and powdered 4Å molecular sieves in dichloromethane (10 mL, 0.5 M) heated to 40°C. General protocol has been shown in general protocol of Chan-Lam Coupling Final Step. O_2 atmosphere yield: 46%; Ag_2O yield: 52%. **^{1}H NMR** (300 MHz, $CDCl_3$) δ 7.40 – 7.28 (m, 2H), 7.27 – 7.05 (m, 2H), 6.99 (p, *J* = 1.6 Hz, 1H), 6.30 (p, *J* = 1.4 Hz, 1H), 2.01 (t, *J* = 1.6 Hz, 3H); **^{13}C NMR** (75 MHz, $CDCl_3$): δ 171.8, 156.7, 142.7, 135.0, 131.1, 124.0, 117.4, 99.57, 10.96; **HRMS** (ESI, *m/z*) calculated for $C_{11}H_{10}O_3Na$ $[M+Na]^+$ 213.0528, found 213.0530.

S-phenyl 2-chloroethanethioate

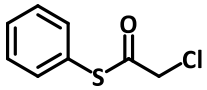

245

Pyridine (1.86 mL, 23.0 mmol, 1.2 eq.) was added dropwise to a stirred solution of chloroacetyl chloride (1.80 mL, 22.6 mmol, 1.2 eq.), thiophenol (2.0 mL, 19.5 mmol, 1.0 eq.) and a catalytic amount of DMAP in CH_2Cl_2 (50 mL) at 0 ºC. The mixture was stirred at 0 ºC for 15 min, then warmed to rt and allowed to stir overnight. The reaction was quenched by the addition of saturated aqueous NH_4Cl (15 mL), diluted in EtOAc (200 mL), H_2O added to just dissolve the formed precipitate (5 mL), organic phase washed with H_2O (2 × 10 mL), brine, dried over Na_2SO_4 and concentrated *in vacuo*. Flash chromatography over silica gel, using 5% EtOAc in hexanes to give compound **216** (3.18 g, yield: 87%) as a pure white solid. **m.p.** 40.2 ℃~41.7 ℃; **^{1}H NMR** (300 MHz, $CDCl_3$): δ 7.44 (br, 5H), 4.29 (s, 2H); **^{13}C NMR** (75 MHz, $CDCl_3$): δ 192.6, 134.7, 130.0, 129.5, 126.4, 47.98. **LRMS** (ESI, *m/z*) calculated for C_8H_8ClOS $[M+H]^+$ 187.00, found 187.09. Data in agreement with literature.[198]

2-bromo-1-butylpyridin-1-ium bromide

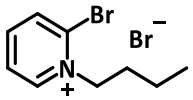

261

In a resealable round bottom flask was placed a solution of 2-bromopyridine (1.91 mL, 3.16 g, 20 mmol, 1.0 eq.) into 6 mL of CH_2Cl_2. The solution was degassed by pump and the flask was purged with argon for three times. Then the solution was cooled to -78°C and 1-bromobutane (2.16 mL, 2.74 g, 20 mmol, 1.0 eq.) was added slowly dropwise with stirring under the protecting atmosphere. The cooling bath was removed and the flask was sealed with septum and wrapped with parafilm, then the reaction mixture was stirred for 36 hours at room temperature. After concentrated in vacuo, toluene (20 mL) was added to the yellow oil, and after stirring for 30 minutes, the reaction mixture was stored in a refrigerator overnight to precipitate the pyridinium salt. The clear supernatant was removed via syringe and an additional 20 mL of dry diethyl ether was added to wash the precipitate. The diethyl ether was removed via syringe again and all subsequent operations were done under a stream of nitrogen to exclude moisture and prevent hydrolysis. The washed solid was dried under highvac for 48 h at 25 °C to afford the product as a brown crystal (3.85 g, yield: 65%). **^{1}H NMR** (300 MHz, $CDCl_3$) δ 10.27 (dd, J = 6.5, 1.7 Hz, 1H), 8.50 (td, J = 7.9, 1.6 Hz, 1H), 8.26 (ddt, J = 7.5, 3.0, 1.5 Hz, 2H), 5.19 – 5.08 (m, 2H), 2.60 (s, 2H), 2.08 – 1.92 (m, 2H), 1.53 (dq, J = 14.8, 7.4 Hz, 2H), 1.01 (t, J = 7.3 Hz, 3H); **IR** (neat/cm^{-1}) 2950, 2376, 1999, 1610, 1442, 1159, 1079, 771, 725, 465. Data in agreement with literature.[199]

S-phenyl 2-((4-methyl-5-oxo-2,5-dihydrofuran-2-yl)oxy)ethanethioate

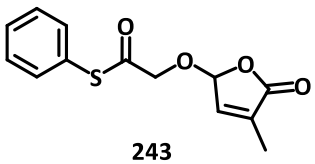

243

Thiophenylacetyl chloride (372 mg, 2 mmol, 1.0 eq.) was added to a solution of potassium carbonate (552 mg, 4 mmol, 2.0 eq.) and Dring furanone (228 mg, 2 mmol, 1.0 eq.) in 20 mL acetone. And potassium iodide (66 mg, 0.4 mmol, 20 mol%) was partly added to the solution. The reaction mixture was stirred at room temperature overnight. 1 M HCl was added to quench the excess base and ether was added. The organic phase was washed with brine two to three times, dried with sodium sulfate, concentrated in vacuo and purified by column chromatography (25% EtOAc in hexanes) to afford title compound (213 mg, yield: 41%). **^{1}H NMR** (300 MHz, $CDCl_3$) δ 7.48 – 7.23 (m, 5H), 6.82 (d, *J* = 6.8 Hz, 1H), 5.54 (s, 1H), 3.66 (d, *J* = 2.3 Hz, 2H), 1.97 (s, 3H); **^{13}C NMR** (75 MHz, $CDCl_3$) δ 193.4, 139.6, 134.1, 129.7, 128.2, 103.9, 75.2, 10.6; Mass spectrum cannot be found (several times *via* ESI, APCI and even GCMS).

1-(3-(2,6,6-trimethylcyclohex-2-en-1-yl)oxiran-2-yl)ethan-1-one

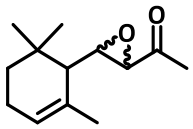

291

To a solution of α-ionone (5.00 g, 26.0 mmol, 1.0 eq.) in methanol (30 mL) at 0 °C was added aqueous hydrogen peroxide (30%, 11.5 mL, 104 mmol, 4.2 eq.) followed by dropwise addition of sodium hydroxide solution (6 M, 2.5 mL) with vigorous stirring. The reaction mixture was held at 0 °C for 144 hours, with daily addition of a portion of methanol (5 mL) and aqueous hydrogen peroxide (30%, 5 mL, 49 mmol). Progress of reaction was monitored by **^{1}H NMR**. Once complete, water (50 mL) was added, and the organic layer was collected. The aqueous layer was extracted with diethyl ether (3 × 100 mL) and the combined organic layers were washed with brine (100 mL), dried over sodium sulfate, and concentrated in vacuo. The crude product was purified by column chromatography on silica gel (3% ethyl acetate in hexane) as a colourless oil (4.22 g, yield: 78%). **^{1}H NMR** (300 MHz, $CDCl_3$) δ 5.51 (s, 2H), 3.29 (d, *J* = 2.0 Hz, 1H), 2.90 (dd, *J* = 8.7, 2.0 Hz, 1H), 2.06 – 1.97 (m, 5H), 1.70 (d, *J* = 2.2 Hz, 3H), 1.52 (dt, *J* = 13.5, 8.2 Hz, 1H), 1.38 (d, *J* = 8.7 Hz, 1H), 1.28 (dt, *J* = 13.6, 4.5 Hz, 1H), 1.09 (s, 3H), 0.92 (s, 3H); **^{13}C NMR** (75 MHz, $CDCl_3$) δ 206.1, 130.5, 124.8, 59.3, 58.8, 52.6, 32.8, 31.8, 27.5, 27.1, 24.6, 23.7, 23.1; **LRMS** (ESI, *m/z*) calculated for $C_{13}H_{20}O_2Na$ $[M+Na]^+$ 231.14, found 231.32; **IR** (neat/cm^{-1}) 2958, 2920, 1709, 1523, 1452, 1389, 1180, 934, 877, 547. Data in agreement with literature.[200]

(1*S*)-1-hydroxy-1-((1*S*,2*S*,6*R*)-2-hydroxy-1,5,5-trimethylbicyclo[4.1.0]heptan-7-yl)propan-2-one

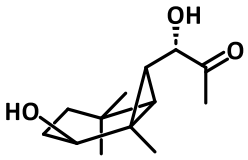

290

To a stirring solution of alpha-ionone epoxide **291** (3.0 g, 14.5 mmol, 1.0 eq.) in acetone (30 mL) were added aqueous solution of 1 M sulfuric acid (3.0 mL). The resulting mixture was heated under reflux for more than 16 hours after which the reaction mixture was cooled to room temperature and poured into a mixture of diethyl ether (50 mL) and saturated aqueous sodium bicarbonate (50 mL), with organic layer collected. The aqueous layer was extracted with diethyl ether (3 × 50 mL). The combined organic layer was washed with brine (80 mL), dried over sodium sulfate and concentrated in vacuo to yield a yellow oil. The crude product was then purified by column chromatography on silica gel (30% ethyl acetate in hexane), followed by recrystallization from hexane to yield the cyclopropane as a white crystalline solid (839 mg, yield: 25%). **m.p.**: 110.4 °C~112.5 °C; **^{1}H NMR** (300 MHz, $CDCl_3$) δ 4.29 (dd, *J* = 5.5, 3.9 Hz, 1H), 2.55 (dd, *J* = 8.5, 5.8 Hz, 1H), 2.28 (s, 3H), 2.11 – 1.98 (m, 2H), 1.91 – 1.66 (m, 4H), 1.44 (s, 3H), 0.83 (s, 3H), 0.77 (s, 3H); **^{13}C NMR** (75 MHz, $CDCl_3$) δ 210.0, 75.6, 70.9, 49.2, 49.2, 43.4, 40.9, 39.9, 27.2, 25.9, 25.7, 23.5, 23.4; **LRMS** (ESI, *m/z*) calculated for $C_{13}H_{22}O_3Na$ $[M+Na]^+$ 249.15, found 249.11; **IR** (neat/cm^{-1}) 3455, 3411, 2951, 2865, 1702, 1455, 1403, 1361, 1238, 1203, 1080, 1054, 1013, 985, 896, 861. Data in agreement with literature.[201,202]

(1*S*)-1-((1*S*,2*S*,6*R*)-2-hydroxy-1,5,5-trimethylbicyclo[4.1.0]heptan-7-yl)propane-1,2-diol

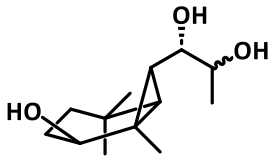

289

Cyclopropane **290** (2.28 g, 10 mmol, 1.0 eq.) and $CeCl_3 \cdot 7H_2O$ (3.73 g, 10 mmol, 1.0 eq.) were dissolved in methanol. After the mixture had been stirred for 20 minutes, $NaBH_4$ (0.500 g, 13.2 mmol, 1.3 eq.) was then added at 0 °C over a period of 20 minutes. The reaction was left to react for at least 21 hours before diluted with diethyl ether and neutralized with saturated ammonium chloride solution until a clear solution was obtained. The organic layer was separated, and the water layer was extracted with diethyl ether (3 × 150 mL). The combined extracts were washed with saturated aqueous sodium bicarbonate and brine, then dried over sodium sulfate. The solvent was removed in vacuo, and the crude product was purified by column chromatography on silica gel (60% ethyl acetate) to give a diastereomeric mixture of the diol (1.87 g, yield: 82%) as a white solid. **^{1}H NMR** (300 MHz, $CDCl_3$) δ 3.73 & 3.66 (dq, 1H), 3.51 & 3.37 (dd, *J* = 9.9, 5.6 Hz & *J* = 9.6, 1.8 Hz, 1H), 2.52 – 2.44 (m, 1H), 2.10 (br, 1H), 2.05 – 1.96 (m, 1H), 1.91 – 1.62 (m, 4H), 1.45 – 1.37 (m, 1H),1.32 & 1.25 (s, 3H), 1.27 & 1.26 (s, 3H), 1.00 & 0.99 (s, 3H), 0.88 & 0.87 (s, 3H) ratio of two isomers = 7 : 3; **^{13}C NMR** (75 MHz, $CDCl_3$) δ 207.01, 77.23, 74.66, 74.34, 71.23, 69.85, 69.71, 68.83, 49.85, 48.97, 48.78, 48.57, 45.56, 45.46, 41.06, 41.03, 39.64, 39.61, 30.94, 27.25, 27.22, 26.42, 25.59, 23.72, 22.58, 22.43, 19.72, 18.43; **LRMS** (ESI, *m/z*) calculated for $C_{13}H_{24}O_3Na$ $[M+Na]^+$ 251.16, found 251.21. Data in agreement with literature.[202]

(1*S*,2*S*,6*R*)-1,5,5-trimethyl-7-((4*S*)-2,2,5-trimethyl-1,3-dioxolan-4-yl)bicyclo [4.1.0]heptan-2-ol

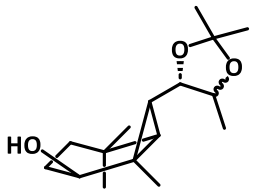

304

To a stirred solution of diol **289** (585 mg, 2.6 mmol, 1.0 eq) and 2,2-dimethoxypropane (813 mg, 0.94 mL, 8.4 mmol, 3.0 eq) in acetone at 0 °C was added p-toluenesulfonic acid monohydrate (25 mg, 0.13 mmol, 0.05 eq). The reaction was raised to room temperature and stirred for 21 h, whereupon it was quenched with saturated solution of $NaHCO_3$, and acetone was removed in vacuo. The reaction mixture was extracted with diethyl ether (3 × 60 mL), and the combined organic layers were washed with brine (100 mL), dried over sodium sulfate and concentrated in vacuo. The crude product was purified by column chromatography with 40% ethyl acetate in hexanes on silica gel to get the product (647 mg, yield: 93%) as a colourless oil. **^{1}H NMR** (300 MHz, $CDCl_3$) δ 4.29 (p, *J* = 6.3 Hz, 0.4 H), 4.09 – 3.97 (m, 0.4 H), 3.72 – 3.59 (m, 1.2 H), 2.52 (t, *J* = 7.6 Hz, 1H), 2.09 (dd, *J* = 7.1, 6.4 Hz, 0.6 H), 1.98 (dd, *J* = 10.6, 6.9 Hz, 0.4 H), 1.87 – 1.66 (m, 4H), 1.41 & 1.39 (s, 6H), 1.35 & 1.35 (s, 2H), 1.18 (d, *J* = 6.5 Hz, 1H), 0.99 & 0.94 (s, 3H), 0.86 (s, 3H). **^{13}C NMR** (75 MHz, $CDCl_3$) δ 107.4, 107.0, 80.3, 78.8, 75.1, 73.8, 70.5, 69.1, 49.1, 47.5, 47.0, 46.9, 43.5, 41.2, 40.8, 40.0, 28.5, 27.7, 27.6, 27.2, 26.3, 26.1, 25.6, 24.1, 23.5, 23.1, 17.6, 16.8. Data in agreement with literature.[202]

2-(diethoxyphosphoryl)acetic acid

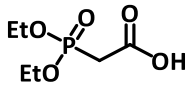

305

To an aqueous solution of 1M sodium hydroxide (22.5 mL, 22.5 mmol, 1.02 eq.) was added triethyl phosphono acetate (4.40 mL, 22.2 mmol, 1.0 eq.) and the mixture was stirred at room temperature for 4 hours. The mixture was concentrated in vacuo and the residue was acidified with aqueous 2M hydrochloric acid until pH=1. The mixture was extracted with dichloromethane (5 × 20 mL). The organic phase was dried over sodium sulfate and concentrated in vacuo to give the carboxylic acid **275** (3.95 g, yield: 91 %) without any further purifications. **^{1}H NMR** (300 MHz, $CDCl_3$) δ 8.52 (br, 1H), 4.23 – 4.12 (m, 4H), 2.99 (d, *J* = 22 Hz, 2H), 1.33 (t, *J* = 7.0 Hz, 6H); **^{13}C NMR** (75 MHz, $CDCl_3$) δ 167.8, 63.3, 34.2, 16.3; **LRMS** (ESI, *m/z*) calculated for $C_6H_{11}O_5P$ $[M-H]^-$ 195.04, found 195.22; **IR** (neat/cm^{-1}) 2984, 2934, 1723, 1392, 1233, 1017, 971, 593. Data in agreement with literature.[203]

(1*S*,2*S*,6*R*)-1,5,5-trimethyl-7-((4*S*)-2,2,5-trimethyl-1,3-dioxolan-4-yl)bicyclo [4.1.0]heptan-2-yl 2-(diethoxyphosphoryl)acetate

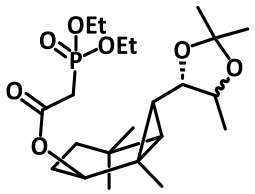

288

To a solution of **304** (320 mg, 1.2 mmol, 1.0 eq.), diethylphosphonoacetic acid (470 mg, 2.4 mmol, 2.0 eq.) and DMAP (67 mg, 0.55 mmol, 4.7 mol%) in dichloromethane (6 mL) at 0°C was added DCC (560 mg, 2.71 mmol, 2.2 eq.) and the mixture was stirred for 6 hours. The mixture was filtered through a pad of silica and the solvent was removed in vacuo. The mixture was redissolved in a minimum amount of diethyl ether and filtered again, with the solvent removed in vacuo. The crude material was purified by column chromatography on silica gel (40% to 50% ethyl acetate in hexanes) to afford an inseparable diastereomeric mixture of the product (341 mg, yield: 64%). **m.p.**: 87.7 °C~90.5 °C; **^{1}H NMR** (300 MHz, $CDCl_3$) δ 4.23 – 4.10 (m, 4H), 3.98 (dd, *J* = 9.0, 2.1 Hz, 1H), 3.70 – 3.55 (m, 1H), 2.97 & 2.91 (d, *J* = 21.8 Hz, 2H), 2.67 (t, *J* = 7.9 Hz, 1H), 2.28 (dd, *J* = 7.6, 6.6 Hz, 1H), 2.09 (d, *J* = 6.9 Hz, 1H), 1.91 (dd, *J* = 13.1, 7.7 Hz, 2H), 1.67 (s, 2H), 1.54 (d, *J* = 4.3 Hz, 3H), 1.40 – 1.31 (m, 12H), 1.21 (d, *J* = 6.0 Hz, 3H), 0.91 (s, 3H), 0.86 (s, 3H); **^{13}C NMR** (75 MHz, $CDCl_3$) δ 164.5 (d, *J* = 7.1 Hz), 153.6, 107.6, 81.1, 79.7, 74.2, 63.3 (d, *J* = 6.6 Hz), 62.6 (d, *J* = 6.4 Hz), 50.6, 48.6, 44.5, 44.0, 41.0. 40.3, 35.2 (d, *J* = 133.6 Hz), 31.9, 27.6, 27.2, 26.1, 25.6, 24.9, 24.1, 21.4. Data in agreement with literature.[203]

(1*S*,2*S*,6*R*)-7-((1*S*)-1,2-dihydroxypropyl)-1,5,5-trimethylbicyclo[4.1.0]heptan-2-yl-2-(diethoxyphosphoryl)acetate

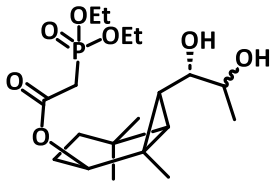

309

To a stirred solution of acetonide **288** (341 mg, 0.75mmol, 1.0 eq.) in ethanol was added *p*-toluenesulfonic acid (1.48 g, 7.5 mmol, 10 eq.) and the mixture was stirred for 3 days. The solvent was removed in vacuo, and the crude residue was diluted with diethyl ether 10 mL and quenched with saturated sodium bicarbonate solution. The water layer was extracted with diethyl ether (3 × 30 mL). The combined organic layer was washed with brine dried over sodium sulfate and concentrated in vacuo. The crude product was purified by column chromatography on silica gel (80% ethyl acetate in hexanes) to give an inseparable diastereomeric mixture of the diol as a colourless oil (188 mg, yield: 63%). **^{1}H NMR** (300 MHz, $CDCl_3$) δ 4.13 (h, *J* = 7.4 Hz, 4H), 3.82 – 3.70 (m, 1H), 3.54 – 3.42 (m, 1H), 2.93 (d, *J* = 4.9 Hz, 1H), 2.86 (dd, *J* = 20.8, 4.6 Hz, 2H), 2.74 (t, *J* = 8.0 Hz, 1H), 2.23 (dd, *J* = 7.6, 7.5 Hz, 1H), 2.02 (q, *J* = 7.2, 5.8 Hz, 0H), 1.68 (qt, *J* = 21.0, 11.0 Hz, 3H), 1.52 (s, 3H), 1.44 (s, 3H), 1.24 (d, *J* = 6.7 Hz, 3H), 0.97 (s, 3H), 0.85 (s, 3H); **^{13}C NMR** (75 MHz, $CDCl_3$) δ 165.1, 80.9, 74.0, 67.4, 62.7, 49.1, 46.8, 46.2, 41.6, 40.0, 35.3, 27.5, 24.3, 24.0, 21.2, 19.7, 16.5; **IR** (neat/cm^{-1}) 3399, 3018, 2952, 2872, 1728, 1485, 1367, 1290, 1020, 841. Data in agreement with literature.[203]

(1*S*,2*S*,6*R*)-7-formyl-1,5,5-trimethylbicyclo[4.1.0]heptan-2-yl-2-(diethoxyphosphoryl)acetate

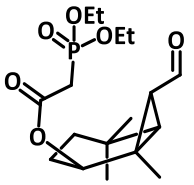

287

To a solution of the diol **309** (250 mg, 0.615 mmol, 1.0 eq.) in THF-H_2O (3:1) (6.1 mL), sodium periodate (397 mg, 1.86 mmol, 3.0 eq.) was added and the resulting suspension was stirred for 3 h. The mixture was partially concentrated *in vacuo* and diluted with water (10 mL) and diethyl ether (10 mL). The organic layer was separated, and the aqueous layer was extracted with diethyl ether (3 × 50 mL). The combined organic layer was washed with brine (100 mL), dried with sodium sulfate, and concentrated in vacuo. The crude product was purified by column chromatography on silica gel (50% ethyl acetate in hexanes) to give the aldehyde (210 mg, yield: 95%) as a colourless oil. **^{1}H NMR** (300 MHz, $CDCl_3$) δ 10.05 (s, 1H), 4.26 – 4.08 (m, 4H), 3.01 (d, J = 2.7 Hz, 1H), 2.94 (dd, J = 21.7, 2.7 Hz, 2H), 2.58 (dd, J = 9.1, 7.0 Hz, 1H), 2.41 (t, J = 7.2 Hz, 1H), 2.05 (dd, J = 14.1, 8.2 Hz, 1H), 1.91 – 1.74 (m, 1H), 1.68 – 1.52 (m, 2H), 1.50 (s, 3H), 1.36 (td, J = 7.1, 1.4 Hz, 6H), 0.89 (s, 3H), 0.88 (s, 3H); **^{13}C NMR** (75 MHz, $CDCl_3$) δ 202.5, 165.0, 78.7, 62.8, 55.7, 48.4, 44.6, 41.3, 39.0, 35.0, 26.6, 23.7, 22.6, 21.7, 16.3; **LRMS** (ESI, *m/z*) calculated for $C_{17}H_{29}O_6PNa$ $[M+Na]^+$ 383.16, found 383.21. Data in agreement with literature.[203]

(1*S*)-1-((1*S*,2*S*,6*R*)-2-(allyloxy)-1,5,5-trimethylbicyclo[4.1.0]heptan-7-yl)-1-hydroxypropan-2-one

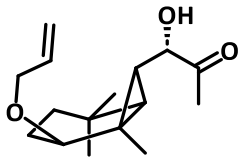

315

To a round bottom flask was added ionone epoxide **291** (3.00 g, 14.4 mmol, 1.0 eq.), acetone (15 mL) and *p*TsOH (two crystals catalyst amount) at room temperature followed by adding allyl alcohol (15 mL, much excessed) and allowing the reaction stirring for overnight at room temperature. The reaction mixture was quenched by saturated sodium bicarb, dried and removed the solvent *in vacuo*. The residue was finally purified by column chromatography to afford product **297** as a pale yellow oil (1.19 g, yield: 31%). **^{1}H NMR** (500 MHz, $CDCl_3$) δ 5.89 (ddt, *J* = 17.3, 10.6, 5.4 Hz, 1H), 5.23 (dt, *J* = 17.3, 1.8 Hz, 1H), 5.12 (dt, *J* = 10.4, 1.6 Hz, 1H), 4.10 – 4.02 (m, 1H), 3.97 – 3.87 (m, 1H), 3.76 (d, *J* = 9.3 Hz, 1H), 3.53 (dd, *J* = 6.9, 5.4 Hz, 1H), 3.45 – 3.37 (m, 1H), 2.37 (s, 2H), 1.59 (tq, *J* = 12.1, 5.1, 4.0 Hz, 2H), 1.37 (s, 3H), 1.08 (s, 3H), 0.90 (s, 3H). **^{13}C NMR** (126 MHz, $CDCl_3$) δ 209.83, 135.66, 135.16, 116.43, 116.02, 79.83, 75.3, 70.72, 69.64, 63.43, 47.05, 43.15, 40.63, 40.12, 37.40, 33.64, 31.55, 29.52, 29.04, 28.46, 27.65, 26.99, 25.61, 23.68, 21.75, 20.68, 17.81; **HRMS** (ESI, *m/z*) calculated for $C_{16}H_{26}O_3Na$ $[M+Na]^+$ 289.1780, found 289.1773; **IR** (neat/cm^{-1}) 3285, 3169, 2921, 2888, 1740, 1692, 1458, 1262, 1125, 965, 834.

(1*S*,2*S*,6*R*)-2-(allyloxy)-1,5,5-trimethylbicyclo[4.1.0]heptane-7-carbaldehyde

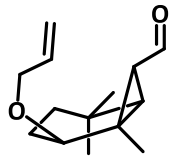

314

To a solution of the hydroxy ketone **315** (862 mg, 3.24 mmol, 1.0 eq.) in THF-H_2O (3:1) (10 mL), sodium periodate (680 mg, 4.53 mmol, 1.4 eq.) was added and the resulting suspension was stirred for 3 h. The mixture was partially concentrated *in vacuo* and diluted with water (10 mL) and diethyl ether (10 mL). The organic layer was separated, and the aqueous layer was extracted with diethyl ether (3 × 50 mL). The combined organic layer was washed with brine (100 mL), dried with sodium sulfate, and concentrated in vacuo. The crude product was purified by column chromatography on silica gel (50% ethyl acetate in hexanes) to give the aldehyde **296** as a colourless oil (558 mg, yield: 77%). **^{1}H NMR** (300 MHz, $CDCl_3$) δ 9.48 (d, *J* = 4.8 Hz, 1H), 5.92 (ddt, *J* = 16.0, 10.7, 5.6 Hz, 1H), 5.28 (dq, *J* = 17.4, 1.8 Hz, 1H), 5.17 (dt, *J* = 10.3, 1.6 Hz, 1H), 4.10 – 3.91 (m, 2H), 3.58 (t, *J* = 5.0 Hz, 1H), 2.07 (dd, *J* = 5.9, 4.8 Hz, 1H), 1.69 – 1.52 (m, 3H), 1.36 (s, 4H), 1.18 (ddd, *J* = 13.9, 10.7, 2.9 Hz, 2H), 1.10 – 1.00 (m, 4H), 0.92 (s, 3H); **^{13}C NMR** (75 MHz, $CDCl_3$) δ 209.89, 135.56, 116.05, 79.78, 76.36, 69.63, 37.54, 33.54, 31.53, 28.50, 27.82, 27.03, 26.96, 25.76, 23.15, 21.72; **HRMS** (ESI, *m/z*) calculated for $C_{14}H_{22}O_2Na$ $[M+Na]^+$ 245.1512, found 245.1509.

ethyl 2-(triphenyl-λ^5-phosphaneylidene)acetate

320 320

To a solution of triphenylphosphine (1.75 g, 6.5 mmol, 1.3 eq.) in ethyl acetate (10 mL) was added a solution of bromoacetate (0.6 mL, 5mmol, 1.0 eq.) in ethyl acetate (3 mL). The formation of a white solid precipitate was observed after one hour reaction and the reaction was left to react overnight. The mixture was filtered and the solid was rinsed with cold ethyl acetate (3 × 2 mL) and then dried *in vacuo*. The solid was then dissolved in 10 mL dichloromethane and aqueous solution of 4% NaOH (10 mL, 10 mmol, 2.0 eq.) was added. Then the solution was stirred vigorously for another 15 minutes. The phases were separated, and the organic layer was washed with brine, dried and concentrated *in vacuo*. The residue was taken up in tiny bit of diethyl ether and filtered again, dried and concentrated to afford the Wittig ester **302** (1.49 g, yield: 85%). **^{1}H NMR** (300 MHz, $CDCl_3$) δ 7.65 (dd, *J* = 12.5, 7.8 Hz, 6H), 7.55 (dd, *J* = 8.4, 6.2 Hz, 3H), 7.46 (d, *J* = 7.6 Hz, 6H), 3.96 (s, 2H), 2.87 (s, 1H), 1.59 (d, *J* = 2.0 Hz, 3H); **^{13}C NMR** (75 MHz, $CDCl_3$) δ 133.0, 133.0, 132.0, 131.8, 128.5, 128.4, 57.9, 13.7; **HRMS** (ESI, *m/z*) calculated for $C_{22}H_{22}O_2P$ $[M+H]^+$ 349.1352, found 349.1348; **IR** (neat/cm^{-1}) 1604, 1482, 1369, 1328, 1103, 889, 753, 716, 691, 505.

ethyl 3-((1*R*,2*S*,6*R*)-2-(allyloxy)-1,5,5-trimethylbicyclo[4.1.0]heptan-7-yl)acrylate

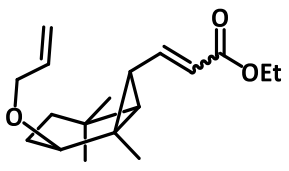

322

Aldehyde **314** (362 mg, 1.63 mmol, 1.0 eq.) was added into a solution of Wittig ester **302** (567 mg, 1.63 mmol, 1.0 eq.) in dichloromethane (20 mL) and the reaction was allowed to stir at room temperature overnight. The crude was concentrated in vacuo and purified by flash column chromatography on silica gel (2% to 10% ethyl acetate in hexanes) to give the Wittig product 304 (427 mg, 89%) as a light-yellow oil. **^{1}H NMR** (300 MHz, $CDCl_3$) δ 6.68 (dd, *J* = 15.5, 10.4 Hz, 1H), 5.88 (dd, *J* = 16.6, 4.5 Hz, 2H), 5.29 – 5.17 (m, 1H), 5.11 (d, *J* = 10.5 Hz, 1H), 4.13 (q, *J* = 7.2 Hz, 2H), 4.01 – 3.79 (m, 2H), 3.56 (t, *J* = 4.3 Hz, 1H), 1.67 (dd, *J* = 10.2, 5.9 Hz, 1H), 1.52 (t, *J* = 9.7 Hz, 3H), 1.25 – 1.18 (m, 2H), 1.00 (s, 6H), 0.87 (d, *J* = 5.4 Hz, 3H); **HRMS** (ESI, *m/z*) calculated for $C_{18}H_{28}O_3Na$ $[M+Na]^+$ 315.1936, found 315.1933; **IR** (neat/cm^{-1}) 2954, 2867, 1710, 1637, 1368, 1262, 1125, 1039, 754, 504.

1-(2,6,6-trimethylcyclohex-2-en-1-yl)butane-2,3-dione

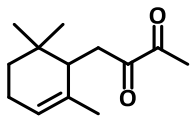

329

To a solution of hydroxy ketone **315** (133 mg, 0.5 mmol, 1.0 eq.) in dichloromethane (2.5 mL) was added tetrabromomethane (166 mg, 0.5 mmol, 1.0 eq.) at 0 °C ice bath. The reaction mixture was stirred for 3 minutes before adding previously prepared 0.4 M lithium diisopropylamine solution in THF (1.25 mL, 0.5 mmol, 1.0 eq.). The ice bath was removed and the reaction mixture was allowed to warm up to room temperature and stirred for another 2 hours. Solvents were removed in vacuo and the crude residue was purified by flash chromatography with 5% to 10% EtOAc in hexanes to afford the diketone 309 (8 mg, yield: 7.6%). **^{1}H NMR** (300 MHz, $CDCl_3$) δ 6.44 (d, *J* = 1.3 Hz, 0H), 5.50 – 5.35 (s, 1H), 3.04 – 2.87 (m, 1H), 2.56 – 2.42 (m, 1H), 2.36 (s, 3H), 2.00 – 1.91 (m, 2H), 1.58 (h, *J* = 2.0 Hz, 3H), 1.32 – 1.14 (m, 2H), 0.91 (s, 3H), 0.72 (s, 3H); **^{13}C NMR** (75 MHz, $CDCl_3$) δ 138.60, 133.23, 121.64, 43.99, 36.97, 32.15, 31.90, 31.27, 27.62, 26.84, 26.75, 24.07, 22.87; **HRMS** (ESI, *m/z*) calculated for $C_{13}H_{21}O_2$ $[M+H]^+$ 209.1542, found 209.1546.

3-bromo-4-(2,6,6-trimethylcyclohex-2-en-1-yl)but-3-en-2-one

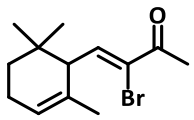

331

To a solution of hydroxy ketone **315** (133 mg, 0.5 mmol, 1.0 eq.) in dichloromethane (2.5 mL) was added tetrabromomethane (166 mg, 0.5 mmol, 1.0 eq.) at 0 °C ice bath. The reaction mixture was stirred for 3 minutes before adding previously prepared 0.4 M lithium diisopropylamine solution in THF (1.25 mL, 0.5 mmol, 1.0 eq.). The ice bath was removed and the reaction mixture was allowed to warm up to room temperature and stirred for another 2 hours. Solvents were removed in vacuo and the crude residue was purified by flash chromatography with 5% to 10% EtOAc in hexanes to afford the bromo ketone 310 (17 mg, 12%). **^{1}H NMR** (300 MHz, $CDCl_3$) δ 6.44 (s, 1H), 5.50 – 5.38 (m, 1H), 2.94 (dd, *J* = 11.0, 2.4 Hz, 1H), 2.36 (s, 3H), 2.17 (s, 1H), 1.59 (q, *J* = 1.9 Hz, 3H), 1.46 (dt, *J* = 13.3, 8.0 Hz, 2H), 1.37 – 1.15 (m, 2H), 0.95 (s, 3H), 0.86 (s, 3H); **^{13}C NMR** (75 MHz, $CDCl_3$) δ 194.79, 148.57, 134.30, 121.19, 119.32, 47.02, 32.66, 31.76, 27.11, 26.85, 23.10, 23.03, 22.84; Mass spectrum cannot be found.

2,4,4-trimethylcyclohex-2-en-1-one

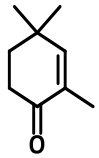

348

To a solution of isobutyraldehyde (3.00 g, 41.6 mmol, 1.0 eq.) and methyl vinyl ketone (2.91 g, 41.6 mmol. 1.0 eq.) was added tiny bit of *p*-toluenesulfonic acid. And the reaction mixture was stirred for at least 5h with a Dean-Stark apparatus in refluxing benzene 20 mL. After finishing, the reaction mixture was neutralized by sat. $NaHCO_3$ to pH = 7. The organic layer was separated and the water phase extracted with EtOAc (3 × 20 mL). The combined organic phases were dried over Na_2SO_4 and concentrated *in vacuo*. Crude was separated by fractional distillation to afford an oil, and the residue oil was further purified by flash chromatography eluting with 5% to 15% EtOAc in hexanes. And the product was obtained as a colourless oil (2.09 g, yield: 36%). **^{1}H NMR** (300 MHz, $CDCl_3$) δ 6.40 – 6.33 (br, 1H), 2.40 (dd, *J* = 7.4, 6.2 Hz, 2H), 1.78 (dd, *J* = 6.8, 5.8 Hz, 2H), 1.68 (d, *J* = 1.3 Hz, 3H), 1.08 (s, 6H); **^{13}C NMR** (75 MHz, $CDCl_3$) δ 199.5, 154.7, 132.2, 36.18, 34.29, 32.81, 27.77, 16.00. Data in agreement with literature.[180]

2,4,4-trimethylcyclohex-2-en-1-ol

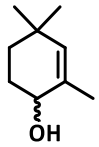

347

To a solution of cyclohexenone **348** (1.02 g, 7.6 mmol, 1.0 eq.) and $CeCl_3 \cdot 7H_2O$ (3.49 g, 9.2 mmol, 1.2 eq.) in methanol (mL) was added $NaBH_4$ (0.35 g, 9.2 mmol, 1.2 eq.) portionwise at 0°C with vigorously stirring over a period of 20 minutes. The reaction was left to react for at least 1 hour before solvent removed *in vacuo* and then diluted with diethyl ether and neutralized with saturated ammonium chloride solution. The organic layer was separated, and the water layer was extracted with diethyl ether (3 × 150 mL). The combined extracts were washed with saturated aqueous sodium bicarbonate and brine, then dried over sodium sulfate. The solvent was removed in vacuo, and the crude product was purified by column chromatography on silica gel with 10% ethyl acetate in hexanes to give alcohol **316** as a yellow oil (623 mg, yield: 61%). **^{1}H NMR** (300 MHz, $CDCl_3$) δ 5.23 (s, 1H), 3.93 (t, *J* = 4.9 Hz, 1H), 1.88 (dddd, *J* = 13.8, 10.4, 4.8, 3.5 Hz, 2H), 1.73 (s, 3H), 1.52 (ddd, *J* = 13.6, 10.5, 3.3 Hz, 1H), 1.45 (s, 1H), 1.38 (ddd, *J* = 13.8, 4.8, 3.5 Hz, 1H), 0.99 (s, 3H), 0.92 (s, 3H); **^{13}C NMR** (75 MHz, $CDCl_3$) δ 136.0, 132.8, 68.62, 32.75, 32.10, 29.97, 29.32, 28.48, 20.44; **IR** (neat/cm^{-1}) 3327, 3024, 2933, 2865, 2842, 1973, 1450, 1428, 1387, 1280, 1048, 997. Data in agreement with literature.[180]

Three-Steps Synthesis of Dibromo Alcohol 313

346: 2-(((*R*)-2,4,4-trimethylcyclohex-2-en-1-yl)oxy)tetrahydro-2H-pyran;

345:2-(((1*S*,2*R*,6*S*)-7,7-dibromo-1,5,5-trimethylbicyclo[4.1.0]heptan-2-yl)oxy)tetrahydro-2H-pyran;

344: (1*S*,6*S*)-7,7-dibromo-1,5,5-trimethylbicyclo[4.1.0]heptan-2-ol

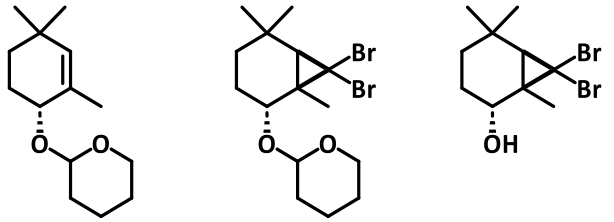

346 345 344

Step 1: To a solution of alcohol **347** (600 mg, 4.35 mmol, 1.0 eq.) in dihydropyran (0.62 mL, 7.8 mmol, 1.5 eq.) was added aluminium chloride (3 mg, 0.5 mol%) with stirring in room temperature water bath in five minutes. The reaction mixture was allowed to react a further hour, then filtered through a pad of silica gel eluting with 5% EtOAc in hexanes. The flushed solvent was removed in vacuo and the compound **346** was afforded as a light-yellow oil (780 mg, yield: 80%).

Step 2: To a solution of THP protected alcohol **346** (390 mg, 1.7 mmol, 1.0 eq.) in dichloromethane (20 mL) was added bromoform (0.5 mL, 5.7 mmol, 3.3 eq.), triethylbenzylammonium chloride (36 mg, catalytic amount, 8 mol%) as phase transferring catalyst and ethanol (50 μL, 0.5 mmol, 0.30 eq.) separately. Followed by adding aqueous sodium hydroxide (50%, 544 mg in 1.5 mL DI H_2O, 13.5 mmol, 8.0 eq.) dropwise in 0℃ ice bath with vigorously stirring. The reaction was then heated up to 40℃ with vigorously stirring for 3 weeks, with portions of bromoform (0.25 mL, 2.8 mmol, 1.6 eq.) in dichloromethane and aqueous sodium hydroxide solution (50%, 0.75 mL, 6.8 mmol, 4.0 eq.) added every 4 days. The reaction was finally cooled to 0℃ again with ice bath and acidified by aqueous HCl and the organic layer collected. The aqueous layer was washed with diethyl ether (3 × 50 mL) and the combined organic

phases were washed with brine, dried and concentrated *in vacuo*. And the crude product was purified by column chromatography on silica gel (15% ethyl acetate in hexanes) to give dibromo THP ether **345** (283 mg, yield: 42%) as a bright yellow oil.

Step 3: To a solution of compound **345** (283 mg, 0.7 mmol, 1.0 eq.) in methanol (30 mL) was added catalytic amount *p*-toluenesulfonic acid (12 mg, 0.07 mmol, 10 mol%) and the reaction was allowed to stir for 2 hours before concentrated *in vacuo*. And the crude mixture was then purified by column chromatography on silica gel (5% to 10% ethyl acetate in hexanes) to give the title alcohol **313** (103 mg, yield: 46%; overall yield: 15.4%) as a white solid. **m.p.:** 119.8 °C~ 121.3 °C; **^{1}H NMR** (300 MHz, $CDCl_3$) δ 4.08 (dt, *J* = 10.8, 5.2 Hz, 1H), 1.73 (d, *J* = 5.5 Hz, 1H), 1.70 – 1.63 (m, 1H), 1.57 (td, *J* = 13.8, 2.2 Hz, 1H), 1.45 (dd, *J* = 13.8, 11.2 Hz, 1H), 1.29 (s, 1H), 1.23 (s, 3H), 1.14 (d, J = 3.5 Hz, 1H), 1.08 (s, 3H); **^{13}C NMR** (75 MHz, $CDCl_3$) δ 69.6, 47.8, 47.3, 33.5, 32.1, 31.2, 31.0, 28.9, 25.9, 22.0; **LRMS** (ESI, *m/z*) calculated for $C_{10}H_{15}Br_2$ [M-OH]+ 292.95, 294.95, 296.95, found 293.11. Data in agreement with literature.[180]

(1*S*,6*S*)-7,7-dibromo-1,5,5-trimethylbicyclo[4.1.0]heptan-2-one

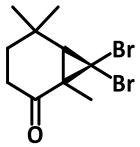

343

To a solution of dibromo alcohol **344** (401 mg, 1.29 mmol, 1.0 eq.) in dichloromethane (5 mL) at room temperature was added (diacetoxyiodo)benzene (460 mg, 1.42 mmol, 1.1 eq.) slowly under vigorously stirring and TEMPO (20 mg, 0.129 mmol. 0.1 eq.). The reaction was allowed to react for 3 hours. The reaction mixture was concentrated *in vacuo* and purified by flash column chromatography with 20% EtOAc in hexanes to afford the title product (384 mg, yield: 96%) as a yellow oil. **^{1}H NMR** (300 MHz, $CDCl_3$) δ 2.44 – 2.09 (m, 4H), 1.62 (d, *J* = 1.4 Hz, 1H), 1.55 (s, 3H), 1.38 (s, 3H), 1.23 (s, 3H); **^{13}C NMR** (75 MHz, $CDCl_3$) δ 205.49, 48.25, 37.85, 35.57, 34.18, 31.96, 30.53, 30.29, 27.42, 21.99; **HRMS** (APCI, *m/z*) calculated for $C_{10}H_{14}Br_2ONa$ $[M+H]^+$ 308.9490, found 308.9484; **IR** (neat/cm^{-1}) 3276, 2999, 2957, 2928, 2864, 1452, 1364, 1340, 1260, 1173, 1135, 1091, 1053, 1011, 774, 719.

5-hydroxyfuran-2(5H)-one

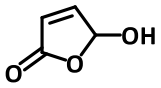

368

To a mechanically stirred, cooled ice-bath solution of furan (5.00 g, 0.0735 mol) in water (100 mL) was added OXONE (56.4 g, 0.0919 mol) solid portion-wise and stirred at 0 °C for 8 h. The mixture was allowed to warm to room temperature and stirred for the next 8 h. The reaction mixture was filtered off, solid was thoroughly washed with ethyl acetate, and the layers were separated. The aqueous layer was extracted with ethyl acetate (50 mL x 3). Additionally, the aqueous layer was saturated with NaCl and extracted with ethyl acetate (50 mL × 3). The combined organic layers were dried with anhydrous Na_2SO_4, filtered and concentrated below 40 °C under reduced pressure to give crude 5-hydroxy-2(5H)-furanone as a clear liquid which solidified on cooling. **m.p.**: 50.4°C~52.7°C; **^{1}H NMR** (300 MHz, $CDCl_3$) δ 7.33 (dd, *J* = 1.1, 5.6 Hz, 1H), 6.27 (s, 1H), 6.22 (dd, *J* = 1.1, 5.6 Hz, 1H), 5.32 (br s, 1H); **^{13}C NMR** (75 MHz, $CDCl_3$) δ 172.7, 153.4, 124.8, 99.1. Data in agreement with literature.[204]

cyclohexyl (*E*)-2-oxo-4-(2,6,6-trimethylcyclohex-1-en-1-yl)but-3-enoate

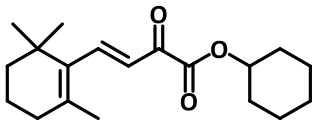

385

To a 250 mL two-neck round bottom flask equipped with a reflux condenser was added toluene (60 mL), β-ionone (2.50 g, 13 mmol, 1.0 eq.), 2,2,6,6-tetramethylpiperidine (384 mg, 2.72 mmol, 0.21 eq.), cyclohexanol (2.76 g, 27.6 mmol, 2.1 eq.) and copper bromide (220 mg, 1.53 mmol, 12 mol%). The reaction mixture was then stirred at 100°C (no more than 110°C) under a continuously supply of oxygen from the cylinder with a needle sticking beneath the surface of the reaction mixture in the speed of one bubble/second overnight. The solvent was then removed in vacuo and the crude residue was purified by flash column chromatography with 2% to 5% diethyl ether in hexanes to afford the cyclohexyl ester 359 (1.48 g, yield: 37%) as a pale yellow oil. **^{1}H NMR** (500 MHz, $CDCl_3$) δ 7.63 (d, J = 16.4 Hz, 1H), 6.68 (d, *J* = 16.4 Hz, 1H), 4.96 (tt, J = 9.4, 4.0 Hz, 1H), 2.17 (s, 2H), 2.13 (t, *J* = 6.4 Hz, 2H), 1.99 – 1.90 (m, 2H), 1.85 (d, *J* = 1.0 Hz, 3H), 1.78 (dp, *J* = 13.6, 4.5 Hz, 2H), 1.67 – 1.57 (m, 2H), 1.40 (dtq, *J* = 13.6, 10.0, 3.3 Hz, 2H), 1.33 – 1.24 (m, 2H), 1.12 (s, 6H), 0.92 – 0.81 (m, 2H); **^{13}C NMR** (126 MHz, $CDCl_3$) δ 184.38, 162.59, 148.17, 141.52, 136.62, 124.61, 75.11, 40.09, 34.30, 34.17, 31.59, 31.40, 30.92, 28.78, 25.23, 23.70, 21.97, 18.73, 14.11; **HRMS** (ESI, *m/z*) calculated for $C_{19}H_{29}O_3$ $[M+H]^+$ 305.2117, found 305.2111.

methyl (*E*)-2-oxo-4-(2,6,6-trimethylcyclohex-1-en-1-yl)but-3-enoate

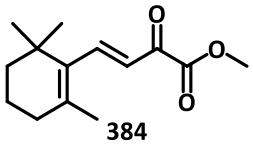

384

To a solution of cyclohexyl ester **385** (608 mg, 2 mmol, 1.0 eq.) in ultra dry methanol (10 mL) was added sodium methoxide (54 mg, 1 mmol, 0.5 eq.) under argon protection in 0℃ ice bath and the reaction was stirred at 0℃ for 10 minutes. The ice bath was removed then and the reaction was allowed to warm up to room temperature and stirred for another 30 minutes. The solvent was removed in vacuo and the crude residue was purified by flash column chromatography with 10% diethyl ether in hexanes to afford the methyl ester (374 mg, 72 %) as a yellow oil (solidified in fridge and freezer). **m.p.**: 6 ℃~25 ℃; **^{1}H NMR** (500 MHz, $CDCl_3$) δ 7.72 (d, J = 16.3 Hz, 1H), 6.78 (d, J = 16.3 Hz, 1H), 3.90 (s, 4H), 2.14 (t, J = 6.3 Hz, 3H), 1.87 (s, 4H), 1.67 – 1.59 (m, 2H), 1.52 – 1.47 (m, 2H), 1.13 (s, 8H); **^{13}C NMR** (126 MHz, $CDCl_3$) δ 182.85, 163.16, 148.35, 142.40, 136.71, 123.81, 52.83, 40.14, 34.40, 34.18, 28.78, 28.77, 22.01, 18.70; **HRMS** (ESI, *m/z*) calculated for $C_{28}H_{40}O_6Na$ $[2M+Na]^+$ 495.2723, found 495.2717.

methyl (*E*)-2-methylene-4-(2,6,6-trimethylcyclohex-1-en-1-yl)but-3-enoate

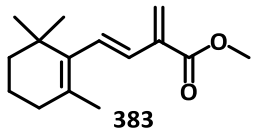

383

To a solution of methyl ester **384** (360 mg, 1.5 mmol, 1.0 eq.) in diethyl ether (5 mL) at 0 °C was added triphenylphosphonomethyl bromide (590 mg, 1.65 mmol, 1.1 eq.) in diethyl ether (2.5 mL). Then the mixture was cooled down to -78 °C and KHMDS in THF solution (0.5 M, 3.3 mL, 1.65 mmol, 1.1 eq.) was added dropwise. The reaction was allowed to stir at -78 °C for 30 minutes and warmed up to room temperature with stirring for another 1 hour. The reaction mixture was then concentrated in vacuo and purified by flash column chromatography 10% diethyl ether in hexanes to obtain the title product (157 mg, yield: 44%) as a yellow oil. **^{1}H NMR** (500 MHz, $CDCl_3$) δ 6.54 (d, *J* = 16.4 Hz, 1H), 6.10 (d, *J* = 16.3 Hz, 1H), 5.95 (d, *J* = 1.4 Hz, 1H), 5.69 (d, *J* = 1.4 Hz, 1H), 3.74 (s, 3H), 1.94 (dd, *J* = 18.6, 13.0 Hz, 2H), 1.66 (d, *J* = 1.0 Hz, 3H), 1.45 – 1.35 (m, 2H), 1.00 (s, 3H), 0.97 (s, 3H), 0.92 – 0.75 (m, 2H); **^{13}C NMR** (126 MHz, $CDCl_3$) δ 144.46, 133.36, 132.11, 130.14, 129.35, 74.31, 63.89, 40.76, 34.89, 30.34, 28.85, 27.50, 23.49, 20.60, 2.65; **HRMS** (ESI, *m/z*) calculated for $C_{15}H_{22}O_2$ $[M+H]^+$ 235.1693, found 235.1699.

5-allyl-3-methylfuran-2(5H)-one

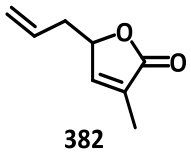

382

Zinc powder (1.44 g, 22.5 mmol, 3.0 eq.) was added into the solution of DringOH **66** (851 mg, 7.5 mmol, 1.0 eq.) and allyl bromide (1.79 g, 15 mmol, 2.0 eq.) in THF (10 mL). Then, saturated ammonium chloride solution (0.5 mL) was added dropwise at 0℃ in ice bath and stirred for an hour. The ice bath was removed, and the temperature was allowed to warm up to room temperature slowly and stirred for another 16 hours. When finished, the reaction mixture was diluted by another portion of THF (5 mL) and filtered. The filtrate was then concentrated *in vacuo* and acidified with 7% aqueous HCl till pH=2. Then the reaction mixture was stirred for another 30 minutes before diluting with dichloromethane (10 mL). Water phase was then extracted by dichloromethane (10 mL × 3), dried over Na_2SO_4, and the combined filtrate was then concentrated *in vacuo*. The crude was then purified by flash chromatography eluting with 10% EtOAc in hexanes to obtain product 352 as a colourless oil (744 mg, yield: 71%). **^{1}H NMR** (500 MHz, $CDCl_3$) δ 7.03 (p, J = 1.6 Hz, 1H), 5.85 – 5.65 (m, 1H), 5.23 – 5.10 (m, 2H), 4.91 (tp, J = 6.0, 1.9 Hz, 1H), 2.57 – 2.32 (m, 2H), 1.91 (t, J = 1.8 Hz, 3H); **^{13}C NMR** (126 MHz, $CDCl_3$) δ 172.83, 138.60, 132.19, 108.18, 99.46, 65.16, 54.72, 10.43; **HRMS** (ESI, *m/z*) calculated for $C_8H_{10}O_2$ $[M+Na]^+$ 161.0573, found 161.0573.

dimethyl-(1*S*,2*R*)-2',6',6'-trimethyl-2-((*E*)-2-(2,6,6-trimethylcyclohex-1-en-1-yl)vinyl)-[1,1'-bi(cyclohexane)]-1',5-diene-2,5-dicarboxylate

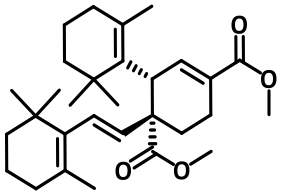

403

Dichloromethane (20 mL) was degassed by reducing pressure at -78 °C and was purged with argon several times to remove the gas contained in the solvent. Alkyl ester **383** (120 mg, 0.51 mmol, 1.0 eq.) and allyl butenolide **382** (360 mg, 2.60 mmol, 5.1 eq.) were added into dichloromethane (8 mL) at -78 °C with vigorously stirring. Second generation Grubbs catalyst (10 mg, 0.02 mmol, 5mol%) in degassed dichloromethane (5 mL) was then added dropwise into the reaction mixture. The reaction was then warmed up to room temperature slowly and stirred for another 3 hours under argon atmosphere. After reaction finishing, solvent was removed in vacuo and the crude residue was purified by flash column chromatography with 10% diethyl ether in hexanes to obtain the Diels-Alder by-product 379 (7 mg, 5.8 %) as a pale-yellow oil. **^{1}H NMR** (500 MHz, $CDCl_3$) δ 6.83 (t, *J* = 3.0 Hz, 1H), 5.78 (d, *J* = 16.3 Hz, 1H), 5.51 (d, *J* = 16.3 Hz, 1H), 3.74 (s, 3H), 3.71 (d, *J* = 19.7 Hz, 1H), 3.57 (s, 3H), 3.42 (t, *J* = 3.5 Hz, 1H), 2.64 – 2.48 (m, 1H), 2.00 – 1.78 (m, 6H), 1.65 (d, *J* = 0.9 Hz, 3H), 1.58 (s, 3H), 1.52 – 1.34 (m, 8H), 1.07 (s, 3H), 1.04 (s, 3H), 0.95 (s, 3H), 0.95 (s, 3H); **^{13}C NMR** (126 MHz, $CDCl_3$) δ 175.27, 167.63, 143.34, 138.19, 137.23, 136.89, 135.12, 128.49, 127.40, 126.71, 51.98, 51.64, 51.24, 42.69, 40.31, 39.26, 36.98 , 34.84, 34.20, 32.62, 29.88, 28.70, 28.65, 28.00, 27.92, 22.91, 21.28, 19.92, 19.36, 19.30; **HRMS** (ESI, *m/z*) calculated for $C_{30}H_{44}O_4$ $[M+Na]^+$ 491.3137 & 492.3171, found 491.3132 & 492.3165; amount of sample was not enough for IR.

dimethyl-(1*R*,5*S*)-2',6',6'-trimethyl-5-((*E*)-2-(2,6,6-trimethylcyclohex-1-en-1-yl)vinyl)-[1,1'-bi(cyclohexane)]-1',2-diene-3,5-dicarboxylate

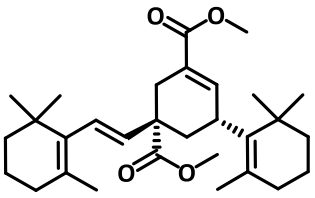

404

Dichloromethane (20 mL) was degassed by reducing pressure at -78 °C and was purged with argon several times to remove the gas contained in the solvent. Alkyl ester **383** (120 mg, 0.51 mmol, 1.0 eq.) and allyl butenolide **382** (360 mg, 2.60 mmol, 5.1 eq.) were added into dichloromethane (8 mL) at -78 °C with vigorously stirring. Second generation Grubbs catalyst (10 mg, 0.02 mmol, 5mol%) in degassed dichloromethane (5 mL) was then added dropwise into the reaction mixture. The reaction was then warmed up to room temperature slowly and stirred for another 3 hours under argon atmosphere. After reaction finishing, solvent was removed in vacuo and the crude residue was purified by flash column chromatography with 10% diethyl ether in hexanes to obtain the Diels-Alder by-product 380 (23 mg, 19%) as a pale-yellow oil. **^{1}H NMR** (500 MHz, $CDCl_3$) δ 6.80 (dd, *J* = 3.7, 2.0 Hz, 1H), 5.97 (dd, *J* = 16.4, 1.0 Hz, 1H), 5.51 (d, *J* = 16.3 Hz, 1H), 4.30 (td, *J* = 3.9, 1.3 Hz, 1H), 3.73 (s, 3H), 3.69 (s, 3H), 2.64 – 2.56 (m, 1H), 2.51 – 2.43 (m, 1H), 2.08 – 1.97 (m, 2H), 1.97 – 1.92 (m, 2H), 1.87 (t, *J* = 6.0 Hz, 2H), 1.58 – 1.57 (m, 4H), 1.56 (s, 3H), 1.48 (s, 3H), 1.45 – 1.38 (m, 4H), 1.14 (s, 3H), 1.11 (s, 3H), 0.95 (s, 3H), 0.93 (s, 3H); **^{13}C NMR** (126 MHz, $CDCl_3$) δ 176.54, 167.71, 144.38, 137.21, 137.05, 134.61, 134.05, 128.34, 127.16, 126.48, 52.83, 52.43, 51.56, 41.07, 40.15, 39.46, 37.00, 34.84, 34.21, 32.69, 29.11, 28.77, 28.54, 28.07, 26.90, 22.89, 21.29, 21.13, 19.25, 19.23; **HRMS** (ESI, *m/z*) calculated for $C_{30}H_{44}O_4$ $[M+Na]^+$ 491.3137 & 492.3171, found 491.3132 & 492.3165; amount of sample was not enough for IR.

References

[1]F. W. Went, K. V. Thimann, “Phytohormones,” **1937**.

[2]J. A. Feurtado, S. J. Ambrose, A. J. Cutler, A. R. S. Ross, S. R. Abrams, A. R. Kermode, *Planta* **2004**, *218*, 630–639.

[3]A. Walz, S. Park, J. P. Slovin, J. Ludwig-Müller, Y. S. Momonoki, J. D. Cohen, *Proceedings of the National Academy of Sciences* **2002**, *99*, 1718–1723.

[4] A. K. Grennan, Plant Physiology 2006, 141, 524–526.

[5]D. L. Sipes, J. W. Einset, *J Plant Growth Regul* **1983**, *2*, 73–80.

[6]Y. Wang, C. Liu, K. Li, F. Sun, H. Hu, X. Li, Y. Zhao, C. Han, W. Zhang, Y. Duan, M. Liu, X. Li, *Plant Mol Biol* **2007**, *64*, 633–644.

[7]O. Leyser, *Dev Cell* **2008**, *15*, 337–338.

[8]M. Umehara, M. Cao, K. Akiyama, T. Akatsu, Y. Seto, A. Hanada, W. Li, N. Takeda-Kamiya, Y. Morimoto, S. Yamaguchi, *Plant Cell Physiol* **2015**, *56*, 1059–1072.

[9]C. E. Cook, L. P. Whichard, B. Turner, M. E. Wall, G. H. Egley, *Science* **1966**, *154*, 1189–1190.

[10]X. Xie, K. Yoneyama, K. Yoneyama, *Annual Review of Phytopathology* **2010**, *48*, 93–117.

[11]S. Mutinda, F. M. Mobegi, B. Hale, O. Dayou, E. Ateka, A. Wijeratne, S. Wicke, E. S. Bellis, S. Runo, *J Exp Bot* **2023**, *74*, 5294–5306.

[12]C. E. Cook, L. P. Whichard, M. E. Wall, G. H. Egley, P. Coggon, P. A. Luhan, A. T. McPhail, *J. Am. Chem. Soc.* **1972**, *94*, 6198–6199.

[13]D. W. Brooks, H. S. Bevinakatti, D. R. Powell, *J. Org. Chem.* **1985**, *50*, 3779–3781.

[14]X. Xie, *Journal of Pesticide Science* **2016**, *41*, 175–180.

[15]M. Bürger, J. Chory, *Trends in Plant Science* **2020**, *25*, 395–405.

[16]C. Hauck, S. Müller, H. Schildknecht, *Journal of Plant Physiology* **1992**, *139*, 474–478.[1]F. W. Went, K. V. Thimann, “Phytohormones,” **1937**.

[2]J. A. Feurtado, S. J. Ambrose, A. J. Cutler, A. R. S. Ross, S. R. Abrams, A. R. Kermode, *Planta* **2004**, *218*, 630–639.

[3]A. Walz, S. Park, J. P. Slovin, J. Ludwig-Müller, Y. S. Momonoki, J. D. Cohen, *Proceedings of the National Academy of Sciences* **2002**, *99*, 1718–1723.

[4] A. K. Grennan, Plant Physiology 2006, 141, 524–526.

[5]D. L. Sipes, J. W. Einset, *J Plant Growth Regul* **1983**, *2*, 73–80.

[6]Y. Wang, C. Liu, K. Li, F. Sun, H. Hu, X. Li, Y. Zhao, C. Han, W. Zhang, Y. Duan, M. Liu, X. Li, *Plant Mol Biol* **2007**, *64*, 633–644.

[7]O. Leyser, *Dev Cell* **2008**, *15*, 337–338.

[8]M. Umehara, M. Cao, K. Akiyama, T. Akatsu, Y. Seto, A. Hanada, W. Li, N. Takeda-Kamiya, Y. Morimoto, S. Yamaguchi, *Plant Cell Physiol* **2015**, *56*, 1059–1072.

[9]C. E. Cook, L. P. Whichard, B. Turner, M. E. Wall, G. H. Egley, *Science* **1966**, *154*, 1189–1190.

[10]X. Xie, K. Yoneyama, K. Yoneyama, *Annual Review of Phytopathology* **2010**, *48*, 93–117.

[11]S. Mutinda, F. M. Mobegi, B. Hale, O. Dayou, E. Ateka, A. Wijeratne, S. Wicke, E. S. Bellis, S. Runo, *J Exp Bot* **2023**, *74*, 5294–5306.

[12]C. E. Cook, L. P. Whichard, M. E. Wall, G. H. Egley, P. Coggon, P. A. Luhan, A. T. McPhail, *J. Am. Chem. Soc.* **1972**, *94*, 6198–6199.

[13]D. W. Brooks, H. S. Bevinakatti, D. R. Powell, *J. Org. Chem.* **1985**, *50*, 3779–3781.

[14]X. Xie, *Journal of Pesticide Science* **2016**, *41*, 175–180.

[15]M. Bürger, J. Chory, *Trends in Plant Science* **2020**, *25*, 395–405.

[16]C. Hauck, S. Müller, H. Schildknecht, *Journal of Plant Physiology* **1992**, *139*, 474–478.

[17]K. Akiyama, K. Matsuzaki, H. Hayashi, *Nature* **2005**, *435*, 824–827.

[18]X. Xie, K. Yoneyama, D. Kusumoto, Y. Yamada, Y. Takeuchi, Y. Sugimoto, K. Yoneyama, *Tetrahedron Letters* **2008**, *49*, 2066–2068.

[19]T. Kisugi, X. Xie, H. I. Kim, K. Yoneyama, A. Sado, K. Akiyama, H. Hayashi, K. Uchida, T. Yokota, T. Nomura, K. Yoneyama, *Phytochemistry* **2013**, *87*, 60–64.

[20]S. Müller, C. Hauck, H. Schildknecht, *J Plant Growth Regul* **1992**, *11*, 77–84.

[21]E. B. Aliche, C. Screpanti, A. De Mesmaeker, T. Munnik, H. J. Bouwmeester, *New Phytol* **2020**, *227*, 1001–1011.

[22] J. Matsui, M. Bando, M. Kido, Y. Takeuchi, K. Mori, *European Journal of Organic Chemistry* **1999**, *1999*, 2195–2199.

[23] H. Matsuura, K. Ohashi, H. Sasako, N. Tagawa, Y. Takano, Y. Ioka, K. Nabeta, T. Yoshihara, *Plant Growth Regul* **2008**, *54*, 31–36.

[24] K. Yoneyama, X. Xie, H. Sekimoto, Y. Takeuchi, S. Ogasawara, K. Akiyama, H. Hayashi, K. Yoneyama, *New Phytologist* **2008**, *179*, 484–494.

[25] K. Ueno, S. Nomura, S. Muranaka, M. Mizutani, H. Takikawa, Y. Sugimoto, *J. Agric. Food Chem.* **2011**, *59*, 10485–10490.

[26] X. Xie, D. Kusumoto, Y. Takeuchi, K. Yoneyama, Y. Yamada, K. Yoneyama, *J. Agric. Food Chem.* **2007**, *55*, 8067–8072.

[27] H. Takikawa, S. Jikumaru, Y. Sugimoto, X. Xie, K. Yoneyama, M. Sasaki, *Tetrahedron Letters* **2009**, *50*, 4549–4551.

[28] M. Umehara, A. Hanada, S. Yoshida, K. Akiyama, T. Arite, N. Takeda-Kamiya, H. Magome, Y. Kamiya, K. Shirasu, K. Yoneyama, J. Kyozuka, S. Yamaguchi, *Nature* **2008**, *455*, 195–200.

[29] X. Xie, K. Yoneyama, Y. Harada, N. Fusegi, Y. Yamada, S. Ito, T. Yokota, Y. Takeuchi, K. Yoneyama, *Phytochemistry* **2009**, *70*, 211–215.

[30] X. XIE, K. YONEYAMA, J. KURITA, Y. HARADA, Y. YAMADA, Y. TAKEUCHI, K. YONEYAMA, *Bioscience, Biotechnology, and Biochemistry* **2009**, *73*, 1367–1370.

[31] T. Tokunaga, H. Hayashi, K. Akiyama, *Phytochemistry* **2015**, *111*, 91–97.

[32] K. Yoneyama, X. Xie, K. Yoneyama, T. Kisugi, T. Nomura, Y. Nakatani, K. Akiyama, C. S. P. McErlean, *Journal of Experimental Botany* **2018**, *69*, 2231–2239.

[33] Y. Seto, A. Sado, K. Asami, A. Hanada, M. Umehara, K. Akiyama, S. Yamaguchi, *Proceedings of the National Academy of Sciences* **2014**, *111*, 1640–1645.

[34] A. Alder, M. Jamil, M. Marzorati, M. Bruno, M. Vermathen, P. Bigler, S. Ghisla, H. Bouwmeester, P. Beyer, S. Al-Babili, *Science* **2012**, *335*, 1348–1351.

[35] S. Abe, A. Sado, K. Tanaka, T. Kisugi, K. Asami, S. Ota, H. I. Kim, K. Yoneyama, X. Xie, T. Ohnishi, Y. Seto, S. Yamaguchi, K. Akiyama, K. Yoneyama, T. Nomura, *Proceedings of the National Academy of Sciences* **2014**, *111*, 18084–18089.

[36]K. Yoneyama, N. Mori, T. Sato, A. Yoda, X. Xie, M. Okamoto, M. Iwanaga, T. Ohnishi, H. Nishiwaki, T. Asami, T. Yokota, K. Akiyama, K. Yoneyama, T. Nomura, *New Phytologist* **2018**, *218*, 1522–1533.

[37]M. Jamil, F. K. Kanampiu, H. Karaya, T. Charnikhova, H. J. Bouwmeester, *Field Crops Research* **2012**, *134*, 1–10.

[38]H. I. Kim, T. Kisugi, P. Khetkam, X. Xie, K. Yoneyama, K. Uchida, T. Yokota, T. Nomura, C. S. P. McErlean, K. Yoneyama, *Phytochemistry* **2014**, *103*, 85–88.

[39]T. V. Charnikhova, K. Gaus, A. Lumbroso, M. Sanders, J.-P. Vincken, A. De Mesmaeker, C. P. Ruyter-Spira, C. Screpanti, H. J. Bouwmeester, *Phytochemistry* **2017**, *137*, 123–131.

[40]K. Ueno, T. Furumoto, S. Umeda, M. Mizutani, H. Takikawa, R. Batchvarova, Y. Sugimoto, *Phytochemistry* **2014**, *108*, 122–128.

[41]T. V. Charnikhova, K. Gaus, A. Lumbroso, M. Sanders, J.-P. Vincken, A. De Mesmaeker, C. P. Ruyter-Spira, C. Screpanti, H. J. Bouwmeester, *Phytochemistry Letters* **2018**, *24*, 172–178.

[42]X. Xie, N. Mori, K. Yoneyama, T. Nomura, K. Uchida, K. Yoneyama, K. Akiyama, *Phytochemistry* **2019**, *157*, 200–205.

[43]K. Kodama, M. K. Rich, A. Yoda, S. Shimazaki, X. Xie, K. Akiyama, Y. Mizuno, A. Komatsu, Y. Luo, H. Suzuki, H. Kameoka, C. Libourel, J. Keller, K. Sakakibara, T. Nishiyama, T. Nakagawa, K. Mashiguchi, K. Uchida, K. Yoneyama, Y. Tanaka, S. Yamaguchi, M. Shimamura, P.-M. Delaux, T. Nomura, J. Kyozuka, *Nat Commun* **2022**, *13*, 3974.

[44]V. Lailheugue, I. Merlin, S. Boutet, F. Perreau, J.-B. Pouvreau, S. Delgrange, P.-H. Ducrot, B. Cottyn-Boitte, G. Mouille, V. Lauvergeat, *Phytochemistry* **2023**, *215*, 113837.

[45]H. J. Bouwmeester, R. Matusova, S. Zhongkui, M. H. Beale, *Current Opinion in Plant Biology* **2003**, *6*, 358–364.

[46]C. Ruyter-Spira, S. Al-Babili, S. van der Krol, H. Bouwmeester, *Trends in Plant Science* **2013**, *18*, 72–83.

[47] B. Zwanenburg, A. S. Mwakaboko, C. Kannan, *Pest Management Science* **2016**, *72*, 2016–2025.

[48] B. A. Kountche, M. Jamil, D. Yonli, M. P. Nikiema, D. Blanco-Ania, T. Asami, B. Zwanenburg, S. Al-Babili, *PLANTS, PEOPLE, PLANET* **2019**, *1*, 107–118.

[49] S. Al-Babili, H. J. Bouwmeester, *Annual Review of Plant Biology* **2015**, *66*, 161–186.

[50] Y. Kapulnik, P.-M. Delaux, N. Resnick, E. Mayzlish-Gati, S. Wininger, C. Bhattacharya, N. Séjalon-Delmas, J.-P. Combier, G. Bécard, E. Belausov, T. Beeckman, E. Dor, J. Hershenhorn, H. Koltai, *Planta* **2011**, *233*, 209–216.

[51] C. Ruyter-Spira, W. Kohlen, T. Charnikhova, A. van Zeijl, L. van Bezouwen, N. de Ruijter, C. Cardoso, J. A. Lopez-Raez, R. Matusova, R. Bours, F. Verstappen, H. Bouwmeester, *Plant Physiology* **2011**, *155*, 721–734.

[52] W. Kohlen, T. Charnikhova, M. Lammers, T. Pollina, P. Tóth, I. Haider, M. J. Pozo, R. A. de Maagd, C. Ruyter-Spira, H. J. Bouwmeester, J. A. López-Ráez, *New Phytologist* **2012**, *196*, 535–547.

[53] K. C. Snowden, A. J. Simkin, B. J. Janssen, K. R. Templeton, H. M. Loucas, J. L. Simons, S. Karunairetnam, A. P. Gleave, D. G. Clark, H. J. Klee, *The Plant Cell* **2005**, *17*, 746–759.

[54] M. G. Cline, *Physiologia Plantarum* **1994**, *90*, 230–237.

[55] Shinohara N., Taylor C., Leyser O., *PLOS Biology* **2013**, *11*, e1001474.

[56] A. Besserer, V. Puech-Pagès, P. Kiefer, V. Gomez-Roldan, A. Jauneau, S. Roy, J.-C. Portais, C. Roux, G. Bécard, N. Séjalon-Delmas, *PLOS Biology* **2006**, *4*, e226.

[57] H. J. Bouwmeester, C. Roux, J. A. Lopez-Raez, G. Bécard, *Trends in Plant Science* **2007**, *12*, 224–230.

[58] A. Genre, M. Chabaud, C. Balzergue, V. Puech-Pagès, M. Novero, T. Rey, J. Fournier, S. Rochange, G. Bécard, P. Bonfante, D. G. Barker, *New Phytologist* **2013**, *198*, 190–202.

[59] R. Matusova, K. Rani, F. W. A. Verstappen, M. C. R. Franssen, M. H. Beale, H. J. Bouwmeester, *Plant Physiology* **2005**, *139*, 920–934.

[60]J. Booker, M. Auldridge, S. Wills, D. McCarty, H. Klee, O. Leyser, *Current Biology* **2004**, *14*, 1232–1238.

[61]M. E. Auldridge, A. Block, J. T. Vogel, C. Dabney-Smith, I. Mila, M. Bouzayen, M. Magallanes-Lundback, D. DellaPenna, D. R. McCarty, H. J. Klee, *The Plant Journal* **2006**, *45*, 982–993.

[62]V. Gomez-Roldan, S. Fermas, P. B. Brewer, V. Puech-Pagès, E. A. Dun, J.-P. Pillot, F. Letisse, R. Matusova, S. Danoun, J.-C. Portais, H. Bouwmeester, G. Bécard, C. A. Beveridge, C. Rameau, S. F. Rochange, *Nature* **2008**, *455*, 189–194.

[63]S. Crawford, N. Shinohara, T. Sieberer, L. Williamson, G. George, J. Hepworth, D. Müller, M. A. Domagalska, O. Leyser, *Development* **2010**, *137*, 2905–2913.

[64]T. Nomura, Y. Seto, J. Kyozuka, *Journal of Experimental Botany* **2024**, *75*, 1134–1147.

[65]K. Yoneyama, P. B. Brewer, *Current Opinion in Plant Biology* **2021**, *63*, 102072.

[66]K. Mashiguchi, Y. Seto, S. Yamaguchi, *The Plant Journal* **2021**, *105*, 335–350.

[67]T. Wakabayashi, K. Shida, Y. Kitano, H. Takikawa, M. Mizutani, Y. Sugimoto, *Planta* **2020**, *251*, 97.

[68]T. Wakabayashi, M. Hamana, A. Mori, R. Akiyama, K. Ueno, K. Osakabe, Y. Osakabe, H. Suzuki, H. Takikawa, M. Mizutani, Y. Sugimoto, *Science Advances* **2019**, *5*, eaax9067.

[69]N. Mori, A. Sado, X. Xie, K. Yoneyama, K. Asami, Y. Seto, T. Nomura, S. Yamaguchi, K. Yoneyama, K. Akiyama, *Phytochemistry* **2020**, *174*, 112349.

[70]N. Mori, T. Nomura, K. Akiyama, *Planta* **2020**, *251*, 40.

[71]Y. Seto, S. Yamaguchi, *Current Opinion in Plant Biology* **2014**, *21*, 1–6.

[72]B. Zwanenburg, S. Ćavar Zeljković, T. Pospíšil, *Pest Management Science* **2016**, *72*, 15–29.

[73]M. J. Harrison, *Annual Review of Microbiology* **2005**, *59*, 19–42.

[74]K. S. Elias, G. R. Safir, *Applied and Environmental Microbiology* **1987**, *53*, 1928–1933.

[75]B. Andreo-Jimenez, C. Ruyter-Spira, H. J. Bouwmeester, J. A. Lopez-Raez, *Plant Soil* **2015**, *394*, 1–19.

[76]M. Umehara, A. Hanada, H. Magome, N. Takeda-Kamiya, S. Yamaguchi, *Plant and Cell Physiology* **2010**, *51*, 1118–1126.

[77]K. Mashiguchi, E. Sasaki, Y. Shimada, M. Nagae, K. Ueno, T. Nakano, K. Yoneyama, Y. Suzuki, T. Asami, *Bioscience, Biotechnology, and Biochemistry* **2009**, *73*, 2460–2465.

[78]E. Foo, E. Bullier, M. Goussot, F. Foucher, C. Rameau, C. A. Beveridge, *The Plant Cell* **2005**, *17*, 464–474.

[79]R. S. M. Drummond, N. M. Martínez-Sánchez, B. J. Janssen, K. R. Templeton, J. L. Simons, B. D. Quinn, S. Karunairetnam, K. C. Snowden, *Plant Physiology* **2009**, *151*, 1867–1877.

[80]A. Hayward, P. Stirnberg, C. Beveridge, O. Leyser, *Plant Physiology* **2009**, *151*, 400–412.

[81]E. A. Dun, A. de Saint Germain, C. Rameau, C. A. Beveridge, *Plant Physiology* **2012**, *158*, 487–498.

[82]H. Ueda, M. Kusaba, *Plant Physiology* **2015**, *169*, 138–147.

[83]I. Visentin, M. Vitali, M. Ferrero, Y. Zhang, C. Ruyter-Spira, O. Novák, M. Strnad, C. Lovisolo, A. Schubert, F. Cardinale, *New Phytologist* **2016**, *212*, 954–963.

[84]M. Ueguchi-Tanaka, M. Ashikari, M. Nakajima, H. Itoh, E. Katoh, M. Kobayashi, T. Chow, Y. C. Hsing, H. Kitano, I. Yamaguchi, M. Matsuoka, *Nature* **2005**, *437*, 693–698.

[85]T. Arite, M. Umehara, S. Ishikawa, A. Hanada, M. Maekawa, S. Yamaguchi, J. Kyozuka, *Plant and Cell Physiology* **2009**, *50*, 1416–1424.

[86]C. Hamiaux, R. S. M. Drummond, B. J. Janssen, S. E. Ledger, J. M. Cooney, R. D. Newcomb, K. C. Snowden, *Current Biology* **2012**, *22*, 2032–2036.

[87]H. Nakamura, Y.-L. Xue, T. Miyakawa, F. Hou, H.-M. Qin, K. Fukui, X. Shi, E. Ito, S. Ito, S.-H. Park, Y. Miyauchi, A. Asano, N. Totsuka, T. Ueda, M. Tanokura, T. Asami, *Nat Commun* **2013**, *4*, 2613.

[88]R. Yao, Z. Ming, L. Yan, S. Li, F. Wang, S. Ma, C. Yu, M. Yang, L. Chen, L. Chen, Y. Li, C. Yan, D. Miao, Z. Sun, J. Yan, Y. Sun, L. Wang, J. Chu, S. Fan, W. He, H. Deng, F. Nan, J. Li, Z. Rao, Z. Lou, D. Xie, *Nature* **2016**, *536*, 469–473.

[89]G. Dodson, A. Wlodawer, *Trends in Biochemical Sciences* **1998**, *23*, 347–352.

[90]Ö. D. Ekici, M. Paetzel, R. E. Dalbey, *Protein Science* **2008**, *17*, 2023–2037.

[91]R. Wieczorek, K. Adamala, T. Gasperi, F. Polticelli, P. Stano, *Life* **2017**, *7*, 19.

[92]E. M. Mangnus, Binne. Zwanenburg, *J. Agric. Food Chem.* **1992**, *40*, 1066–1070.

[93]B. Zwanenburg, T. Pospíšil, S. Ćavar Zeljković, *Planta* **2016**, *243*, 1311–1326.

[94]A. Scaffidi, M. T. Waters, C. S. Bond, K. W. Dixon, S. M. Smith, E. L. Ghisalberti, G. R. Flematti, *Bioorganic & Medicinal Chemistry Letters* **2012**, *22*, 3743–3746.

[95]J. Park, Y. Lee, E. Martinoia, M. Geisler, *BMC Biol* **2017**, *15*, 93.

[96]X. Xie, K. Yoneyama, T. Kisugi, T. Nomura, K. Akiyama, T. Asami, K. Yoneyama, *Journal of Pesticide Science* **2015**, *40*, 214–216.

[97]L. Borghi, J. Kang, D. Ko, Y. Lee, E. Martinoia, *Biochemical Society Transactions* **2015**, *43*, 924–930.

[98]P. B. Brewer, K. Yoneyama, F. Filardo, E. Meyers, A. Scaffidi, T. Frickey, K. Akiyama, Y. Seto, E. A. Dun, J. E. Cremer, S. C. Kerr, M. T. Waters, G. R. Flematti, M. G. Mason, G. Weiller, S. Yamaguchi, T. Nomura, S. M. Smith, K. Yoneyama, C. A. Beveridge, *Proceedings of the National Academy of Sciences* **2016**, *113*, 6301–6306.

[99]J. B. Heather, R. S. D. Mittal, C. J. Sih, *J. Am. Chem. Soc.* **1974**, *96*, 1976–1977.

[100]G. A. MacAlpine, R. A. Raphael, A. Shaw, A. W. Taylor, H.-J. Wild, *J. Chem. Soc., Chem. Commun.* **1974**, 834–835.

[101]D. W. Brooks, H. S. Bevinakatti, E. Kennedy, J. Hathaway, *J. Org. Chem.* **1985**, *50*, 628–632.

[102]O. D. Dailey, *J. Org. Chem.* **1987**, *52*, 1984–1989.

[103]J. B. Heather, R. S. D. Mittal, C. J. Sih, *J. Am. Chem. Soc.* **1976**, *98*, 3661–3669.

[104]C. Sun, S. Wu, Y. Wu, B. Sun, P. Zhang, K. Tang, *Process Biochemistry* **2023**, *124*, 132–139.

[105]K. Hirayama, K. Mori, *European Journal of Organic Chemistry* **1999**, *1999*, 2211–2217.

[106]J. Matsui, T. Yokota, M. Bando, Y. Takeuchi, K. Mori, *European Journal of Organic Chemistry* **1999**, *1999*, 2201–2210.

[107]K. Mori, J. Matsui, T. Yokota, H. Sakai, M. Bando, Y. Takeuchi, *Tetrahedron Letters* **1999**, *40*, 943–946.

[108]M. Lachia, P.-Y. Dakas, A. De Mesmaeker, *Tetrahedron Letters* **2014**, *55*, 6577–6581.

[109]J. Matsui, M. Bando, M. Kido, Y. Takeuchi, K. Mori, *European Journal of Organic Chemistry* **1999**, *1999*, 2183–2194.

[110]V. S. Mahalwal, Mohd. Ali, *Flavour and Fragrance Journal* **2003**, *18*, 73–76.

[111]S. Kitahara, T. Tashiro, Y. Sugimoto, M. Sasaki, H. Takikawa, *Tetrahedron Letters* **2011**, *52*, 724–726.

[112]K. Frischmuth, E. Samson, A. Kranz, P. Welzel, H. Meuer, W. S. Sheldrick, *Tetrahedron* **1991**, *47*, 9793–9806.

[113]A. Reizelman, B. Zwanenburg, *European Journal of Organic Chemistry* **2002**, *2002*, 810–814.

[114]V. X. Chen, F.-D. Boyer, C. Rameau, P. Retailleau, J.-P. Vors, J.-M. Beau, *Chemistry – A European Journal* **2010**, *16*, 13941–13945.

[115]L. J. Bromhead, A. R. Norman, K. C. Snowden, B. J. Janssen, C. S. P. McErlean, *Org. Biomol. Chem.* **2018**, *16*, 5500–5507.

[116]K. Uchida, H. Okamura, Y. Ogura, H. Takikawa, *Tetrahedron* **2024**, *159*, 134016.

[117]M. C. Dieckmann, P.-Y. Dakas, A. De Mesmaeker, *J. Org. Chem.* **2018**, *83*, 125–135.

[118]E. W. Colvin, B. J. Hamill, *J. Chem. Soc., Perkin Trans. 1* **1977**, 869–874.

[119]M. Yoshimura, M. Dieckmann, P.-Y. Dakas, R. Fonné-Pfister, C. Screpanti, K. Hermann, S. Rendine, P. Quinodoz, B. Horoz, S. Catak, A. De Mesmaeker, *Helvetica Chimica Acta* **2020**, *103*, e2000017.

[120]S. Woo, C. S. P. McErlean, *Org. Lett.* **2019**, *21*, 4215–4218.

[121]A. Scaffidi, M. T. Waters, E. L. Ghisalberti, K. W. Dixon, G. R. Flematti, S. M. Smith, *The Plant Journal* **2013**, *76*, 1–9.

[122]H. Malik, F. P. J. T. Rutjes, B. Zwanenburg, *Synthesis* **2010**, *2010*, 3271–3273.

[123]O. Doebner, *Berichte der deutschen chemischen Gesellschaft* **1902**, *35*, 1136–1147.

[124]E. Knoevenagel, *Berichte der deutschen chemischen Gesellschaft* **1898**, *31*, 2596–2619.

[125]N. A. Milas, S. W. Lee, E. Sakal, H. C. Wohlers, N. S. MacDonald, F. X. Grossi, H. F. Wright, *J. Am. Chem. Soc.* **1948**, *70*, 1584–1591.

[126]N. A. Milas, in *Vitamins & Hormones* (Eds.: R.S. Harris, K.V. Thimann), Academic Press, **1947**, pp. 1–38.

[127]C. C. Tung, A. J. Speziale, H. W. Frazier, *J. Org. Chem.* **1963**, *28*, 1514–1521.

[128]M. Ballester, *Chem. Rev.* **1955**, *55*, 283–300.

[129]L. J. Bromhead, J. Visser, C. S. P. McErlean, *J. Org. Chem.* **2014**, *79*, 1516–1520.

[130]J.-P. Corbet, G. Mignani, *Chem. Rev.* **2006**, *106*, 2651–2710.

[131]C. C. C. Johansson Seechurn, M. O. Kitching, T. J. Colacot, V. Snieckus, *Angewandte Chemie International Edition* **2012**, *51*, 5062–5085.

[132]P. Ruiz-Castillo, S. L. Buchwald, *Chem. Rev.* **2016**, *116*, 12564–12649.

[133]P. Y. S. Lam, C. G. Clark, S. Saubern, J. Adams, M. P. Winters, D. M. T. Chan, A. Combs, *Tetrahedron Letters* **1998**, *39*, 2941–2944.

[134]D. M. T. Chan, K. L. Monaco, R.-P. Wang, M. P. Winters, *Tetrahedron Letters* **1998**, *39*, 2933–2936.

[135]B. M. Rosen, K. W. Quasdorf, D. A. Wilson, N. Zhang, A.-M. Resmerita, N. K. Garg, V. Percec, *Chem. Rev.* **2011**, *111*, 1346–1416.

[136]L. Dai, J. Gonzalez, K. Zhang, *Journal of Chromatography Open* **2022**, *2*, 100036.

[137]Q. Zhong, K. K. Ngim, M. Sun, J. Li, A. Deese, N. P. Chetwyn, *Journal of Chromatography A* **2012**, *1229*, 216–222.

[138]S. Darses, J.-P. Genet, *Chem. Rev.* **2008**, *108*, 288–325.

[139]G. A. Molander, B. Canturk, *Angewandte Chemie International Edition* **2009**, *48*, 9240–9261.

[140]R. Martin, S. L. Buchwald, *Acc. Chem. Res.* **2008**, *41*, 1461–1473.

[141]G. W. Kabalka, B. Venkataiah, G. Dong, *Tetrahedron Letters* **2004**, *45*, 729–731.

[142]S. R. Inglis, E. C. Y. Woon, A. L. Thompson, C. J. Schofield, *J. Org. Chem.* **2010**, *75*, 468–471.

[143]K. Brak, J. A. Ellman, *J. Am. Chem. Soc.* **2009**, *131*, 3850–3851.

[144]A. J. J. Lennox, G. C. Lloyd-Jones, *Angewandte Chemie International Edition* **2012**, *51*, 9385–9388.

[145]T. D. Quach, R. A. Batey, *Org. Lett.* **2003**, *5*, 1381–1384.

[146]L. Steemers, L. Wijsman, J. H. van Maarseveen, *Advanced Synthesis & Catalysis* **2018**, *360*, 4241–4245.

[147]F. Huang, T. D. Quach, R. A. Batey, *Org. Lett.* **2013**, *15*, 3150–3153.

[148]J.-J. Sui, D.-C. Xiong, X.-S. Ye, *Chinese Chemical Letters* **2019**, *30*, 1533–1537.

[149]R. E. Shade, A. M. Hyde, J.-C. Olsen, C. A. Merlic, *J. Am. Chem. Soc.* **2010**, *132*, 1202–1203.

[150]W. Jo, J. Kim, S. Choi, S. H. Cho, *Angewandte Chemie International Edition* **2016**, *55*, 9690–9694.

[151]J. C. Vantourout, H. N. Miras, A. Isidro-Llobet, S. Sproules, A. J. B. Watson, *J. Am. Chem. Soc.* **2017**, *139*, 4769–4779.

[152]J.-Q. Chen, J.-H. Li, Z.-B. Dong, *Advanced Synthesis & Catalysis* **2020**, *362*, 3311–3331.

[153]X. Liu, T. M. Deaton, F. Haeffner, J. P. Morken, *Angewandte Chemie International Edition* **2017**, *56*, 11485–11489.

[154]Z.-Q. Zhang, C.-T. Yang, L.-J. Liang, B. Xiao, X. Lu, J.-H. Liu, Y.-Y. Sun, T. B. Marder, Y. Fu, *Org. Lett.* **2014**, *16*, 6342–6345.

[155]T. Klis, S. Lulinski, J. Serwatowski, *Current Organic Chemistry* **n.d.**, *14*, 2549–2566.

[156]C. Sun, B. Potter, J. P. Morken, *J. Am. Chem. Soc.* **2014**, *136*, 6534–6537.

[157]W. Adam, H. H. Fick, *J. Org. Chem.* **1979**, *44*, 356–359.

[158]H. Henry-Riyad, C. Lee, V. C. Purohit, D. Romo, *Org. Lett.* **2006**, *8*, 4363–4366.

[159]G. S. Cortez, R. L. Tennyson, D. Romo, *J. Am. Chem. Soc.* **2001**, *123*, 7945–7946.

[160]R. L. Danheiser, J. S. Nowick, *J. Org. Chem.* **1991**, *56*, 1176–1185.

[161]M. Yasui, R. Ota, C. Tsukano, Y. Takemoto, *Nat Commun* **2017**, *8*, 674.

[162]B. E. Maryanoff, A. B. Reitz, *Chem. Rev.* **1989**, *89*, 863–927.

[163]W. S. Wadsworth Jr., in *Organic Reactions*, John Wiley & Sons, Ltd, **2005**, pp. 73–253.

[164]J. Boutagy, R. Thomas, *Chem. Rev.* **1974**, *74*, 87–99.

[165]L. Horner, H. Hoffmann, H. G. Wippel, *Chemische Berichte* **1958**, *91*, 61–63.

[166]W. S. Wadsworth, W. D. Emmons, *J. Am. Chem. Soc.* **1961**, *83*, 1733–1738.

[167]S. K. Thompson, C. H. Heathcock, *J. Org. Chem.* **1990**, *55*, 3386–3388.

[168]B. Bardili, H. Marschall-Weyerstahl, P. Weyerstahl, *Liebigs Annalen der Chemie* **1985**, *1985*, 275–300.

[169]J. L. Luche, *J. Am. Chem. Soc.* **1978**, *100*, 2226–2227.

[170]B. Neises, W. Steglich, *Angewandte Chemie International Edition in English* **1978**, *17*, 522–524.

[171]K. Ando, K. Narumiya, H. Takada, T. Teruya, *Org. Lett.* **2010**, *12*, 1460–1463.

[172]A. de Meijere, *Angewandte Chemie International Edition in English* **1979**, *18*, 809–826.

[173]E. Honegger, E. Heilbronner, A. Schmelzer, W. Jian-Qi, *Israel Journal of Chemistry* **1982**, *22*, 3–10.

[174]F. H. Allen, O. Kennard, D. G. Watson, L. Brammer, A. G. Orpen, R. Taylor, *J. Chem. Soc., Perkin Trans. 2* **1987**, S1–S19.

[175]H. E. Simmons, R. D. Smith, *J. Am. Chem. Soc.* **1958**, *80*, 5323–5324.

[176]E. J. Corey, M. Chaykovsky, *J. Am. Chem. Soc.* **1965**, *87*, 1353–1364.

[177]A. W. Johnson, R. B. LaCount, *J. Am. Chem. Soc.* **1961**, *83*, 417–423.

[178]O. Silberrad, C. S. Roy, *J. Chem. Soc., Trans.* **1906**, *89*, 179–182.

[179]W. von E. Doering, A. K. Hoffmann, *J. Am. Chem. Soc.* **1954**, *76*, 6162–6165.

[180]K. Kikuchi, C. S. P. McErlean, *Tetrahedron Letters* **2021**, *70*, 153003.

[181]M. Fedoryński, *Chem. Rev.* **2003**, *103*, 1099–1132.

[182]D. Bourissou, O. Guerret, F. P. Gabbaï, G. Bertrand, *Chem. Rev.* **2000**, *100*, 39–92.

[183]W. S. Rapson, R. Robinson, *J. Chem. Soc.* **1935**, 1285–1288.

[184]M. L. Lepage, G. Alachouzos, J. G. H. Hermens, N. Elders, K. J. van den Berg, B. L. Feringa, *J. Am. Chem. Soc.* **2023**, *145*, 17211–17219.

[185]S. P. Chavan, A. L. Kadam, *Results in Chemistry* **2021**, *3*, 100170.

[186]A. Besserer, G. Bécard, A. Jauneau, C. Roux, N. Séjalon-Delmas, *Plant Physiology* **2008**, *148*, 402–413.

[187]Y. Krasylenko, G. Komis, S. Hlynska, T. Vavrdová, M. Ovečka, T. Pospíšil, J. Šamaj, *Front. Plant Sci.* **2021**, *12*, DOI 10.3389/fpls.2021.675981.

[188]N. Mori, K. Nishiuma, T. Sugiyama, H. Hayashi, K. Akiyama, *Phytochemistry* **2016**, *130*, 90–98.

[189]K. Kawada, T. Saito, S. Onoda, T. Inayama, I. Takahashi, Y. Seto, T. Nomura, Y. Sasaki, T. Asami, S. Yajima, S. Ito, *ACS Omega* **2023**, *8*, 13855–13862.

[190]X. Huang, X. Li, M. Zou, J. Pan, N. Jiao, *Org. Chem. Front.* **2015**, *2*, 354–359.

[191]S. T. Nguyen, L. K. Johnson, R. H. Grubbs, J. W. Ziller, *J. Am. Chem. Soc.* **1992**, *114*, 3974–3975.

[192]G. C. Vougioukalakis, R. H. Grubbs, *Chem. Rev.* **2010**, *110*, 1746–1787.

[193]R. H. Grubbs, T. M. Trnka, in *Ruthenium in Organic Synthesis*, John Wiley & Sons, Ltd, **2004**, pp. 153–177.

[194]J. S. Kingsbury, J. P. A. Harrity, P. J. Bonitatebus, A. H. Hoveyda, *J. Am. Chem. Soc.* **1999**, *121*, 791–799.

[195]X. Xia, Z. Lao, P. H. Toy, *Synlett* **2019**, *30*, 1100–1104.

[196]J. R. Coombs, L. Zhang, J. P. Morken, *J. Am. Chem. Soc.* **2014**, *136*, 16140–16143.

[197]S. Gobbi, Q. Hu, M. Negri, C. Zimmer, F. Belluti, A. Rampa, R. W. Hartmann, A. Bisi, *J. Med. Chem.* **2013**, *56*, 1723–1729.

[198]T. Imamoto, M. Kodera, M. Yokoyama, *Synthesis* **2002**, *1982*, 134–136.

[199]S. H. Oh, G. S. Cortez, D. Romo, *J. Org. Chem.* **2005**, *70*, 2835–2838.

[200]S. Serra, C. Fuganti, *Tetrahedron: Asymmetry* **2006**, *17*, 1573–1580.

[201]K. Kikuchi, *MPhil Thesis* **2021**.

[202]Z. Wang, *Honours Thesis* **2022**.

[203]D. Brandt, A. Dittoo, V. Bellosta, J. Cossy, *Org. Lett.* **2015**, *17*, 816–819.

[204]S. P. Chavan, A. L. Kadam, *Results in Chemistry* **2021**, *3*, 100170.

Appendix

Compound **329** ^{1}H NMR

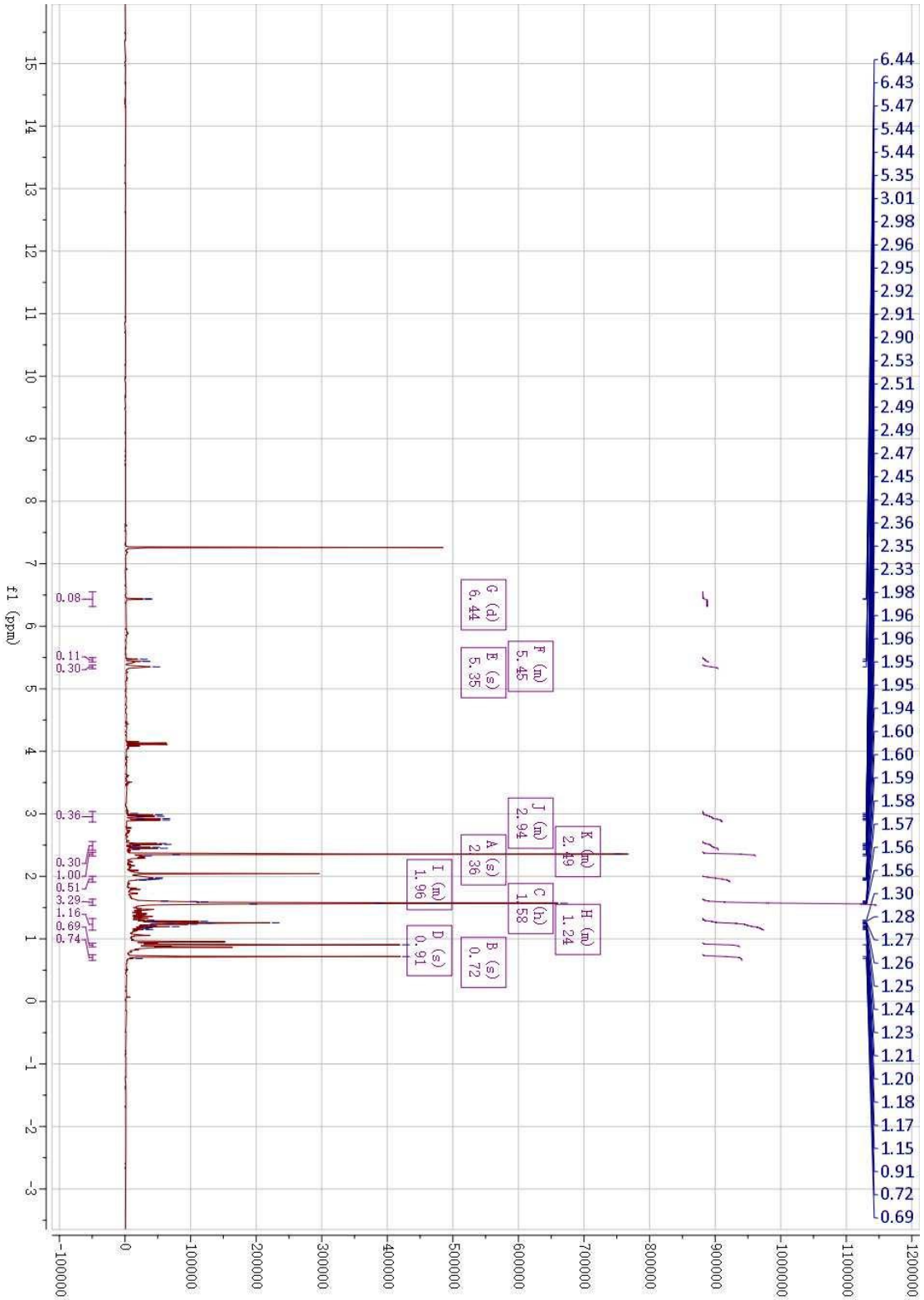

Compound **329** ^{13}C NMR

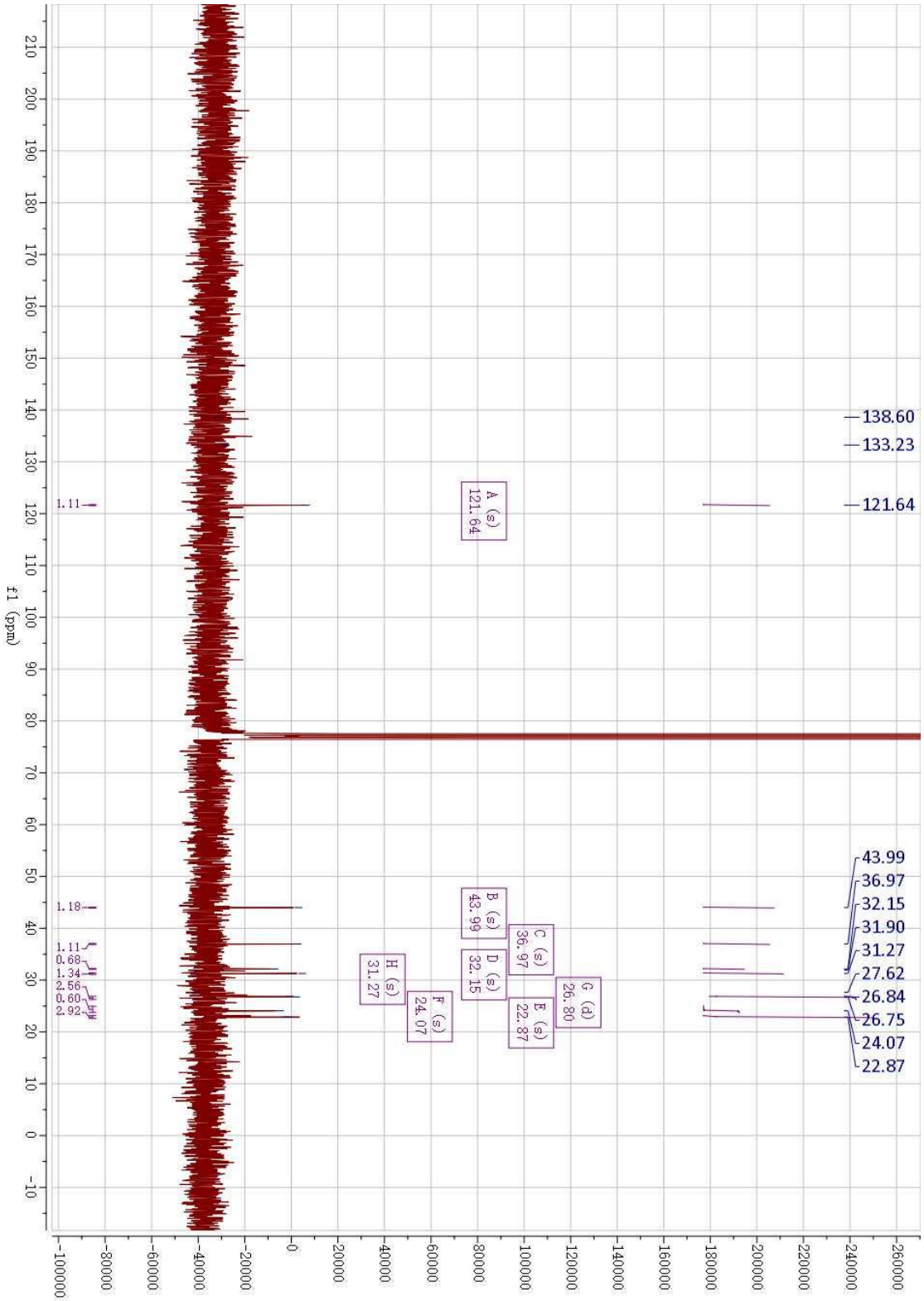

Compound **331** ^{1}H NMR

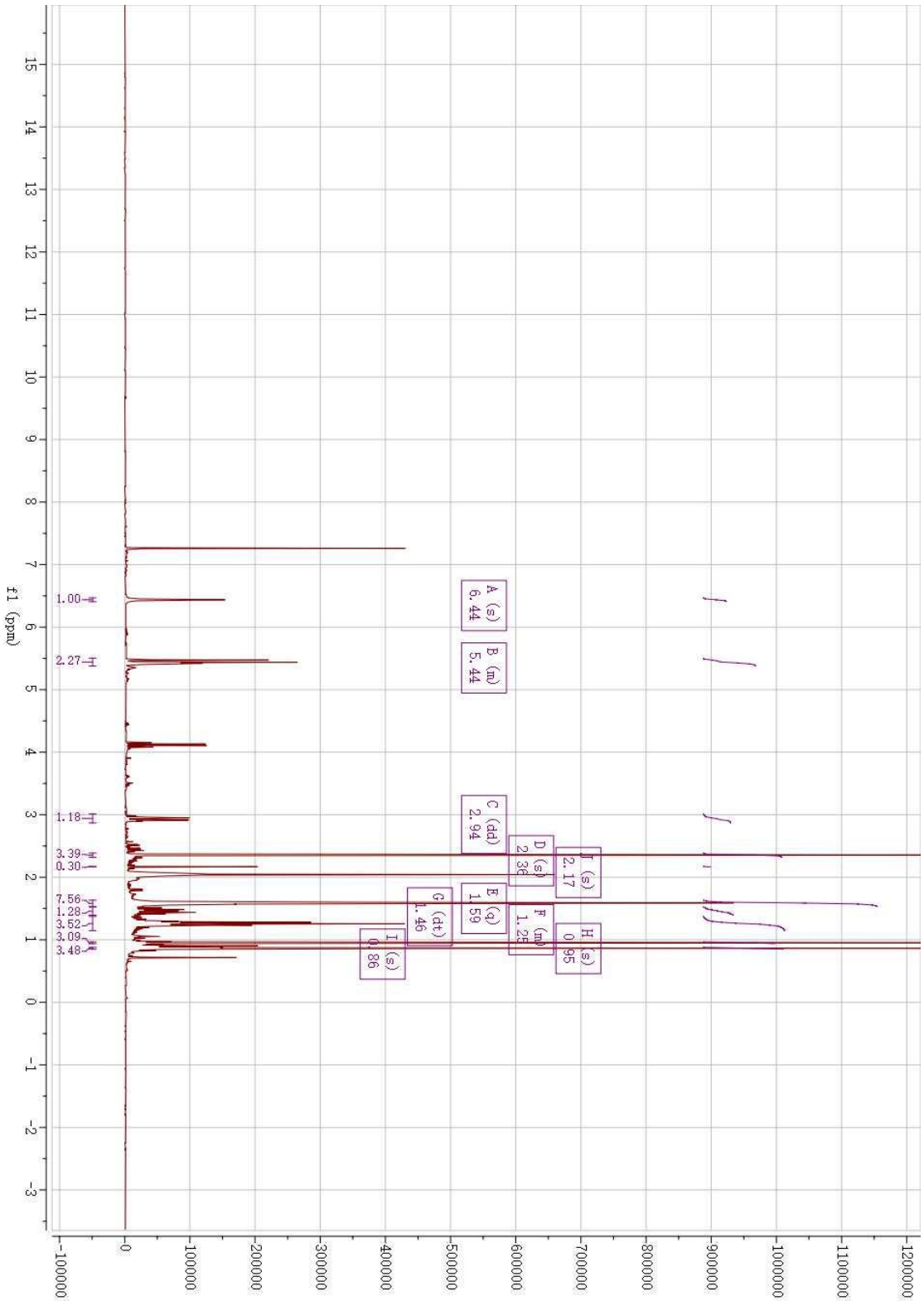

Compound **331** ^{13}C NMR

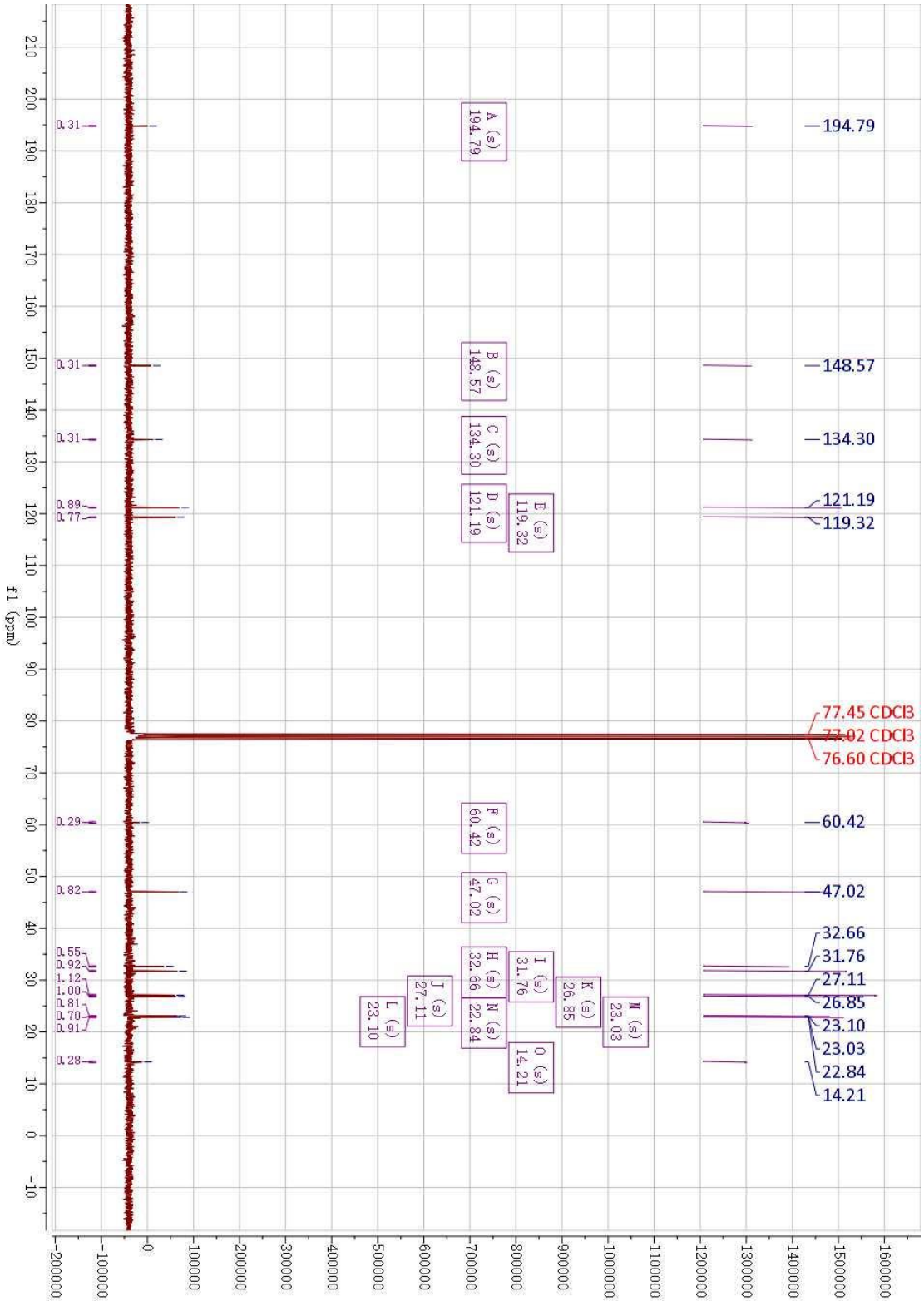

Compound **382** ^{1}H NMR

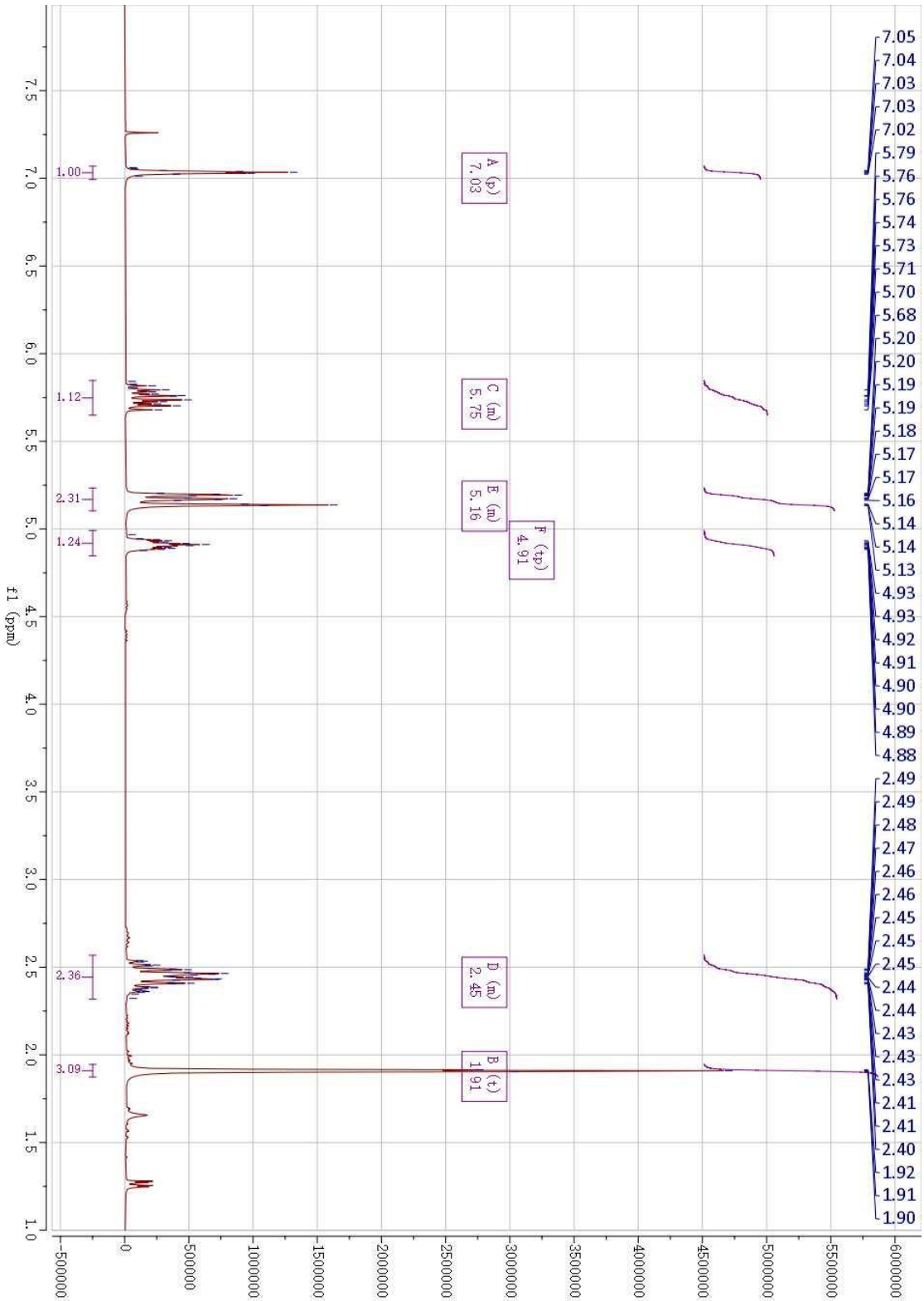

Compound **382** ^{13}C NMR

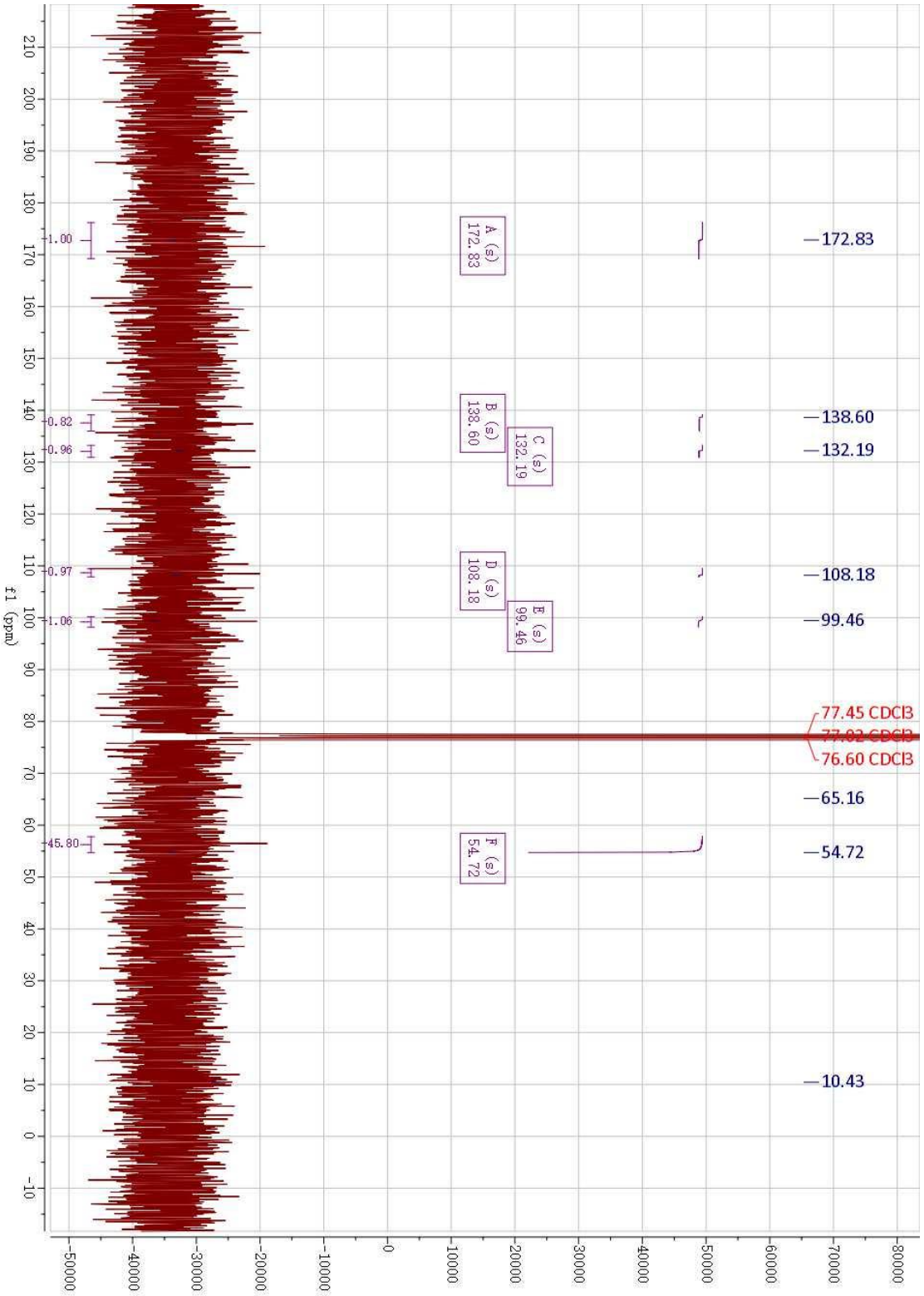

Compound **403** ^{1}H NMR

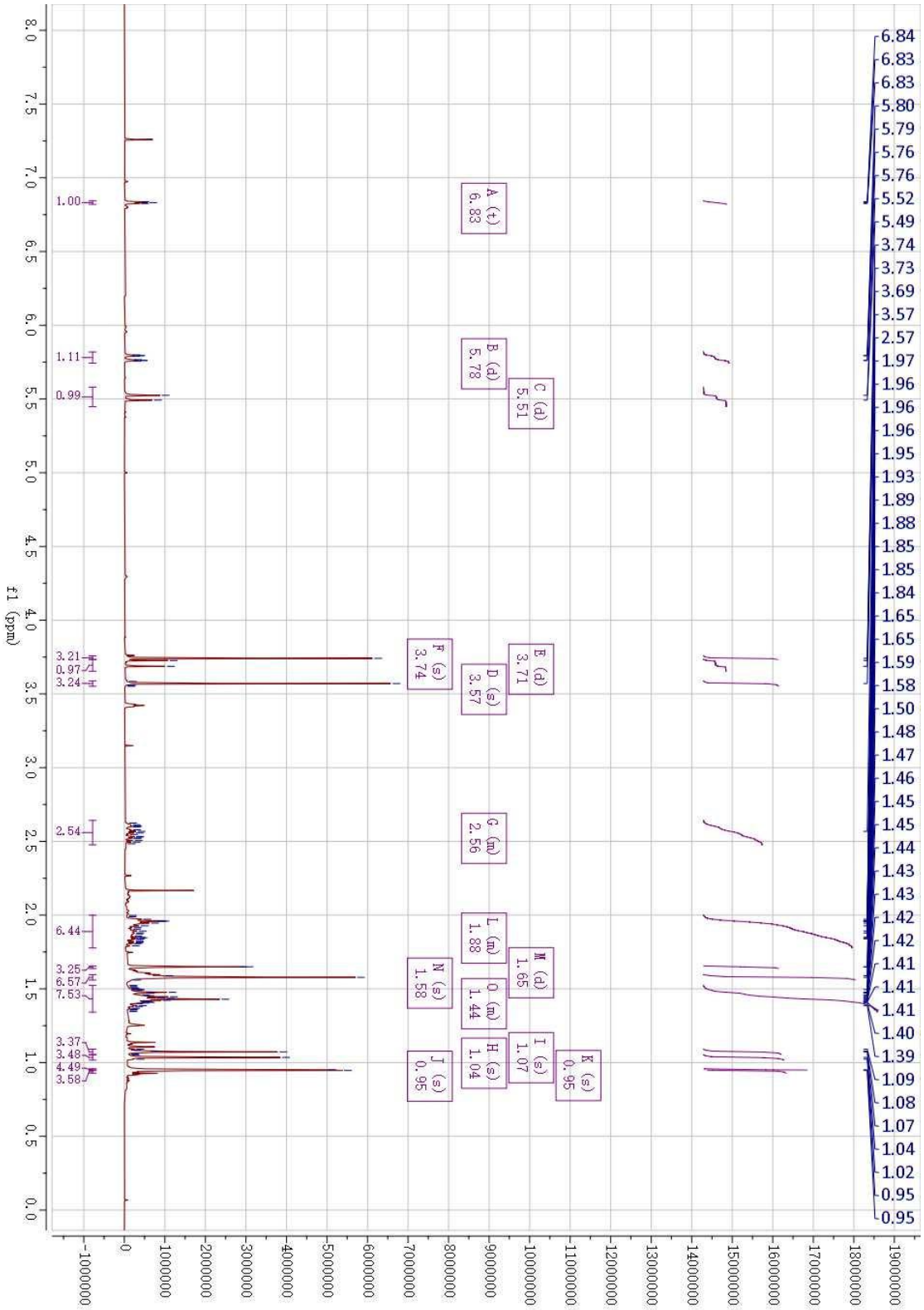

Compound **403** ^{13}C NMR

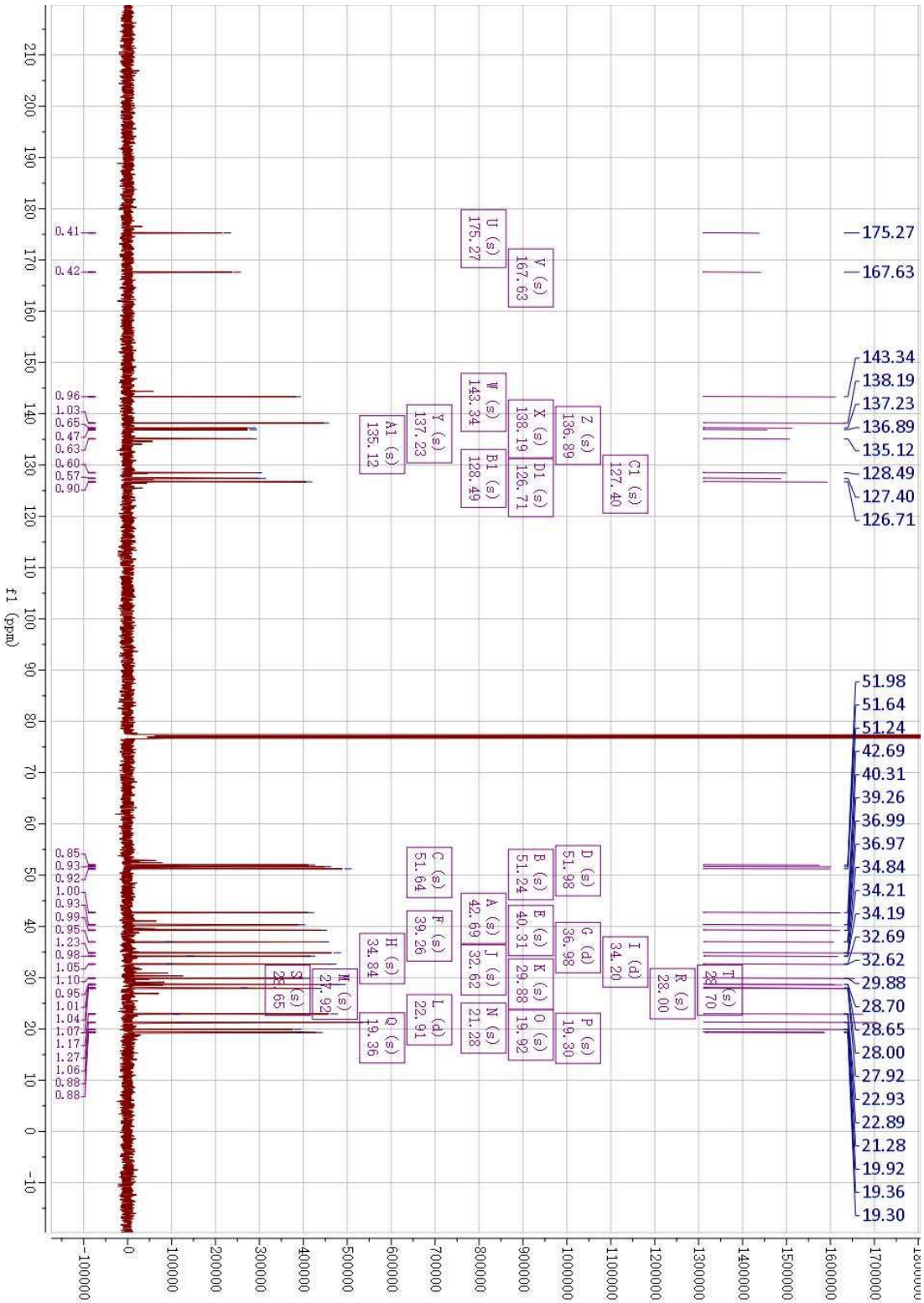

Compound **403** COSY

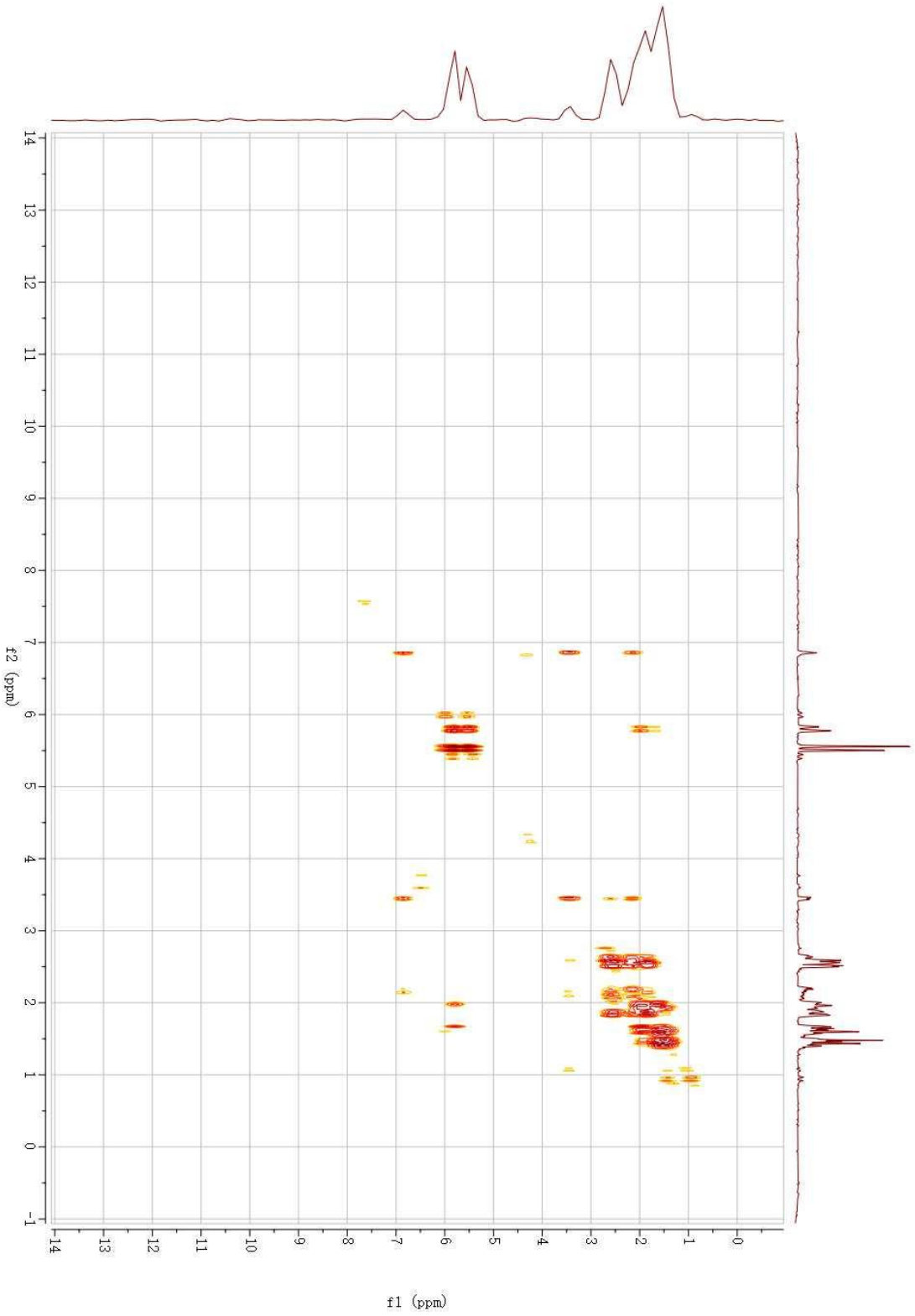

Compound **403** NOESY

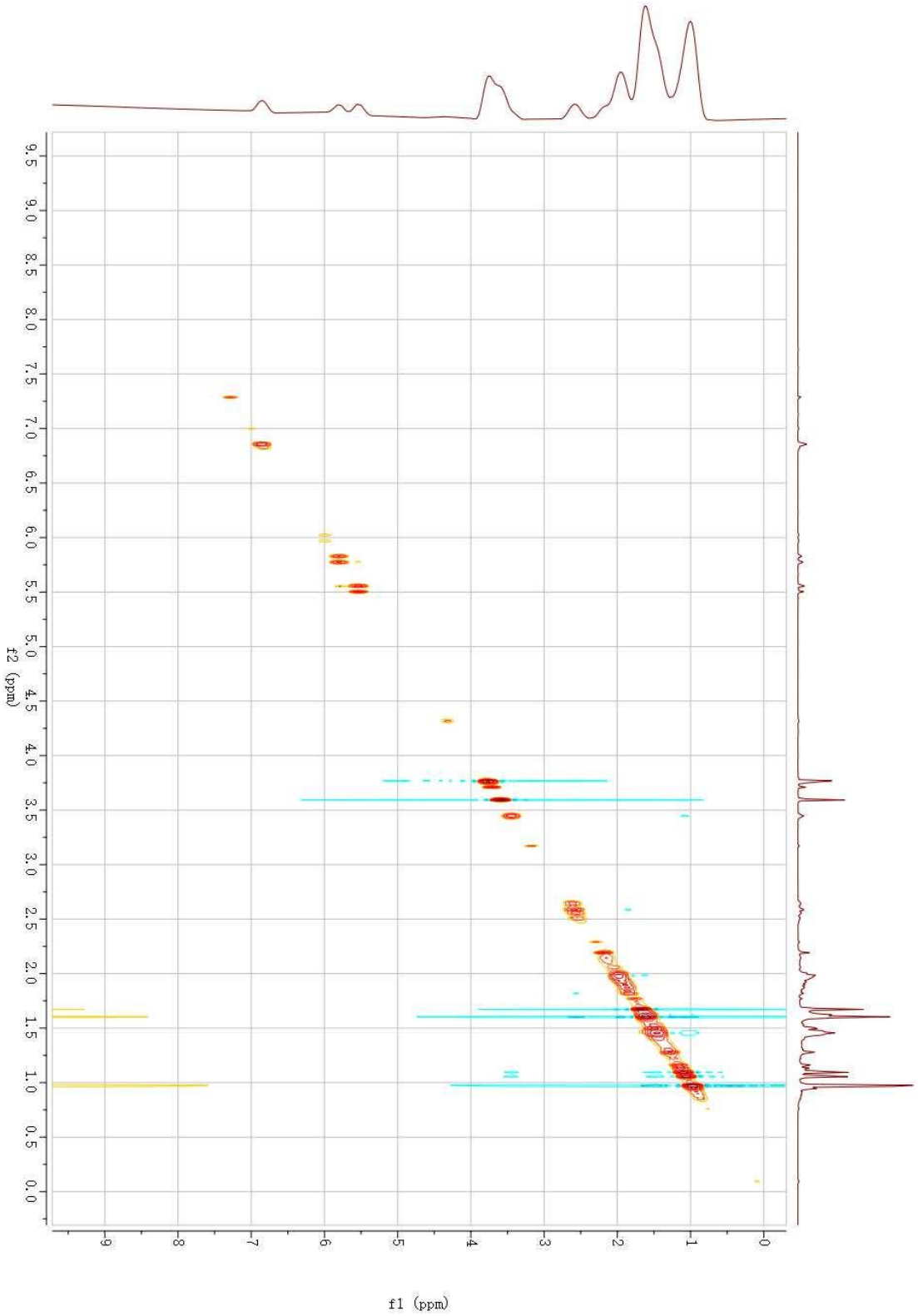

Compound **403** HSQC

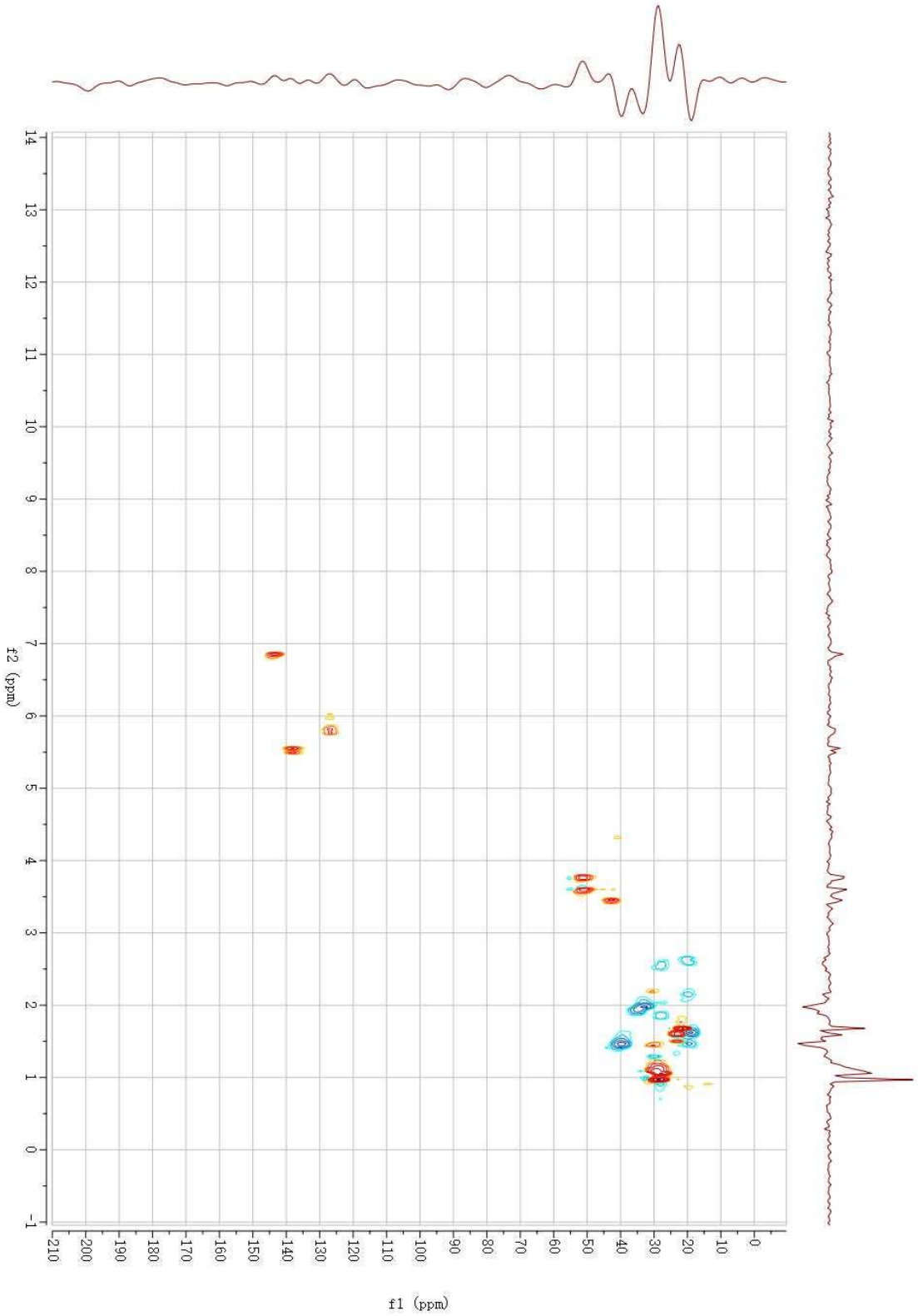

Compound **403** HMBC

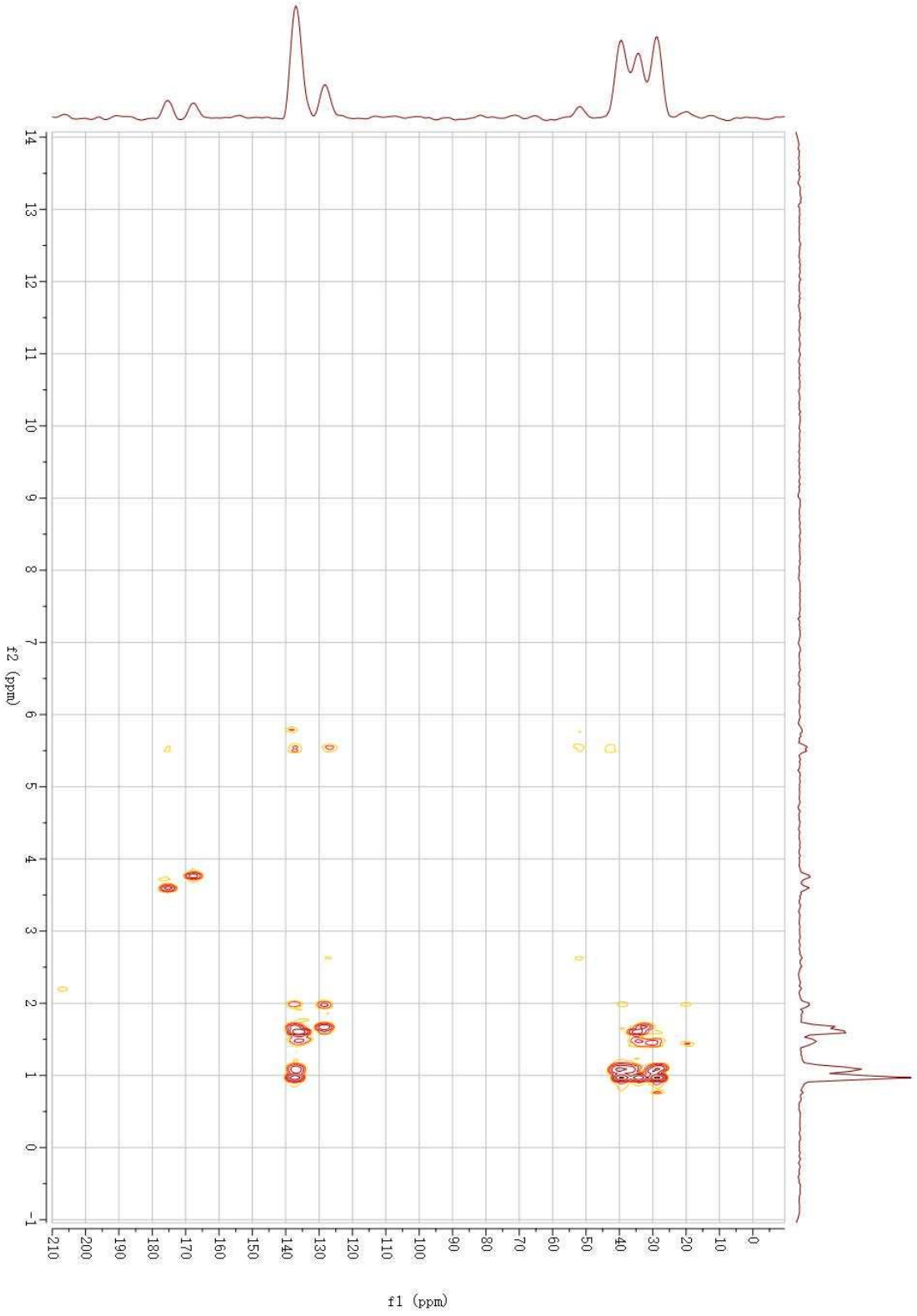

Compound **404** ^{1}H NMR

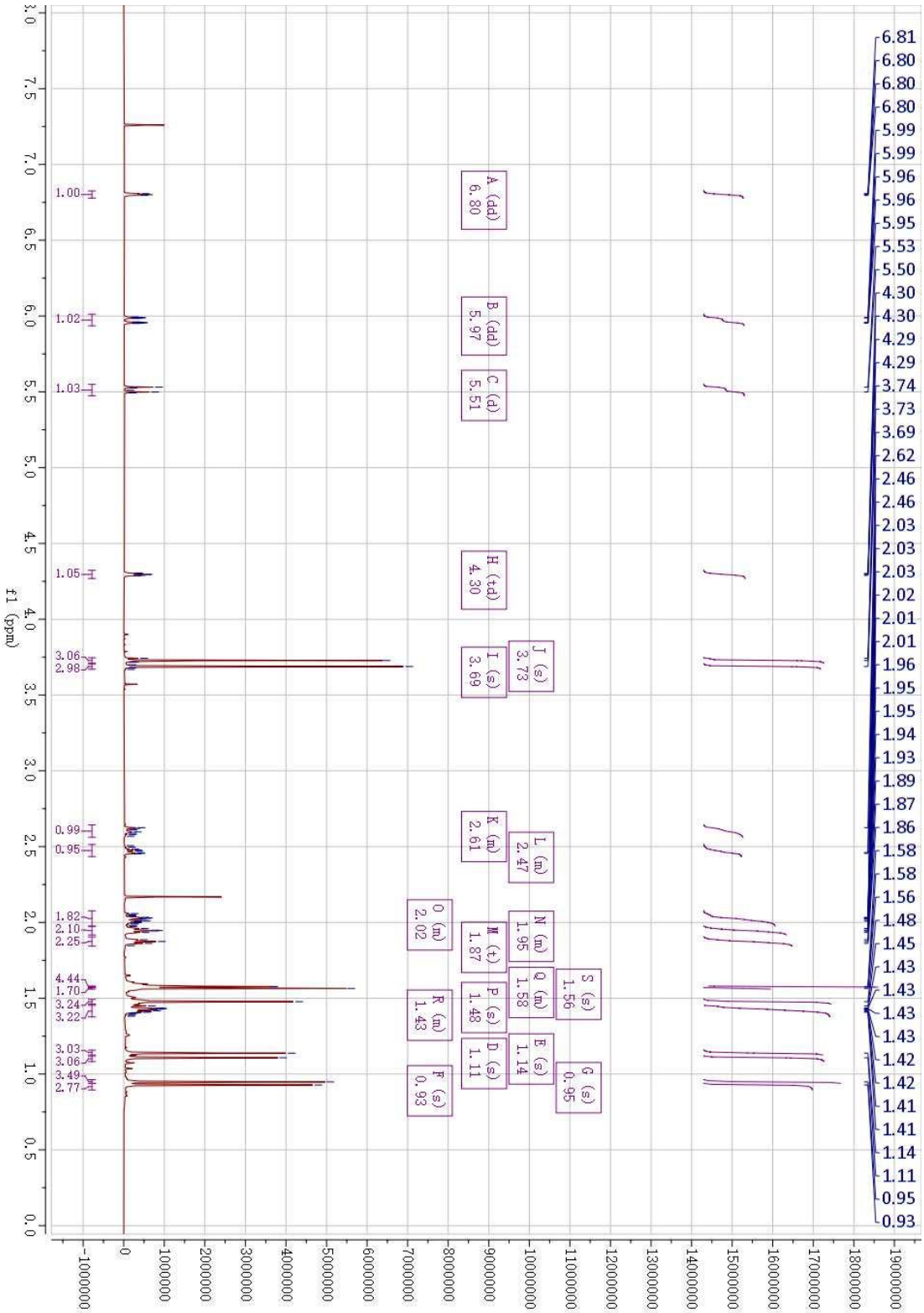

Compound **404** ^{13}C NMR

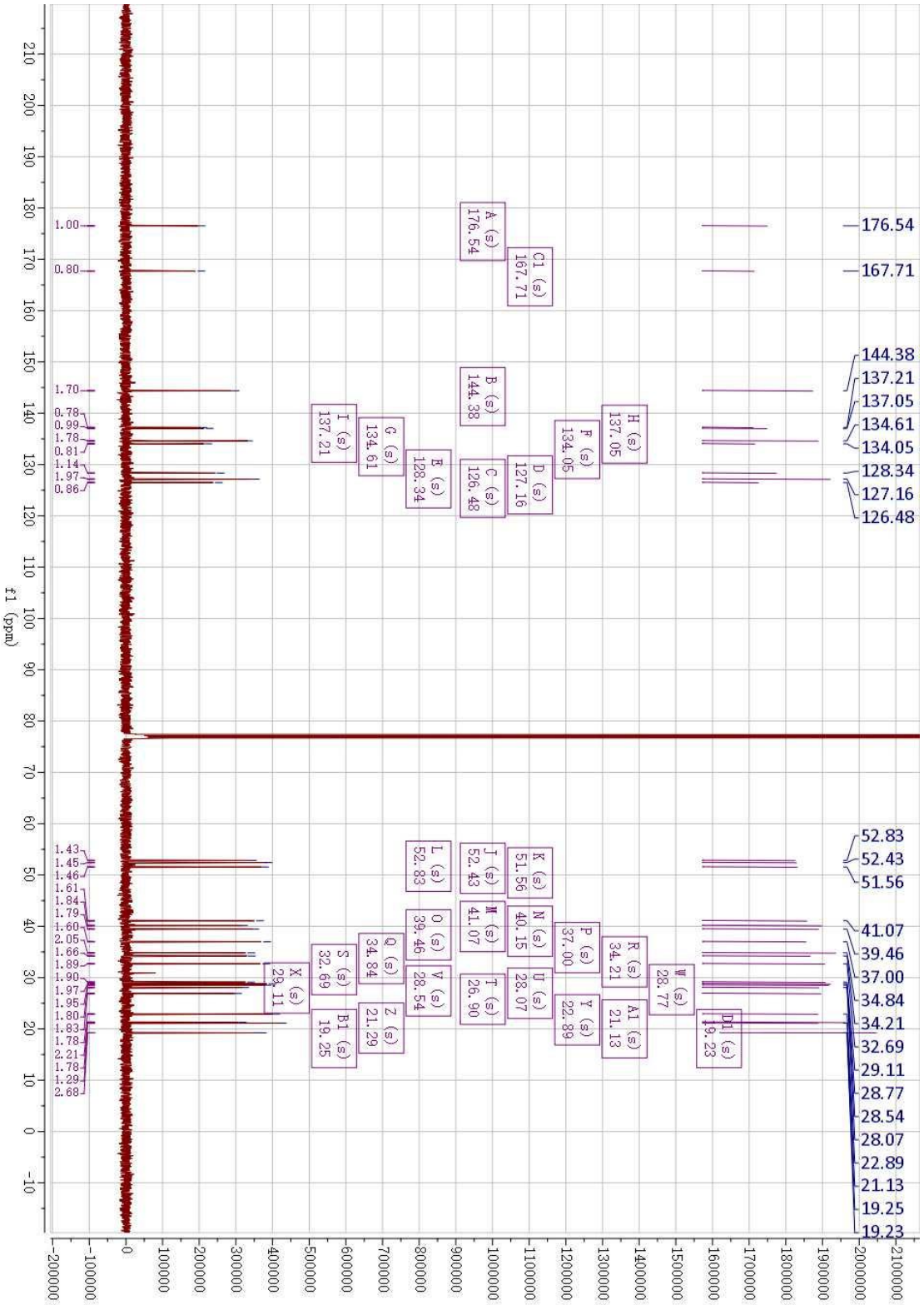

Compound **404** COSY

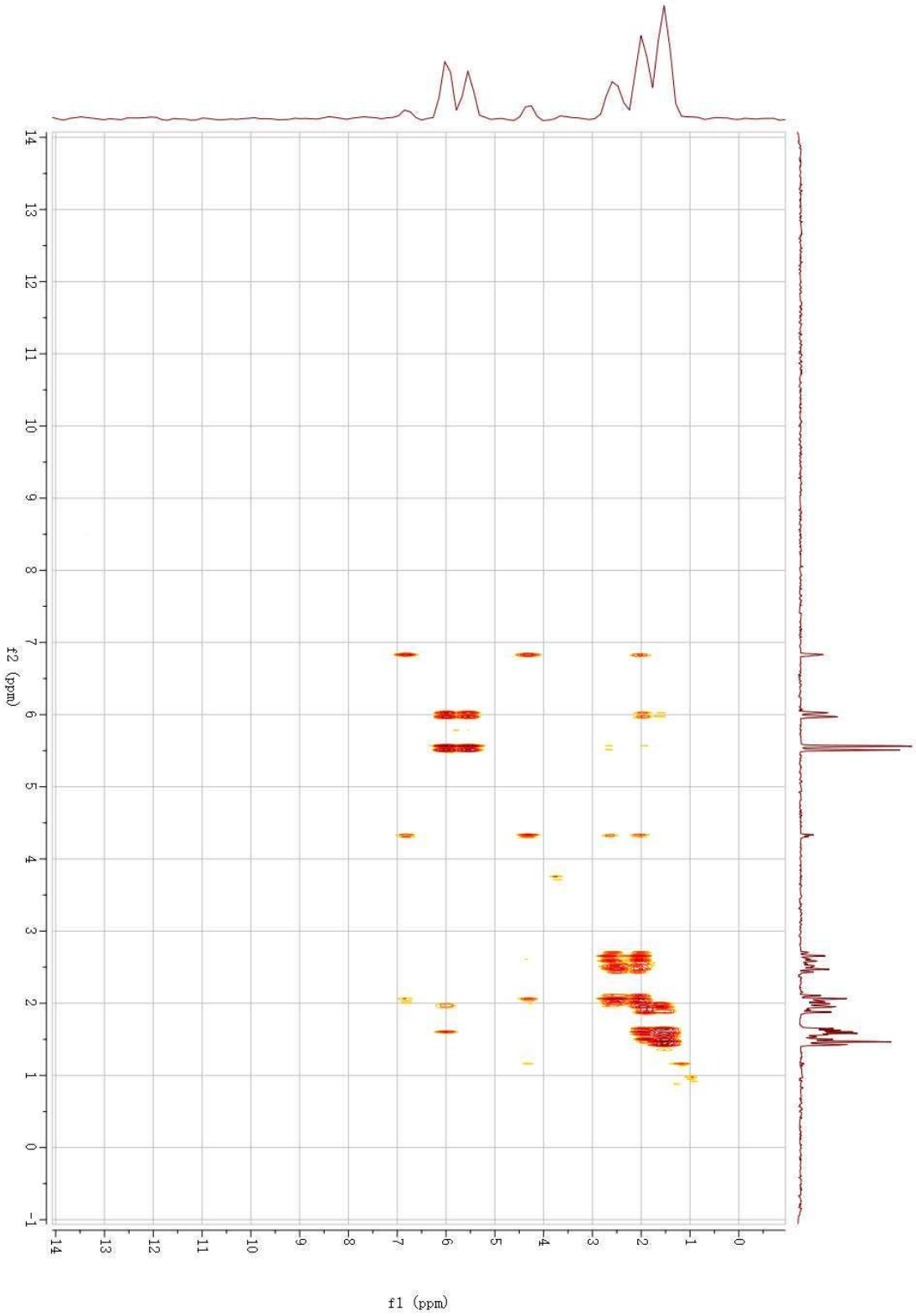

Compound **404** NOESY

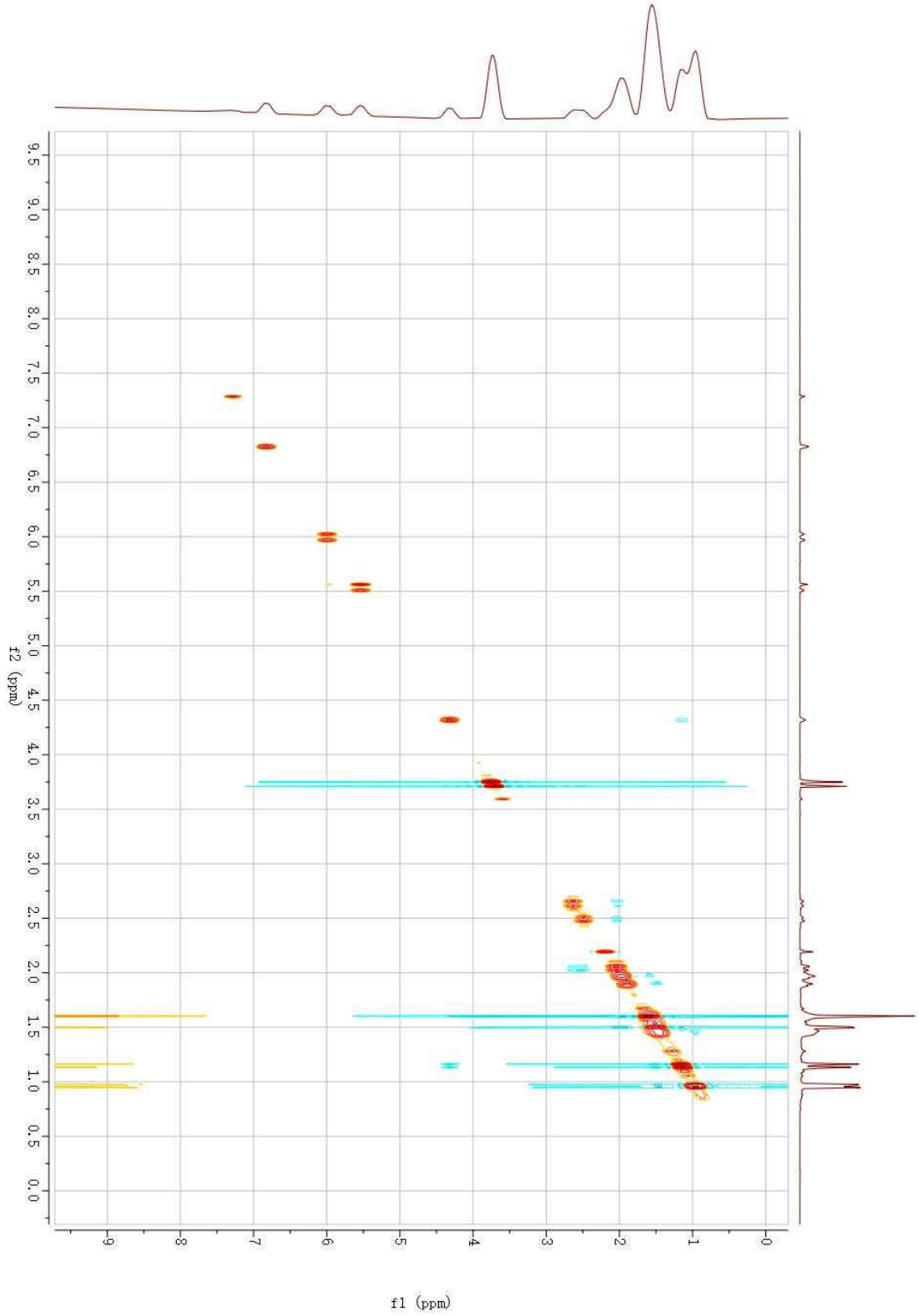

Compound **404** HSQC

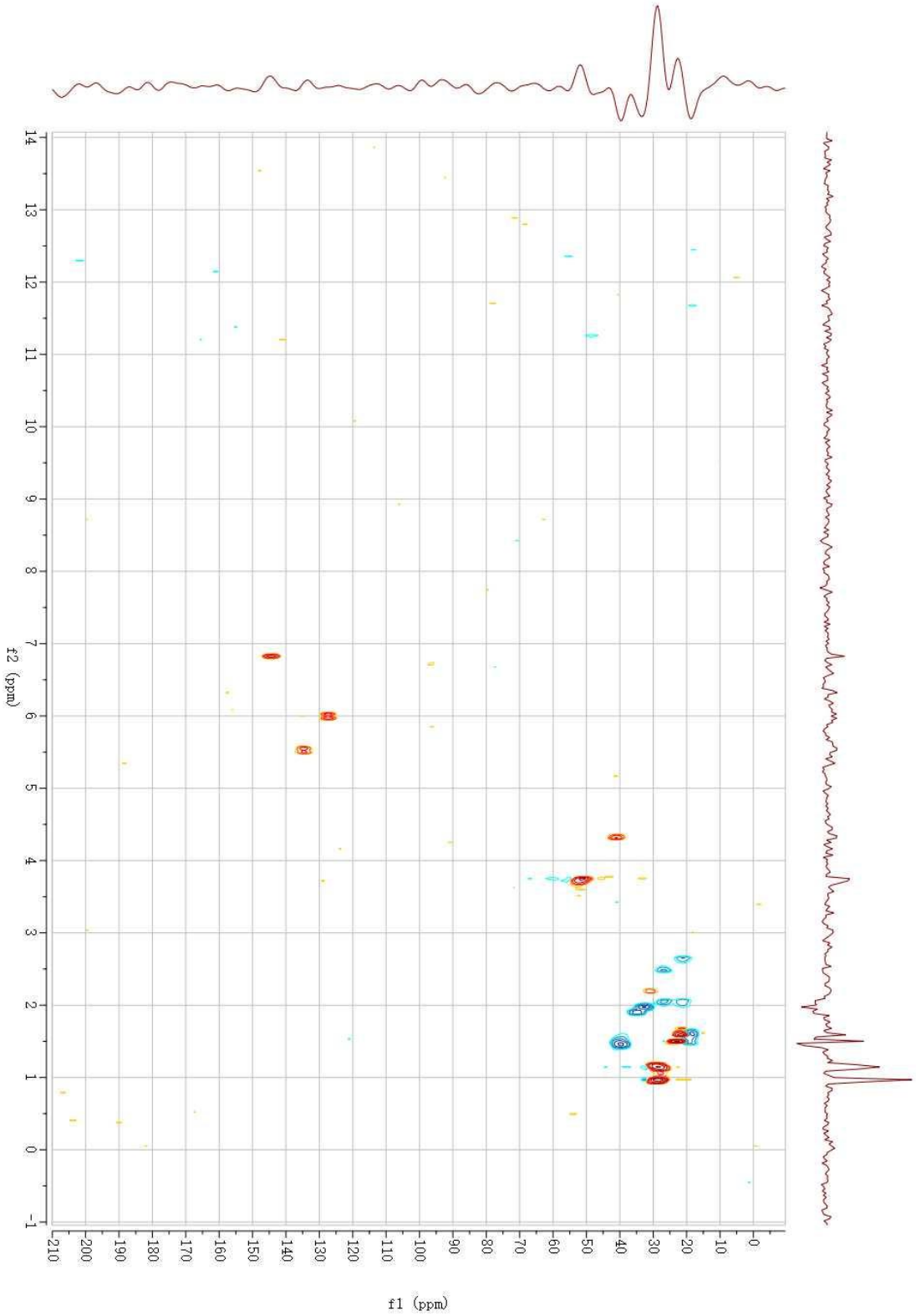

Compound **404** HMBC